Energy Saving Impact of Air Curtains in Commercial Buildings

Sherif Goubran

A Thesis in
the Department of
Building, Civil, Environmental Engineering

Presented in Partial Fulfillment of the Requirements
for the Degree of
Master of Applied Science (Building Engineering) at
Concordia University
Montreal, Quebec, Canada

April 2016

CONCORDIA UNIVERSITY

School of Graduate Studies

This is to certify that the thesis prepared

By: Sherif Nader Alphonse Goubran

Entitled: Energy Saving Impact of Air Curtains in Commercial Buildings

and submitted in partial fulfillment of the requirements for the degree of

Master of Applied Science (Building Engineering)

complies with the regulations of the University and meets the accepted standards with respect to originality and quality.

Signed by the final Examining Committee:

Dr. R. Zmeureanu — Chair

Chair's name

Dr. B. Lee — Examiner

Examiner's name

Dr. H. d. Ng — External Examiner

Examiner's name

Dr. L. Wang — Supervisor

Supervisor's name

Approved by: _____

Chair of Department or Graduate Program Director

_____ 2016 _____

Dean of Faculty

ABSTRACT

Energy Saving Impact of Air Curtains in Commercial Buildings

Sherif Goubran

This study investigates the energy saving impact replacing vestibules with air curtain doors (single doors fitted with air curtain units) has on energy usage of commercial buildings. Laboratory experiments were used to investigate the infiltration characteristics of air curtains in a small size chamber and to validate numerical simulation methods. Experimental flow and pressure as well as particle image velocimetry data confirmed that air curtains can significantly reduce air infiltration when compared to the single and vestibule doors. In addition, the results indicated that the CFD modeling methods used are valid in capturing the characteristics of the airflow at the door with air curtains. CFD simulations were conducted for a full scale door with consideration for the door operation cycle and the existence of people in the doorway. The results of the simulations were used to conduct energy simulations for two reference building models. The end use site-energy performances of the whole buildings with air curtain, vestibule and single doors are compared using two infiltration calculation methods. The energy simulations conducted show that, on a national average level, air curtain doors save energy (in comparison to code requirements). Finally, considering the space saving benefit of air curtains and their lower initial costs, air curtains are concluded to be a valid and energy saving alternative to vestibule doors in climate zones 3 to 8 and a valuable energy saving addition in climate zones 1 & 2.

ACKNOWLEDGEMENT

I would like to express my gratitude to my supervisor Dr. Leon Wang and I would like to thank him for his continuous support, guidance and dedication. I would also like to thank him for all the resources he made available which allowed me and this work to excel.

The author acknowledges the support from the Air Management and Control Association (AMCA) and the valuable inputs from Mr. Frank Cuaderno at Mars Air Systems, Mr. David Johnson at Berner International, Mr. Brian Jones at Powered Aire, and Ms. Amanda Hickman at InterCode Incorporated. The author would also like to thank Mr. William Stuart Dols and Mr. Brian Polidoro at the Engineering Lab of the U.S. National Institute of Standards and Technology (NIST) for developing the "CONTAM Results Export Tool" used in this study. The author also thanks Mrs. Bing Liu and Mr. Rahul Athalye at the Pacific Northwest National Laboratories (PNNL) for answering various inquiries regarding energy modeling and DOE reference building models' details. Finally, the author would like to thank Mr. Thierry Lafrance and the MËKANIC team for their work in the fabrication and assembly of the experimental chamber used in this research within a very short time frame.

I would like to thank all the research group members, Dahai Qi and Dr. Wael Fayrouz, who have been of great support and above all great friends. The author would like to specifically thank Dr. Fayrouz for his great guidance in the experimental work of this research.

I want to acknowledge the support of my parents without which I would not have been able to pursue my studies at Concordia. I would also like to thank my beloved Nadra who helped me every single step of the way during my studies. I have to also thank all my family members in Canada and abroad who have helped me, supported me and encouraged me. I also want to thank the fellow researchers and friends who helped me throughout my work in my masters.

CONTRIBUTION OF RESEARCHERS

This study was conducted within a team and was mainly designed and coordinated by Dr. Leon Wang. The research team and their contributions are as follows:

1. **Dahai Qi** contributed mainly in the numerical simulation component of this research:
   It is important to note that the CFD model for the full size door that will be presented in chapter 4 was made available (based on the previous study) by Dr. Wang at the beginning of the research. (Wang, 2013)
   - Modeling, setup, running and data extraction (velocity fields and pressure/flow data) of the CFD simulations (ANSYS FLUENT 14.0) cases for the experimental validation study (presented in chapter 3). **NOTE** the author however contributed in that work by assisting in the modeling and simulation process of the different cases that were used
   - Setup, running and analysis of data for the CFD simulations for the full size door with different air curtains presented in section 4.3.1. **NOTE** The author assisted in the setup, running and data extraction process for more than half of these simulation cases
   - Setup, running and extracting the data of the CFD simulations for the full size door with the door open at 20 m/s and 20° (presented in section 4.3.2). **NOTE** the analysis and correlation of the data (development of the infiltration curves presented in section 4.3.2) was completed by the author.
2. **Dr. Wael Fayrouz:** contributed mainly in the experimental validation study presented in chapter 3 as follows:
   - The design, testing and assembly of the helium filled soap bubble nozzles used in this study (presented in section 3.2.2.2) and in the design process of the experimental chamber (presented in section 3.2.1.1)
   - The acquisition of PIV data presented in chapter 3. **NOTE** The author assisted in all the PIV data acquisition of this study, he also processed (correlation and analysis) the data and completed the presentation work of the data.

All researchers have consented to the inclusion of the work within this academic thesis.

TABLE OF CONTENTS

LIST OF FIGURES

LIST OF TABLES

ABBREVIATIONS & NOMENCLATURE

η_{air}	Efficiency factor for infiltration reduction (air curtain)
A	Area
b_0	Width of the air curtain nozzle (air outlet width)
C	Automatic door coefficient (for specific door size)
C_A	Airflow coefficient (Yuill, 1996)
C_d	Discharge coefficient
$C_{D,\ section}$	Average discharge coefficient for each door operation section
C_{Dave}	Average flow coefficient for a full door operation cycle
CZ	Climate zone
D_d & D_{Dave}	Discharge modifier (air curtains)
D_m	Deflection modulus of air curtain jet
E_{fe}	Air curtain annual total fan energy
E_{saving}	Energy savings
Eu	Euler number
Fr	Froude number
F_u	Air curtain infiltration usage correction factor
H	Door height
η	Efficiency factor for heat transfer reduction (air curtain)
ϕ	Heat flux
P_h	People per hour (door usage)
$P_{savings}$	Energy savings in percent
P_u	Number of people per use (doors)
Q	Volume flow rate
Re	Reynolds number
R_p	Pressure factor (ASHRAE, 2009)
T_h	Usage per hour (doors)
T_u	Time per usage (doors)
u_0	Air curtain discharge speed
UA_c	Total heat loss of the building
U_h	Number of door usages per hour
V_0	Air curtain volume supply rate
α_0	Air curtain discharge angle

$\Delta\emptyset$	Total different in the door openings in °
ΔP_a	Pressure difference across the air curtain door due to the air curtain (Floyd C Hayes, 1968)
ΔP_{lc}	Lower Critical pressure difference
ΔP_{uc}	Upper Critical pressure difference

The following list is alphabetically ordered

AC	Air curtain
Air curtain door	Double swing doors opening out with air curtain unit
AMCA	Air Movement and Control Association Inc. (International)
ASHRAE Method	Energy simulation using the design infiltration rates calculation method
BSRIA	Building Services Research and Information Association
CFD	Computational fluid dynamics
CONTAM-EnergyPlus Method	Energy simulation using airflow simulations for infiltration calculation
Door mid-plane	Vertical plane 30.5 cm away from the left side of the chamber door edge (in the middle of the door opening) - in the experimental chamber
Door side-plane	Vertical plane 8.5 cm away from the left side of the chamber door edge - in the experimental chamber
Fully open door	Door open at 90°
HFSB	Helium Filled Soap Bubbles
LG	Large store (in the strip mall reference building model)
NIST	National Institute of Standard and Technology
NREL	National Renewable Energy Laboratory
PIV	Particle Image Velocimetry
PNNL	Pacific Northwest National Laboratory
RMS	Root mean square values (PIV velocity fields)
Single door	Double swing doors opening out (without vestibule or air curtain) (Yuill, 1996)
Single door, vestibule door and air curtain doors	Three (3) door scenarios (referring to)
SM	Small store (in the strip mall reference building model)
US. DOE (DOE)	United States Department of Energy
Vestibule door	Vestibule with double swing doors opening out (2 set of double swing doors) (Yuill, 1996)

1 INTRODUCTION

1.1 Background

Air infiltration is the uncontrolled inward leakage of outdoor air into buildings through cracks in the building envelope or through large openings such as doors (ASHRAE, 2009). Air leakage, movement of air in or out of buildings, is mainly caused by the pressure difference across the various building enclosure elements. Differences in pressure can be caused by many factors such as wind, stack effect, and/or HVAC system imbalances. (ASHRAE, 2010)

The building sector (residential, institutional and commercial buildings) consumes about 41% of the primary energy use in the USA. In a survey completed in 1998 for office buildings in the US, it was estimated that air infiltration can account on average for 13% of the heating loads (Emmerich & Persily, 1998). In general for different commercial building types, estimates go up to 18% (Wang & Zhong, 2014b; Nicklas Karlsson, 2013). As the construction materials and building methods develop, modern buildings are more tightly built and are better insulated. In newer (modern and well insulated) buildings, a larger portion of the heat losses are contributed to air infiltration. It is calculated that, on average, air infiltration is responsible for about 25% of the modern buildings' heating loads (Emmerich & Persily, 1998). New studies confirm that with the increase of efficiency of equipment and buildings, the energy loss due to air infiltration is becoming more significant - bigger portion of the heat losses are contributed to air infiltration (Ng, Emmerich, & Persily, 2014; Deru, Field, Studer, & Benne, 2011) . With even more tight building envelopes and enclosures, one of the major sources of air infiltration that remain in commercial buildings are entrance doors and the infiltration related to their frequent use (ASHRAE, 2009, 2010).

Many energy codes[A] have opted, based on literature available (Yuill, 1996), to require fitting main entrances of commercial buildings with vestibule doors. More specifically, ASHRAE

[A] Such as the American Society of Heating, Refrigerating and Air-Conditioning Engineers (ASHRAE) Standard 90.1 – Energy Standard for Buildings Except Low-Rise Residential Buildings, as well as International Energy Conservation Code

Standard 90.1 (Addendum 'q' to ASHRAE 90.1 - 2007 vestibule) requires vestibules to be installed in almost all types of building entrances located in climate zones 3 to 8 (ASHRAE, 2007). Vestibules are not the ideal solution for building owners and developers since they are space demanding and costly to construct (especially in tight and valuable real estate, estimates of costs go as high as $60,000) (Wang, 2013). In addition, vestibule doors are only effective in reducing air infiltration if both doors are not open simultaneously: an assumption that is generally not true in high traffic doors of most commercial buildings (Wang & Zhong, 2014b).

Another solution to restrict air infiltration, a method that has been used for more than 50 years, is the use of air curtains. These units, typically made of a fan and casement with a jet outlet, are used to create air barriers at openings in many applications: they have become a standard in cold storages and food cabinets. (Belleghem et al., 2012; Chen, 2009; Johnson, Thomas, Kordecki, & Berner International Corporation, 2008; Alamdari, 1997)

The main concept of an air curtain operation is for the unit, most commonly mounted above the doorway/opening, to supply one (or more) jet(s) of air that are engineered to reach the floor and seal the opening aerodynamically (Costa, Oliveira, & Silva, 2006). Using air curtain doors (single doors equipped with air curtain units) in buildings, as an alternative for vestibule doors, can provide building owners with space and cost savings during construction (the units can cost below $6000) (Wang, 2013). They can also provide users with un-obstructed entrance ways while still sealing the doorway opening. In addition, air curtains can help in blocking outdoor pollutants, respirable dust, insects, and moisture. Manufacturers of the units claim that air curtain doors can reduce the energy losses from doors by 70% (Cremers, 2012; Indac, 2011).

Even though literature on air curtains has been available for a while (details of the literature review on air curtains can be found in section 2.2), it mainly focuses on closed room applications rather than entrance doors which are open and exposed to the exterior. Focusing on entrance doors of buildings subject to different weather and wind conditions, a study conducted by Wang et al. (Wang & Zhong, 2014b, 2014a; Wang, 2013) quantified the impact of air curtain doors on whole building energy usage (details can be found in 2.3). The study concluded that air curtain doors reduced air infiltration and energy losses through doors significantly when compared to vestibule or single doors under the same conditions. However, the study of the air curtain performance was mainly numerical and only dealt with one air curtain unit with and air

discharge of 15 m/s at 20° outwards with no people in the doorway. Moreover, the energy simulations were conducted only for 1 building model in 8 climate zone locations - simulations were conducted using the energy software TRNSYS 17.1 ("TRNSYS," n.d.) for the medium office reference building model (Wang, 2013).

1.2 Methodology, Scope and Objectives

Based on the background (presented in section 1.1 of this chapter) and the research gaps identified in the literature (presented in chapter 2), the general scope of this research is to extend the investigation about the impact of air curtain doors on whole building energy usage in comparison to buildings with vestibule doors and/or single doors (depending on the codes' requirements). The general objectives of this research are:

1. to experimentally validate existing modeling and numerical simulation methods for air curtain doors - previously proposed by Wang et al. and other (Wang & Zhong, 2014a; Wang, 2013; Belleghem et al., 2012),
2. to investigate some of the factors that affect the performance of air curtain doors and
3. to conduct energy simulations to capture the energy savings impact of air curtain doors in more commercial buildings.

Based on the scope and objectives proposed three (3) main tasks are formulated:

Task 1: a laboratory experimental study for the validation of computational fluid dynamics (CFD) and theoretical modeling methods available in literature - namely Wang's study on air curtain doors (Wang & Zhong, 2014a; Wang, 2013),

Task 2: an extended CFD numerical study to investigate the effect of the change in supply angle and speed as well as the effect of people on the performance of air curtain doors, and finally

Task 3: an energy simulation study for two reference building models to calculate the savings realized by air curtain doors in comparison to vestibule doors (where required by code).

Further details about each of the tasks as well as their specific scope and objectives are presented in the subsequent sub-sections.

The general framework of the research is to conduct the validation study for CFD modeling methods of air curtains, use the validated methods to conduct a new and extended numerical

CFD study then to use the results of the CFD study to conduct energy simulations for the buildings 3 doors scenarios (namely: single, vestibule and air curtain doors).

This document is organized using a chapter based structure. In the Chapter 1, the general background of the study is set, general and task specific scopes and objectives are presented and some of the limitations of this study are discussed. An extensive review of literature is presented in Chapter 2, covering the basic physics of airflow through large openings and specifically automatic doors, air curtains and infiltration through doors with air curtains, simulations of commercial reference building energy models, the different methods of modeling air infiltration, vestibule related energy savings as well as large scale velocimetry particularly particle image velocimetry (PIV). The detailed methodologies, results and conclusions of each of tasks of this study are presented in individual chapters. Chapter 3 presents the experimental validation study (Task 1); Chapter 4 presents the numerical CFD simulation study (Task 2); and Chapter 5 presents the energy simulation study (Task 3). Finally, chapter 6 presents the general conclusions of this study and the possible scope of future work.

1.2.1 Task 1: Experimental Study and CFD Validation

The study conducted by Wang (2013) was found to be the most methodologically developed and complete in regards to the performance of air curtain external doors. However, no experimental measurements that could be used to validate the numerical data were found (literature review sections 2.2.3 and 2.3). Most importantly, no general models for scaling or theoretical models were found in literature which required the validation study to focus on the existing methods to model air curtains numerically or theoretically

An experimental setup was designed and constructed at Concordia University building envelope lab to enable the acquisition of experimental data for the air curtain doors to be used in the validation CFD modeling methods. In order to correctly validate the air curtains CFD modeling method, and due to the absences of a general equations for air curtain doors and their performance, a numerical CFD model is created for the test chamber and its surroundings using the similar methods as those proposed by Wang et al. and other researcher (Wang & Zhong, 2014a; Wang, 2013; Belleghem et al., 2012).

1.2.1.1 Scope and Objective

The general scope of this task is to conduct controlled laboratory experiments on a double swing door equipped with air curtain in order to validate the air curtain modeling method proposed by Wang (2013).

The specific objectives of this task are:

- to design an experimental setup that can be used to test air curtain doors under different pressure difference conditions
- to validate the CFD modeling methods proposed by Wang (2013) for an air curtain operating under isothermal conditions:
    - to compare the experimental and numerical infiltration characteristics of air curtain doors, i.e. airflow infiltrations as functions of pressure differences
    - to compare experimental and numerical airflow fields at the doorway using experimental flow visualization techniques for an air curtain operating under isothermal conditions
- to validate the theoretical modeling method of air curtains proposed by Wang (2013)
- to experimentally investigate different factors that can affect the performance of air curtains such as the effect of the supply angle and speed, presence of people in the doorway and external wind

The details of the methodology and the conclusions of this task are presented in Chapter 3 and the details of the literature referenced are presented in Chapter 2.

1.2.2 Task 2: Computational Fluid Dynamics (CFD) Simulations

Previous numerical studies conducted by Wang, regarding the performance of air curtain doors performance, were mainly based on the performance of one air curtain unit with an air discharge of 15 m/s at 20° outwards with no people in the doorway (Wang & Zhong, 2014a; Wang, 2013).

1.2.2.1 Scope and Objective

Following validation of the air curtain modeling method, the main scope of this task is to conduct an extensive CFD numerical study that considers different air curtain units (units with

different discharge angles and speeds) as well as to investigate the effect of the presence of people in the doorway.

The specific objectives of this task are:

- to use the CFD model proposed by Wang et al. (Wang & Zhong, 2014a; Wang, 2013) and presented in the literature review (section 2.3) to investigate the following aspects on the performance of air curtains doors:
    - the effect of supply angle
    - the effect of supply speed
    - the effect of the presence of people in the doorway
- to use the methods proposed by Wang et al. (Wang & Zhong, 2014a; Wang, 2013), which are based on the model developed by Yuill (1996), to generate a new correlated air curtain door performance curve for the air curtain door that provides the best performance (based on the new CFD results)

The details of the methodology and the conclusions of this task are presented in Chapter 4 and the details of the literature referenced are presented in Chapter 2.

1.2.3 Task 3: Annual Whole-Building Energy Simulations

Different sources of literature indicate that DOE commercial reference building models, available as input files for EnergyPlus (US DOE, 2010), are generally used in the development, assessment and researching of new technologies and codes. The study regarding the energy impact of vestibules (Cho, Liu, & Gowri, 2010) simulated ASHRAE 90.1 compliant energy models with EnergyPlus using annual constant infiltration rates for single and vestibule doors following the methods proposed by ASHRAE - and developed by Yuill (ASHRAE, 2009; Yuill, 1996). The results of the study (presented in section 02.4.3.3) showed that the maximum national weighted energy saving was achieved in the strip mall building and the lowest was achieved in the outpatient healthcare building (Cho et al., 2010). Other sources in the literature (section 2.4.2) indicated that using airflow simulation, in software such as CONTAM, might provide a better hourly/sub-hourly estimates for the infiltration rates through building envelopes (Ng et al., 2014).

However, no previous studies used EnergyPlus to model air curtains or air curtain doors. Also no studies have been found that used CONTAM and EnergyPlus for airflow and energy simulations. In addition, no direct coupling methods between the two programs are available.

The Energy and Environment Division of the Engineering Laboratory at NIST were informed of this study and have accelerated the process of development of a specialized tool for exporting zone-specific CONTAM results into data table formats (or EnergyPlus input files) which were used in this study (National Institute of Standards and Technology, 2014). The details of the tool can be found in the NIST Technical note 1873 (Polidoro, Ng, Dols, & Emmerich, 2015). It is important to note that the fulfillment of some of objectives proposed in the following sub-section would not have been possible without the development of this tool.

1.2.3.1 Scope and Objective

Using the correlated results of the CFD simulations (for the best performing air curtain door), the general scope of this task is investigate the annual energy saving impact of using air curtain doors in two commercial reference building models (namely, strip mall building and outpatient healthcare building) in comparison to vestibule doors and single doors (depending on code requirements) in 16 climate zone locations.

The specific objectives of this task are:

- to develop a method for modeling and controlling air curtains in EnergyPlus
- to use EnergyPlus to simulate the two buildings with the design infiltration rates calculation method proposed by ASHRAE (ASHRAE, 2009; Yuill, 1996) (ASHRAE Method) with three door setups (single, vestibule and air curtain doors) and to calculate the national weighted average energy savings of air curtain doors
    - Also, to study the sensitivity of the infiltration rates calculated for the three door setups to the following factors:
        - outdoor temperature
        - door usage frequency
        - air curtain operation temperature control

- to model, and simulate the infiltration through the three door setups in the two buildings using CONTAM using the methods proposed by Wang presented in section 2.4.4.1 (Wang, 2013)
- to use EnergyPlus to simulate the two buildings with three door setups (single, vestibule and air curtain doors) using the infiltration rates exported from CONTAM (National Institute of Standards and Technology, 2014) in order to calculate the national weighted average energy saving of air curtain doors
    - Also, to study the sensitivity of energy consumption in the two building to the following factors:
        - door usage rate
        - building orientation
        - wind pressure coefficients
        - air curtain operation temperature control

The details of the methodology and the conclusions of this task are presented in Chapter 5 and the details of the literature referenced are presented in Chapter 2.

1.2.3.2 Selection of the Simulation Programs and Methods

There are a variety of methods to simulate airflow in buildings. Despite the fact that EnergyPlus (US DOE, 2010) includes airflow network models which can be used for airflow simulations, the ASHRAE 90.1-2013 models (Deru et al., 2011) do not use them. In addition, no previous studies have been found that investigate air infiltration using EnergyPlus' airflow network models. Also, and since one of the main objectives of the study was to simulate the ASHRAE 90.1 models, it had to be ensured that the least amount of changes (changes in the inputs of the models) are to be made to the original models available online. CONTAM ("CONTAM User Manual," n.d.) is a specialized program for the simulation of airflow in buildings. The reference building models are available as airflow network models for CONTAM with published detailed inputs (Ng, Musser, Persily, & Emmerich, 2012). At the start of the research, no co-simulation methods existed between CONTAM and EnergyPlus. Alternatively, the NIST CONTAM result export tool (Polidoro et al., 2015) provided a manual method to export infiltration rates simulated by CONTAM to EnergyPlus.

It was then concluded that using this tool, with manual export of the results from CONTAM to EnergyPlus would ensure:

1. Minimum changes in the ASHRAE 90.1 models
2. Focus on the scope of investigating air infiltration in buildings rather than the development/testing of co-simulation methods
3. Provide a double checking method to review infiltration inputs and models in both software which can help in the validation of the results

1.3 Limitations

The main limitation of this study, as well as previous air curtain studies regarding air infiltration through air curtain doors, is the absences of a general model that can describe the performance of air curtains operating under external pressure conditions (non-sealed room). As a consequence, the conclusions and results obtained and presented this study are only limited to the air curtain units tested and simulated.

Also the experimental results obtained and presented for the effects of supply angle, external wind and presence of the people in the doorway are only exploratory and they are a topic of future research.

This research is one of the first in using the CONTAM/EnergyPlus uncoupled simulation methods; minor differences in the models available and compatible with each of the two programs can lead to possible sources of error (details discussed in section 2.4.1.6). It is also important to note that the energy simulation results obtained are only valid for the two reference building models simulated and that these models are not intended to represent energy use in any real building: they are hypothetical models (Deru et al., 2011). In addition, the methods used to model infiltration in EnergyPlus (US DOE, 2010) neglects the negative infiltration rates (exfiltration) which may lead to errors in the savings estimates presented. Finally, it is important to note that the helium filled soap bubble (HFSB) system (designed and fabricated by the research team) that was used with the large-scale particle image velocimetry, is still undergoing validation.

The research, experiment design, laboratory experiments, simulations as well as the reporting (including the writing of this thesis) were successfully completed within a time frame of 15

months, which is short considering the scope and objectives set and presented in the subsequent sub-sections.

1.4 Overall Objectives and Research Framework

Figure 1 illustrates the overall objectives and the framework of the research by clarifying the relations between the different tasks and their fulfillment of the main goals.

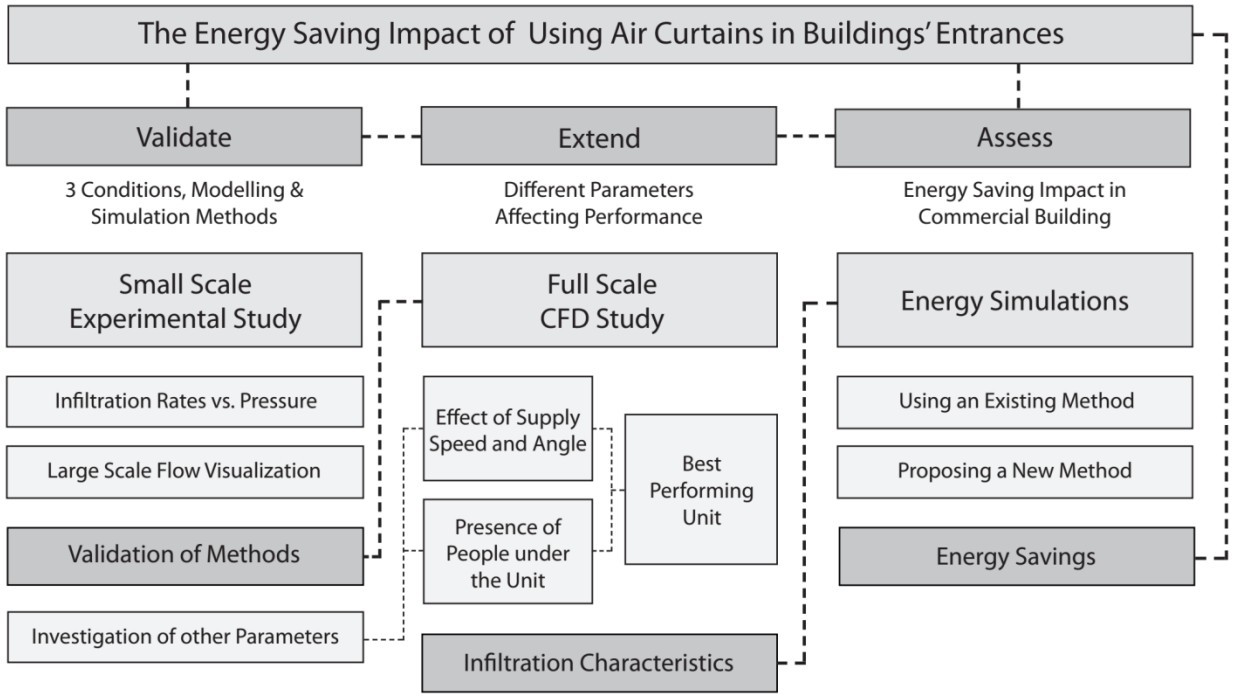

Figure 1. Illustration for the objectives and the overall framework of the research

2 LITERATURE REVIEW

2.1 Air Infiltration through Doors

Understanding airflow through large openings in buildings (exterior and interior openings) is one of the main topics of interest for building engineers. Many research aimed to further understand the complex airflow and air motion through openings: consideration of three-dimensional flow, effect of temperature gradients and the causes of large variations in the discharge coefficients through openings (Van der Mass, 1992). In this section an overview of the basics physics of airflow through openings is presented. In addition, various literature and studies concerning air infiltration through doors in specific are presented and reviewed.

2.1.1 Physics of Airflow through Large Openings

The simplified approach to understanding the flow in large openings is to apply the continuity equation and the Bernoulli theorem on both sides of the openings. This requires assuming a steady flow of incompressible constant density non-viscous fluid that is driven by the pressure differential (Van der Mass, 1992). Considering the hydrostatic pressure at the opening, Equation 1 suggests that the fluid is only at equilibrium when the density and the pressure are constant through all horizontal planes.

Equation 1.

$$p = p_0 - g \int_0^z \rho \, dz$$

Through consideration of Newton's second law of motion and the conservation of mechanical energy along the trajectory of an irrotational flow, Bernoulli's theorem for inviscid flow is obtained with a constant valid for all streamlines in the flow. Additionally the loss of pressure due to internal flow friction when moving through a duct can be added as a pressure drop term.

Equation 2.

$$p_2 - p_1 + \rho \frac{1}{2} ({u_2}^2 - {u_2}^2) + \rho g(z_2 - z_1) + \Delta p_f = 0$$

Even though most fluid flow is turbulent, they can be generally described using the perfect fluid theories (Van der Mass, 1992). In fact, many factors determine the flow's conditions which are usually described in non-dimensional numbers:

- Froude number: used to compare the inertial and buoyancy terms where the larger the ratio, the smaller the effect of gravity on the flow.

  Equation 3.

$$Fr = \frac{u}{\sqrt{gL}}$$

  Where u is a typical velocity and L is a typical length.

- Reynolds number: used to compare the inertial forces to viscous forces where the higher the Reynolds number the higher the pressure losses (more turbulent flow regime) and less it is dependent on the viscosity of the fluid. Where for Re smaller than 2000 the flow in considered laminar and for larger than 4000 it is considered turbulent (and the range in between is a transitional flow) (Landau & Lifshitz, 1987).

  Equation 4.

$$Re = \frac{\rho u L}{\mu}$$

  Where ρ is density,
  u is the flow velocity,
  L is a typical length, and
  μ is the dynamic viscosity.

  It is important to note that large openings in buildings usually have small "duct lengths" which can result in small Reynolds numbers (Van der Mass, 1992).

- Euler number: used to provide a measure of the importance of other factors other than the pressure gradient in the flow pattern.

  Equation 5.

$$Eu = \frac{u}{\sqrt{2\frac{\Delta p}{\rho}}}$$

  Where ρ is density,
  u is the flow velocity, and
  ΔP is the pressure difference.

It is important to note that large openings in buildings usually have small "duct lengths" which can result in small Reynolds numbers (Van der Mass, 1992).

The most important aspects when dealing with building openings is the size of the opening itself. The sizes of the opening and the boundary conditions have major effects in determining the flow that can go through it at any pressure difference. The discharge coefficient, C_d, is used to compute the discharge through the orifice. (Van der Mass, 1992)

It is the ratio between the flow through an opening, and the theoretical flow through an opening of the same area that faces no resistance.

Equation 6.

$$C_d = \frac{Q}{A \times \sqrt{\frac{2\Delta P}{\rho}}}$$

Or the better known orifice equation

Equation 7.

$$Q = C_d \times A \times \sqrt{\frac{2\Delta P}{\rho}}$$

In many studies that consider flow through large building openings, especially when dealing with isothermal cases of flow, the discharge coefficient is used to describe the flow through the opening under different pressure conditions (Mahajan, Cho, Shanley, & Kang, 2015; Yuill, Upham, & Hui, 2000; Yuill, 1996).

2.1.2 Air Infiltration in Buildings and Infiltration Related Energy Loads

Air infiltration/leakage is defined by the U.S. Department of energy as the uncontrolled or unintentional movement of air through the building envelope through cracks or openings. Many studies have aimed to quantify the effect of air infiltration on buildings' energy consumption. In a survey completed in 1998 for office buildings in the U.S., it was estimated that air infiltration can account for up to 13% of the heating loads (Emmerich & Persily, 1998). In newer and tighter more insulated construction, it is calculated that, on average, air infiltration is, on average, responsible for about 25% of the building heating loads (with cases where infiltration was

responsible for up to 42% of the heating loads) (Emmerich & Persily, 1998). Newer studies confirm that infiltration is still an ongoing problem in buildings and that with the increase of efficiency of equipment and buildings, the energy loss due to air infiltration is becoming more significant (Ng et al., 2014; Deru et al., 2011). The significant role air infiltration plays in deterring the energy consumption of buildings has led many standards and codes to include limits on the allowed air infiltration in buildings. These limits aim to minimize the energy loss and to minimize the other harmful effect air movement through the envelope might cause in buildings. With even more tight building envelopes and enclosures, the major sources of air infiltration that remain in building are generally exterior openings (doorways) (ASHRAE, 2010).

Large efforts have been made by enforcing regulations to minimize the infiltration through large openings in building and energy codes. This includes addendum 'q' to ASHRAE 90.1 - 2007 which requires the addition of vestibules (double entrance doors) in building entrances situated in climate zones 3 to 8 to minimize the air infiltration from main doors (ASHRAE, 2010). The infiltration reductions of such design interventions are discussed thoroughly in subsequent sections.

The most basic method for calculating heat transfer through openings is presented in the IEA's Annex 20 of the air flow patterns within buildings report (Van der Mass, 1992). It explains that if constant temperature and pressure differences exist between two zones (Zone 1 & Zone 2); the net heat flow (in watts) is simply equal to the product of the mass flow, temperature and heat capacity.

Equation 8.

$$\Phi = C_p \left(M_{1-2} \times T_1 - M_{2-1} \times T_2\right)$$

In a PhD thesis submitted in 1992 at Texas A&M University, Liu indicates another common equation that is used to quantify the heat loss factor due to air infiltration (Liu, 1992)

Equation 9.

$$UA_C = UA_0 + \dot{M} C_p$$

Where UA_c is the total heat loss of the building,

UA_0 is the heat loss of the building with no infiltration (in W/°C),

$\dot{M}$ is the mass flow rate (in Kg/s), and

C_p is the heat capacity of the air (J/Kg°C).

In fact, the PhD dissertation published in 1992 indicates that even though Equation 9. is widely used for quick calculations of HVAC and loads in buildings, it ignores a lot of the real life condition of the heat flow. In addition, the interaction between the air flow and the heat transfer is ignored (Liu, 1992)

With the development of modern modeling and advanced numerical calculation tools, the effect of the air infiltration on building energy performance and HVAC equipment loads is better measured and quantified (based on building specific models and location specific weather) (Ng et al., 2014). New methods which have been developed to better measure the infiltration through building envelopes are discussed in subsequent sections.

2.1.3 Air Infiltration through Single and Vestibule Entrance Automatic Doors

Air infiltration through entrance doors of real buildings is a complex topic of research (Cho et al., 2010). It is common for researchers to assume the entrance doors of commercial buildings (small scale commercial buildings in specific) to be automatic doors (Yuill et al., 2000; Yuill, 1996). This assumption allows for certain simplifications that can avoid the difficulties that could result from considering manual door opening patterns (difficulties in quantifying the door opening area, opening time and time of use that are mainly based on independent users' patterns) (Cho et al., 2010). However, one of the limitation/drawbacks of assuming the doors to be automatic is that, automatic doors, generally, stay open longer than manually operated doors which can result in over-estimations of the air infiltration rates (Cho et al., 2010; Yuill, 1996). Currently, simplified methods for estimating air infiltration through these automatic doors are available in literature and are constantly used in calculating the air flow through entrance doors of buildings (Cho et al., 2010; ASHRAE, 2009; Yuill, 1996).

2.1.3.1 Calculating Infiltration Rates for Door Full Operation Cycles

One of the most extensive studies available for the estimation of air flow through automatic doors was conducted by Professor Grenville K. Yuill in 1996 within the ASHRAE Research Project 763-TRP. This study used laboratory scaled experiments to calculate the discharge coefficient of 15 different entrance door configurations (mainly for single and vestibule doors) as well as field study to record the door operation characteristics for the doors. In addition, Yuill

used a scaled down doll (dummy) to determine the effect of door users on the flow rates. (Yuill, 1996)

Some aspects of Yuill's study that are focused on double swing single doors are presented in more details in following sub-sections (as some of the methodology and models in his study were used in this research).

2.1.3.1.1 Yuill's laboratory experimental for measuring air infiltration through doors

The apparatus used in the experiments conducted by Yuill at Pennsylvania State University was described as a 2.44 m × 2.44 m × 1.3 m (W × L × H) air tight box with a door opening of 0.61 m × 0.71 m (W × H) that represented a double swing door (a door with two leaves). The chamber was a one third (1/3) scaled down model of a real building. Across from the door, a bower-door (fan) was placed which draws air out to create a negative pressure condition and to draw air into the 'building'. A multi-configuration attachment was created for the chamber to represent and be used as the entrance vestibules. Figure 2 shows the drawings of the described chamber. (Yuill, 1996)

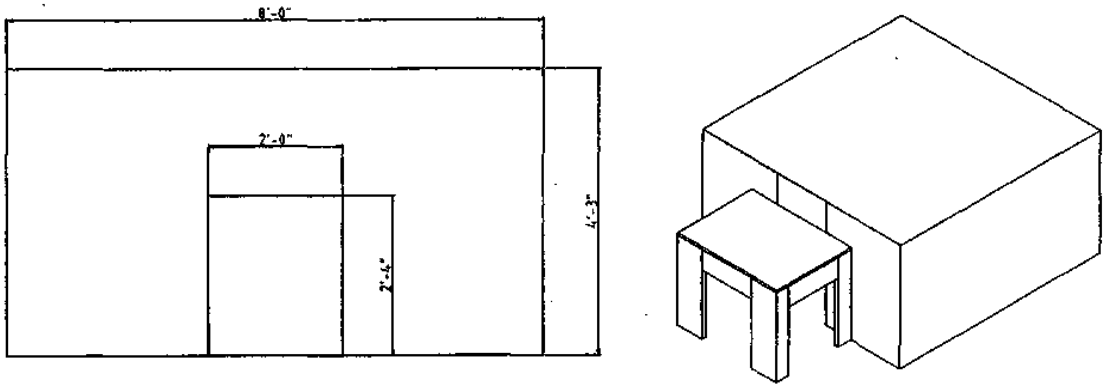

Figure 2. View of the experimental chamber used in Yuill's study - dimensions in inches (Yuill, 1996)

For the different entry configurations, the difference in pressure across the door (or through each door in the vestibule cases) was measured along with the corresponding airflow (measured at the blower door) (Yuill, 1996). These measurements allowed for the discharge coefficient (C_D) to be calculated using Equation 6 for each door opening angle, $C_{D,angle}$. The discharge coefficients were calculated for different door opening conditions; however, for the single door, $C_{D,\ angle}$ was calculated with the angle of the doors (door leaves) at 30°, 60° and 90°. The door operation cycle

was then simplified to 4 distinct sections: the opening of the door (from 0° to 90°) - *a* , the fully open time of the door (90°) - *b*, the closing of the door (90° to 10°)- *c* and *d* - is the gap when the door slows down before its full closure (from 10° to 0°). (Yuill, 1996)

An averaged C_D was calculated based on the openness range observed at each section based on the experimentally calculated $C_{D,\ angle}$. Finally, using a time-weighted average, the overall average discharge coefficient for a full opening cycle, C_{Dave}, was calculated. Figure 3, taken form literature (Wang & Zhong, 2014a), visually presents the discussed concepts.

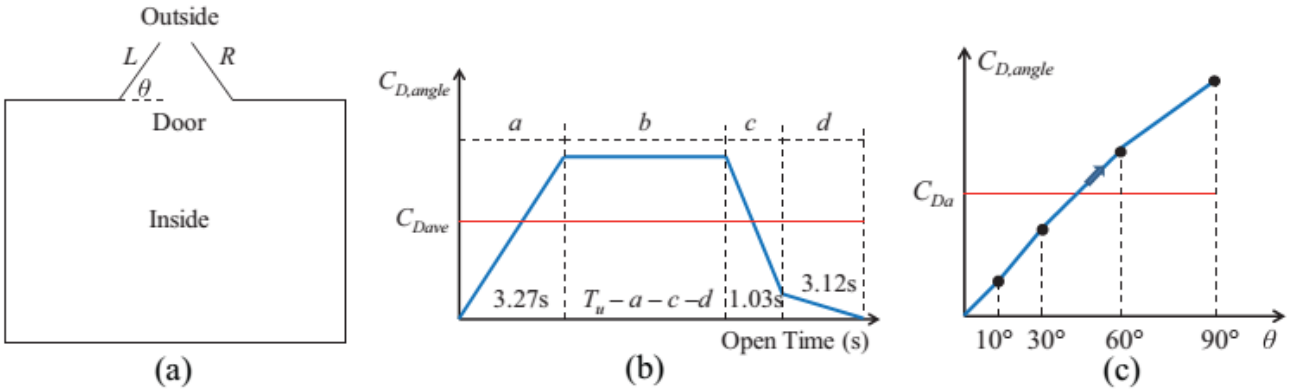

Figure 3. Door operation and C_D schematics (a) double swing single door, (b) C_D of different door operation status and (c) calculation of the average C_D for section *a* of the door operation (Wang & Zhong, 2014a)

Equation 10 and Equation 11 show the calculations for the overall average C_D of an operation cycle and the calculation of the $C_{D,\ section}$ at each of the door operation sections. (Yuill, 1996)

Equation 10.

$$C_{Dave} = \frac{C_{D\,a}a + C_{D\,b}b + C_{D\,c}c + C_{D\,d}d}{a + b + c + d}$$

Where C_{Dave} is the overall average discharge coefficient,

$C_{D,\ section\ (a,b,c,d)}$ is the average discharge coefficient for each door operation section, and

a, b, c & d are the time period (in seconds) for each door operation section (from field observations)

Equation 11.

$$C_{D,section} = \frac{1}{\Delta\emptyset} \int_{\emptyset 1}^{\emptyset 2} C_{D,angle}\, d\theta$$

Where $C_{D,\ section\ (a,b,c,d)}$ is the average discharge coefficient for each door operation section, $C_{D,angle}$ is the experimentally calculated discharge coefficient at a certain door opening angle,
$\emptyset 1$ & $\emptyset 2$ are the angle limits in ° (range of door openness) at each door operation sections and,
$\Delta\emptyset$ is the total difference in the door openings in ° ($\Delta\emptyset = \emptyset 1 - \emptyset 2$).

It is important to note that the time period of each of the door states were obtained from the field observations conducted, which are be presented in section 2.1.3.1.2.

2.1.3.1.2 Results of Yuill's field study

The results of the field study conducted by Yuill's were used to determine the relationship between the number of people using the door each hour and the air flow coefficients of the door. (Yuill et al., 2000; Yuill, 1996)

The results of this observation study were the calculated time periods for the different door operation sections as well as various mathematical relationships and terminology that became a standard in this field of research until today (Mahajan et al., 2015; Wang & Zhong, 2014a; Nicklas Karlsson, 2013; Cho et al., 2010)

For automatic single double swinging doors, and as explained in section 2.1.3.1.1, four distinct operation sections were found: (Yuill et al., 2000; Yuill, 1996)

1. Base open time: is the full time needed for the door to be fully opened (from the fully closed position) and then to return to its fully closed position when no people are using it (was found to be 11.71 s)
2. Opening time: is the time the doors takes to be opened (fully open from the fully closed position) (Section a)
3. Fully open time: is the time the doors remain open for people to pass through (Section b)
4. Closing time: is the time it takes the door to fully close after they were fully open (Section c & d - 4.15s)

a. Slow close time: within the closing time, the doors slow down just before it is fully closed and move in slower speed (Section d)

The calculated operation time for each section were found to be as follows (Yuill et al., 2000; Yuill, 1996):

- (Time) a = 3.27s
- (Time) b = depends on the number of people using the door (s)
- (Time) c = 1.03 s (4.15s - Section d)
- (Time) d = 3.12 s

For the door operation section b, Equation 12 to Equation 16 are used to determine its duration:

Equation 12.

$$b = T_u - (a + c + d)$$

Equation 13.

$$T_u = \frac{T_h}{U_h}$$

Equation 14.

$$T_h = 1 - e^{-0.002233 P_h}$$

Equation 15.

$$U_u = \frac{P_h}{P_u}$$

Equation 16.

$$P_u = 0.0098\, P_h + 1.7541$$

Where T_u is the total door usage time (h),

T_h is the door usage per hour (h/h),

U_h is number of door usages per hour (usage/h),

P_h is the number of people passing through the door per hour (people/h), and

P_u is the number of people passing through the door every usage (people/usage).

Equation 17 is then used to calculate the total infiltration rate through a door based on its door usage time, its area, pressure difference across it and its discharge coefficient.

Equation 17.

$$Q = C_{Dave}\, A\, T_h \sqrt{\frac{2\Delta P}{\rho}}$$

2.1.3.1.3 Conclusion of Yuill's study

The final outcomes of the Yuill's study, and its follow up literature (ASHRAE, 2009; Yuill et al., 2000; Yuill, 1996), are a series of simplified equations and figures were developed that can be used by designers to estimate of the infiltration through entrance doors of buildings.

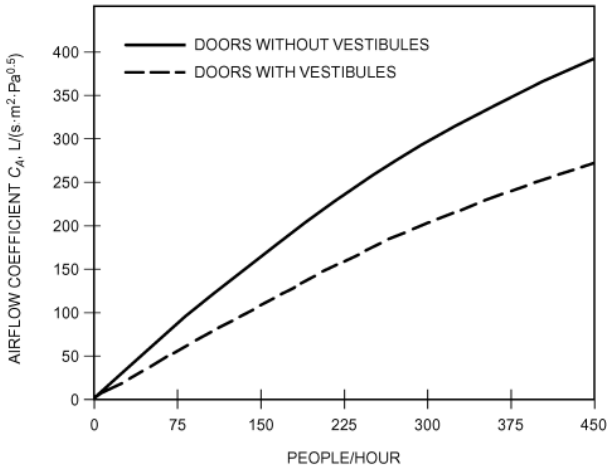

Figure 4. Airflow coefficients for automatic doors (ASHRAE, 2009; Yuill et al., 2000)

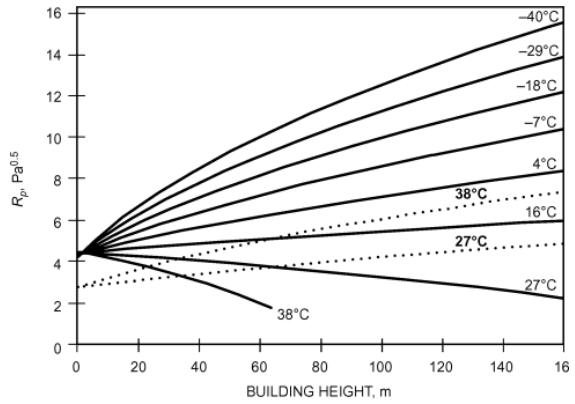

Figure 5. Pressure factor for automatic doors (ASHRAE, 2009; Yuill et al., 2000)

Equation 18.

$$Q = C_A\ A\ \ R_p$$

Where C_A is the overall air coefficient for the door (single door or vestibule door),
A is the full door size (m^2), and
R_p is the pressure factor obtained from Figure 4 and Figure 5 ($Pa^{0.5}$).

It is important to note that R_p is a calculated factor for the pressure $\sqrt{\Delta P}$ (where $\Delta P = P_{out} - P_{in}$) based on the assumption of steady winds of 6.7 m/s (15 mph), that does not consi &der the effect of terrain and that assumes uniformly distributed openings (neutral pressure plane location at the middle of the building height) in the calculation of stack effect and for the draft coefficient in the building to be 0.9 (Mahajan et al., 2015; Cho et al., 2010; Yuill, 1996). It is important to note that it is common for designers or researchers to use one set temperature to calculated an average (or design) infiltration rate through the door for all year; usually based on 16 °C (60 °F) (Cho et al., 2010).

2.1.3.2 Development on the Yuill Model

Other studies have focused on developing the model proposed by Yuill (1996) in order to better incorporate some of the aspects overlooked by the use of the pressure factor R_p. One study uses the equations and concepts proposed by ASHRAE (2009) for calculating the infiltration based on the actual wind pressure and stack pressure of building. The study proposes and tests an analytical process (shown in Figure 6), with the aid of simulation programs, for better estimations of the pressure across entrance doors. (Mahajan et al., 2015)

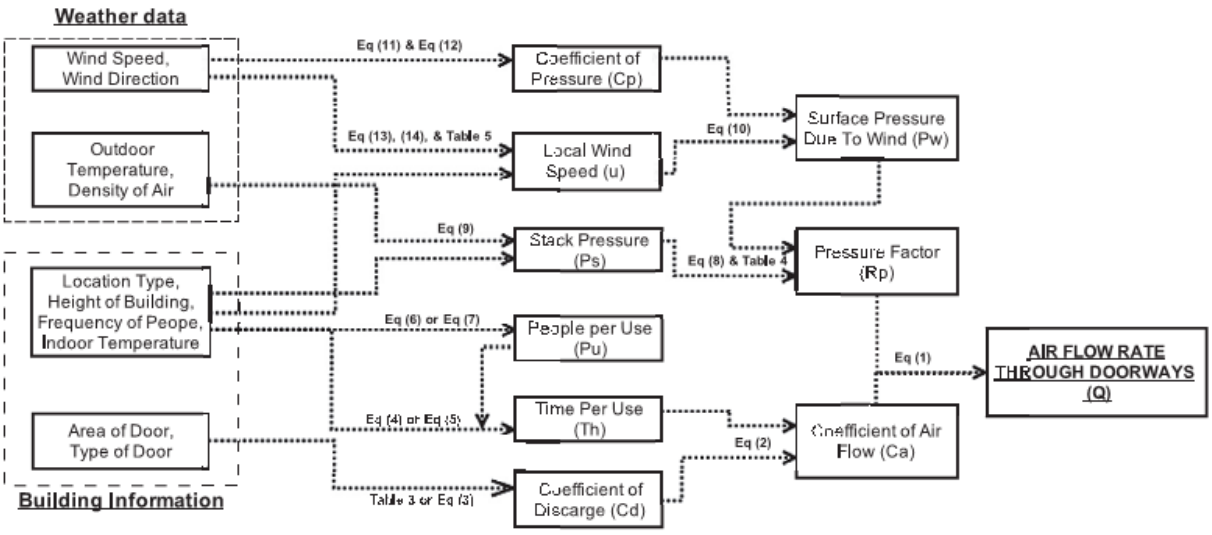

Figure 6. Process proposed by Mahajan et al. for calculating airflow rate through doorways (Mahajan et al., 2015)

It is important to note that the proposed model's results were only reported for daily calculations and that incorporating such iterative process in yearly energy simulations might result in complications. The study also reported that the proposed model is not applicable for all door configurations and specifically doors with air curtains (Mahajan et al., 2015). Other more recent studies (Ng et al., 2014; Wang, 2013) suggested using airflow simulations, which consider climate, wind and stack effect, to have more realistic hourly or sub-hourly estimates of the air infiltration through openings (more about these methods are discussed in section 2.4.2.2).

Yuill's study was used and implemented in many simulation and calculation based studies that consider air infiltration through entrance doors. The model and equations proposed for the calculation of infiltration and coefficient was also used in many studies later dealing with different door types such as doors with air curtains and revolving doors. (Goubran, Qi, & Wang, 2015; Mahajan et al., 2015; Qi, Goubran, Zmeureanu, & Wang, 2015; Wang & Zhong, 2014a; Nicklas Karlsson, 2013; Wang, 2013; Verhaeghe & Belleghem, 2010)

2.2 Air Curtains

Air curtains are defined by the American Society of Heating, Refrigeration and Air-conditioning Engineers as "*a continuous broad stream of air circulated across a doorway of a conditioned space. It reduces penetration of insects and unconditioned air into a conditioned space by*

forcing an air stream over the entire entrance. The air stream layer moves with a velocity and angle such that any air that tries to penetrate the curtain is entrained" (ASHRAE, 2007). Many studies dealing with various aspects of air curtains have been conducted. The main focus of these studies were generally to understand the characteristics (flow characteristics) of air curtains under different operation conditions, to quantify the effectiveness of air curtain in sealing spaces (minimize penetration of air into spaces), to calculate the heat loss through openings (doors in specific) equipped with air curtains, and to understand the factors that affect the performance of the units. It is important to note that no general models are available in the literature to estimate or calculate the performance of air curtains (general/universal models that describe of all or any air curtain unit).

2.2.1 Characteristics of Air Curtains

One of the earliest studies conducted for air curtains was that completed by Hayes as his PhD thesis at the University of Illinois in 1968. In his study, Hayes investigated and developed theoretical models that describe the airflow and jet of vertically blowing air curtains for isothermal and non-isothermal cases using the setup shown in Figure 7. (Floyd C Hayes, 1968)

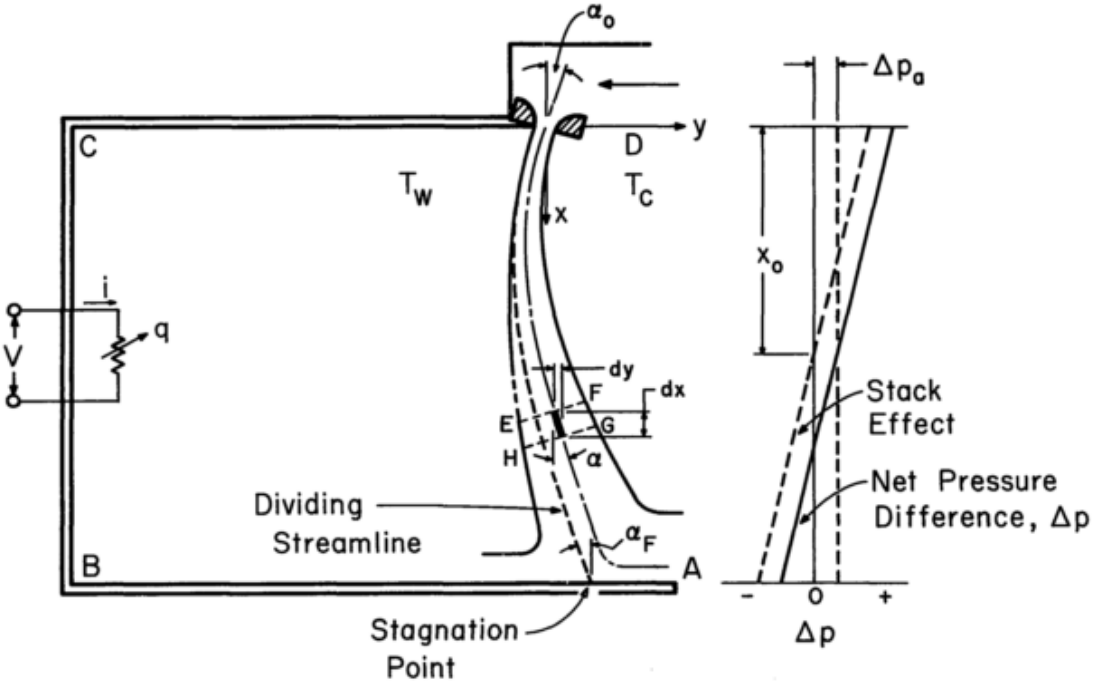

Figure 7. Schematic of the setup used in Haye's study (Floyd C Hayes, 1968)

A key concept that Hayes described in his thesis is the general operation condition of air curtain placed at the doorway of a closed room (as seen in Figure 7). For an air curtain that primarily takes air from outside of the enclosure and supplies air vertically downward ($\alpha_0 = 0°$), the air stream is first divided equally across the door. This equal division results in the spilling of more air into the room than that which is entrained by the jet. As the pressure builds up in the room, the jet begins to curve (as shown in Figure 7) and the angle of impingement is balanced so that the amount of air entrained from the room is equal to the amount of air spilled into the room (steady-state equilibrium). Hayes defines this specific angle at equilibrium as α_F and the pressure across the doorway at equilibrium as ΔP_a. ΔP_a is the pressure difference across a specific door (with a certain height and width) generated only by the existence of the air curtain flow which is supplied at a specific angle and speed. It is important to note that, the study assumed that the air curtain stream (jet) width is exactly the size of the door opening with a perfectly uniform flow condition. (Floyd C Hayes, 1968)

Hayes derived the basic equations using non-dimensional terms that can describe the flow of the air curtain based on the momentum conservation in the isothermal case. The equation combines the conditions of the air as well as the properties of the door and air curtain. No indication on the significance of the non-dimensional term of Equation 19 is indicated in literature. (F.C. Hayes & Stoecker, 1969; Floyd C Hayes, 1968)

Equation 19.

$$\frac{\Delta P_a}{\rho u_o^2} = \frac{b_0}{H}\left[2.4\sqrt{\frac{b_0}{H}\left(1 - 2.56\,\frac{b_0}{H}\right)} - \sin\alpha_0\right]$$

Where ΔP_a is the pressure difference across the door ($\Delta P_a = P_{out} - P_{in}$),
b_0 is the width of the air curtain nozzle (air outlet width - m),
H is the door height (m),
α_0 is the discharge angle (supply angle) of the air curtain unit,
u_0 is the discharge speed, and
ρ is the air density.

It is clearly stated that this equation is used to describe the operation of the air curtain under the assumption that the jet reaches the floor. No calculations were made for the isothermal case with

any pressure difference other than ΔP_a acting on the door. (F. C. Hayes & Stoecker, 1969; F.C. Hayes & Stoecker, 1969; Floyd C Hayes, 1968)

Hayes also developed a model that can incorporate and consider the effect of the temperature difference across the door (creating stack effect). Based on the setup proposed in Figure 7, it is considered that the "breakthrough" condition (where the air curtain jet no longer reaches the floor), occurs only at the upper portion of the flow. This assumption is supported by some calculations that show that, when the jet passes the point of 0 pressure without breaking, it remains unbroken (this is only try for the air curtain units taking air from outside the closed room). It is also noted that the pressure across the door for the non-isothermal case only differs from the isothermal case's ΔP_a if the neutral pressure plane position is changed (moved upwards or downwards depending on the temperature conditions). Hayes again derives equations that describe the minimum (limiting value - to ensure the jet reaches the floor) of the outlet momentum $(\rho_c\, b_0\, u_0^2)_{\,min}$ within a non dimensional expression. The study shows that when the outlet momentum is below $(\rho_c\, b_0\, u_0^2)_{\,min}$ the air jet is broken and that if it greater than $(\rho_c\, b_0\, u_0^2)_{\,min}$ the jet remains unbroken until it reaches the floor.

Equation 20.

$$\frac{(\rho_c\, b_0\, u_0^2)_{\,min}}{g\, H^2(\rho_c\, -\, \rho_c\,)} = \frac{1}{8(1-\sin\alpha_0)}$$

ρ_c is the air density at the cold side of the door,

ρ_w is the air density at the warm side of the door, and

g is the gravitational constant.

The literature also clarified that the left side of Equation 20 (a non-dimensional group) is named the deflection modulus of the jet. D_m, which is shown in Equation 21, is indicative of the deflection of the air curtain jet. The nominator of the D_m is the outlet momentum and the denominator indicated the transverse forces created by the difference in temperatures across the door: The higher the value of D_m the lower the deflection in the jet. (Floyd C Hayes, 1968)

Equation 21.

$$D_m = \frac{(\rho_c\, b_0\, u_0^2)_{\,min}}{g\, H^2(\rho_c\, -\, \rho_c\,)}$$

The proposed equations were validated using laboratory experiments, further details on the experimental setup and the results of the validation can be found in the original sources (F.C. Hayes & Stoecker, 1969; Floyd C Hayes, 1968). Other studies have indicated that, in cases where the temperature difference across the air curtain door is high, the $D_{m,\ min}$ might not be sufficient to predict a stable air curtain jet (Belleghem et al., 2012).

In a subsequent paper to his thesis, Hayes and Stoecker indicate that for the case where the air curtain is installed inside a room and takes air from inside the closed room, the jet's flow is usually concave inwards as seen in Figure 8 (the jet hits the floor in a position closer to the enclosure). (F. C. Hayes & Stoecker, 1969)

It is important to note however, that in all the analysis conducted in the studies presented (and in the development of the deflection modulus), only the stack pressure through the opening and the pressure created by the air curtain unit are considered (no extra or added pressure difference across the door is considered - pressure that can be generated due to wind or height of the building).

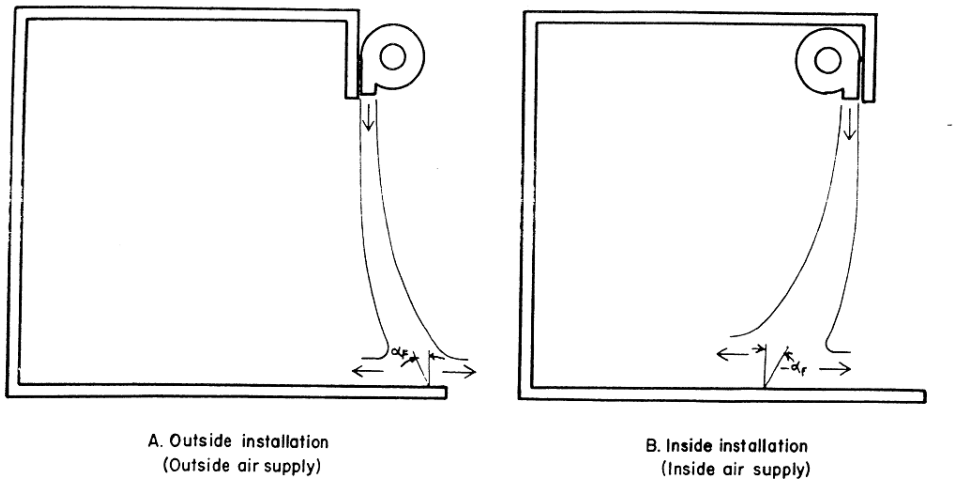

Figure 8. Jet deflection for the inside and outside installed air curtains (F. C. Hayes & Stoecker, 1969)

Based on the extensive studies conducted by Hayes, the most important parameters in designing air curtain are the discharge angle, the air curtain supply width b_0 and the supply speed u. It is indicated that the air curtain is less likely to break (experience a breakthrough condition where

the jet does not reach the floor) if the jet is directed toward the warm side when the air curtain is placed outside of an enclosure. (F. C. Hayes & Stoecker, 1969)

However, it can be argued that, based on the understanding of the models proposed, the air jet should be directed opposite the supply position (i.e. if the supply is from outside, it is better to direct the jet toward the inside and if the supply is from inside it is better to direct the flow towards the outside). Research presents various methods to quantify the effectiveness of the air curtain units in sealing of entrance doors. The most commonly used is the efficiency factor, η_{air} (Belleghem et al., 2012; F.C. Hayes & Stoecker, 1969).

Equation 22.

$$\eta_{\text{air}} = 1 - \frac{Q}{Q_{open}}$$

Where η_{air} is the efficiency factor of the air curtain in reducing the infiltration through the door,
Q is the infiltration volume flow rate through the door with the air curtain used, and
Q_{open} is the infiltration through the door with no air curtain.

The higher the value of η_{air} the better the unit performs. It is important to note that η_{air} is calculated for the air curtain at one set operation condition (at specific discharge and pressure different condition). Another commonly used measurement is the sealing effectiveness which is based on the ratio between the air flow through an opening and with the opening fitted with an air curtain (E_Q, as the air curtain completely blocks the airflow $E_Q \rightarrow \infty$.
It is proposed the a $D_{m,\,min} = 1$ should be respected to achieve the needed performance with a good safety factor against weather and usage conditions (Costa et al., 2006)

2.2.2 Heat Transfer through Air Curtain Doors

Hayes and Stoecker also proposed a simplified calculation method for the for the sensible heat transfer through doors equipped with air curtains (F. C. Hayes & Stoecker, 1969).

Equation 23.

$$q = h''\, W\, H\, (T_W - T_c)$$

Where q is the heat transfer rate (W),
h" is the heat transfer coefficient ($W/m^2.°C$),
H & W are the door height and width (m), and

T is the absolute temperature difference across the door.

The heat transfer coefficient was presented in figures for a doorway of height 7" (2.1 meters) and temperature conditions of 75 °F & -10 °F. Both heated and cooled building conditions are presented as curves for different supply outlet widths and different supply speeds. In addition, the corrections for other door heights and temperatures are given and are used as factors. The same figures are used to denote the minimum outlet velocity required (based on the calculated minimum outlet momentum) to maintain an unbroken jet at the condition stated for the different supply outlet widths and different supply speeds. (F. C. Hayes & Stoecker, 1969)
This model was then developed further by considering the latent and sensible heat transfer through the opening. This was achieved by relating the heat transfer to the mass transfer through the door opening. (Pappas & Tassou, 2003)

Using the method and models proposed by Hayes and Stoecker, many research and studies were conducted aiming to calculate the heat transfer (energy losses) through doorways fitted with air curtains (Pappas & Tassou, 2003; Sirén, 2003b; Alamdari, 1997). Another factor for measuring the efficiency of the air curtains in reducing heat transfer through openings was then proposed, η (ASHRAE, 2007).

Equation 24.

$$\eta = 1 - \frac{q}{q_{open}}$$

Where q is the heat transfer rate calculated based on Equation 23.

The efficiency factor, η of air curtain in most cases was reported to reach up to 0.7 (ASHRAE, 2006) and can be below 0 (an air curtain that is not set up or sized properly can increase air infiltration, thus increasing the heat flow through the door) (Belleghem et al., 2012). It is important to note that η is calculated for the air curtain at one set operation condition (specific discharge and specific pressure and temperature difference conditions).

Some studies suggest that an air curtain working at D_m close to or greater than the $D_{m,\,min}$ can provide energy savings up to 80% (Costa et al., 2006). Other studies reported efficiencies up to 0.79 for inclined supply (towards cooled room) and 0.72 for air curtain units supplying air downwards. The study by Pappas & Tassou suggested that using a thicker jet (a wider air supply

outlet) and inclining the supply towards the colder zone can increase the efficiency of the air curtain. It is also indicated that, in a lot of cases, using heated air curtain (air curtain supplying heated air) can reduce the efficiency of the unit. It was also suggested that the optimized operation for summer condition differ from the operation configuration of the unit in winter. (Pappas & Tassou, 2003)

Some studies aimed to capture the energy savings of air curtain through modeling/simulating theatrical air curtains (based on efficiency factors and heat transfer formulas presented). The results show that, fitting air curtains in commercial buildings can reduce energy consumption and that the payback period for the units can be as low as two seasons (Lawton & Howell, 1995). Only the recent the study by Wang et al. was found to numerically investigate the building heating and cooling energy savings achieved by fitting air curtains in building entrances which experience transient conditions (Wang & Zhong, 2014a; Wang, 2013).

2.2.3 Studies on Real Life Air Curtains Applications

A number of experimental studies were conducted to measure the effectiveness of air curtains in sealing entrance ways. The most important of which was based on the numerical models developed by Verhaeghe and Belleghem, a setup of an air curtain unit that is sealing a cooled room (closed refrigerated room) was used (Belleghem et al., 2012; Verhaeghe & Belleghem, 2010).

The study used thermo-graphic measurements across the door to compare them with the isotherms obtained from the CFD simulations. The comparison was successful and resulted in the validation of the numerical model used. Foster et al. (Foster, Swain, Barrett, D'Agaro, & James, 2006) suggested in their experimental and numerical study that air curtains can be significantly effected by 3-dimensional effects (edge of door effect and supply profile). The numerical model used by Belleghem et al., ensured that the air curtain unit exceeded the size of the opening to avoid such complications (Verhaeghe & Belleghem, 2010; Foster et al., 2006). The numerical model used the k-ε turbulence model. The Boussinesq and Sutherland approximations are applied while solving using the 2^{nd} order upwind scheme and the SIMPLE algorithm was utilized for the pressure-velocity coupling (Belleghem et al., 2012; Verhaeghe & Belleghem, 2010). The most significant finding in their experimental/numerical study was the presentation of the sealing efficiency factor of the air curtain with varying supply speeds (seen in

Figure 9). The results suggest a discontinuity and sudden improvement of the performance of the air curtain once the jet reaches the floor. (Belleghem et al., 2012)

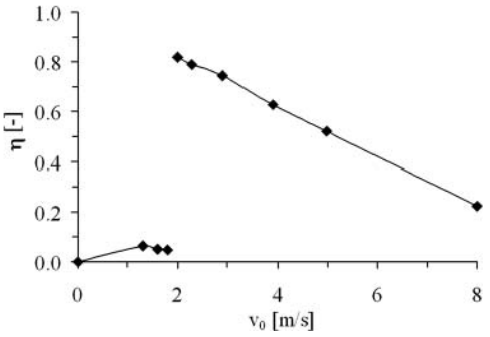

Figure 9. Sealing effectiveness as a function of air curtain speed (Verhaeghe & Belleghem, 2010)

It is important to note that, the study used a uniform average supply velocity assumption calculated based on 10 measurements across the air curtain nozzle. However, it was highlighted that the supply velocity differed significantly across the air curtain outlet and that, when studying 3D phenomena of the supply, these variations might have to be considered. (Belleghem et al., 2012)

Some sources of literature are available in the form of reports developed by manufacturers. These reports are mainly based on numerical simulations conducted following similar methods as Belleghem et al. and Foster et al. (Cremers, 2012; Howell, 2008; Johnson et al., 2008)

Chen investigated the effect of air supply angle, in cold refrigerators, on the amount air entrained through the jet. A quadratic relationship was found: for a given air supply speed and conditions an optimum supply angle for the air curtain exists (Chen, 2009)

Many of the literature available, even though some of which are experimental, are not presented in this review since they deal with special air curtain application in sealing cold cabinets and refrigeration display units or with air curtains that supply air upwards or sideways. (Indac, 2011; Chen, 2009; Jaramillo, Oliva, Perez-Segarra, & Oliet, 2008; Sirén, 2003b, 2003a; Alamdari, 1997).

2.2.4 Sizing and Design Data for Air Curtains

Many design and application guides are available for air curtains' operation, configuration and design. The most useful of them is the application guide developed by BSRIA. The report uses 3D CFD simulations, and a compilation of the reviewed studies, to provide a step by step process

for selecting and setting up (discharge angle and speed setup) air curtains in buildings. (Alamdari, 1997)

Perhaps the most important aspect about this guide is that it proposed a method for offsetting the effect of air leakage (air movement) into buildings by increasing the supply speed of the air curtain.

Equation 25.

$$V_0 \geq 1.2 \frac{V_0(t_w - t_c)}{(t_0 - t_w)}$$

Where V_0 is air curtain supply air volume flow rate,

V_i is the incoming (outdoor) air flow rate,

t_w is the warm temperature, t_c is the cold temperature, and

t_0 is the supply temperature of the air curtain.

2.2.5 Testing Methods and Standards

A number of technical testing methods and standards pertaining to air curtains were reviewed. The most important of which are those published by the AMCA. In the AMCA publication 222-08, the main definitions as well as the different designs and variations of air curtains are overviewed. In addition, some of the aspects affecting performance are discussed and presented (Air Movement and Control Association International, 2012a). The AMCA standard 220-05 presents the main laboratory tests needed to calculate the performance variables of the air curtain units (i.e. uniformity, average speeds, core speeds and air flow rates) (Air Movement and Control Association International, 2012b). The review of these standards was crucial for the selection and understanding of air curtain products' data sheets.

2.3 Infiltration through Entrance Doors Equipped with Air Curtains

All the studies presented in the preceding sections, even if dealing with infiltration through entrance doors, have considered a steady-state condition for the door (usually with the doors considered to be fully open) to evaluate the performance of the air curtains. In the study by Wang and Zhong (Wang & Zhong, 2014b, 2014a), the methods proposed by Yuill (1996) in regards to the door opening cycle, were extended to include the analysis single double swing doors equipped with air curtains. (Wang & Zhong, 2014a; Wang, 2013)

In the study, a full numerical (CFD) study was conducted using ANSYS Fluent 14.0 (ANSYS, 2011) for a 20 m × 24 m × 10 m (L×W×H) building within a full domain of 50 m × 24 m × 10 m (L×W×H). A double swing automatic door was modeled at the center of the building's width to be 2 m × 2.4 m (W×H). The door opening angles were considered from 10° to 90° (fully open). The air curtain was modeled following the methods similar to those proposed by Belleghem et al (2012) with a supply slot of 0.08 m × 2 m (b_0 = 0.08 m), an indoor air intake, and an air supply of 15 m/s at 20° outwards. The door was then simulated with different pressure conditions that were set at the boundaries of the CFD model (pressure inlet and outlet), the stack effect was considered by setting different indoor and outdoor temperatures. In addition, the door opening angles were varied (presented in Figure 10 and Table 1). The actual pressure difference across the door (in order to consider the effect of temperature) was calculated at the mid-section of the model (as seen in Figure 10). The CFD cases assumed steady-state flow and uniform supply velocity based on the standard k − ε model.

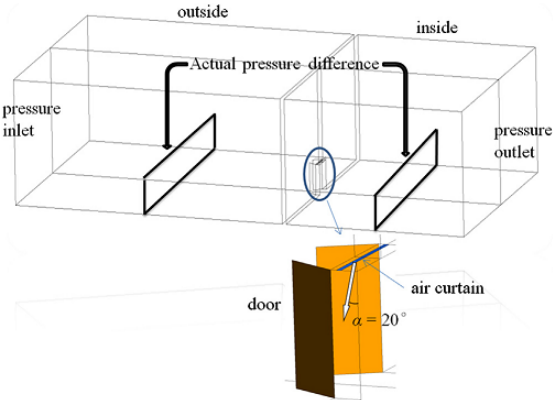

Building	Size	20 m × 24 m × 10 m ($L \times W \times H$)
	Indoor temperature	24 °C for the summer and 21 °C for the winter
Door	Door size	2 m × 2.4 m ($W \times H$)
	Door open/closing angles	10°, 30°, 60°, 90° (fully open)
Air Curtain	Supply velocity/temperature	21 °C for the winter and 24 °C for the summer at 15 m/s with an angle of 20° outwards
	Supply slot size	0.08 m × 2 m ($W \times L$)
	Return slot size	0.2 m × 2 m ($W \times L$)
CFD	Domain size	50 m × 24 m × 10 m ($L \times W \times H$)
	Total grid number per case	1,260,000
	Transient/steady simulation	Steady state
	Turbulence model	Standard $k-\varepsilon$
	Boundary conditions	The prescribed outdoor and indoor pressure difference (pressure inlet and outlet) of 40, 30, 20, 10, 0, −0.5, −1, −1.5, −2.5, −3.5, −5, −10, −20 Pa
	Outdoor temperature	−40 °C, −20 °C and 10 °C for the winter and 25 °C, 30 °C and 40 °C for the summer

Figure 10. CFD setup and model of the building used in Wang's study (Wang & Zhong, 2014a)

It is important to note however that the air curtain in Wang's study was modeled as a perfectly uniform jet (i.e. it was assumed that the air curtain is supplying air at a perfectly uniform speed and angle throughout the width of the door) (Wang, 2013). As seen in Table 1, more than 330 simulations were conducted in order to develop the air curtain infiltration characteristics curves with pressure differences across the door ranging from -30 Pa to 50 Pa.

Table 1.CFD scenarios used in Wang's study (Wang & Zhong, 2014a)

Categories	Winter mode	Summer mode
Door opening angle (°)	10, 30, 45, 60, 90	
Outdoor temperature (°C)	−40, −20, 10	25, 30, 40
Indoor temperature (°C)	21	24
Pressure difference (Pa)	−20, −10, −5, −3.5, −2.5, −1.5, −1, −0.5, 0, 10, 20, 30, 40	
Air curtain velocity (m/s)	15	
Air curtain temperature (°C)	21	24
Total CFD runs	336	

The results of the simulation corresponded and extended the concepts proposed by Hayes' study (Floyd C Hayes, 1968) as it identified 3 main operational conditions (seen in Figure 11)

- Optimum condition; where the air curtain flow reaches the flow and seals the door
- Inflow breakthrough: where the air curtain flow is curved inward and does not reach the floor
- Outflow breakthrough: where the air curtain flow is curved outwards and does not reach the floor

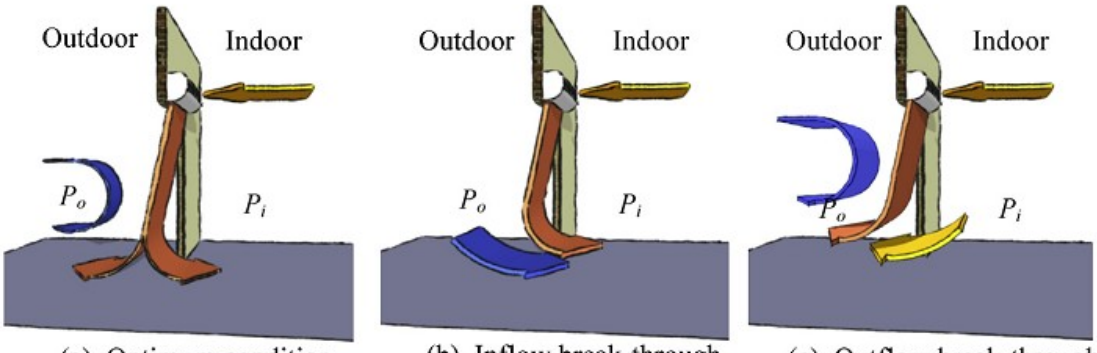

Figure 11. The three operation conditions of air curtains (Wang & Zhong, 2014a)

The results indicated that there exist two critical pressure differences across the door: the upper critical pressure, ΔP_{uc}, at which the air curtain operates at the inflow breakthrough condition, and the lower critical pressure, ΔP_{lc}, after which the air curtain operates in the outflow breakthrough condition. It is important to also note that the study uses the net air flow through the door and that when the pressure difference across the door is 0 Pa, the net air flow is not zero (due to the air curtain jet air that escapes through the door with the outwards supply angle). (Wang, 2013)

Wang developed a model, similar to that proposed by Yuill (1996), by adding to orifice equation a discharge modifier, $D_{d,\ angle}$ ($Pa^{0.5}$). This indicated that, for air curtain doors, the airflow is determined by both the pressure difference and the air curtain jet. Equation 26, which is primarily based on to Yuill's method and model, was developed and used in the study to calculate the infiltration rates through the air curtain door. (Wang, 2013)

Equation 26.

$$Q = (-1)^i\ C_{Dave}\ \ A\ T_h \sqrt{\frac{2|\Delta P_{oi}|}{\rho}} +\ D_{Dave}\ T_h \sqrt{\frac{2}{\rho}}$$

Where

$$D_{Dave} = \frac{D_{D\ a} a + D_{D\ b} b + D_{D\ c} c + D_{D\ d} d}{a + b + c + d}$$

And i = 0 when $\Delta P_{oi} \geq 0$ and i=1 when $\Delta P_{oi} < 0$. Or in shorter term:

$$Q = (-1)^i C \sqrt{|\Delta P_{oi}|} +\ D$$

The correlation and calculation of the coefficients at each door opening angle was completed using Equation 27:

Equation 27.

$$\frac{Q_{angle}}{A\sqrt{\frac{2}{\rho}}} = (-1)^i\ C_{D,angle} \sqrt{|\Delta P_{oi}|} +\ D_{D,angle}$$

Based on the correlations presented in Equation 26, the air infiltration through the air curtain door was calculated for the various door usages and the results were compared to the theoretical curves of developed by Yuill (1996). It was found that the air curtain door modeled can significantly reduce the air infiltration through the door when compared to the single doors and

vestibule doors even when the air curtain is operating in a breakthrough condition (beyond the upper and lower critical pressures). Figure 12 shows the correlation completed for the 3 air curtain operation conditions for the door opening angle 90°. Figure 13 shows the infiltration characteristics of air curtain with an air supply of 15 m/s and 20° outwards (Wang, 2013).

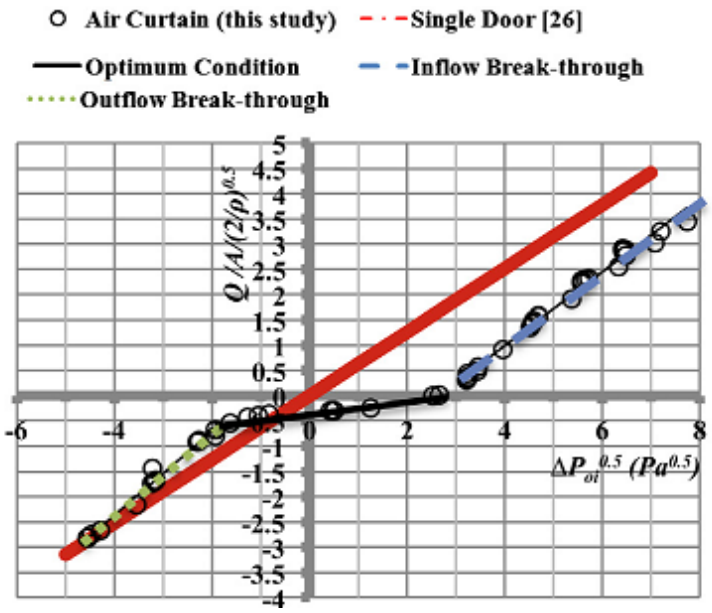

Figure 12. Correlation of air curtain door infiltration at door opening angle 90° (Wang & Zhong, 2014a)

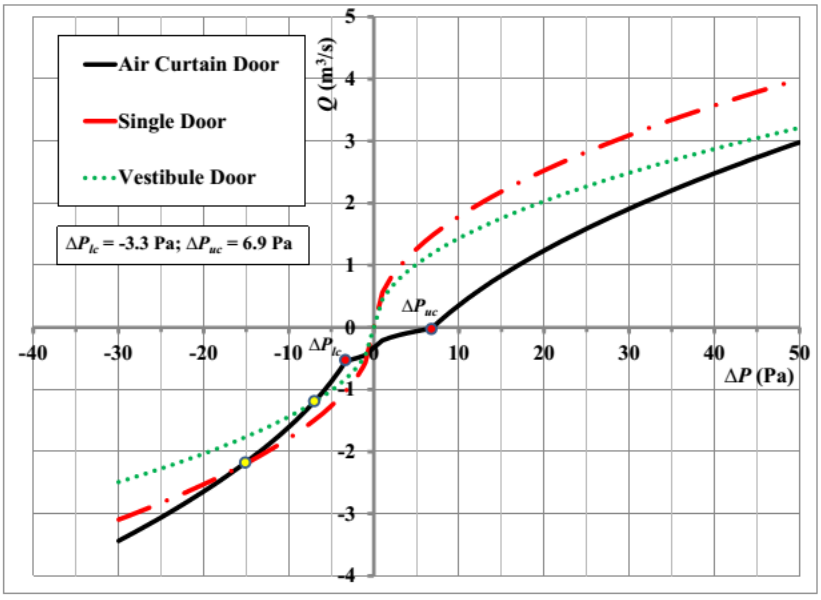

Figure 13. Infiltration and exfiltration characteristics of air curtain door in comparison to single and vestibule doors at 100 P_h door usage (supply 15 m/s at 20° outwards) (Wang, 2013)

Perhaps one of the most interesting findings of Wang et al.'s study (Wang & Zhong, 2014a) is that, even under inflow breakthrough conditions, air curtains can still outperform the single and vestibule doors with high pressure differences across the door. Also, in the outflow breakthrough conditions, air curtains might cause excessive infiltration when compared to vestibule and single doors. It is very important to note that the simulations and methods developed were based on a non-heated air curtain model (air curtain with no heating element) and assuming no convective heat transfer from the air curtain to the air or surrounding.

Wang proposed that, by using the airflow simulation software CONTAM ("CONTAM User Manual," n.d.), the infiltration characteristics of the air curtain can be input and the infiltration rates based on weather files can be calculated for specific buildings in specific locations. It was also concluded that the infiltration rates through the air curtain door has direct and constant relationship with the door usage frequency throughout all pressure ranges. A correction factor (named F_u in this thesis) was then used to express the ratio of the air infiltration through the air curtain door at any given door usage to that at 100 P_h seen in Figure 13 (Wang, 2013).

2.4 Commercial Reference Buildings and Energy Simulations

In order to achieve the objectives of this research (in section 1.2), a literature review was conducted in regards to the two commercial reference building models that are used in this research (namely the strip mall and outpatient healthcare building). In addition, literature dealing with the model's inputs, development, enhancements and configurations was reviewed in order to inform the methodology of this research. Finally, literature regarding the methods for modeling infiltration and the various simulation analyses was reviewed. This review is presented in the subsequent sections.

2.4.1 U.S. DOE Commercial Reference Building Energy Models of the National Building Stock

The reference building models of the national building stock were developed by a number of national laboratories (namely PNNL and NREL) in collaboration with the U.S. DOE. According to the NREL, the national building models were developed to represent the existing and new buildings. They are used in the development, assessment and researching of new technologies and codes (DOE and PNNL use these reference models for the development of new ASHRAE Standard 90.1 Versions). It is important to note that these models are not intended to represent

energy use in any real building but rather they are hypothetical models. More than 768 models (for 16 building types in 16 climate zone locations) were developed and are available as EnergyPlus input files. (Deru et al., 2011)

2.4.1.1 Energy Models for DOE Reference Buildings

Many versions and variations of the DOE reference building models are available (available to download online), namely new construction models and models for old existing construction types. However, the model that are most readily used and referred to in simulation studies are the ANSI/ASHRAE/IES Standard 90.1 Prototype Building Models (Zhang, Athalye, Hart, Rosenberg, & Xie, 2013; B Thornton et al., 2011; BA Thornton, Wang, Huang, Lane, & Liu, 2010; Cho et al., 2010; Gowri, Winiarski, & Jarnagin, 2009; Jiang, Gowri, Lane, Thornton, & Liu, 2009). These energy reference building models, derived from the DOE reference models, are updated constantly to match the ASHRAE 90.1 evolving standards (models available for to comply with 2004, 2007, 2010 and 2013 standards) and are location specific. (Jiang et al., 2009; "Commercial Prototype Building Models | Building Energy Codes Program," n.d.)

The latest updated models are the ASHRAE 90.1 - 2013 compliant versions, the technical details and the documentations of these models can be found online through the DOE's website page ("Commercial Prototype Building Models | Building Energy Codes Program," n.d.). It is important to note that the models, if used only with EnergyPlus (US DOE, 2010), are considered non-directional (Deru et al., 2011)

2.4.1.1.1 EnergyPlus energy simulation software

EnergyPlus (US DOE, 2010) is software developed and funded by the U.S. Department of Energy Building Technologies Office and is used to conduct whole building energy simulations ("Building Technologies Office: EnergyPlus Energy Simulation Software," n.d.). The software is a collection of many modules that work in synchronization to calculate energy loads. EnergyPlus uses building models that are based on the fundamentals of heat balance principles and, as opposed to other building energy simulation software, it solves the building, system and plant components simultaneously. The engineering details and technical reference of the program are outside the scope of this research and are not reviewed. It is important to note that significant changes have been made in the software through updates and that the DOE recommends the use

of the most current versions. Further data is available in the technical documentations of the software. (US DOE, 2010)

2.4.1.2 Energy Models General Details and Description

Based on the models' description and scoreboard data sheets available for the models, general details were gathered for the two models of interest and are presented in Table 2. Further details on the inputs and setup of these models can be found in the relevant sources (Deru et al., 2011; US DOE, 2010). As seen in Table 2, , the entrance zone (zones directly affected by the air infiltration through the doors) in the strip mall building is 100% of the building area while in the outpatient healthcare building the entrance zone represents a very small area in relation to the building size (0.18%). This, intern, could reflect on the relative building savings that can be achieved by door infiltration reduction.

Table 2. DOE reference building models' general details

	Strip Mall Building	Outpatient Healthcare Building
Height - ft (m)	17 (5.19)	30 (9.15)
Gross Floor area - ft^2 (m^2)	22500 (2070)	40950 (3767.4)
Footprint area - ft^2 (m2)	22500 (2070)	13650 (1255.8)
Entrance zone - ft^2(m^2)	LG-3750/ LS-1875 (345/172)	1096 (1008.3)
Number of Doors (where infiltration is calculated)	10	1
Door Opening zone area - ft^2(m^2)	2×3750 + 8×1875 = 22500 (2070)	72 (6.6)
Door Opening zone area in relation to gross floor area (%)*	100%	0.18%

**The details of the entrance zones and the infiltration zone were determined with the help from Dr. Bing Liu and Mr. Athalye from PNNL.*

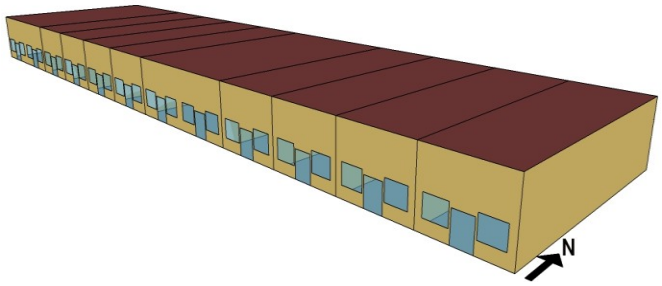

Figure 14. Retail strip mall building prototype view (Deru et al., 2011)

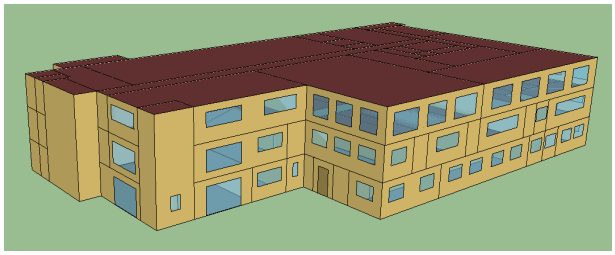

Figure 15. Outpatient healthcare building prototype view (Deru et al., 2011)

2.4.1.3 Models Development and Enhancement

PNNL and other national laboratories (in collaboration with the U.S. DOE) continuously review and update the building models posted online. Furthermore, PNNL regularly publishes and documents the enhancements and developments done to the prototype building through technical reports. ("Commercial Prototype Building Models | Building Energy Codes Program," n.d.).

It is important to note that, according to some of PNNL's documentation, using a different model version (namely 2004 compliant models in comparison to the 2010 complaint models) can lead to changes in energy consumption of more than ±30% in the strip mall building and more than ± 35% in the outpatient healthcare building. Also, some single enhancements or changes applied in the models (for each single version of the models, i.e. only 2004 or 2010 compliant models) were shown to change energy consumptions by more than ±6% in the strip mall building and more than ±5% in the outpatient healthcare building. (Goel, Rosenberg, Athalye, & Xie, 2014; Jiang et al., 2009)

With this indicated, it important to note that the absence of previously published models (previous versions) can lead to difficulties in comparative studies: any previously published energy studies might have used model versions that are no longer available or that have been modified/enhanced. Thus this requires every new/current study to simulate its own base cases for comparisons.

2.4.1.4 Weather Data and Representative Cities

According to literature reviewed that discusses and compares different weather data (Crawley, 1998) and according to the proposed weather files by the U.S. DOE and the NREL (Deru et al.,

2011), the TMY3 weather files (updated versions available online through the NREL website) data was selected to be used in this research with their latest updates. It is important to note that some research and simulation studies published by PNNL, including the vestibule study (Cho et al., 2010), used subsequent versions of these weather files (namely TMY2 files). PNNL indicated that the change in the weather files used for the simulations can lead to difference in simulation results (Jiang et al., 2009; Crawley, 1998). According to Crawly, the TMY weather data series are based on improved solar models and correctly match the long term average climatic conditions (Crawley, 1998).

The NREL proposed representative cities the climate zones and sub-zones of the U.S.A and they are shown in Table 3.

Table 3. Representative cities of the US climate zones and sub-zones (Deru et al., 2011)

Climate Zone	Representative City
1A	Miami, Florida
2A	Houston, Texas
2B	Phoenix, Arizona
3A	Atlanta, Georgia
3B-CA	Los Angeles, California
3B-other	Las Vegas, Nevada
3C	San Francisco, California
4A	Baltimore, Maryland
4B	Albuquerque, New Mexico
4C	Seattle, Washington
5A	Chicago, Illinois
5B	Denver, Colorado
6A	Minneapolis, Minnesota
6B	Helena, Montana
7	Duluth, Minnesota
8	Fairbanks, Alaska

Modifications in the represented cities for the climate zone and sub-zones are presented and are based on official published PNNL and DOE reports

Based on PNNL publications and other studies on the commercial reference building models (Cho et al., 2010; Jiang et al., 2009), the appropriate representative city for CZ-3A was found to be Memphis, Tennessee; the one for CZ-3B was found to be El-Paso, Texas; the one for CZ-4C was found to be Salem, Oregon; the one, for CZ-5B was found to be Boise, Idaho; and the one for CZ-6A it was found to be Helena, Montana. Additionally, CZ-5C is not represented by any

city in the US and therefore Vancouver, British Colombia (Canada) was found to be the representative city for this climate sub-zone.

2.4.1.5 National Weighted Average

Based on reports published by NREL, PNNL and U.S. DOE regarding the commercial reference building models of the national building stock, the national weighing factors (based on the construction volume weights for all building prototypes) were found and reviewed. (Deru et al., 2011; Jarnagin & Bandyopadhyay, 2010; Jiang et al., 2009)

For the strip mall and the outpatient healthcare building reference building models, the national weighting factors (in percentage) for the U.S.A. for each location are shown in Table 4.

Table 4. National weighting factors for the strip mall and the outpatient healthcare reference buildings (Jarnagin & Bandyopadhyay, 2010)

Climate Zone		Strip Mall Building	Outpatient Healthcare Building
1A	Miami	2.45%	0.78%
2A	Houston	17.51%	12.01%
2B	Phoenix	4.55%	2.84%
3A	Memphis	18.04%	12.31%
3B	El-Paso	11.03%	5.83%
3C	San Francisco	1.75%	1.29%
4A	Baltimore	17.69%	17.33%
4B	Albuquerque	0.35%	0.49%
4C	Salem	1.93%	3.83%
5A	Chicago	18.04%	22.42%
5B	Boise	3.50%	4.62%
5C	Vancouver*	-	-
6A	Burlington	2.63%	7.25%
6B	Helena	0.35%	0.70%
7	Duluth	0.18%	8.26%
8	Fairbanks	0.00%	0.04%

**Vancouver is a Canadian city and does not represent building of the US (it is not included in the national weighted average calculation method used in this research)*

2.4.1.6 Airflow Models for DOE Reference Buildings

Based on the 16 EnergyPlus models developed by DOE for the reference buildings, NIST developed models for the multizone and contaminant transport program CONTAM. The main reason for their development is to overcome some of the limitation imposed by the constant infiltration rates input in the energy models (Ng et al., 2012). An airflow simulation study was conducted for a number of the models developed and it was concluded that the EnergyPlus constant infiltration rates are not realistic as they do not reflect the impact of weather conditions on the outdoor infiltration rates. Moreover, the EnergyPlus models were found to neglect the interior airflow within the buildings (Deru et al., 2011). It is important to note however, that all the building inputs were based on published reference and standards, that leakages were modeled based on effective leakage area (for all walls, floors and roofs it is 5.27 cm^2/m^2 of leakage) and that consideration for the stack effect in the buildings were made in models. More specific details and inputs of the models can be found in the relevant technical reports. All HVAC systems are modeled in CONTAM with 90% balance for each zone as opposed to neutral balance inputs of EnergyPlus. In addition, all interior zones are considered to have a constant temperature of 20 ºC as opposed to the scheduled temperature inputs of EnergyPlus. However, a number of modifications to the interior zoning of the buildings were made in order "*to more realistically account for airflow*". These modifications in zone/geometries might result in difficulties for using the simulated airflow data in EnergyPlus. (Ng et al., 2012)

2.4.1.6.1 CONTAM airflow simulation software

CONTAM is airflow and contaminant dispersal simulation software developed by NIST. The software assumes all zones are well-mixed and uniform in temperature and assumes only 1-D convection/diffusion. The program mainly uses the principle of mass balance to solve for the mass flow between defined zones. The version used in this research is CONTAM 3.1 (technical documentations are available online) and it allows for the use of weather files to simulate yearly infiltration conditions at different time steps. ("CONTAM User Manual," n.d.)

2.4.1.6.2 HVAC models for the strip mall and outpatient healthcare buildings

Based on (Ng et al., 2012) the Strip Mall Building's New Construction CONTAM model has (where large stores are named LS 1 & 2 and small stores are named SS 1 to 8):

- 10 packaged constant volume single-zone systems
- the HVAC supply rates are presented in Table 5
- exhaust fans are modeled in CONTAM with flow rate 0.03 m^3/s
- all HVAC and exhaust fans operate on the following schedule:
    - Weekdays: on from 6:00 a.m. to 9:00 p.m., off otherwise
    - Saturday: on from 6:00 a.m. to 10:00 p.m., off otherwise
    - Sunday, holidays: on from 8:00 a.m. to 7:00 p.m., off otherwise
    - Outside air is supplied according to this schedule as well

Table 5. Summary of HVAC system flow rates in Strip Mall Building (Ng et al., 2012)

Zone	Supply (m^3/s)	Return (m^3/s)	Outside air (m^3/s)
LS 1	1.38	1.22	0.52
LS 2	1.02	0.89	0.52
SS 1	0.65	0.56	0.26
SS 2	0.59	0.51	0.26
SS 3	0.59	0.51	0.26
SS 4	0.58	0.50	0.26
SS 5	0.53	0.45	0.26
SS 6	0.53	0.45	0.26
SS 7	0.53	0.45	0.26
SS 8	0.60	0.52	0.26

Based on (Ng et al., 2012) the Outpatient Healthcare Building New Construction CONTAM model has:

- 2 Variable air Volume Air Handling Units, one for the 1st floor and the second for the 2nd and 3rd floors - in CONTAM they are modeled as constant volume systems (as opposed to EnergyPlus where their supply volume is variable)
- for the Lobby zone (where the entrance door is located), it is served by AHU 1 with a supply of 0.53 m^3/s with 0.09 m^3/s of outdoor air and the return is 0.47 m^3/s
- all HVAC and exhaust fans operate on the following schedule
    - for AHU 1 (1st floor):
        - Weekdays: 4:00 a.m. to 9:00 p.m., off otherwise
        - Saturdays: 4:00 a.m. to 9:00 p.m., off otherwise
        - Sundays and holidays: off all day
    - For AHU 2 (2nd and 3rd floor):

- Weekdays: 6:00 a.m. to 6:00 p.m., off otherwise
- Saturdays: 6:00 a.m. to 6:00 p.m., off otherwise
- Sundays and holidays: off all day

2.4.2 Calculating Air Infiltration Rates through Doors in Reference Buildings

Literature was reviewed in order to understand the different methods for calculating air infiltration through the entrance doors of the commercial reference building models. Two methods were distinctly found and are discussed in subsequent sections. (Stein & Kung, 2012; Cho et al., 2010)

2.4.2.1 Constant Infiltration Rate (ASHRAE Method)

This infiltration rate calculation method directly uses the models developed by Yuill (ASHRAE, 2009; Yuill, 1996) to calculate the constant design infiltration rates (that are usually input as constant rates in energy models) (Cho et al., 2010). It is important to note that no actual changes in the geometry of the building are made with the change of the door configuration; instead, only the infiltration rate inputs are just changed depending on the door configuration. This method of calculation for infiltration and input in EnergyPlus is widely used for conducting annual energy simulations. In addition, this method is used to calculate the standard inputs of the reference models available (Deru et al., 2011). Other references, such as those presented in section 2.1.3.2, suggest using more specific calculation methods that are based on the climate and wind conditions in the locations where the buildings are simulated (Stein & Kung, 2012). However, no energy simulation studies were found that utilize to calculation for annual energy simulations, which might be due to difficulty in calculating infiltration rates for sub-hourly time steps over a full year period. Other studies tested the effect of vestibule zone that are modeled separately in the energy models (Mahajan et al., 2015). However, no specific conclusions were drawn on the effect of the simplification made in the published DOE building ("Commercial Prototype Building Models | Building Energy Codes Program," n.d.).

2.4.2.2 Airflow Simulation Method (CONTAM)

Based on the development of the reference building airflow multi-zone models by NIST (Ng et al., 2012), some studies suggest using these simulation tools in calculating air infiltration through entrance doors as well as for all of the building model. Since the airflow models use weather data

to calculate transient air infiltration (through openings and leakages) at each time step simulated. It is concluded that this method can provide more accurate estimations for air infiltration due to their consideration of the outdoor weather, internal zone airflow and stack effect in the buildings. Some suggestions are made on how the simulated air infiltration rates can be used in energy simulation using EnergyPlus. However, no studies have utilized coupled or uncoupled CONTAM-EnergyPlus simulations. (Ng et al., 2014)

The study conducted by Wang et al. (Wang & Zhong, 2014b, 2014a; Wang, 2013), which aimed to assess the energy savings realized by the use of air curtain doors (in comparison to vestibule doors), utilized the CONTAM airflow reference building model to calculate yearly air infiltration. Wang used a coupled CONTAM-TRNSYS model to calculate the yearly energy savings in heating and cooling generated by the air infiltration reductions (achieved from the use of the air curtain) in the medium office reference building model in 8 climate zones (Wang, 2013). This study is further reviewed in the subsequent sections.

2.4.3 Vestibule Door Energy Savings

The main source of literature regarding energy savings from the use of vestibule doors is provided by the PNNL report (report -20026) published in 2010 (Cho et al., 2010). PNNL used the ASHRAE Method of infiltration calculation using the models developed by Yuill (ASHRAE, 2009; Yuill, 1996) presented in section 2.1.3.1.3. In their report, 2 cases of 12 of the commercial reference buildings were simulated and compared (end use site-energy consumption) in the 16 climate zone locations presented in Table 4: one with calculated air infiltration for single doors and the other with vestibule doors. The study used TMY2 weather data files, PNNL ASHRAE 90.1 reference building energy models and EnergyPlus V-3.1. (Cho et al., 2010)

A study on the sensitivity of the infiltration rates calculated to the outdoor temperature and peak door usage frequency was conducted for the quick service restaurant. The sensitivity for the energy consumption to the variation of the infiltration rates for the same building in Baltimore was conducted. The sensitivity study showed a maximum variation of 0.7% in energy consumption with an increase of 20% in the infiltration rates. (Cho et al., 2010)

Further details on this study, including the technical data and the standards, used are provided in subsequent sections as they are used to inform the methodology of this research.

2.4.3.1 Vestibule Door Requirements by ASHRAE 90.1

The assessment of energy savings resulting from the use of vestibule doors was conducted based on the vestibule requirements indicated by addendum 'q' to ASHRAE 90.1 - 2007.

Table 6 presents these requirements for the 2 reference buildings of interest. The national weighted average savings realized from the use of vestibule doors was calculated based on factors presented in Table 4 (while assuming that savings in the zones that do not required to have vestibule are 0%). (Cho et al., 2010)

Table 6. Addendum 'q' to ASHRAE 90.1 - 2007 vestibule requirement for prototypes (ASHRAE, 2007)

Climate Zone	Strip Mall Building	Outpatient Healthcare Building
Zone 1	No (h)	No (h)
Zone 2	No (h)	No (h)
Zone 3	Yes	Yes
Zone 4	Yes	Yes
Zone 5	Yes	Yes
Zone 6	Yes	Yes
Zone 7	Yes	Yes
Zone 8	Yes	Yes

(h) Building entrances with revolving doors.

2.4.3.2 Door Usage

Cho et al. used some of the data of the field study conducted by Yuill (1996) in calculating the door usage rates of the buildings. Some assumptions were made for any missing information and other studies were also used to create the operation and intensity of use schedules of the doors. Table 7 presents the door operation schedule reported by PNNL in P_h for the 2 buildings of interest. (Cho et al., 2010)

Table 7. Door usage for the strip mall and outpatient healthcare building in P_h (Cho et al., 2010)

	12-6	6-7	7-8	8-9	9-10	10-11	11-12	12-13	13-14	14-15	15-16	16-17	17-18	18-19	19-20	20-24
Strip Mall (All week) - Large Store				3	3	34	34	34	34	34	34	34	34	3	3	
Strip Mall (All week) - Small Store				2	2	16	16	16	16	16	16	16	16	2	2	
Outpatient (Weekdays)		12	123	123	123	123	123	123	123	123	123	123	123	12		
Outpatient (weekends)																
Peak	Off-Peak		unoccupied													

2.4.3.3 Vestibule Door Savings

PNNL reported the end use energy savings resulting from the use of vestibule doors (in comparison to the use of single doors) for the 12 reference building models studied. It is important to note that door sizes assumed in PNNL's study was 7 × 3 ft (2.1 × 0.9 m , approx. 1.9 m^2). The results of the their analysis showed that, from all the building simulated, the national weighted average maximum savings was 5.61% for the strip mall building and the minimum savings was 0.03% for the outpatient healthcare building model (Cho et al., 2010) . It is important to note that the results confirm and support the reasons of choice of the building models in the proposed method in section 1.2.

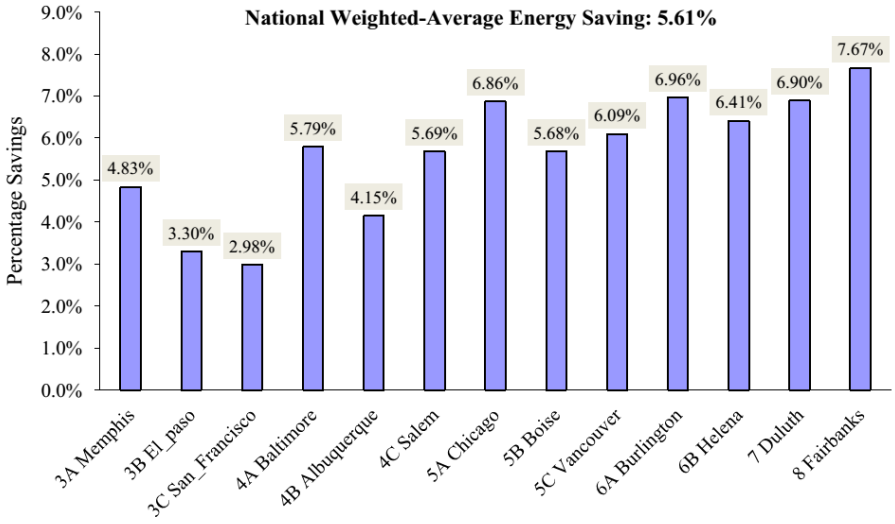

Figure 16. PNNL reported vestibule door savings for the strip mall building (Cho et al., 2010)

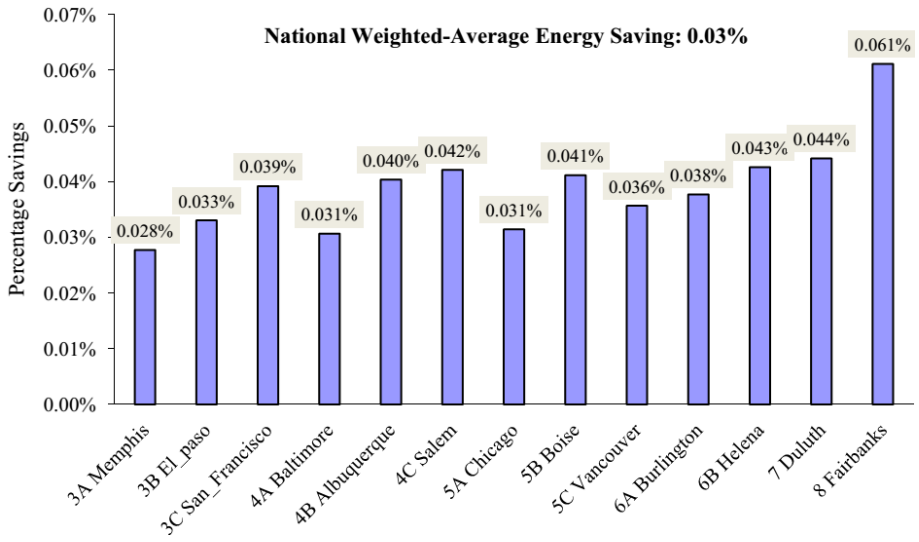

Figure 17. PNNL reported vestibule door savings for the outpatient healthcare building (Cho et al., 2010)

2.4.4 Air Curtain Door Savings and the study of air curtain door energy simulation

Based on CFD simulations results presented in sections 2.3 and the infiltration curves presented in Figure 13, Wang (2013) investigated the energy savings of air curtains using TRNSYS 17.1 ("TRNSYS," n.d.) coupled with CONTAM 3.1 ("CONTAM User Manual," n.d.) through the data interface TYPE 98 developed by NIST (Figure 18 presents a data exchange schematic between TRNSYS and CONTAM). The data interface was based on CONTAM providing TRNSYS with the air infiltration and exfiltration data while TRNSYS provides CONTAM weather and room temperature data in what was described as a "*ping-pong*" manner (Wang, 2013).

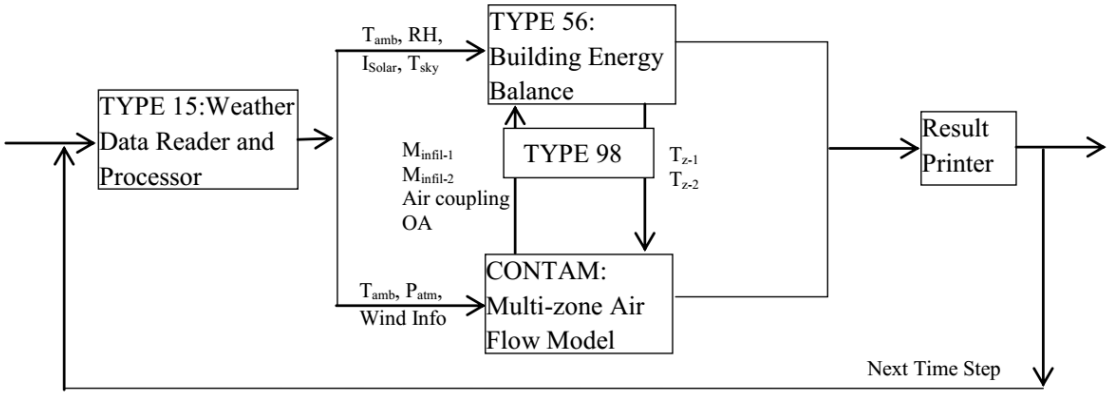

Figure 18. Data exchange schematic between TRNSYS and CONTAM (Wang, 2013)

The heating and cooling energy savings from replacing a 2 × 2.4 m (4.8 m^2) vestibule door (or single door, in accordance to ASHRAE 90.1 requirements) with an air curtain door were calculated for the medium office reference building model (Ng et al., 2012; Deru et al., 2011) for 9 locations representing all the 8 climate zones of the United States (building model presented in Figure 19). It is very important to note that, Wang (2013) used the DOE energy model of the building (new constriction version) as opposed the ASHRAE 90.1 models used by PNNL (Cho et al., 2010). Although the DOE models are still considered to be reference building models, the ASHRAE 90.1 models are the ones used to assess code related aspects due to their compliance with the ASHRAE 90.1 code (Jiang et al., 2009; "Commercial Prototype Building Models | Building Energy Codes Program," n.d.).

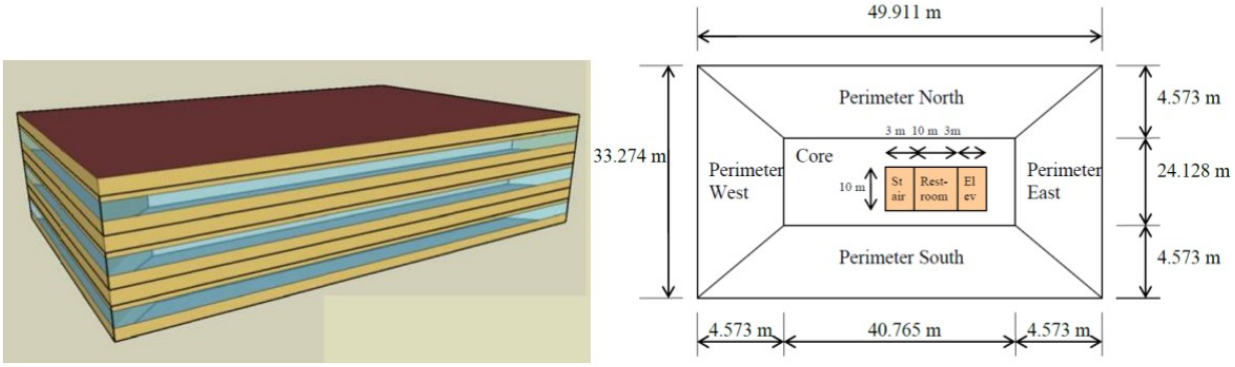

Figure 19. Medium office reference building model (Ng et al., 2012; Deru et al., 2011)

In his study, Wang (2013) used air curtain door infiltration results presented in sections 2.3 which are for a unit supply air at 15 m/s at 20° outwards. He also used a method (Equation 28) similar to that proposed by PNNL in the vestibule savings study (Cho et al., 2010) for calculating energy saving Equation 28 (Wang, 2013).

Equation 28.

$$E_{saving} = E_{base} - E_{ac} - E_{fe}$$

And

$$P_{savings} = \frac{E_{saving}}{E_{base}}$$

Where E_{saving} is the energy savings,

E_{base} is the annual heating/cooling or both heating and cooling loads of the base for comparison: the single door or the vestibule door (kWh),

E_{ac} is the air curtain annual heating load for the regions using air curtain for heating only, or the cooling load for cooling only, or both heating and cooling loads for the regions using air curtain for both heating & cooling (kWh)

E_{fe} is the air curtain annual total fan energy, kWh, which is the air curtain fan power (kW) multiplied by the total operating time (hr), and

$P_{savings}$ is the air curtain door annual total energy savings in percentage. (Wang, 2013)

It is important to note that, in the CONTAM model, the single doors and vestibule doors were modeled using the one way flow - power law model. The schedules for the doors were the flow coefficient (C) values calculated based on door usage frequency and the size of the door as proposed by Yuill (1996) and presented in section 2.1.3.1.3. In CONTAM, air curtain doors were modeled using cubic-Spline fitting model (Q vs. P) where the air curtain door's infiltration characteristics for 100 P_h (shown in Figure 13) was used as input. The schedule values used were the factors, correction factors (referred to in this thesis as F_u), calculated based on the ratio between the air curtain door infiltrations at a specific door usage in relation to that at 100 P_h usage (based on the conclusions obtained from the CFD and presented in section 2.3). (Wang & Zhong, 2014b, 2014a; Wang, 2013)

More details on the methods used by Wang (2013) in modeling and controlling air curtain units in CONTAM, and the method of calculating the units energy consumption are presented in sections 2.4.4.1 and 2.4.4.2 respectively.

The study concluded that, when compared to vestibules (according to ASHRAE 90.1 requirements presented in

Table 6), air curtain doors can reduce the annual energy consumption of the medium office reference building model between 0.3% (1146 kWh, in CZ3) to 2.2% (18986 kWh in CZ8) (Wang, 2013). Figure 21 and Table 8 present the major concluding findings of Wang's study (2013).

Table 8. Annual heating/cooling savings and total energy savings of air curtains in the medium office reference building (Wang, 2013)

Climate Zone	City	Heating/ Cooling	Air Curtain Fan Energy kWh	Air Curtain Annual Performance					
				Basis for Comparison: Single Door			Basis for Comparison: Vestibule		
				Heating/Cooling Saving, kWh (%)	Total Saving		Heating/Cooling Saving, kWh (%)	Total Saving	
					E_{saving} kWh	P_{saving} %		E_{saving} kWh	P_{saving} %
1	Miami	Cooling	94	175 (0.0)	81	0.0	-		
2	Austin	Cooling	158	290 (0.1)	132	0.0			
3	Atlanta	Heating	200	2003 (2.9)	1757	0.4	1172 (1.7)	1146	0.3
		Cooling		-46 (-0.0)			174 (0.1)		
4	Baltimore	Heating	331	-			2425 (1.6)	2217	0.5
		Cooling					123 (0.1)		
5	Chicago	Heating	371				4383 (1.7)	4169	0.9
		Cooling					157 (0.1)		
6	Minneapolis	Heating	372				7379 (2.0)	7007	1.2
7	Fargo	Heating	415				9152 (2.0)	8737	1.4
8	Fairbanks	Heating	529				19515 (2.5)	18986	2.2
For selected zones, when the operation of air curtain is not controlled by outdoor temperature									
3	Atlanta	Heating	786	2161 (3.2)	911	0.2	1330 (2.0)	300	0.0
		Cooling		-464 (-0.1)			-244 (-0.1)		
4	Baltimore	Heating	786	-			2695 (1.7)	1620	0.4
		Cooling					-289 (-0.1)		
5	Chicago	Heating	786				4694 (1.9)	3721	0.8
		Cooling					-187 (-0.1)		

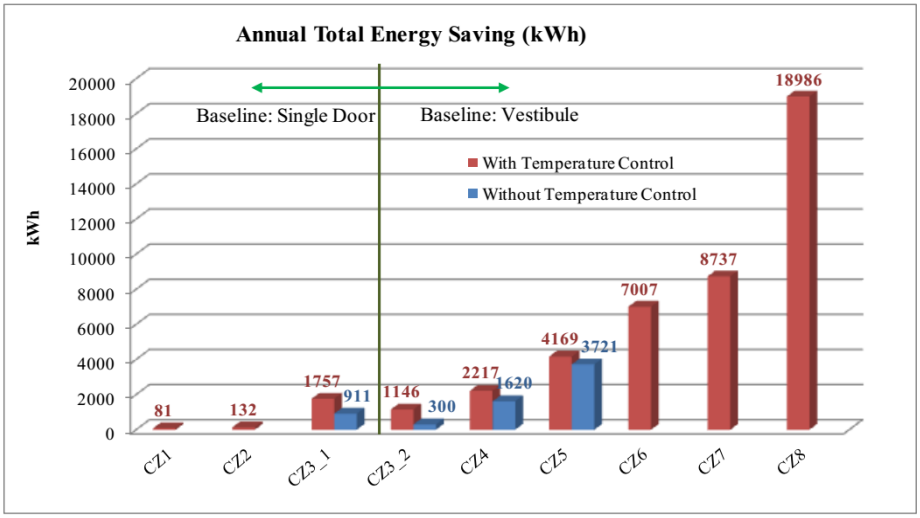

Figure 20. Annual total air curtain door savings in kWh when compared to single and vestibule doors according to ASHRAE 90.1 requirements (Wang, 2013)

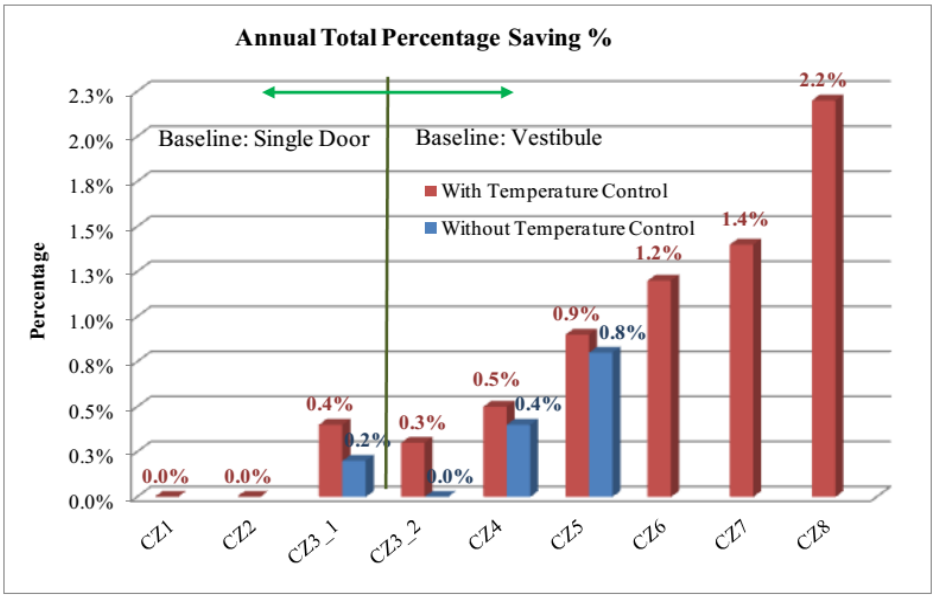

Figure 21. Annual total air curtain door savings in percentage when compared to single and vestibule doors according to ASHRAE 90.1 requirements (Wang, 2013)

It is important to note that, despite providing valid data on the savings achieved from the use of air curtain doors, the results of the study conducted by Wang (2013) differ from the results of PNNL studies (BA Thornton et al., 2010; Cho et al., 2010; Gowri et al., 2009). This is due the differences in methodologies, door usage schedules, software, and energy models used to conduct the energy simulations. The study by Wang (2013) also focused mainly on the annual heating and cooling loads obtained from the TRNSYS model which could defer from the standard models (Deru et al., 2011). In addition, the output of the EnergyPlus simulations also includes all auxiliary building loads which were not all considered by Wang (2013).

2.4.4.1 Modeling and Control of Air Curtains Units in CONTAM

As presented in 2.4.4, the air curtain door was modeled in CONTAM using cubic-Spline fitting model (Q vs. P) with the air curtain door's infiltration characteristics for 100 P_h (shown in Figure 13) input. Wang however modeled the air curtain unit to operate only under the following conditions (Wang, 2013).

- Air curtain operates under temperature control: the unit only operates when $T_{ambient} > 30$ ºC and $T_{ambient} < 10$ º C

- The air curtain only operates when the doors are being used: only for the time of usage of the door T_h (the air curtain is assumed to be off and not consuming energy when the doors are closed) (Wang, 2013)

The modeling of the air curtain door in CONTAM, with the proposed conditions, required for two doors to be modeled (since when the air curtain unit is not functionally, the door operate as single doors). The choice of the door model used and the schedule inputs to the door models was complete in CONTAM through the use control nodes within the program.

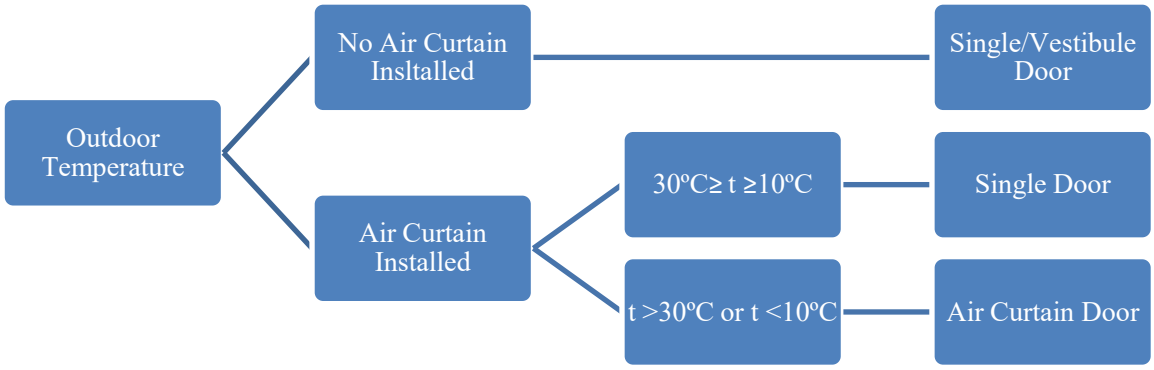

Figure 22. Description of the control modeled used for air curtain in CONTAM (Wang, 2013)

2.4.4.2 Calculating Energy Consumption of Air Curtain Units

The air curtain was considered to operate only when the doors are being used (i.e. based on the door usage frequency) (Wang, 2013).

Equation 14 which calculates the total door usage per hour, T_h. proposed by Yuill and presented in section 2.1.3.1.2, was used to estimate the air curtain's unit operation based on the people per hour usage of the doors used. The calculation of the air curtain energy, E_{fe}, is found more details in the studies. (Wang & Zhong, 2014b; Wang, 2013)

Equation 29.

$$E_{fe} = Fan\ Power\ (Watts) \times Operation\ Hours\ (Hour)$$

Where Operation hours is calculated based on the door time of use (T_h).

Wang proposed a power rating of 1.05 kW for the air curtain fan unit with no consideration for convective or radiative heat exchange between the unit and the surroundings (Wang, 2013). It is important to note that no literature was found regarding the modeling and control of air curtains in EnergyPlus.

2.5 Large Scale Velocimetry

Velocimetry is a term that refers to measuring the velocity of fluids to solve complex engineering and fluid dynamics problems. Large scale velocimetry is a set of methods that are used to quantity the airflow fields in any large scale applications, usually with the purpose of large visualization/quantification of fluid flow. In the field of building engineering, a large amount of research depends on the measurements of airflow in and around buildings. Large scale velocimetry became critical in understanding many of the engineering and physics of the building environments. However, it is not easy to conduct large scale accurate airflow field measurements in building applications due to the complexity of the subject. It is not an easy task to measure the flow without causing significant disturbances or to obtain accurate measurements especially for large scale applications. (X. Cao, Liu, Jiang, & Chen, 2014)

In general, velocimetry is divided into two categories; point-wise and global-wise measurements (Sun & Zhang, 2007). Point wise techniques include technologies that enable the measurement of speed (and sometimes velocity) based on pressure differentials (example: Pitot tube), Doppler shift principles (example: laser Doppler), heat transfer principles (example: hot-wire anemometry) or acoustic principles (example: ultrasonic anemometry) (X. Cao et al., 2014). Global-wise techniques rely mainly on optical principles and include technologies such as particle image velocimetry (PIV), particle tracking velocimetry (PTV) and particle streak velocimetry (PSV) (X. Cao et al., 2014; Adrian, 2005). It has been established that using point wise velocimetry might not be effective or accurate in capturing global turbulent airflow fields for multiple reasons. The later include the perturbation on the flow and the fact that point by point measurements can be time-consuming (X. Cao et al., 2014). Optical based velocimetry, especially PIV, has become one of the most robust and widely used in the flow field studies since it is able to capture velocities in large global domains with minimal flow disturbances (Raffel, Willert, Wereley, & Kompenhans, 2013; Sun & Zhang, 2007).

2.5.1 Particle Image Velocimetry

Particle image velocimetry is a global-wise measurement technique that, apart from providing qualitative flow visualization, is able to achieve almost instantaneous quantitative measurement for velocity fields within a field of view. A typical PIV system consists of a multi-pulsed laser, one or more cameras that are synchronized with the laser, and a computer that is used to control the system and analyze the acquired data. (X. Cao et al., 2014)

Many types of PIV systems are now available in the market. 2D-2C PIV system (2D PIV) generally use one camera and generate 2D (planar, capturing velocity in 2 dimensions) velocity field images while 3D-3C PIV system depend on 2 cameras to capture the 3-dimensional flow. Other types of systems such as tomographic PIV use more than 2 cameras. These systems are generally able to generate volumetric velocity field. (X. Cao et al., 2014; Li, Qin, Xin, Wang, & Wang, 2010)

It is important to note that the available system used in this research is a normal 2D-2C PIV system and that 3D and tomographic PIV systems are not reviewed as they are outside the scope of this research. (G. Cao, Sivukari, Kurnitski, & Ruponen, 2010; Bosbach et al., 2006; Bryant & Johnsson, n.d.)

Figure 23 shows the components, data acquisition and analysis of a 2D PIV system. The laser sheet is fired at known time intervals Δt, and the images are captured (in synchronized manner) by the camera. The processing of the data is generally done through a comparison/correlation (or tracking) of tracer particles (seeds) movement within interrogation areas. A known limitation of 2D PIV systems is the movement of seeding particles outside the plane of measurement (this is specifically true when the flow has strong 3D characteristics). (X. Cao et al., 2014; Sun & Zhang, 2007)

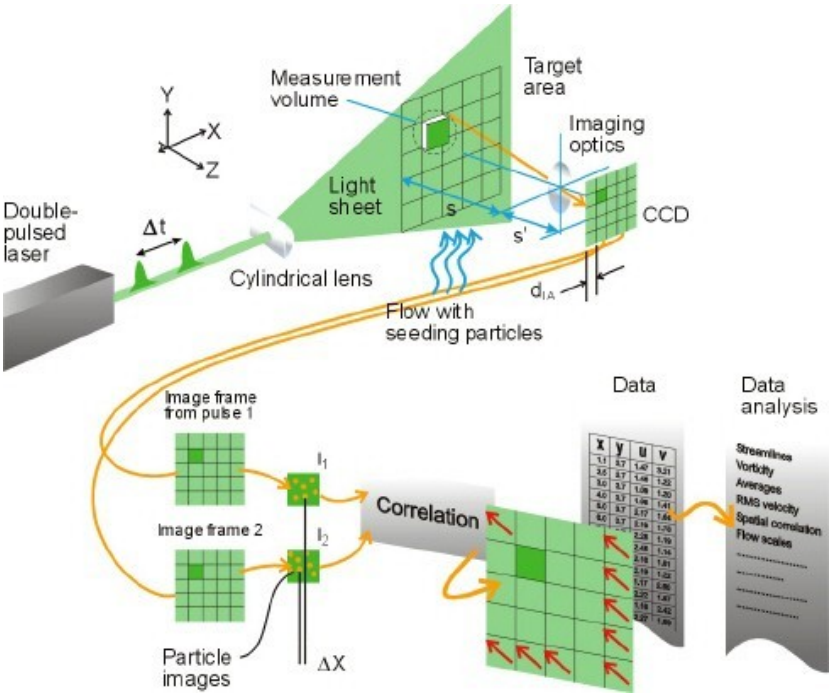

Figure 23. 2D PIV system components and general data acquisition and analysis process ("Laser Optical CCD and sCMOS Cameras | Dantec Dynamics," n.d.)

A double pulsed Nd:Yag laser is usually used in the 2D PIV system. The laser generates a green sheet (2 green sheets) of light of 532 nm. The light can be focused; the sheet's thickness, angle and orientation can be manipulated with the help of a cylindrical lens. (X. Cao et al., 2014; Sun & Zhang, 2007)

In regards to the recording devices, the most widely used technology is the coupled charges devices (CCD) cameras which are known to have a good spatial resolution. CCD cameras in the market today have sensors that range in resolution from 2M (1600 × 1200 pixels) to 29M (6576 × 4384 pixels). It is important to note that large resolution CCD cameras are required in large-scale measurements. (X. Cao et al., 2014; "Laser Optical CCD and sCMOS Cameras | Dantec Dynamics," n.d.)

One of the most important parameters when using laser is the time delay, Δt, between laser pulses (thus between each 2 captured frames). The delay between the pulses have to be long enough from the particles to move a significant amount within the frame (usually ¼ the interrogation area) but has to be short enough to avoid particles moving outside the frame. Many methods are available to estimate the needed time delay. The most widely used is the method

proposed by Li et al. which relate the delay to the maximum velocity that is measured. (X. Cao et al., 2014; G. Cao, Sivukari, Kurnitski, Ruponen, & Seppänen, 2010; Li et al., 2010; Hart, 2000)

Equation 30.

$$U_{max} \times \Delta t\ (\mu s) = 250$$

Where U_{max} is the maximum speed of flow to be captured, and
Δt is the time delay between laser pulses in μs.

Since the PIV system captures and measures the velocity of the tracer particles (not that of the real airflow), the tracer particles (a.k.a. seeds) have a key role in determining the accuracy of the PIV measurements. Many seeding methods are available none of which are completely neutrally buoyant (oil droplets, suspended fluid, vapors, helium filled soap bubbles (HFSB) and solid particles). The effect of gravity (derived from Stoke's law) is usually used to estimate the gravitationally induced velocity. Another important parameter arises when the tracer particles are introduces with an initial velocity. The response of the particles to the flow of interest (change of direction or gain of speed into the flow) can be characterized with by the relaxation time of the particles. However, the relaxation time can be neglected with correct time delay settings. Finally, the scattering characteristics of the particles also need to be considered.

An acceptable range of seeding density within the field of view should provide more than 2 up to 20 particles per interrogation area (data analysis software only detects interrogation areas with sufficient amount of seeding as valid) Based on the analysis of various seeding methods, it was concluded that using the HFSB is the most feasible seeding option for large-scale application considering their low density ratio to air (more literature regarding HFSB is reviewed in section 2.5.1.1). (Scarano et al., 2015; X. Cao et al., 2014; Raffel et al., 2013)
Finally, the data processing method of the acquired images have a deciding factor on the accuracy and precision of the final PIV results. The adaptive correlation method (Dantec Dynamics & Nova Instruments, 2012) is the most widely accepted data processing method and it is considered to be one of the most advanced automatic correlation algorithms. Adaptive correlation calculates velocity vectors at each interrogation area by correlating a set of captured frames and overlaps data from one interrogation area to be uses as information for the surrounding interrogation areas. In large-scale applications, the size of the interrogation area is

usually set to be 64 × 64 pixels with an overlap of 50%. (X. Cao et al., 2014; Dantec Dynamics & Nova Instruments, 2012; G. Cao, Sivukari, Kurnitski, Ruponen, et al., 2010)

2.5.1.1 Helium Filled Soap Bubble (HFSB) Seeding Method

Helium filled soap bubbles (HFSB) are being increasingly used in large-scale PIV experimental studies. The main reason of interest in this relatively new seeding method is mainly due to the high scattering efficiency of these particles (as they can be easily traceable and lit by light sources). Other parameters that distinguish HFSB seeding systems from other methods are the low density ratio when compared to air (making them more neutrally buoyant than other tracer particles) and the flexibility of adjusting their size. Professionally fabricated HFSB systems are available in the market (but they are still undergoing development and they come at very high prices) and specially designed systems have been reported in the literature. (Bosbach et al., 2006; Sage action Inc., 2002)

The key to the HFSB system is the nozzle design. The nozzle consists of 3 coaxial tubes that air, soap and helium are pumped through. Two main types of nozzles are available; the orifice types (shown in Figure 24) and the filtered type nozzles (commercial nozzle which are usually equipped with vortex filters - used as buoyancy filters). (Bosbach et al., 2006; Sage action Inc., 2002)

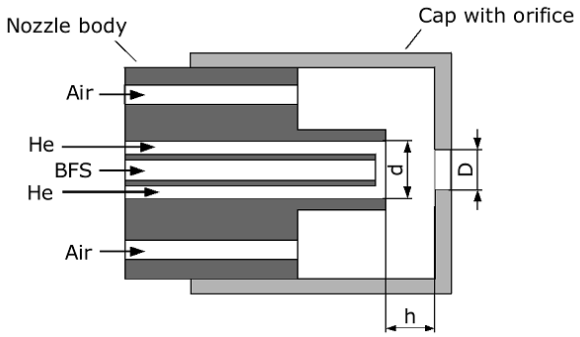

Figure 24. Orifice type HFSB nozzle (Bosbach et al., 2006)

A number of studies utilizing this system have been reviewed. A general agreement on the merits of this seeding methods have been noted considering the ability of high density seeding (using multiple nozzles), better traceability in large scale and the full controllability of the size and weight/density ratio. However, some drawbacks and limitations have been also reported. The

bubbles can have, depending on the soap solution used, short lifetime (a few minutes), the need of injection close to the measurement region (creating disturbances) and finally the large pollution the seeding might cause to test sections. (Scarano et al., 2014, 2015; Bosbach et al., 2006)

The study Scarano et al. aimed to assess the usability of HFSB in high speed wind tunnel experiments, Scarano et al. compared the PIV results obtained with various HFSB (with different weights and sizes). They indicated that some consideration of the double glare conditions (at the 2 walls of the large bubbles) could cause some errors in the PIV results. It was also observed that, when compared to fog tracer particles, the bubbles might show delayed responses to flow speed changes. However, it was concluded that the bubbles were traceable for speeds up to 30 m/s, and that, based on the experiment setup, an optimum size and weight has to be selected for the tracers to exhibit minimum slip velocity (relaxation time). The study concluded positively in regards to the use of HFSB for quantitative studies. Perhaps another important conclusion of the study is that, even without using buoyancy filters, accurate results can be obtained using correctly sized HFSB (these filters are usually used to remove negatively or positively buoyant particles). (Scarano et al., 2015)

2.6 Conclusion

Based on the objectives and scope of this research that were presented in section 1.2, an extensive review of the literature was conducted for the various topics which were used in the establishment of the theoretical background and in the development of the methodological framework of this research.

A review of the literature dealing with airflow and heat flow was conducted (sections 2.1.1 & 2.1.2). It is concluded that the methods proposed by Yuill (1996) for calculating the airflow coefficient of automatic doors in operation are the most established (section 2.1.3). However, the current method proposed by PNNL (Cho et al., 2010; ASHRAE, 2009) for calculating the pressure difference across doorways to be used in energy simulations were seen by many as unrealistic due to their independence from the outdoor and building conditions. It was concluded that airflow simulations could provide better estimates of air infiltration rates through openings in buildings (section 2.1.3.2) (Ng et al., 2014; Wang, 2013; Liu, 1992). The study by Wang

successfully used the airflow simulation method for annual energy assessments in buildings (Wang, 2013).

An extensive literature review on the research and standards regarding air curtain units was conducted (section 2.2). The most developed and widely used models for the air curtains' operation are the those developed by Hayes (F.C. Hayes & Stoecker, 1969; Floyd C Hayes, 1968). It was seen that most of the studies dealing with the topic of air curtains considered a sealed room (no external pressure) with isothermal or non-isothermal conditions. In additions, none of the experimental studies reviewed have been able to visualize airflow of air curtains. In regards to air infiltration through air curtain entrance doors, the numerical study conducted by Wang was found to be most advanced, however some of the limitations of this study were also presented (section 2.3). (Wang, 2013)

In regards to commercial reference buildings energy simulations, it was found that the models developed by PNNL for EnergyPlus (in collaboration with DOE) are the most widely used (section 2.4.1). A review on the ASHRAE standard 90.1 requirements for vestibule and the related study conducted by PNNL (Cho et al., 2010) (section 2.4.3) confirmed the reasons of choice of the building models in the proposed method in section 1.2. The study by Wang (2013) (section 2.4.4), compared the annual energy use of a commercial building with air curtain and vestibule doors. The review also supported the use of EnergyPlus, standard reference buildings (compliant to ASHRAE Standard 90.1 - 2013) in this research.

In regards to the experimental study proposed in section 1.2, the experimental setup used by Yuill et al. (2000) was found to be the most relevant (section 2.1.3.1.1). The review of the literature dealing with large scale velocimetry (section 2.5) confirmed the proposed method in section 1.2 for the experimental validation.

The findings and conclusions of the literature review support the proposed method in section 1.2. The possible contributions of this thesis were therefore determined as follows:

- Validating CFD simulation & infiltration modeling methods of air curtain doors proposed by Wang (2013)
- Visualizing airflow of air curtains in isothermal operation using large scale PIV with HFSB apparatus.

- Investigating the effect of air curtain discharge angles and speed on the sealing of entrance doors under external pressure conditions (non-sealed room conditions).
- Modeling and controlling air curtains in EnergyPlus.
- Using CONTAM for infiltration calculation & EnergyPlus to simulate energy consumption of 2 commercial building reference models.
- Estimate national weighted average savings achieved from the use of air curtain doors in 2 commercial building reference models.

3 EXPERIMENTAL STUDY

3.1 Introduction

This chapter mainly presents the methodology, results and discussion of the experimental validation study conducted for the air curtain door. All experiments have been conducted at Concordia University using research equipment furnished by the Building, Civil and Environmental Engineering Department.

As indicated in the introduction of this thesis (section 1.2.1) and as presented in the literature review (section 2.2.3 and 2.3), existing studies did not provide sufficient experimental or field data that can be used in to validate the modeling methods of air curtains proposed by Wang (2013). An experimental study had to be developed in order to acquire the correct experimental data for the validation of the numerical study. It is important to note that the realization of the experimental setup used would not have been possible without the support of the AMCA.

The experimental study aims to validate:

- the existence of the three air curtain flow conditions as shown in Figure 11:

  The experiments aim to confirm the different air curtain flow patterns (conditions) as proposed by previous studies (Wang & Zhong, 2014a; Wang, 2013; F. C. Hayes & Stoecker, 1969). The study also aims to confirm that the air curtains can be modeled by Equation 27 and Equation 26.

- the method of modeling air curtain supply in CFD:

  The supply velocity of air curtains can be variable and sometimes highly non-uniform at different locations of the air curtain supply slot. The experiments aim to investigate the impact of the supply non-uniformity on the air curtain performance.

- the method of defining and locating pressures and volumetric flow rates in Equation 27 and Equation 26:

  In 3D-CFD simulations, pressures calculated can be highly non-uniform across the door. The experimental study aims to confirm the definition and the locations of pressure results obtained from simulations. It also aims to confirm the modeling method of the duct blaster

fan from which the volumetric flow rates are obtained (often defined by the fan curve provided from its manufacturer).

- the choice and use of turbulence model:

  The experimental study aims to confirm that the standard k-ε model (found to be repeatedly used in literature) is suitable to use when modeling air curtain doors. It also aims to confirm the associated turbulence parameters used (turbulence intensities and boundary conditions).

- other CFD-related settings:

  CFD simulations have many parameters such as grid resolutions, high gradient flow regions, discretization schemes and their accuracy ($1^{st}/2^{nd}$ order), wall functions, under-relaxation factors, etc. The comparison between the CFD simulation and the experimental data can confirm these settings. The experimental study can also help to adjust these parameters if necessary by providing experience of modeling air curtain and its characteristics.

Finally, and as presented in the contribution of authors section, it is a must to indicate that the inputs of Dr. Fayrouz were key in obtaining the PIV results presented in this chapter. Also, his input regarding the design of the chamber and HFSB nozzles were crucial for their success. In addition, the efforts of Dahai Qi in modeling and simulating the cases for the experimental study have to be mentioned.

3.2 Methodology

3.2.1 Experiment Design

An experimental setup (Figure 25 shows a conceptual setup illustration which includes the different components) was proposed for the validation study consisted generally of:

- an air tight transparent/translucent chamber with an exhaust fan and a door equipped with an air curtain
- pressure sensors located inside of the enclosure and flow gauge at the exit of the fan
- a PIV system to capture the airflow field at the door of the chamber

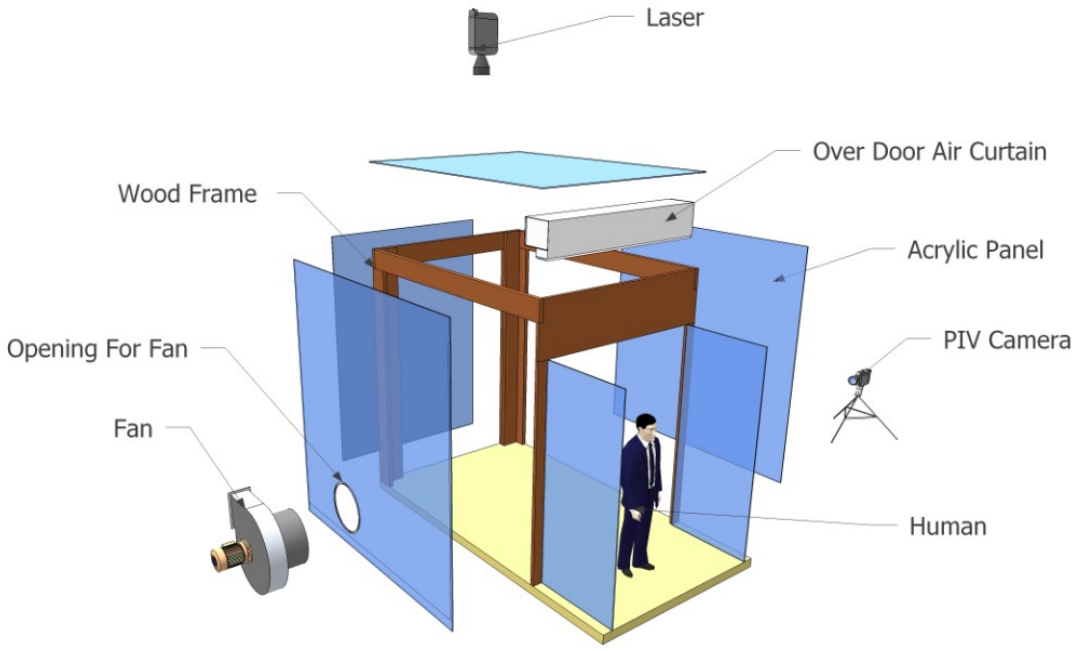

Figure 25. Conceptual 3D representation for the components of the proposed experimental setup (not the final setup used)

The detailed design and selection process of each of these elements are presented in the following sub-sections and the final setup used is presented in section 3.2.1.5.

3.2.1.1 Experimental Chamber

Due to the infeasibility of constructing a full scale model/setup as proposed by Wang (2013) (20 m × 24 m × 10 m (L × W × H) building within a full domain of 50 m × 24 m × 10 m (L×W×H) with a door size of 2 m × 2.4 m (W × H) and presented in Figure 10), a number CFD simulations were conducted to evaluate different chamber designs. The experimental chamber used by Yuill (1996) in his study on the impact of using automatic doors (2.44 m × 2.44 m × 1.3 m (W × L × H) with a door opening of 0.61 m × 0.71 m (W × H) that represents 1/3 scaled down model of a real building and presented in (Figure 2) was finally selected. This selection was important in the experimental study as it provided the research with reference for carrying out the calibration of the setup (using the infiltration through the single door as a reference).

The design of the chamber enclosure itself was critical to the success of the proposed objectives of this research. It relied mainly on fabricating a transparent (minimum framing elements)

enclosure to allow for the use of particle image velocimetry (PIV) tests to measure airflow fields of air curtains

A full design proposal for a wood and acrylic enclosure with the dimensions of 2.44 m × 2.44 m × 2.44 m and a movable suspended mid-ceiling was prepared by the project team - presented in APPENDIX (A). However, the more flexible and rapidity constructible aluminum frames design proposed for this chamber by MËKANIC was more successful in catering the needs (specifically in regards to time) of this research. This chamber (Concordia University Building Environment - CUBE - test lab shown in Figure 26) was fabricated using aluminum frames and enclosed with Lexan panels. The movable ceiling of the chamber is positioned so that only a portion (1.3 m high) is used in for this research. The chamber is purposely made transparent for particle image velocimetry (PIV) measurements to be feasible. It is important to note that the drawings, pictures and renders of the chamber are the intellectual property rights of MËKANIC and that the fabrication of this chamber was completed by KATIM (Disca Automation Inc.). More pictures of the final test chamber are shown in APPENDIX (A).

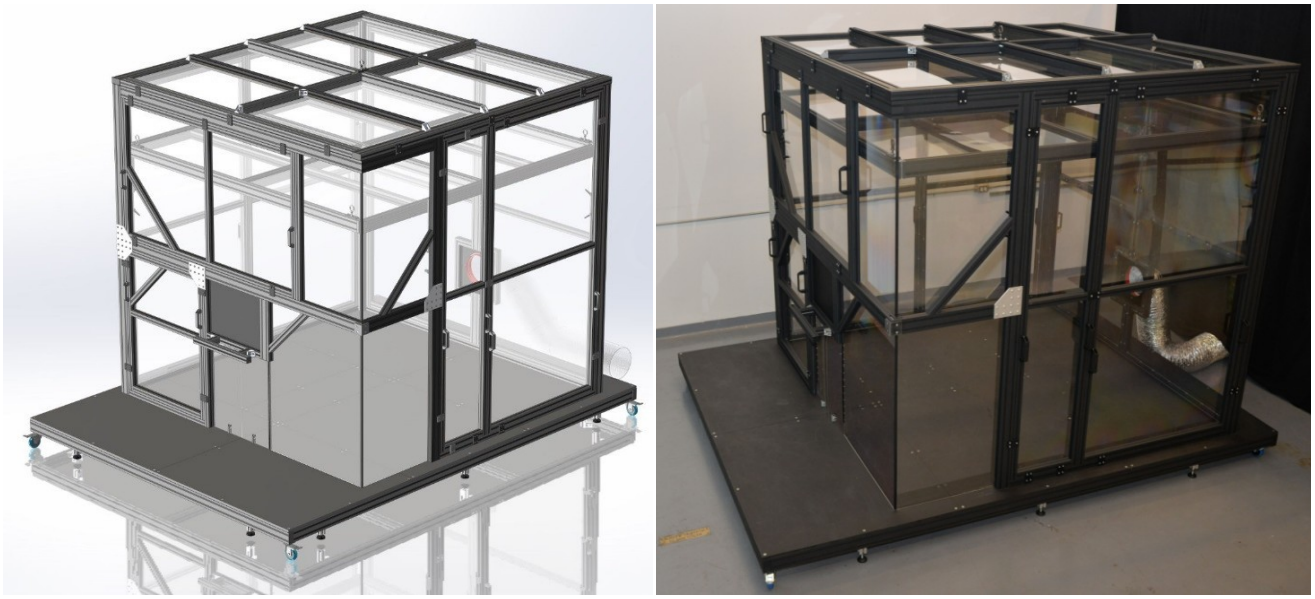

Figure 26. A design render (left) and a real picture (right) of the CUBE (pictures provided by MËKANIC)

As indicated, the equipment fitted in the chamber is discussed in the subsequent sub-section and the details and characteristics of the air curtain used are presented in section 3.2.1.4.

3.2.1.2 Blower-Door Test

The chamber was fitted with a Minneapolis Duct Blaster® System ("Minneapolis Duct Blaster® System - The Energy Conservatory," n.d.). The system consists of a flexible duct (fitted in the chamber at the opposing surface to the door), a Series-B fan (details of which can be found in the manufacturer manual) as well as various flow rings. The duct was equipped with an air diffuser (hat type diffuser) to limit the direct flow of air to the door. The correct configurations (flow rings and tube connections) as suggested by the manufacturer were used in the measurement of the flow through the fan. (The Energy Conservatory, 2015)

The system used was equipped with digital pressure and flow gauges. The gauges are calibrated to measure the flow of the selected fan with its various configurations by the manufacturer: the measurement of flow is based on the pressure difference between two inputs. The original gauge of the system was the DG-3 (The Energy Conservatory, 2007). However, due to some limitations in the operation of this old gauge model, the newer DG-700 model was used. ("DG-700 Pressure and Flow Gauge - The Energy Conservatory," n.d.). It is important to note that all the equipment used were timely calibrated by the manufacturer (i.e. The Energy Conservatory) and that the models of the gauges were cross checked to ensure their calibration. The digital gauges are designed to measure two inputs (input A and input B), each with two inputs: a pressure and a reference (the detail of the equipment can be found in the manuals ("DG-700 Pressure and Flow Gauge - The Energy Conservatory," n.d.). In the experiments conducted, one of the inputs of the DG-700 digital gauge was used to measure the flow through the fan and the other was used to measure the pressure inside the chamber in reference to the laboratory. The details of the pressure measurements are presented in the following sub-section. The manufacturer ("Minneapolis Duct Blaster® System - The Energy Conservatory," n.d.) reported range of error for the measurements (using the DG-700) is up to ± 3% (more details on the error calculations are presented in section 3.2.5.1).

3.2.1.2.1 Interior Chamber Pressure

The interior pressure in the room was measured at the center plane of the room between the door and the fan - following the same concept used by Wang et al. (Wang & Zhong, 2014a). In order to obtain a close-to-average pressure at this plane, sensors (tube endings) at 4 different points (nodes) throughout this plane were placed (details of the specific pressure measurement position

can be seen in Figure 31). The 4 tubes were then reconnected (joined) and input into the DG-700 for the pressure measurement. Since the chamber would have had airflow at significant speed, the tube endings were fitted with protectors to ensure only the static pressure (rather than the total pressure) is being measured (as illustrated in Figure 27).

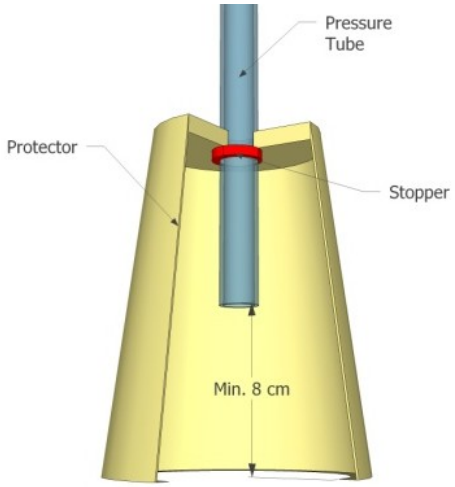

Figure 27. Tube ending protection for static pressure measurements

3.2.1.3 Particle Image Velocimetry

Based on the literature presented in section 2.5, PIV was considered to be the best method to visualize the airflow fields at the door way of the experimental chamber. Based on the air curtain's jet characteristics, it was assumed that a 2 dimensional PIV (2D-PIV) system would successfully capture the air flow at the doorway.

The PIV system used in this research is the Solo PIV 120XT model by New Wave Research with its controller (New Wave Research, 2004). The laser is a Nd:YAG dual laser head system with a pulse energy of 120 mJ at 532 nm equipped with a telescope lens. The CCD camera - DANTEC Dynamics ("Laser Optical CCD and sCMOS Cameras | Dantec Dynamics," n.d.) - used in the experiment is a thermo-electrically cooled 14 bit camera with a 2M (1200 × 1600 pixels) resolution. The camera is equipped with a 60 mm lens (2.8/32, manufactured by Nikon).

Based on the literature presented in section 2.5, the best seeding method indentified is the HFSB. After researching the market, the available commercial apparatuses were deem not fit to the application due to the requirement of multiple seeding points to account of the high speed sealing effect of the air curtain. A specially designed, tested and fabricated a HFSB system was used in

this research (details of the system are presented in following sub-section). The system used 4 nozzles each capable of producing about 80 - 150 HFSB/s between 0.8 to 1.6 mm.

Accordingly, and considering the air curtain velocity exceeding 10 m/s, the laser light sheets were adjusted to coincide (maximum 1 - 2 mm apart) at the doorway to capture the seeds within the same plane. The specific setup of the system is illustrated in Figure 30, Figure 31 and Figure 32. The details of the data acquisition are presented in section 3.2.2 and analysis process in section 0.

3.2.1.3.1 Helium Filled Soap Bubble Seeder

Based on the commercial HFSB system available (Sage action Inc., 2002) and the concepts presented by Bosbach et al. and Scarano et al. (Scarano et al., 2014; Bosbach et al., 2006), HFSB nozzles were designed specifically for this research (seen in Figure 28). The nozzles consist of a 3D printed plastic polymer body fitted with 5 needle stainless steel tubes. The nozzles created present a novel design since they use no filter and they do not have an orifice cap. In total, 6 nozzles were fabricated each optimized independently to all reach an acceptable operation level. A control station that can accommodate the operation of 4 nozzles simultaneously was also designed and fitted in the chamber (seen in Figure 28). More details on the HFSB system can be found in APPENDIX (A).

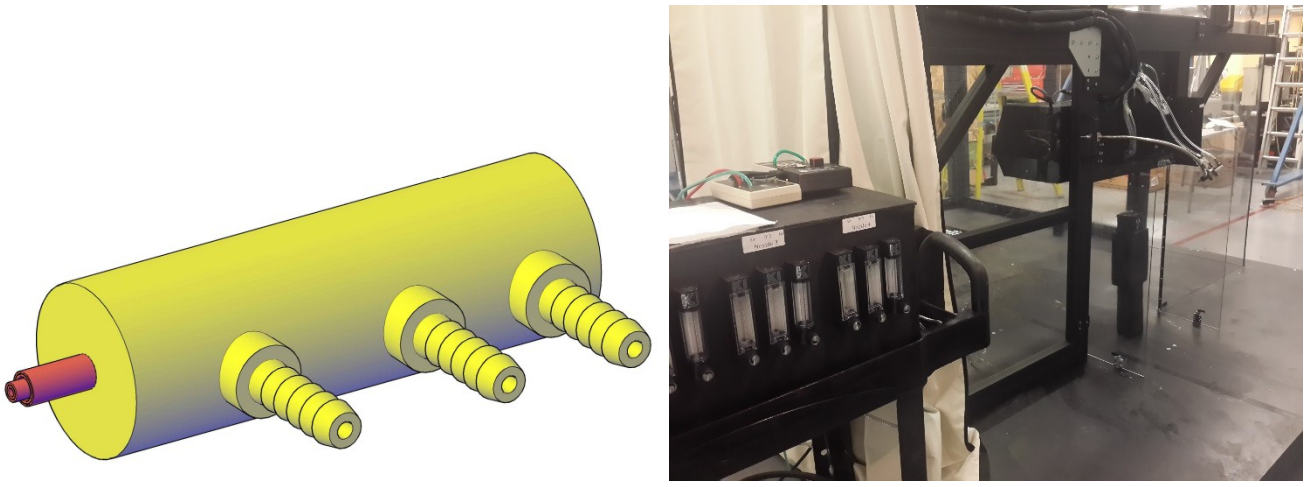

Figure 28. Design of the HFSB nozzle (left) and the system after being fitted in the chamber (right)

3.2.1.4 Air Curtain Unit and Supply Speeds Profile

A process of air curtain unit selection in collocation in the AMCA was required. Finally, MARS Air System agreed to manufacture and provide a specially designed unit for this project. The air curtain is a 120V center motor unit (motor placed in the center of the unit) with centrifugal fans on each side (total 2 fans). The unit's outlet nozzle is 6.35 cm × 61 cm (depth × width - same width as the door) equipped with 3 discharge direction vanes (which were set to 20° outwards for this study, unless stated otherwise). The unit was provided with a stepped VFD controller with 6 configurations (5 Hz and 10 to 60 Hz with 10 Hz steps). It is important to note that the unit provided included interior longitudinal flow deflectors (placed at angles within the interior of the unit) to enhance the nominal uniformity according to AMCA standards (Air Movement and Control Association International, 2012b).

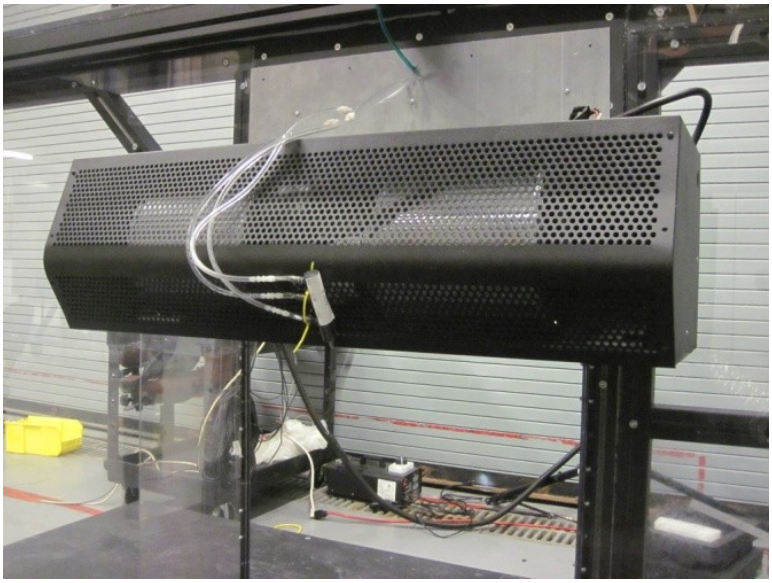

Figure 29. The air curtain unit fitted inside the CUBE

Before fitting the air curtain in the chamber, the direction vanes were removed and the surface supply speeds of the unit at 2 VFD levels were tested (namely: medium speed 40 Hz, and maximum speed 60 Hz). The detailed method of the testing is presented in APPENDIX (A). This test was crucial for replicating the supply characteristics of this specific air curtain in CFD simulations. The tests were also used in the selection of the PIV measurement planes. It is important to note that the speed measurements were conducted using a calibrated hot wire

anemometer (using average measurement over 10 seconds, with measurements repeated twice at each speed)

It was found that for the 40 Hz configuration, the air curtain average supply speed at the surface was 9.10 m/s (measured based on 2 speed measurements at 45 points) and for the 60 Hz configuration the air curtain average supply speed at the nozzle surface was 13.75 m/s - the detailed results of the testing is presented in APPENDIX (A). It is important to note the average variance in the supply speed through the air curtain for both configurations was ±40% (calculated based on the standard deviation supply speed data). However, according to the manufacturer, the unit had a nominal uniformity of more than 90% tested based on AMCA 220 Standard (Air Movement and Control Association International, 2012b). At both configurations, the highest air supply speed was recorded approximately 8.5 cm away from the edges and the lowest supply speed was at the center of the unit. It was observed that the center motor design, and the deflectors, created strong 3D flow phenomena. These observations can be the field of future studies as they are unit specific and cannot be generalized to all air curtains.

3.2.1.5 Final Experimental Setup

The experimental setup was finalized and construction following the details presented in sections 3.2.1.1 to 3.2.1.4. Two PIV measurement planes were set, at 8.5 cm from the edge (door side-plane) and at the center of the door (door mid-plane). The locations were selected to be coinciding with the highest and lowest supply velocities of the air curtain unit. The field of view (decided by the CCD camera position) was set to be 60 × 90 cm (W × H). 2 HFSB were placed inside the air curtain and 2 were placed on the outside at each side of the door. Figure 30, Figure 31 and Figure 32 Illustrate the final experimental setup in details. It is important to note that the placement of the nozzles inside the air curtain was necessary to achieve the needed seeding density. However, it might have contributed to some measurement errors. Based on the equipment and setup used, the flow rate achieved from the duct fan (airflow through the door/fan) was of a maximum of approximately 0.4 m^3/s (infiltration) and a minimum of approximately -0.3 m^3/s (0.3 m^3/s of exfiltration).

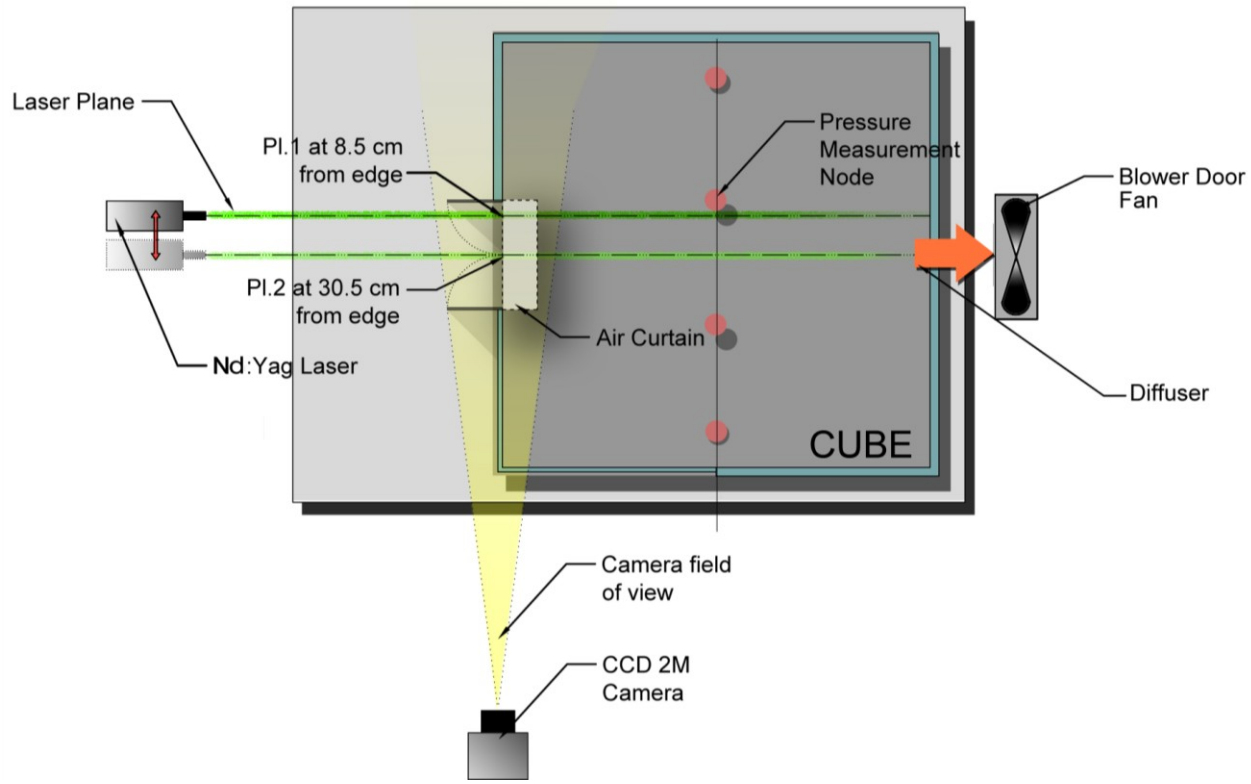

Figure 30. Final experimental setup plan view showing equipment and measurement positions

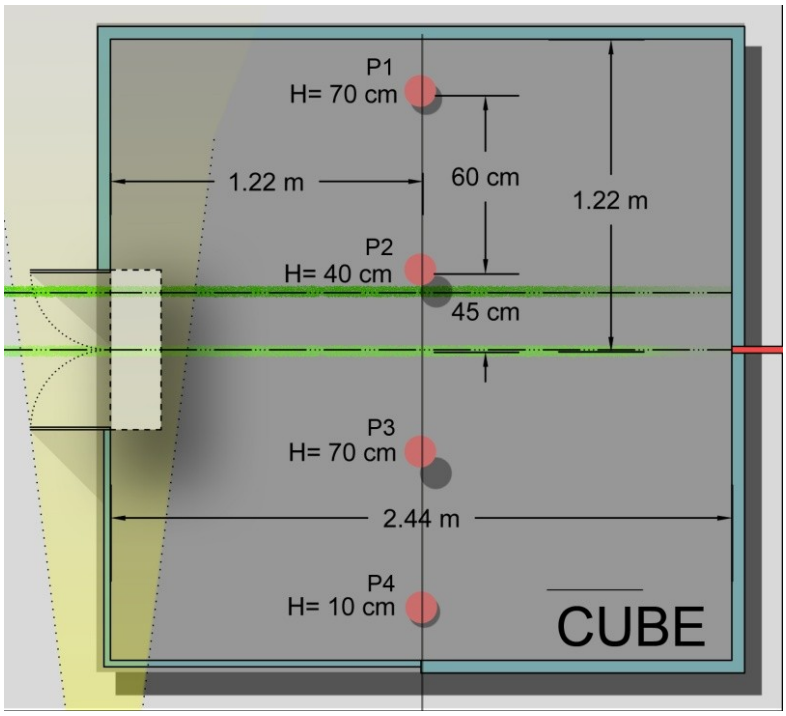

Figure 31. Pressure measurement nodes' positions inside the CUBE

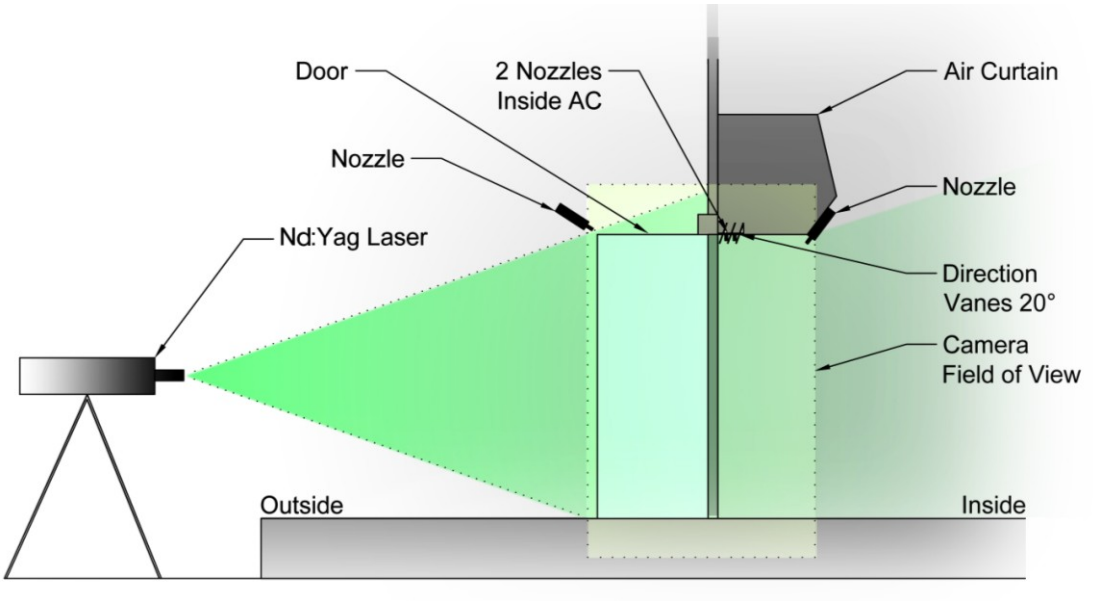

Figure 32. Illustration of the chamber view with the field of view and seeding (nozzle) positions highlighted

It is important to note that all experiments were conducted with the door fully open (both door leaves open at 90°). Based on this final setup, and as seen in Figure 32, the flow through the door could be captured fully. This setup allowed for a high seeding density to be achieved at the doorway - APPENDIX (A) shows pictures of the seeding density. It is important to note that other sending methods were also tested in the chamber.

3.2.2 Experiment Data Acquisition

3.2.2.1 Air Flow and Interior Chamber Pressure

Using the equipment described in section 3.2.1.2, the airflow through the fan (same airflow through the door by mass balance), was measured using the pressure and airflow gauge for the duct blaster system. The process of the measurements would start by (1) activating the air curtain at the desired speed, (2) setting the duct blaster fan's flow to a certain known rate (using the fan controller), (3) waiting for a period of 2-5 minutes for the flow to stabilize, (4) measuring the 10 seconds time average pressure in the chamber (in reference to the ambient pressure). In order to insure the repeatability of the reading, each case was tested twice at different days as seen in the results presented in APPENDIX (B). It is important to note that the average temperature over the testing time was recorded to be 23 °C. In addition, measurements were conducted for the single

door (air curtain off) to be compared with the theoretical curves obtained by Yuill (1996). Table 9 shows the total number of data sets (flow and pressure points).

Table 9. Experimental flow/pressure measurements completed for the validation study

Condition	Measurements
AC Speed 1: Avg. 9.1 m/s	15
AC Speed 2 Avg. 13.75 m/s	16
Single Door	10
Total Number of measurements	**82 (41 conditions × 2)**

3.2.2.2 Particle Image Velocimetry (PIV)

the PIV data acquisition was completed using the software package of the PIV system, FlowManager 4.71 (Dantec Dynamics & Nova Instruments, 2012). Based on the size of the seeds, the airflow conditions of the air curtain and the models available in the literature (presented in section 2.5.1), the optimum delay time, Δt, was calculated to be 800 ųs. By comparing the same flow analyzed using different number of captured frames (images), it was concluded that 31 frame pairs (62 images) for each PIV case was the optimum number (i.e. the minimum number that allowed for the flow to be correctly captured). As proposed by literature, the interrogation area was selected to be 64 × 64 pixels. (X. Cao et al., 2014; G. Cao, Sivukari, Kurnitski, Ruponen, et al., 2010; Li et al., 2010; Hart, 2000)

Based on the methods presented in the literature review (section 2.5.1), the process of processing for the PIV captured data was (1) to correlate the data using the adaptive correlation method with an overlap of 50% (central differencing method with 1.2/2 min peak for validation and an acceptance factor of 0.1), (2) to filter the correlated data using the average filter (3×3 averaging area), and (3) to generate the RMS values of the velocity vectors. The flow scale was generated by using the flow ranges observed in the cases and the average error calculations were based on the standard deviation data reported by the software. Again, to insure the repeatability of the data measured, some selected cases' data were captured two times and compared. Table 10 shows the total number of PIV measurements completed for the validation study.

Table 10. Experimental PIV measurements completed for the validation study

Condition	PIV measurements
AC Speed 1: Avg. 9.1 m/s	12 (incl. 3 repeated)
AC Speed 2 Avg. 13.75 m/s	12 (incl. 3 repeated)
Total Number of PIV measurements	**24**

It is important to note that the pressure ranges and seen in the results are limited by the test equipment used (future research can consider larger pressure ranges) and that the CFD simulations conducted for chamber were only meant to replicate the test conditions. It is also important to note, that despite the limitations, the test results are considerably sufficient to complete the validation of the CFD model.

3.2.3 CFD Simulations for Experimental Setup

Using the data presented in the previous sections, a CFD model of the CUBE and it surrounding was developed using ANSYS Fluent 14.0 (seen in Figure 33). The CFD model used the similar boundary conditions as those available in the real laboratory. The air curtain's supply was modeled based on the real speed profile of the unit with an outward angle of (using UDF input). In addition, the duct blaster fan was modeled as a velocity outlet (with a diffuser modeled as a surface inside the chamber): the pressure in the chamber was controlled and decided by the airflow through the fan. The pressure was calculated based on the same points illustrated in Figure 31. The CFD cases, as proposed by Wang (2013), assumed steady-state flow based on the standard k − ε model (all cases are isothermal, i.e. no temperature differences between the interior and exterior of the chamber).

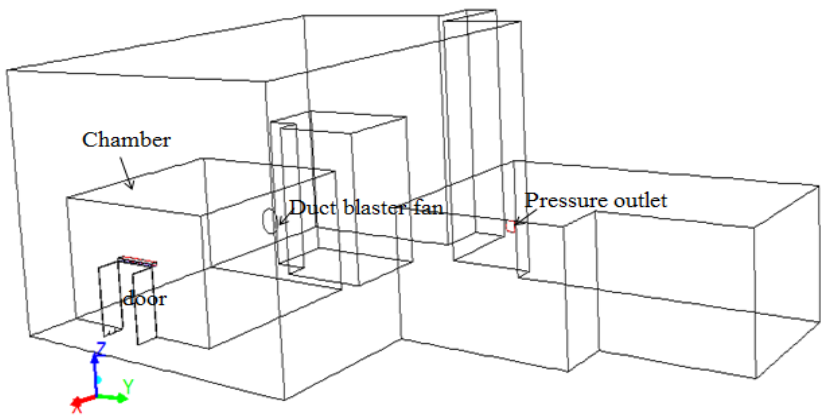

Figure 33. CFD model of the experimental chamber and its surroundings

It is important to note that the 3D and transient characteristics of the real air curtain's flow were not modeled in CFD: only the speed variations were considered. (i.e. a uniform jet at 20° outwards with the variations in speed was modeled). Simulations were conducted for the two experimental supply speeds (namely 9.10 m/s and 13.75 m/s average supply speed) as well as for the single door (air curtain off). The number of simulations conducted is presented in Table 11.

It is also worthy of mentioning that, the CFD model used for the experiments assumes the same CFD parameters as proposed by Wang and Zhong (2014a) in regards to grid sizes and wall functions (and other boundary conditions). Also the CFD modeling method proposed in literature (Wang & Zhong, 2014b, 2014a) of the air curtain unit was used. Only two grid sizes were used and compared for the simulations. However, further simulations with different grid sizes might be needed for a full grid independence study.

3.2.3.1 Air Curtain Modeling Simplifications

Since the model proposed by Wang (2013) assumed a uniform supply speed for the air curtain, a number of simulations were conducted with this assumption (using the average speeds calculated for the two VFD configurations). This step was crucial in the validation process of the modeling method of air curtains. The total number of simulations is presented in Table 11.

Table 11. CFD simulations completed for the experimental validation study

Model	Air Curtain Speed	Simulations
Model including supply speed profile	AC Speed 1: Avg. 9.1 m/s	10
	AC Speed 2 Avg. 13.75 m/s	13
Model assuming uniform speed	AC Speed 1: Avg. 9.1 m/s	4
	AC Speed 2 Avg. 13.75 m//s	4
Single Door	NA	9
Total Number of simulations		40

3.2.4 Testing Different Parameters Affecting Performance

3.2.4.1 Effect of Presence of people

A person model was created and placed in the doorway of the air curtain door and experimental measurements (PIV & flow/pressure) were obtained (presented in Table 12). The location of the person model in reference to the doorway and the setup is illustrated in APPENDIX (A) presents more details about the person model.

Table 12. Experimental data gathered for with a person model in the doorway

Flow/pressure	10 (5 conditions × 2)
PIV	2

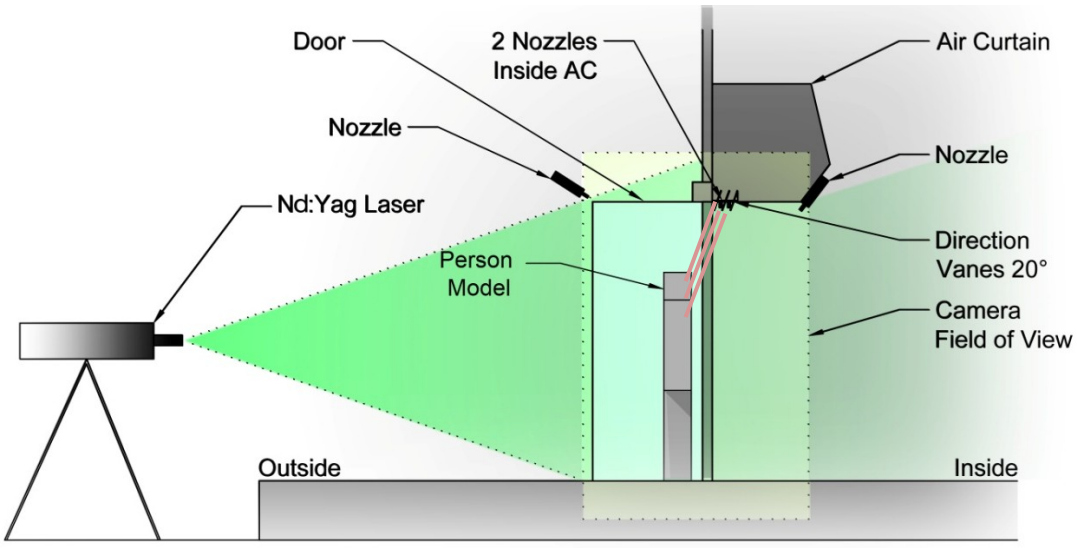

Figure 34. Illustration of the location of the person model within the field of view

3.2.4.2 Effect of Angle

The supply angle of the air curtain operating with an average speed of 13.75 m/s was changed from 20° to 0° (vertical). The effect of the change of angle on the air curtain performance was captured using 11 flow/pressure measurements (22 total measurement points).

3.2.4.3 Effect of Wind

An external fan (a second Duct Blaster Fan) was placed 1.4 meters perpendicular to the door opening plane at the ground level. The supply fan speed (using the flow gauge) was recorded and the experimental measurements were completed (Table 13). The pressure difference across the door was measured at the same points for the main cases

Table 13. Experimental data gathered for the effect of wind on performance

Flow/pressure	12 (6 conditions × 2)
PIV	3

3.2.5 Analysis of Results

3.2.5.1 Calculating of Error in Experiment Results

For the pressure measurements, the DG-700 gauge's reported random error ("DG-700 Pressure and Flow Gauge - The Energy Conservatory," n.d.) is ±1% or ±0.15 Pa. However, since 2 measurements are averaged, the error range of the averaged measurement was calculated based on the measurements (considering the variations in the readings) to be ±1.3% or ±0.21 Pa. The reported random error for the flow measurements with the Series B fan is ±1% or ±0.00472 m^3/s ("Minneapolis Duct Blaster® System - The Energy Conservatory," n.d.).

However, since some error could result from the infiltration of air into the experimental chamber - air leakage from sources other the door (air tightness of the construction), this systematic error was calculated using an air tightness test - seen in APPENDIX (A). The calculated total random and systematic average error in the flow measurements (based on the average error for all the cases presented) in the flow measurements is ±9% or ±0.02 m^3/s.

For the PIV RMS value velocities, the average standard deviation reported by the software for all the PIV cases was calculated to be approximately ±20%.

It is important to note that no propagation of uncertainty analysis was conducted for the experimental data.

3.2.5.2 Comparing Experimental and Simulation Results

For the flow and pressure data, the experimental measurements and the CFD results are both plotted on the same Pressure vs. Flow graphs and direct comparison is used to evaluate the cases. Some numerical comparisons are conducted between the correlated CFD data and the experimental results to calculate the differences in the flow rates at the door.

For airflow fields, the velocity field obtained from the PIV RMS values are compared, qualitatively, to the CFD data at the two measurement planes (namely at the door side-plane and mid-plane). The CFD results were exported to match the field of view captured by PIV. It is important to note that all the results presented in the following section for the PIV and CFD are for the field of view region as illustrated by Figure 35 .

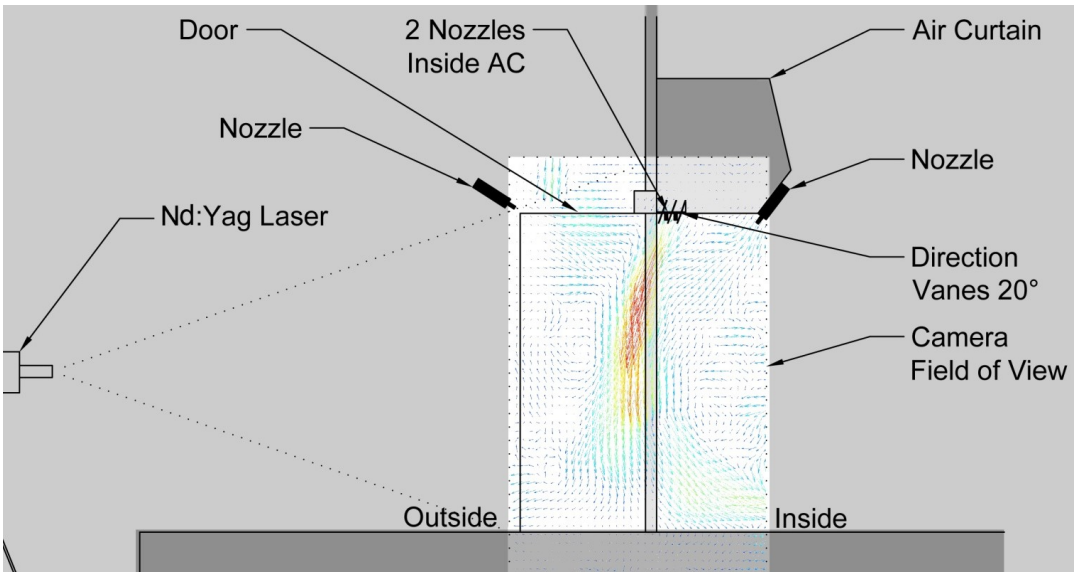

Figure 35. Field of view captured by PIV in relation to the experimental setup

3.3 Results and Discussion

In this section, following the methods proposed in section 3.2 of this chapter, the main results of the experimental validation of the air curtain's CFD modeling method are presented. The results of the blower-door tests are presented in form of graphs for the air infiltration as a function of pressure difference through the door. In addition, the PIV airflow visualization captured at the door are presented in form of vector flow fields. All the experimental data gathered is compared to the CFD simulations results for the analogous case and a discussion of the comparisons is provided. More detailed results for all the presented cases are available in APPENDIX (B).

It is important to note that the pressure conditions tested in the chamber (seen in Figure 36 specifically) were mainly defined and limited based on the equipment used for the experimentation (the details of the equipment used are indicated in section 3.2.1 of this chapter). It is also important to note that the CFD simulations conducted aimed to replicate the tests for the different door scenarios.

3.3.1 Comparing Experimental and Simulation Results

3.3.1.1 Air Infiltration

As seen in Figure 36, the infiltration rates from the experiments (i.e. "Experiment") are compared the CFD simulations (i.e. "CFD" in the figures) for air curtains with different jet velocities (average jet supply jet speed of 9.1 m/s and 13.75 m/s with 20° outward angle). To better show the trends, correlated CFD results based on Equation 27 (i.e. "Simulation Correlation" in the figure) are plotted. Figure 36 also compares infiltration rates through the single door as measured in the experiments and obtained from CFD simulations. In addition, the single door and vestibule door infiltration models from Yuill's study are presented (Yuill, 1996).

The error range (error bars) for the experimental data was calculated and presented in Figure 36 based on the methods proposed in section 3.2.5.1 of this chapter. The results shown in Figure 36 indicate an agreement between the experimental measurements and CFD simulations for both average air curtain supply speeds of 9.1 m/s and 13.75 m/s under different pressure differences. Figure 36 also indicate that both the experiment results and CFD simulations data agree well with the empirical curve developed by Yuill (1996) for the pressure difference range $\Delta P = -0.35 \sim 1.25$ Pa (the experimental data fits Yuill's theoretical curve with an average difference of 3.48%).

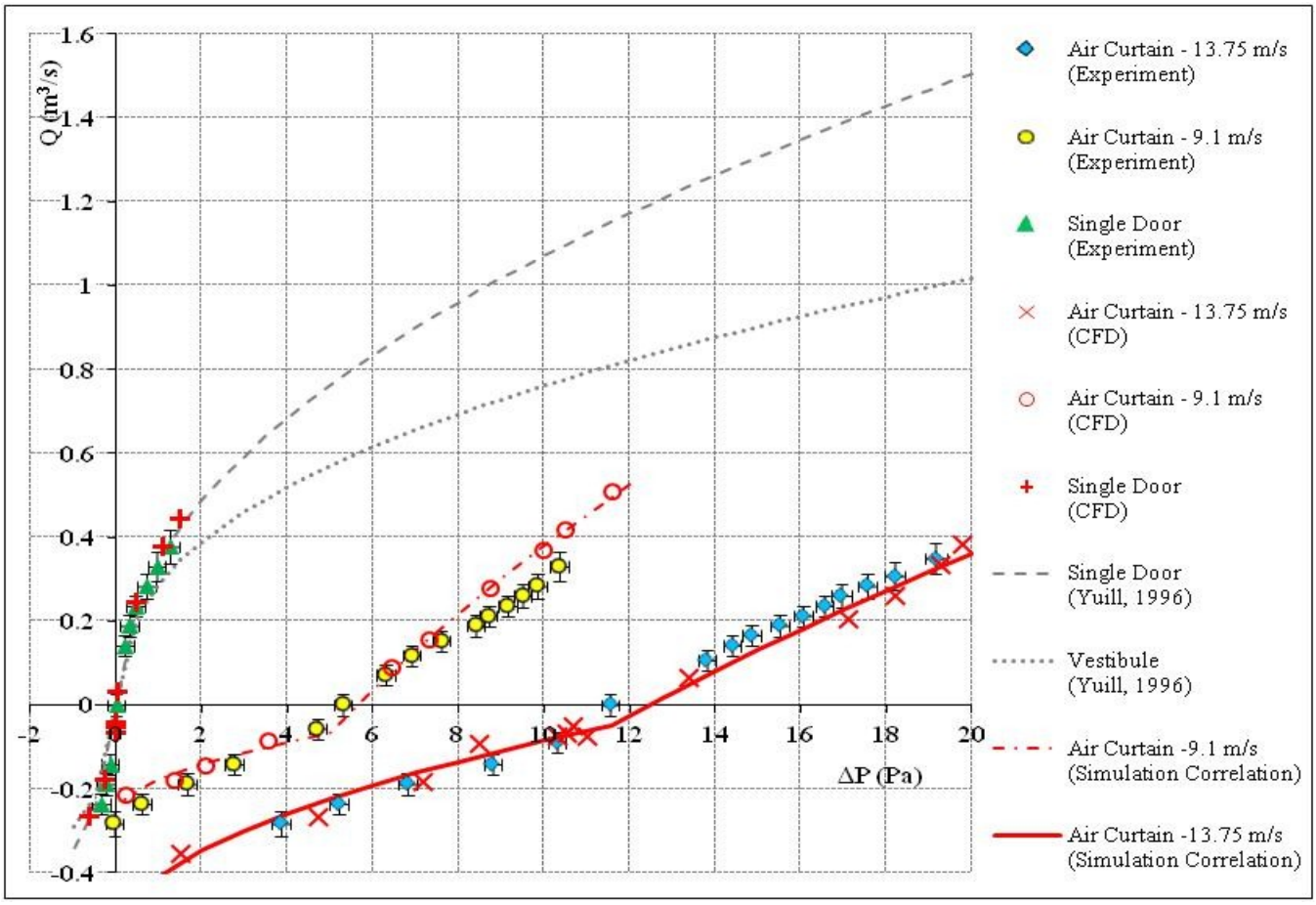

Figure 36. Comparison of experiments and CFD simulations data for the air curtains with different jet velocities (average jet supply speed of 9.1 m/s and 13.75 m/s at 20° outward) and for the single door

Based on the correlation completed for CFD results using Equation 27, the $C_{D,\,90°}$ as well as the $D_{D,\,90°}$ for the air curtains operating at the two speeds were calculated and are presented in Table 14. It can be seen that the flow modifier (which represent the air curtain unit outwards flow) for the 9.1 m/s supply speed case is lower than at that of 13.75 m/s case. For the 9.1 m/s supply the flow coefficient in the optimum condition range is lower than that of the 13.75 m/s case. However, in the inflow breakthrough condition, the 9.1 m/s flow coefficient is much higher than that of the 13.75 m/s. This suggests that when the air curtain is broken through (i.e. the jet does not reach the floor), the unit with the higher supply speed will perform better that those with lower supply speeds. As seen in Figure 36, the upper critical pressure. ΔP_{uc}, for the 9.1 m/s case was approximately 5.3 Pa while that for the 13.75 m/s case was significantly higher at approximately 11.5 Pa.

Table 14. $C_{D,\,90°}$ and $D_{D,\,90°}$ calculated for the tested cases based on the CFD simulations

Air Curtain Average Supply Speed (m/s)	$C_{D,\,90°}$		$D_{D,\,90°}$	
	Optimum Condition	Inflow Breakthrough	Optimum	Inflow Breakthrough
9.1 (ΔP_{uc} = 5.3 Pa)	0.160	0.858	-0.478	-2.033
13.75 (ΔP_{uc} = 11.5 Pa)	0.268	0.684	-0.999	-2.417

It is clear that, compared to the single door and the vestibule door, the measured experiment data and the correlated curves for the air curtain (with both supply speeds) show a significant reduction of air infiltration through the door for a given pressure difference (i.e. The infiltration curves for the air curtain doors are further to the right of Figure 36). The experimental data for the air curtain at both speeds, as well as the CFD data, show the transition from the optimum condition to the inflow breakthrough conditions in both air curtain jet supply speeds validating the proposed theoretical model presented in previous numerical air curtain studies (Wang & Zhong, 2014a; Wang, 2013).

Finally, both the experimental and CFD data indicate that, for the same outward supply angle, the higher jet supply speed (in this research 13.75 m/s average supply speed) can achieve better performance than the lower jet supply speed (in this research compared to 9.1 m/s average supply speed). Thus, when the air curtain is supplying air outwards (in this research 20° outward), the higher the air supply rate the better the air curtain door performs. For the 9.1 m/s average supply speed case, the average difference between the experimental data and the correlated simulation curve was calculated to be 15.07% and for the 13.75 m/s average supply case the average difference was calculated to be 20.67%. This range of difference is acceptable considering that the flow measurements equipment random and systematic error can be as high as 9%. More details on the calculated errors are presented in APPENDIX (B).

It is important to note that the blower-door tests conducted were mostly focused depressurization tests, following similar methods in Yuill's study (1996). The current experimental setup and the equipment allowed for reaching a minimum pressure difference of 0 Pa (with the air curtain average supply of 9.1 m/s). However, testing the more extreme exfiltration breakthrough conditions needs further pressurization and might require modifications to test setup. The detailed results obtained for the experimental cases are provided in APPENDIX (B).

3.3.1.2 Air Curtain Door Airflow and Velocity Profile

Using the PIV system, the captured airflow patterns and velocity fields of the air curtain were captured and are presented in Figure 37, Figure 38, Figure 39 and Figure 40 as the root mean square values of velocity (RMS values). The PIV RMS values are compared the in-plane velocity magnitude extracted from the CFD simulations for the corresponding case - PIV data labeled in (letter) and the corresponding CFD case labeled with (letter)'. Example PIV (A) and CFD (A'). It is important to note that, based on the methods proposed in section 3.2.5.1 of this chapter, the deviation of the PIV RMS values calculated exceeded ±20% based on the reported standard deviation for all the data sets. In addition, the results obtained from the PIV were repeatable based on the repeatability check proposed (section 3.2.2). This large deviation needs further investigations. However, it can be due to a number of factors including the transient and three-dimensional (3D) nature of the air curtain flow (that are intensified limitations of the used 2D PIV) as well as the errors due to the seeding method used.

The PIV RMS values and the CFD velocity fields presented in Figure 37, Figure 38, Figure 39 and Figure 40 confirm the three (3) flow scenarios (operation conditions) exist for air curtains: optimum condition, inflow breakthrough, and outflow breakthrough as defined in the previous studies (Wang & Zhong, 2014b, 2014a; Wang, 2013). The PIV RMS values also confirm that air curtains with higher air supply speed is able better reduce air infiltration. The air curtain with an average supply speed of 13.75 m/s at 20° outwards maintains its optimum condition up to around 10 Pa, while the air curtain with an average supply speed of 9.1 m/s at 20° outwards maintains its optimum condition only up to around 5 Pa. As seen in Figure 37 and Figure 39, the air curtain RMS values captured by PIV present the same trends seen in the CFD simulations at analogous pressure differences for the door side-plane. However, Figure 38 and Figure 40 indicate that the PIV RMS data captured at the door mid-plane are somehow different to the CFD data at analogous pressure differences. This difference can be due to some simplifications in modeling the air curtain unit's supply which can be the scope of further investigations: the air curtain tested had the motor placed at its center which created turbulences in the air jet as clearly seen in Figure 38 and Figure 40. However, what is most interesting to note is that, the PIV results indicate that because of the variations in the supply speed and characteristics of real air curtains, the same unit under the same conditions might experience breakthrough condition in only part of the jet.

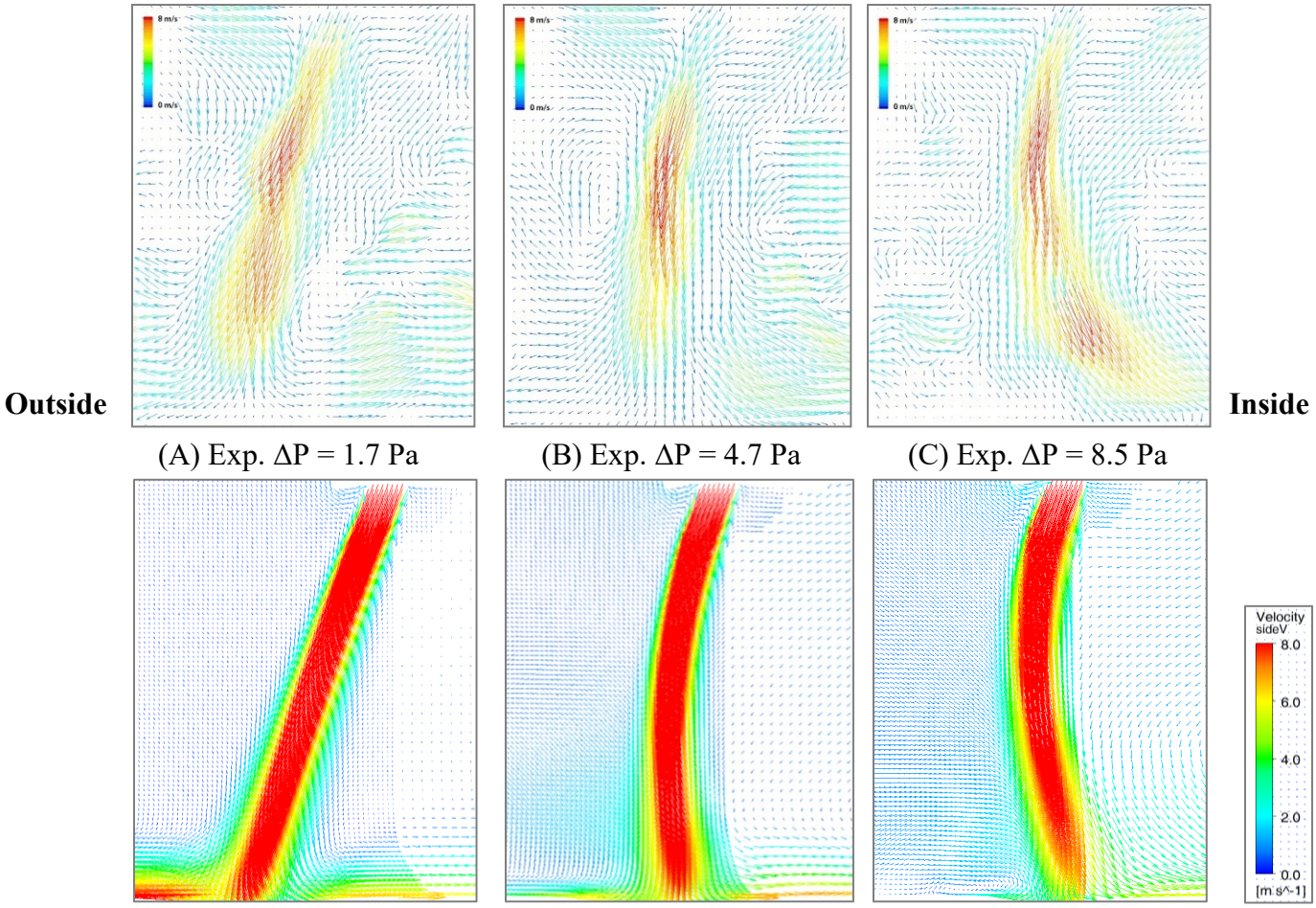

(A) Exp. ΔP = 1.7 Pa (B) Exp. ΔP = 4.7 Pa (C) Exp. ΔP = 8.5 Pa

(A') CFD. ΔP = 1.3 Pa (B') CFD. ΔP = 3.6 Pa (C') CFD. ΔP = 8.7 Pa

Figure 37. Comparison between experimental and CFD simulation flow visualization at door side-plane for the air curtains with an average supply speed of 9.1 m/s at 20° outwards at different pressure conditions - (A) & (B) are optimum condition and (C) is inflow breakthrough

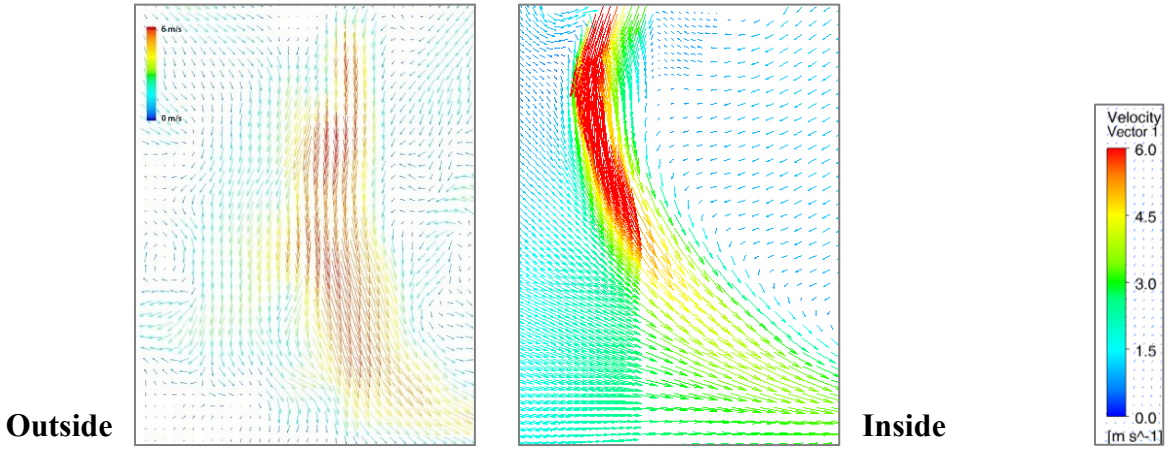

(A) Exp. ΔP = 8.5 Pa (A') CFD. ΔP = 8.7 Pa

Figure 38. Comparison between experimental and CFD simulation flow visualization at door mid-plane for the air curtain with an average supply speed of 9.1 m/s at 20° outwards - Inflow breakthrough

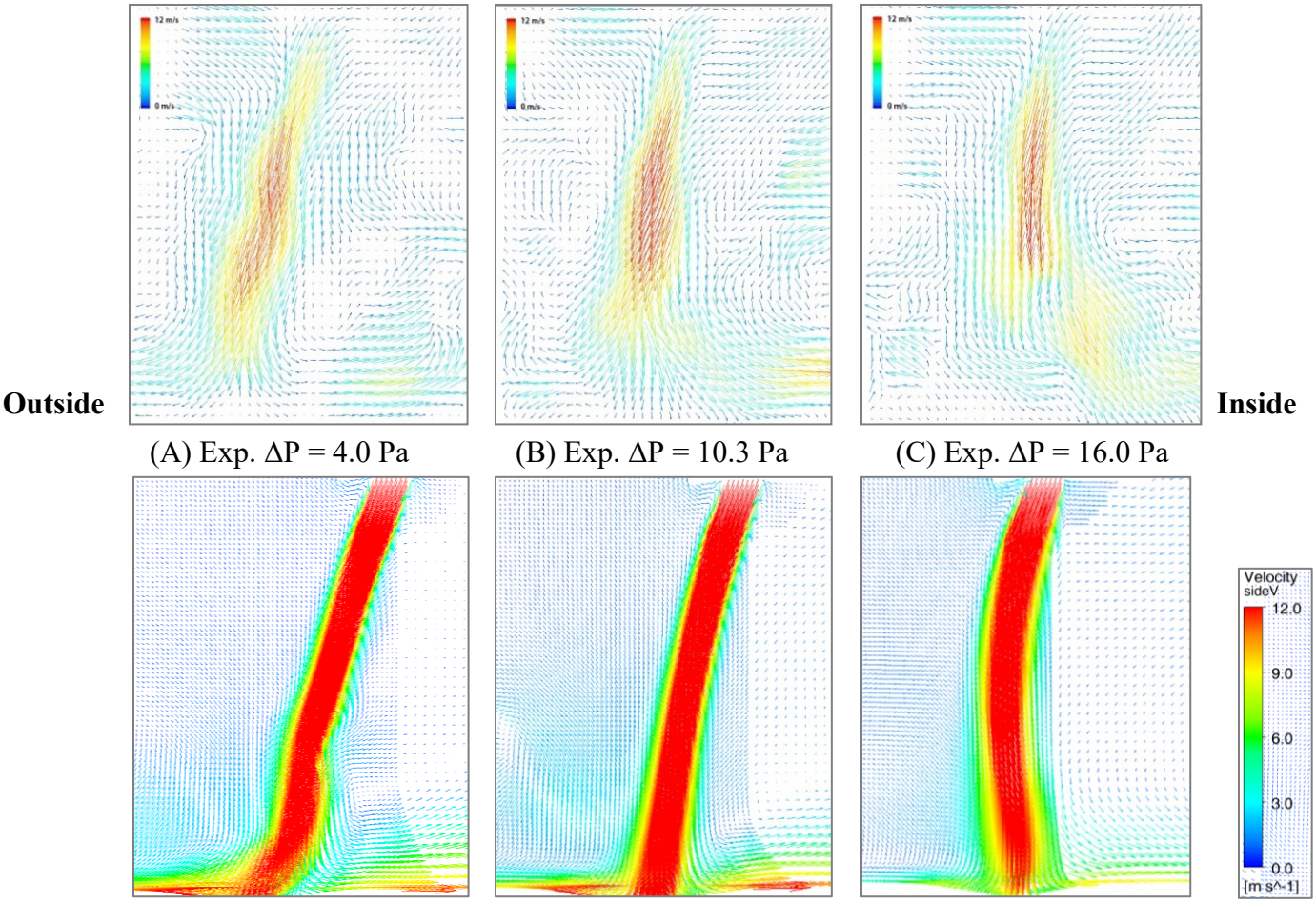

(A) Exp. ΔP = 4.0 Pa (B) Exp. ΔP = 10.3 Pa (C) Exp. ΔP = 16.0 Pa

(A') CFD ΔP = 4.7 Pa (B') CFD. ΔP = 10.3 Pa (C') CFD. ΔP = 17.1 Pa

Figure 39. Comparison between experimental and CFD simulation flow visualization at door side-plane for the air curtain with an average jet supply speed of 13.75 m/s at 20° outwards at different pressure conditions - (A) & (B) are optimum conditions and (C) is inflow breakthrough

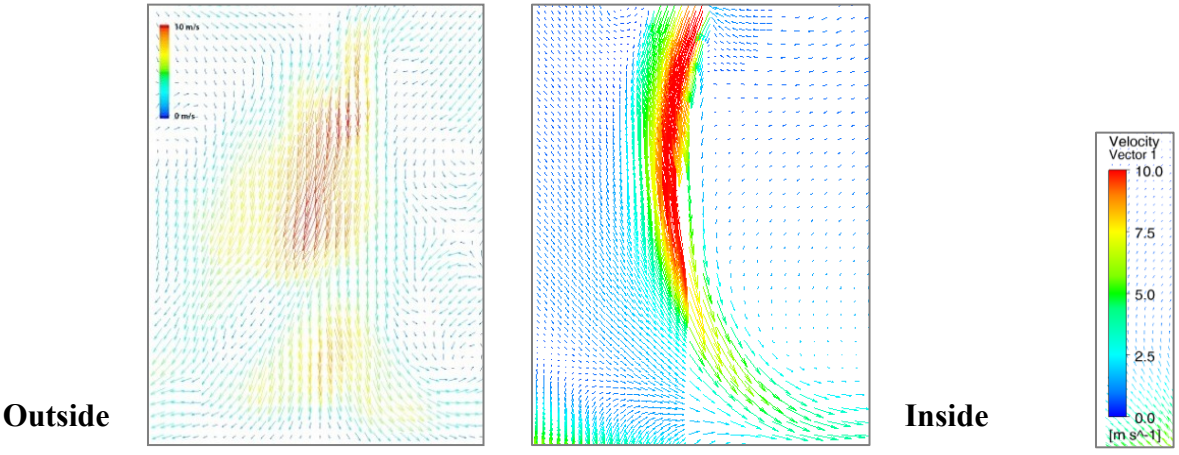

(A) Exp. ΔP = 10.3 Pa (A') CFD. ΔP = 10.3 Pa

Figure 40. Comparison between experimental and CFD simulation flow visualization at door mid-plane for the air curtain with an average supply speed of 13.75 m/s at 20° outwards - Inflow breakthrough

It is important to note that the comparison between the CFD and PIV velocity flow fields was done mainly qualitatively. It is also important to note that the similarity referred to between the two types of data is mainly in regards to the general flow trend. The comparison was completed based on the assessment of the jets' curvature, direction and general velocity profile.

3.3.2 Air Supply Modeling Simplifications

As seen in Figure 41, for the two tested supply speeds, further simplification of the model of the air curtain that assumes a perfectly uniform air supply (disregarding the real supply profile) can still capture the air curtain unit performance. Based on the results obtained, the simplified uniform model used in previous numerical studies (Wang, 2013) is considered to be accurate in capturing the infiltration characteristics of air curtain doors. These findings confirm that the tested air curtain's overall uniformity level (the overall variation of the supply speed, angle and flow condition especially at the center of the unit) is within the acceptable level (i.e. not significantly effecting the performance of the unit overall). However, further testing is needed to investigate further the effect of uniformity of the performance of the air curtain unit.

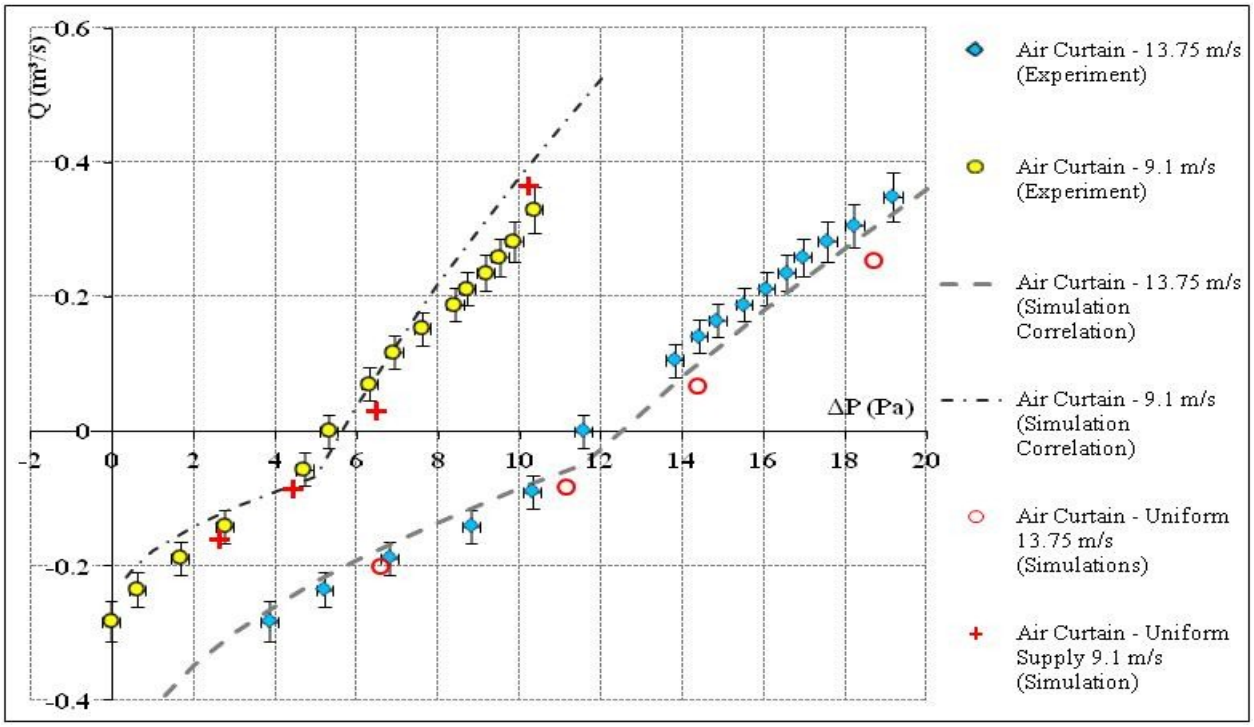

Figure 41. The CFD results for the air curtain with uniform supply compared to experimental tests results and the correlated air curtain simulations that consider the tested unit's supply profile

3.3.3 Effects of Wind, Supply Angle and People on the Air Curtain Performance

Following the methods proposed in sections 3.2 of this chapter, a number of experimental data where gathered for the air curtain door performance for the average supply speed of 13.75 m/s under different conditions. More detailed results obtained for the experimental cases are provided in APPENDIX (B). It is important to note that the scope of the experimental work in this project was limited to the validation of the numerical CFD air curtain simulation and theoretical modeling methods and that the results shown in Figure 42 are only preliminary. Each of the conditions tested and presented can be subject of future investigations and studies.

3.3.3.1 Airflow and Pressure Measurements

As shown by the yellow squares in Figure 42 which fall close to the performance curve of the original case (show by the solid grey line in Figure 42), the air curtain door performance is almost unaffected by external wind of 10 m/s (22 MPH - 20 knots, Beaufort number 5 - fresh breeze). The air curtain door with the external wind continues to outperform the single door and vestibule door (based on the empirical curves developed by Yuill (1996).

Comparing the performance of the air curtain door when the air curtain is supplying air at an average supply speed of 13.75 m/s at 0° angle (shown by the red circles in Figure 42) and at 20° outwards (solid grey line in Figure 42) shows a significant decrease in the performance at the smaller angle (i.e. 0° angle). The red circles are all shifted to the left (illustrate a similar performance as that of the supply of 9.1 m/s at 20° accidentally). This data proves that the supply angle of the air curtain is one of the critical parameters of the air curtain door performance.

Finally, when conducting experiments with the model of dummy person below the air curtain's jet (data shown by the red triangles in Figure 42), the air curtain door performance seems unaffected and even slightly improved (red triangles and positioned slightly right to the original's case curve and data points).

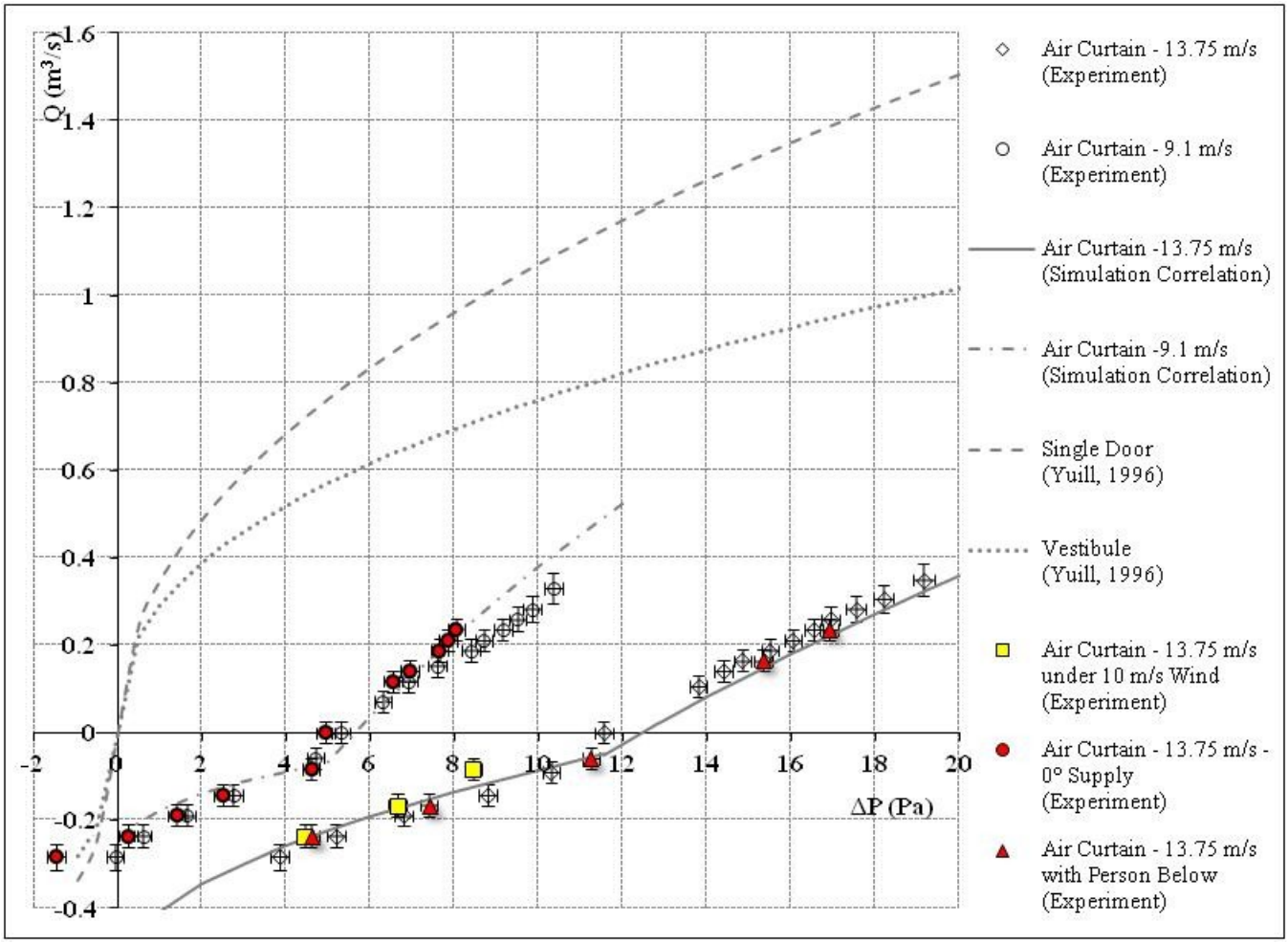

Figure 42. Comparison of measured air curtain performances under the conditions of a) no wind (by default) and 10 m/s wind, b). 0° and 20° (by default) supply jet angles, and c) without person (by default) and with a person below the air curtain

3.3.3.2 Airflow and Velocity Profile

3.3.3.2.1 Effect of external wind on air curtain door performance

As seen the in Figure 43 and Figure 44, when comparing the captured PIV data for the air curtain's flow under normal conditions (no wind and no person) and with 10 m/s external winds under the same pressure difference condition, the air curtain's flow is shows no or minimal change. The presented PIV data confirms the findings shown in Figure 42 that indicated that the air curtain door performance is almost unaffected by the external wind of 10 m/s.

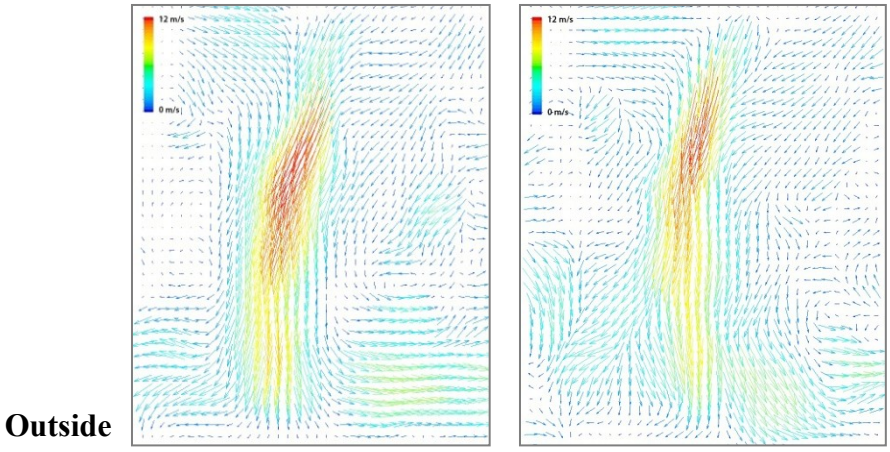

(A) No wind, no person (B) 10 m/s wind, no person

Figure 43. PIV visualization of RMS at the door side-plane with average air curtain supply speed of 13.75 m/s at 20° outwards for (A) no wind and no person , (B) 10 m/s wind (ΔP = 8.5 Pa)

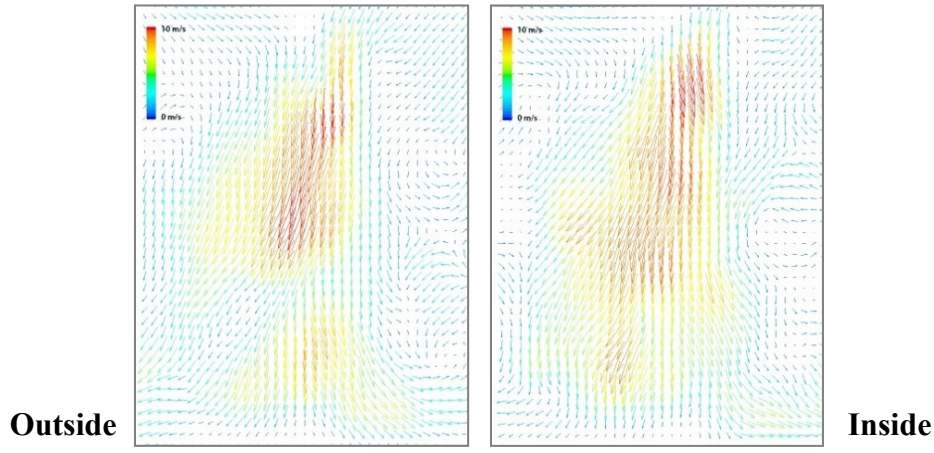

(A) No wind, no person (B) 10 m/s wind, no person

Figure 44. PIV visualization at the door mid-plane with average air curtain supply speed of 13.75 m/s at 20° outwards for (A) no wind and no person, (B) 10 m/s wind (ΔP = 8.5 Pa)

3.3.3.2.2 Effect of presence of a person on air curtain door performance

As shown in Figure 45, the captured PIV RMS data for the air curtain's flow under normal conditions (no wind and no person) and in the case with the person model under the air curtain jet under the same pressure difference condition at the door mid-plane. Figure 45 show that the air curtain's jet moves around the person while still providing the appropriate sealing for the door against air infiltration. Based on the infiltration characteristics shown in Figure 42 and the PIV data for the flow around the person, it is appropriate to conclude that the flow at the door side-plane is unaffected by the presence of the person. In addition, it is concluded that the person

present in the doorway can slightly increases the resistance of flow through the door (i.e. to some extent improving the performance of the air curtain door).

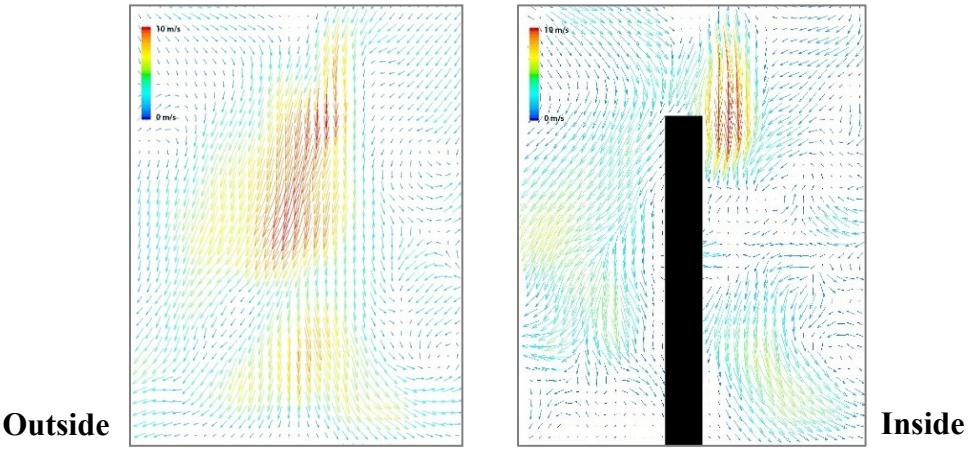

(A) No wind, no person (B) Person below, no wind

Figure 45. PIV visualization at the door mid-plane with average air curtain supply speed of 13.75 m/s at 20° outwards for (A) no wind and no person, (B) dummy person below air curtain's jet (ΔP = 11.2 Pa)

3.4 Conclusion

A specially designed experimental test chamber, similar in dimensions to that used by Yuill (1996), equipped with an air curtain was constructed at Concordia University (the Concordia University Building Environment - CUBE - test chamber). The chamber was used for the validation of the CFD modeling method and the theoretical modeling of air curtains on a small scale door (section 3.2.1.1). The data presented in this chapter indicate that the experimental infiltration rates measured through the chamber's air curtain door conform well to the data obtained from numerical CFD simulations within the pressure difference range of -2 Pa to 20 Pa. The data also confirmed the ability of the model developed by Wang et al. (Wang & Zhong, 2014a; Wang, 2013) to estimate the air curtain performance in the optimum and inflow breakthrough condition using the correlation proposed in Equation 27.

The blower-door tests conducted in the CUBE test chamber also showed that:

- The infiltration rates measured through the air curtain door are significantly lower than the measured infiltrations through the single door

- The infiltration rates measured through the air curtain door are significantly lower than the measured as well as the theoretically calculated infiltrations through a vestibule door of the same size by Yuill (1996).
- The higher the air curtain supply speed, the better the air curtain performs, i.e. it is able to continue to operate in the optimum condition at higher pressure differences. However, the higher supply speed might result in larger exfiltration under optimum operation condition
- The larger the outward angle of the air curtain supply, the better it is able to reduce air infiltration. Again, the higher supply angle might result in larger exfiltration in the optimum and outflow breakthrough conditions
- The performance of the air curtain door tested was barely affected by the outdoor wind of up to 10 m/s and continued to main its better performance
- The presence of a person in the doorway may slightly improve the air curtain performance by blocking air infiltrations

Two-dimensional (2D) Particle image velocimetry (PIV) system with a specially designed and fabricated seeding helium filled soap bubble (HFSB) apparatus (section 3.2.1.3.1) was utilized to visualize the airflow at two vertical planes in the door for an isothermal air curtain operating. The captured PIV RMS data for the airflows at the air curtain door confirmed that the three airflow regions of air curtains found in previous air curtain numerical studies (Wang & Zhong, 2014a): namely, inflow breakthrough, outflow breakthrough and optimum conditions. The captured RMS PIV data is also consistent with the infiltration data gathered from the blower-door tests (i.e. the air curtain's airflow captured by PIV is seen to be conforming to the expected airflow region for each of the pressure conditions tested). In addition, comparing the CFD airflow velocity fields with the experimental PIV RMS values captured show a general agreement. The noticeable differences between the CFD airflow and the captured airflow at the door mid-plane are mainly due to the specific complexities (turbulences and 3D flow) caused by the tested center motor air curtain model (Section 3.3.1.2).

The data presented in this chapter also confirm that modeling the tested air curtain with a uniform air supply in CFD can still accurately capture the air curtain performance (in regards to infiltration at specific pressure difference condition) (section 0). This confirmed that the air curtain tested was within the accepted uniformity level as indicated by standards (Air Movement

and Control Association International, 2012b). Air curtain flow uniformity as well as the effect of wind and people on the sealing efficiency can be the focus of further studies.

Based on both types of experimental data gathered at the doorway, (namely; infiltration/pressure measurements and visualized airflow) at the doorway, it is concluded that the air curtain modeling method used in previous numerical studies (Wang & Zhong, 2014a; Wang, 2013) is valid and is able to accurately capture the performance of various air curtain doors in regards to air infiltration through double swing doors.

It is also recommended that further experiments are needed to investigate the effect of air curtain uniformity on the performance of the units (i.e. the infiltration curves) and its effect on the air curtain jet shape, velocity profile. It is also important to investigate whether the existing theoretical models, by Wang & Zhong (2014a) and Hayes (1968), are accurate to describe the characteristics of air curtains with different uniformities.

4 COMPUTATIONAL FLUID DYNAMICS SIMULATIONS

4.1 Introduction

Following the conclusions of Chapter 3, this chapter presents the methodology, results and discussion of a new and extended numerical study conducted for air curtain doors.

This research uses a similar CFD model and setup as proposed by Wang (Wang, 2013) (the details of the model are presented in section 2.3 of the literature review and illustrated in Figure 10). The main scope of this task is to conduct an extensive CFD numerical study, using ANSYS Fluent 14.0 (ANSYS, 2011), to investigate the performance of different air curtain doors (air curtain units with different discharge angles and speeds) and that investigates the effect of the presence of people in the doorway. In addition, a new correlated performance curve for the air curtain door with the best performance (for this study with an air discharge of 20 m/s at 20° outwards with a person in the doorway) are developed (following the methods proposed by Wang et al. (Wang & Zhong, 2014a; Wang, 2013).

No grid independence study was conducted within the scope of this study since the model used was previously validated and published (Wang & Zhong, 2014a; Wang, 2013).

It is important to note that the input and work of Dahai Qi (as stated in the contributions of authors section), were key in obtaining the results presented this chapter.

4.2 Methodology

4.2.1 Varying the Supply Angle and Speed of Air Curtains

4.2.1.1 Parameters

Using the CFD model (illustrated in Figure 10), 420 CFD simulations were conducted for an air curtain door (2 × 2.4 m (W × H)) with the air curtain supplying air at 10, 15 and 20 m/s and 10°, 15° and 20°. The air supply nozzle size used for this study is 0.08 m × 2 m (W × H). These simulations are conducted for a fully open door (double swing automatic door with both leaves open at 90°. Table 15 presents a summary of the cases simulated.

Table 15. Summary of CFD simulation cases conducted for the units with different supply speeds and angles

	Winter Mode	**Summer Mode**
Outdoor Temperature (˚C)	-40, - 20, 10	25, 30, 40
Indoor Temperature (˚C)	21	24
Pressure Difference (Pa)	-20, -10, -5, -3.5, -2.5, -1.5, -1, -0.5, 0, 10, 20, 30, 40	
Door Opening Angle (˚)	90	
Air Curtain Velocity (m/s)	10,15,20	
Air supply angle (^{0})	10,15,20	
Total number of simulations	**420**	

4.2.1.2 Key Outputs

The results of the simulations conducted for the various air curtain supply speeds and angles are compared and presented non-dimensionally using the correlation methods proposed by Wang (2013) in graphs seen below (based on Equation 27).

$$\frac{Q}{A\sqrt{\left(\frac{2}{\rho}\right)}} \quad VS. \quad \sqrt{\Delta P}$$

Where Q is flow rate in m^3/s,
A is door opening area in m^2 ,
ρ is air density in kg/m^3, and
ΔP is the pressure difference across the door in Pa.

Some results are also compared to the performance of single doors (doors without air curtains) obtained using the model developed by Yuill (1996).

4.2.2 Full Door Operation Simulations Design

Based on the results of the parametric simulations (presented in Table 15), the best performing air curtain door (i.e. air curtain with a supply speed of 20 m/s at 20°) is further investigated. CFD simulations of the door with different opening angles are conducted in order to develop a correlated performance curve using the methods proposed by Wang & Zhong (Wang & Zhong, 2014a; Wang, 2013). The correlation was done using Equation 10 and Equation 26. Table 16

shows the summary of the simulation cases conducted. The summary of all the CFD cases conducted in the study is presented in APPENDIX (C).

4.2.2.1 Effect of People on Air Curtain doors' Performance

A number of simulations are also conducted with a model of person (scaled from model used in the experimental validation presented in 3.2.4.1 to be with a total height of 1.76 m) in the doorway to capture the effect of the presence of the people on the performance of the air curtain door. It is important to note that the person is assumed to be present in the doorway only when the doors are fully open (i.e. doors at 90°). Thus the presence of the person only affects the flow during section (b) of the door operation cycle (the analysis of the door cycle is presented in section 2.1.3.1 and illustrated in Figure 3). It is also important to note that, the definition of people in the doorway used in this research is the presence of the person/people below the air curtain as illustrated by Figure 46.

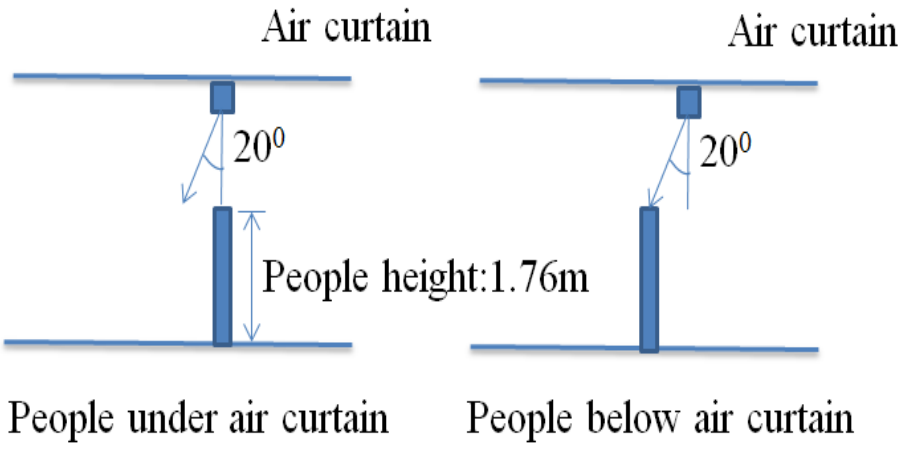

Figure 46. The position of person (people) in the doorway, the people below air curtain condition is used in this research (seen on the right)

Table 16. Summary of CFD cases conducted for the full door operation cycle

	Winter Mode	**Summer Mode**
Outdoor Temperature (˚C)	-40, - 20, 10	25, 30, 40
Indoor Temperature (˚C)	21	24
Air Curtain Temperature (˚C)	21	24
Pressure Difference (Pa)	-20, -10, -5, -3.5, -2.5, -1.5, -1, -0.5, 0, 10, 20, 30, 40	
Door Opening Angle (˚)	10, 30, 45, 60, 90 (90 also with people below)	
Air Curtain Velocity (m/s)	20	
Air supply angle (^{0})	20^0	
Total number of simulations	**390** (270 new simulations)	

4.2.2.2 Key Outputs and Analysis of Results

The main outputs of the CFD simulation for the full door operation cases are the correlated performance curves. The performance is presented in as curves of air infiltration rates as a function of pressure difference. The upper and lower critical pressure differences are also determined through the analysis of the CFD simulation results. ΔP_{uc} is the point over which inflow breakthrough takes place. ΔP_{lc} is the point under which outflow breakthrough takes place. The data is compared to the theoretical infiltration rates of single and vestibule doors of the same size obtained by the model proposed by Yuill (1996).

The models of the air curtain used in this research is not created to reflect the performance of any real unit, but they are rather hypothetical; The air curtain units model are assumed to have perfectly uniform supply. However, it is important to note that, based on the results of the experimental validation; these curves can accurately predict the performance of air curtain units with similar air supply speeds and angles that are within the accepted uniformity level set by the AMCA (Air Movement and Control Association International, 2012b).

4.3 Results and Discussion

In this section, following the methods proposed in section 4.2 of this chapter, the CFD simulations results are presented. Using the full size door model (Wang & Zhong, 2014a), the effects of varying the supply angle and speed of air curtains are presented in the form of graphs that compare the performance of the different a fully open air curtain door. In order to obtain the infiltration characteristics through the air curtain door for a full door operation cycle, the methods detailed in section 4.2.2.2 are then used to conduct further analysis for one air curtain

door (based on the unit that shows the best performance for both supply angle and speed variations). Finally the effect of the presence of people below the jet of the selected air curtain is presented. More detailed results for all the presented data are available in the appendices.

4.3.1 Effect of Varying the Supply Angle and Speed on Air Curtain Door Performance

4.3.1.1 Effect of Supply Speed

As seen in Figure 47, when comparing air curtain units supplying air at 20°, the air curtain door with the unit supplying air at 20 m/s is seen to significantly reduce the infiltration through the fully open door when compared to slower supply speed conditions (the infiltration curve is shifted to the right). It is also important to note that the higher supply speed air curtain door shows lower infiltration in the positive pressure difference region and lower (more positive) exfiltration in the negative pressure difference region when compared to the other two cases. However, during the optimum operation condition the higher the supply speed the more exfiltration is caused by the air curtain door. These results confirm the experimental findings of presented in chapter 3. Cases with other supply angles at the 3 different supply speeds (10, 15 & 20 m/s) are presented in APPENDIX (D).

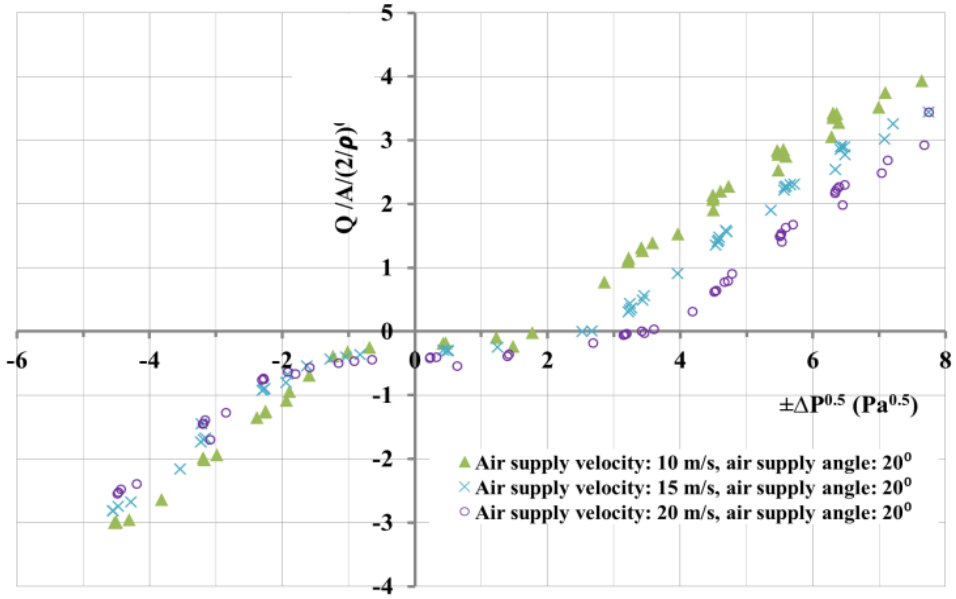

Figure 47. Performance the fully open air curtain door (door at 90°) with air supply of 10, 15 & 20 m/s at 20°

4.3.1.2 Effect of Supply Angle

As seen in Figure 48, when the air curtain unit is supplying air at 20 m/s, the air curtain door performs slightly better with unit supplying air at 20° outwards in the positive pressure difference region in comparison to smaller outwards angles (the infiltration curve is shifted to the right). This observation again confirms the experimental findings presented in Chapter 3. However, it is observed that the air curtain door with larger supply angle (20°) increases the exfiltration rates in the negative pressure difference region; thus, when the indoor pressure is higher than the outdoor pressure, the exfiltration through the door with the air curtain supplying air at 20° is higher than when it is supplying air at lower outwards angles. This case has not been investigated experimentally due to the experimental setup limitations presented in section 3.2.1. Cases with other supply speeds for the 3 different supply angles (10°, 15° & 20°) are presented in APPENDIX (D).

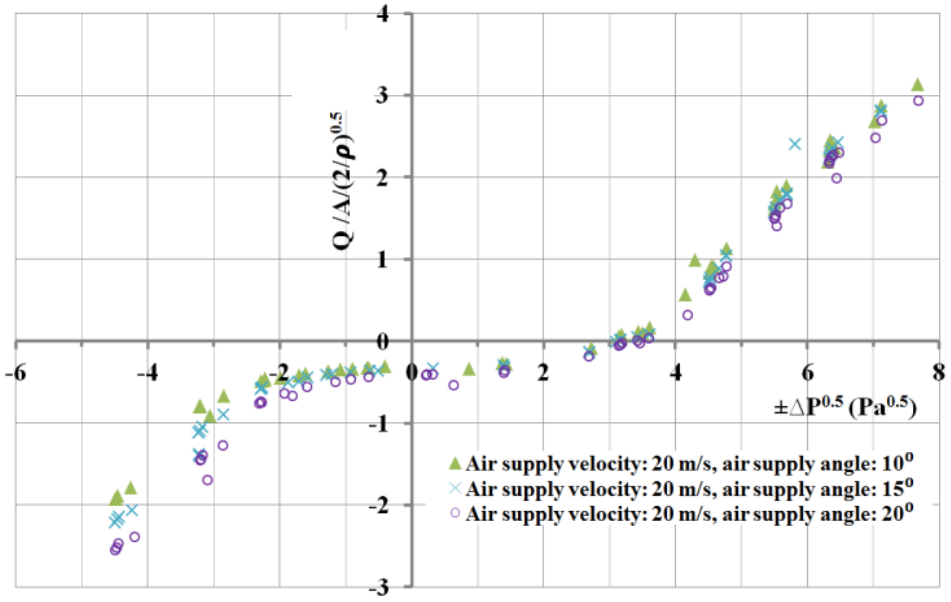

Figure 48. Performance the fully open air curtain door (door at 90°) with air supply of 20 m/s at 10°, 15° and 20°

4.3.1.3 Best Performing Air Curtain Unit

Based on the data presented in Figure 47 and Figure 48, and considering the scope of this research in the reduction of infiltration through doors, it is concluded that, for within the different cases simulated, the air curtain door with a unit supplying air at 20 m/s at 20° shows the

best performance. The air curtain unit with the highest supply speed and largest outwards supply angle showed the lowest infiltration rates through the fully open door in the positive pressure difference range. The air curtain unit with the 20 m/s and 20° is used for all further investigations in this research. However, it is concluded that the air curtain supply angle is an important factor that needs to be well considered during the design, commissioning and installation of the units. It is recommended that further investigation and experimentation for the effect of the supply angle on the air curtain performance is needed, especially in the negative pressure region (exfiltration region).

4.3.2 Full Door Operation Infiltration Calculation

Following the infiltration analysis method proposed in section 4.2.2.2 for full door operation cycles, Figure 49 shows the calculated infiltration characteristics of the full size air curtain door (with air curtain supply of 20 m/s at 20° outwards) for 100 P_h. Figure 49 also shows the infiltration characteristics of the same air curtain door with consideration of a person in the doorway (people below air curtain) as well as the infiltration through a vestibule door and a single door as proposed by Yuill (1996) (extrapolated in the negative pressure range).

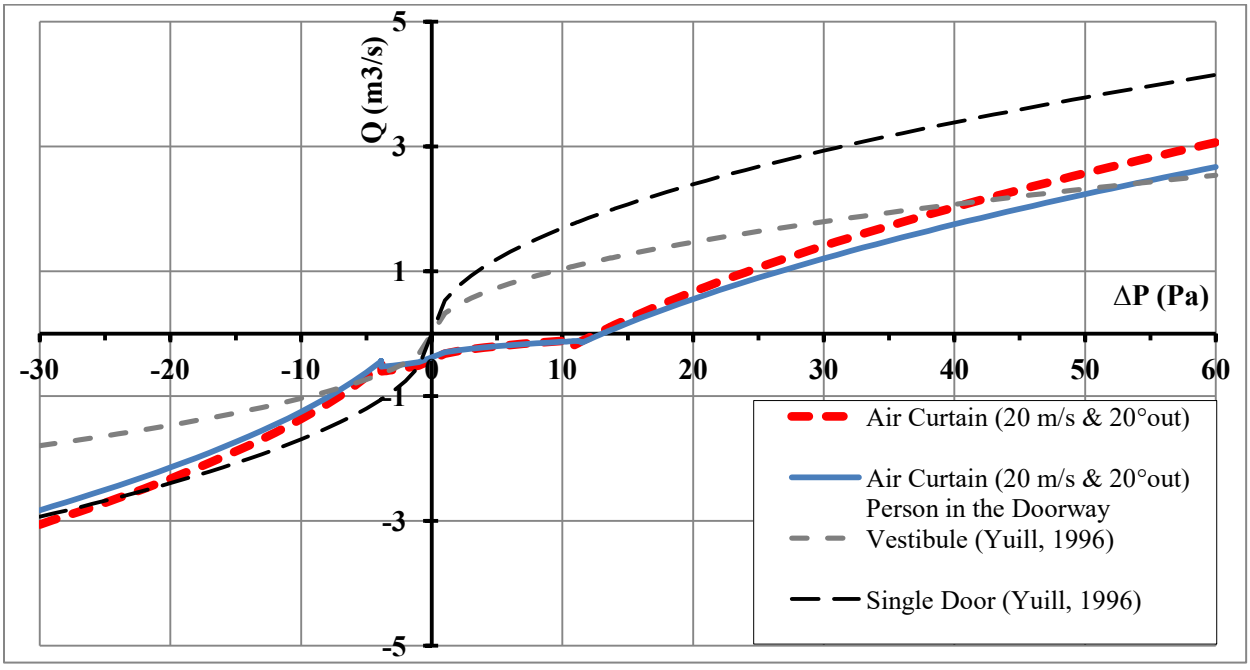

Figure 49. Infiltration and exfiltration characteristic of the air curtain door modeled in with and without consideration of the person model (20 m/s supply at 20° outwards - full operation cycle) in comparison the single and vestibule doors (P_h = 100)

Based on the curves presented in Figure 49, the air curtain door with a supply of 20 m/s at 20° outwards has lower infiltration and exfiltration rates than the vestibule door (outperforms the vestibule door) within the pressure range of -6 Pa < ΔP < 42 Pa. It is also observed that the presence of a person in the doorway, specifically below the air curtain, slightly improves the air curtain performance: the air curtain door outperforms the vestibule door for a wider pressure range of -7 Pa < ΔP < 54 Pa (Qi et al., 2015). Again, this finding is consistent with the experimental data gathered and presented in chapter 3.

It is important to note that a linear relationship between the infiltration rate and the P_h was observed. Thus factors (usage correction factor, F_u) for the infiltration through the air curtain door at different P_h were developed based on the results and were used in the airflow simulations presented in chapter 5 - presented in APPENDIX (D).

4.4 Conclusions

An extensive numerical study of more than 600 CFD cases was conducted for air curtain doors based on the modeling method validated in Chapter 3 using ANSYS Fluent 14.0. Simulations were conducted for air curtains with air supply of 10, 15 and 20 m/s and 10°, 15° and 20° outwards, with different door opening angles and with and without people in the doorway.

The analysis of the parametric CFD results (section 4.3.1) indicated that the air curtain door with an air supply of 20 m/s and 20° outward and with a person in the doorway has the best performance of all the simulated cases (details on the cases and their setup are found in section 4.2.1).

Following Wang's adoption to Yuill's method for determining flow coefficients for single door and vestibule door (Wang & Zhong, 2014a; Yuill, 1996) (section 2.1.3.1 and 2.3), the infiltration correlations for the mentioned air curtain door were developed for a full door opening cycle (Figure 49). The correlated simulation results (for the air curtain supplying air at 20 m/s and 20° outward and with a person in the doorway) demonstrate that the air curtain door outperforms the vestibule door within the pressure range of range of -7 < ΔP < 54 Pa.

It is also seen that more studies are needed to investigate characteristic of air curtain doors in the exfiltration regions (in both the optimum and outflow breakthrough conditions) with a focus on the transition regions (upper and lower critical pressure points). In addition, further

investigations on the effect of the transient movement of the door leaves and the person movement on the performance of the air curtain doors can be the focus of future studies.

5 ENERGY SIMULATIONS

5.1 Introduction

Using the correlated infiltration curve for the air curtain with a supply speed of 20 m/s at 20° (presented in Figure 49) and the infiltration models developed by Yuill (1996), energy simulations for the strip mall and outpatient healthcare reference building model, were conducted using EnergyPlus. The main aim of these simulations is to capture the energy savings impact of air curtain doors in these commercial reference buildings. It is important to note that the buildings were selected based on the results of the PNNL study presented in section 0 (Cho et al., 2010).

Energy simulations are conducted in 16 climate zone locations for the two buildings (strip mall and outpatient healthcare reference building models) using the two infiltration rates calculation methods identified in the literature (namely the ASHRAE Method and CONTAM-EnergyPlus Method presented in section 2.4.2). The results are analyzed and the national weighted average savings are calculated (following the methods presented in section 2.4). When using ASHRAE Method (presented in section 2.1.3.1.3) the sensitivity of the infiltration rates to the outdoor temperature and door usage rate is calculated. When using the airflow simulation method (i.e. CONTAM -EnergyPlus Method), the sensitivity of the energy usage to the door usage frequency, building orientation and wind pressure coefficients is calculated.

5.2 Methodology

5.2.1 Buildings' and Software Parameters

Based on the literature reviewed (presented in section 2.4.1), the commercial reference building models, weather files and simulation software that used are as follows:

- for the energy models, the ANSI/ASHRAE/IES Standard 90.1 Prototype Building Models that are compliant with ASHRAE 90.1-2013 are used (Deru et al., 2011). The distinct models are available as EnergyPlus input files for each of the 16 locations
- for the airflow models, the "New-Construction" version of Airflow and Indoor Air Quality models of DOE Reference Commercial Buildings are used (Ng et al., 2012). The models are available as CONTAM airflow models. Illustrations of the two buildings are found in APPENDIX (E)

- TMY3 weather data files for the 16 climate zones are used in the simulations. TMY3 files are compatible with EnergyPlus and the weather file creator tool ("CONTAM Weather File Creator," n.d.) was used to convert them to compatible formats for CONTAM
- EnergyPlus (US DOE, 2010) Version 8 is used (latest version available at the start of the research)
- CONTAM 3.1 is used in this research ("CONTAM User Manual," n.d.)
- The buildings are simulated with the default north orientation (except for the sensitivity study when using the CONTAM-EnergyPlus Method)

Some of the details of these models are presented in the literature review (sections 2.4.1.1 and 2.4.1.6) and more details of the models and their inputs can be found in the appropriate literature sources (Ng et al., 2012; Deru et al., 2011) and technical sources ("Commercial Prototype Building Models | Building Energy Codes Program," n.d.)

5.2.2 CONTAM Result Export Tool and Zone Matching

In order to complete the energy simulations using the infiltration rates calculated by CONTAM, the CONTAM results export tool (National Institute of Standards and Technology, 2014) developed by NIST was used. The tool exports the infiltration rates data for each time-step of the airflow simulations in data table (CSV) format which can be used as input for EnergyPlus (Polidoro et al., 2015).

However, as indicated in the literature review in section 2.4.1.6, some differences exist between the building zones in the CONTAM models and the EnergyPlus models. A process of manual zone matching was conducted in order to cross link the zones in each of the models - details of the zone matching are presented in APPENDIX (E). For the strip mall building, the EnergyPlus contained 10 zones (8 small and 2 large stores) that were each sub-divided in 3 zones in CONTAM (30 zones for the same 10 stores) (seen in Table 49). For the outpatient healthcare building the EnergyPlus model contained 118 zones (114 single floor zones and 4 multi-floor zones/shafts). In CONTAM the multi-floor zones were modeled separately on each floor, so the multi-floor zones were subdivided in 3 for 3 stories high outpatient healthcare building (seen in Table 50). The infiltration and exfiltration rates calculated for each of the divided zones in CONTAM were input as a sum in EnergyPlus.

5.2.3 Setup of Energy and Airflow Models

Most of parameters of both the EnergyPlus and the CONTAM models were mainly maintained at their original inputs. For EnergyPlus models, only infiltration rates related parameters and door usage schedules were edited (more details are provided in subsequent sections). In CONTAM, door models (and their parameters) and also door usage schedules were added to match the proposed door operation schedule presented in Table 7.

For the strip mall building, 10 doors (1 door for each of the stores of the buildings) were modeled. For the outpatient healthcare building only 1 door was modeled: all the energy simulation results presented in this chapter for the outpatient healthcare building were conducted with the door modeled in the "Lobby" zone - illustration in Figure 94 of APPENDIX (E). However, for the outpatient healthcare building, other door positions were used to conduct some sensitivity analysis cases that are presented in APPENDIX (G).

5.2.3.1 Modeling Doors in EnergyPlus

Based on the available literature discussed in section 2.4.2.1, infiltration through doors is usually modeled in EnergyPlus using the Flow/Zone model with a design flow rate that is controlled by a schedule (i.e. infiltration rates are only affected by the door usage which is based on daily schedules). This method is used when simulating the buildings using the infiltration rates calculate by the ASHRAE Method. However, when using the CONTAM-EnergyPlus Method to calculate the infiltration rates of the building (including the door), a different method for modeling infiltration is used which is presented in section 5.2.3.1.2.

5.2.3.1.1 Modeling air curtain units and air curtain doors in EnergyPlus

The available literature did not provide methods on the modeling of air curtains in EnergyPlus. In this research, the air curtain units are modeled as an electric equipment with a power rating of 1.05 kW as indicated by Wang (2013). The air curtain units are modeled with a multiplier based on the number of entrance doors in each of the two models (for the outpatient building 1 and for the strip mall building 10): the multiplier for the load is used to reflect the number of air curtain units in the buildings.

In order to automatically control the air curtain unit's operation in EnergyPlus (and thus calculate the fan energy consumption within the energy simulation of the building), an ERL program was

developed as part of the Energy Management system (EMS) program of each building. A sample of these control programs is provided in APPENDIX (E).

In accordance to the parameters proposed by Wang (2013) and presented in section 2.4.4.1, the air curtain control program for the unit was based on the outdoor temperature (extracted from the weather file - to only operate when the temperature is below 10 °C or above 30 °C) and based on the operation schedule of the doors in the two buildings as proposed by (Cho et al., 2010) and presented in Table 7. In order to calculate the air curtain units' energy usage (air curtain fan energy), the power rating of the unit (1.05 kW) is multiplied by the T_h (time of use of the door in hour/hour) which is calculated using Equation 14 and based on the hourly door schedule (P_h). The model of the air curtain units in EnergyPlus assumes no convective heat generated from the units (which are assumed to be non-heated models): thus, assuming that the energy of the unit is (1.05 kW) is used for the unit's fan and sensor operation. The results of the calculated T_h related to the door usage schedule for the two building can be found in Table 21 in section 5.3.1.1. When the buildings were simulated with single or vestibule doors the T_h was set to zero (i.e. the air curtain fan energy was 0).

It is important to note that by using this proposed air curtain units control method in EnergyPlus the fan energy (air curtain units' energy consumption) was integrated within the final energy report and the energy use of the buildings. This resulted in a more direct method for calculating energy savings when compared to the method proposed by Wang (2013) (Equation 28).

Also, for the simulations conducted using the ASHRAE Method for the buildings with air curtain doors, a similar control program was used for the doors. The program was needed since the single door infiltration rates are used when the conditions of air curtain units operation are not met.

5.2.3.1.2 Modeling Air Infiltration in EnergyPlus

When using the ASHRAE Method, door infiltration is modeled independently from other sources of infiltration in EnergyPlus. The reference models consider air infiltration through the envelope or walls by a Flow/Exterior-Surface model for which the original inputs of which are used in ASHRAE Method simulations.

When simulating the building using the CONTAM-EnergyPlus Method, the envelope infiltration is accounted for in CONTAM and thus the original envelope infiltration inputs are removed from the energy models. Thus, all the infiltration sources modeled for of the two buildings are removed from the EnergyPlus input file (all door and wall/envelope infiltration). New infiltration inputs, based on the flow/zone model, were then re-defined for each zone with a design flow of 1 m^3/s and a schedule input. The schedule values used were the infiltration rates data tables exported from CONTAM. The infiltration rates data exported from CONTAM are defined as part of the building schedule (schedule based on table) and are used to control the infiltration flow rates for each zone as indicated in section 5.2.2. It is important to note that EnergyPlus (US DOE, 2010) is only able to model positive infiltration rates and that negative ones are considered to be equal to 0 m^3/s.

5.2.3.2 Modeling Doors in CONTAM

The entrance doors in CONTAM were modeled using the methods proposed by Wang (2013). Two door models were used for each entrance door; a single/vestibule door and an air curtain door. For the single and vestibule door cases, the air curtain door was de-activated (i.e. only the single and vestibule door models were used). For the air curtain door cases the method of selecting the door model was done by the method presented in section 5.2.3.2.1.

The single and vestibule doors are modeled using the "Power-Law Model - $Q=C(\Delta P)^n$" with a power of 0.5 ($n = 0.5$) and the flow coefficients (C) input as schedules. The flow coefficients were obtained using the model proposed by Yuill (1996) for 2 × 2.4 m (W × H) doors based on hourly door usage frequency for each building (P_h as proposed by (Cho et al., 2010) and presented in Table 7). APPENDIX (E) shows more details about the single and vestibule doors' coefficients calculated of the door.

The air curtain doors were modeled using the Cubic-Spline Fitting formula (Q vs. P). The infiltration correlation for 100 P_h obtained from chapter 4 (presented in Figure 49) was input in the program - more details are provided in APPENDIX (E). In order to account for the door usage frequency (P_h), the air curtain door door usage correction factors, F_u were input as schedules. F_u factors are the ratio of the infiltration rates at the specific P_h over that of 100 P_h as

presented in section 4.3.2. The factors calculated for the air curtain door used in this research are presented in APPENDIX (E).

5.2.3.2.1 Modeling and Controlling Air Curtain units in CONTAM

Using the method proposed by Wang (2013) for the control of air curtain doors and units in CONTAM, the control node system (illustrated by Figure 22) was re-created in CONTAM for both building and set that:

- the air curtain operates under temperature control: the unit only operates when $T_{ambient} >$ 30 ºC and $T_{ambient} <$ 10 º C
- the schedules of the air curtain door was input as the door usage factors, F_u (as explained in 5.2.3.2)
- when the air curtain is not on (not operating), the doors are considered single doors (the single door model with its coefficients are used using the methods as explained in 5.2.3.2

It is important to note that the process presented above was executed automatically by CONTAM at each time step based the definition of the control nodes, the weather file data and the operation schedule used for each of the two buildings.

It is highly important to note that the operation time calculated by CONTAM and EnergyPlus were cross checked in all simulations: the hours of operation of air curtains in EnergyPlus (based on which fan energy consumption was calculated) are consistent with the hours of operation of air curtains in CONTAM.

5.2.4 Calculating Energy Savings

The methods proposed by PNNL (Cho et al., 2010) were used to calculate the energy savings resulting from the use of the air curtain doors (Similar method were used when calculating savings resulting from the vestibule doors in reference to single doors). It is important to note that the energy usage considered in this research is the end-use site energy and that EnergyPlus outputs the energy usage in MJ/m^2.

Equation 31.

$$E_{saving} = E_{base} - E_{ac}$$

$$P_{saving} = \frac{E_{saving}}{E_{base}}$$

Where E_{base} is the annual site end-use energy of the model simulated with the single or vestibule door,

E_{ac} is the annual site end-use energy of the model simulated with the air curtain door (which includes the air curtain fan energy), and

P_{saving} is the energy savings in percentage.

It is important to note that the base cases used were in accordance with the vestibule requirements mandated by addendum 'q' to ASHRAE 90.1 - 2007 and are presented in Table 17.

Table 17. Base cases used for air curtain doors energy savings calculation (ASHRAE, 2010)

Climate Zone		Base Case
1A	Miami	Single Door
2A	Houston	Single Door
2B	Phoenix	Single Door
3A	Memphis	Vestibule Door
3B	El-Paso	Vestibule Door
3C	San Francisco	Vestibule Door
4A	Baltimore	Vestibule Door
4B	Albuquerque	Vestibule Door
4C	Salem	Vestibule Door
5A	Chicago	Vestibule Door
5B	Boise	Vestibule Door
5C	Vancouver	Vestibule Door
6A	Burlington	Vestibule Door
6B	Helena	Vestibule Door
7	Duluth	Vestibule Door
8	Fairbanks	Vestibule Door

5.2.5 Energy Simulation using ASHRAE Method

This set of simulations were conducted in accordance to the methods proposed in literature: calculating infiltration rates through doors using the design infiltration rates calculation method (ASHRAE Method) is the commonly used method (the standard energy models' infiltration rates are calculated using this method) and has been used by PNNL in their investigation of the vestibule door savings (Cho et al., 2010). It is worthy of mentioning that, before using this method, a sample of the models (with single door and vestibule doors) was sent to PNNL researchers (Rahul Athalye and Bing Liu) who, thankfully, validated our method of

implementation and input of the door infiltration in EnergyPlus. However, It is important to note that the energy simulation conducted for the two buildings in this research use a different, and much larger, door size (2 × 2.4 m) in comparison to the study conducted by PNNL (door size 3 × 7 ft or 0.9 × 2.1 m). Considering that infiltration rates are directly related to the area of the door (Equation 18) and that the infiltration rates calculated in this are in the order of 2.5 times the infiltration rates calculated by PNNL, higher energy consumptions and savings for the buildings are expected (considering that savings are relative to the overall energy consumption of the building).

The details of the methods are explained further in the following sub-sections, however, Figure 50 illustrates the general process of the for energy simulation using ASHRAE Method. Table 18 shows the number of the calculations and simulations that are used to generate the results presented in section 5.3.1 (more details are presented in APPENDIX (E).

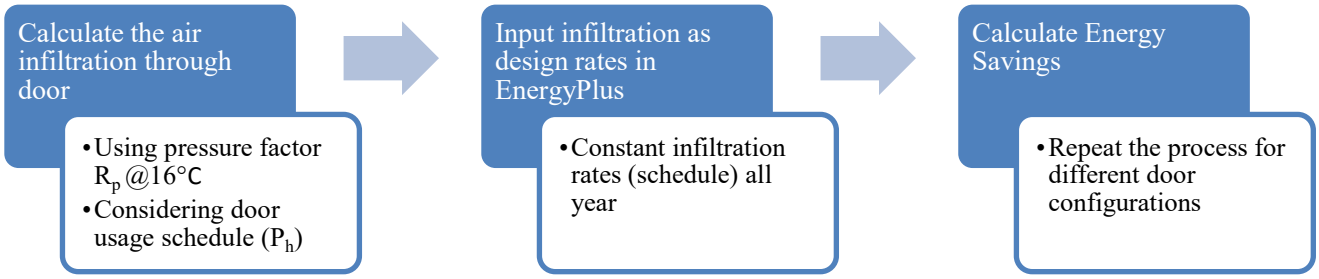

Figure 50. General process for the Energy Simulation using ASHRAE Method

Table 18. Number of the calculations and simulations using ASHRAE Method

	Infiltration Calculations		Energy Simulations	
	Main Cases	Sensitivity	Main Cases	Sensitivity
Strip Mall Building	45	0	45	3
Outpatient Healthcare Building	45	13	45	3
Total	103		96	

5.2.5.1 Calculating Air Infiltration Rates

Based on the model proposed by Yuill and the data available in ASHRAE (ASHRAE, 2009; Yuill, 1996), the pressure factor, R_p, was obtained for each of the two buildings at an outdoor temperature of 16° (R_p is in the order of $\sqrt{\Delta P}$ and it varies with the height of the building as seen in Figure 5. For the strip mall building, with a height of 5.18 m, the R_p was 4.46 $Pa^{0.5}$ and for the outpatient healthcare building, with a height of 9.14 m, the R_p was 4.51 $Pa^{0.5}$. In the case of the

single and vestibule doors, Equation 32 (which is based on Equation 18) was used to calculate the infiltration rates - where C was obtained from the data presented in APPENDIX (E).

Equation 32.

$$Q = C\ R_p$$

Where

$$C = C_A\ A$$

Where C is the door coefficient,
C_A is the airflow coefficient for automatic doors (ASHRAE, 2009; Yuill, 1996),
and A is the area of the door. (For this research the door size is 2 × 2.4 m).

For the air curtain doors, Q was calculated using a simplified method (Equation 33) based the methods proposed by Wang (2013) and presented in section 2.3.
Equation 33.

$$Q = F_u\ Q_{100\ P_h}\ R_p$$

Where F_u is the door usage correction factor, and
Q_{100Ph} is the infiltration rate through the air curtain door with 100 P_h door usage (2 × 2.4 m door with air curtain supply of 20 m/s at 20° outwards).

It is important to note that Equation 33 is a simplification of Equation 26 proposed by Wang (Wang, 2013) that uses correlated data presented in Figure 49 and assumes $\Delta P = {R_p}^2$.

5.2.5.2 Sensitivity Study

Similar to the methods proposed by PNNL (Cho et al., 2010), the sensitivity of the air infiltration rates for the 3 doors scenarios to the outdoor temperature and the door usage frequency (P_h) was assessed for the outpatient healthcare building during peak door usage frequency. For the sensitivity to the outdoor temperature, the R_p was calculated for different outdoor temperature between -40 °C to 37 °C (based on Figure 5). For the sensitivity to the door usage frequency, different values for different P_h (with variance of ±30% at 10% intervals from the base case of 123 P_h) were used to calculate the infiltration through the 3 door scenarios (at the base case R_p - 16 °C). Other simulations have been conducted with variations in the air curtain door control

temperatures. The full results of the sensitivity study using this method are presented in APPENDIX (F).

5.2.6 Energy Simulations using CONTAM-EnergyPlus Method

No literature has been found that conducted energy simulations conducted with the CONTAM-EnergyPlus Method or with similar methods. The details of the modeling and parameters considered in both software (i.e. CONTAM and EnergyPlus) were discussed in section 5.2.3.

Further details of the methods are presented in the following sub-sections. Figure 51 illustrates the general process for the energy simulation using the CONTAM-EnergyPlus Method. Table 18 shows the number of the simulations that are used to generate the results presented in section 5.3.1 - more details are presented in APPENDIX (E).

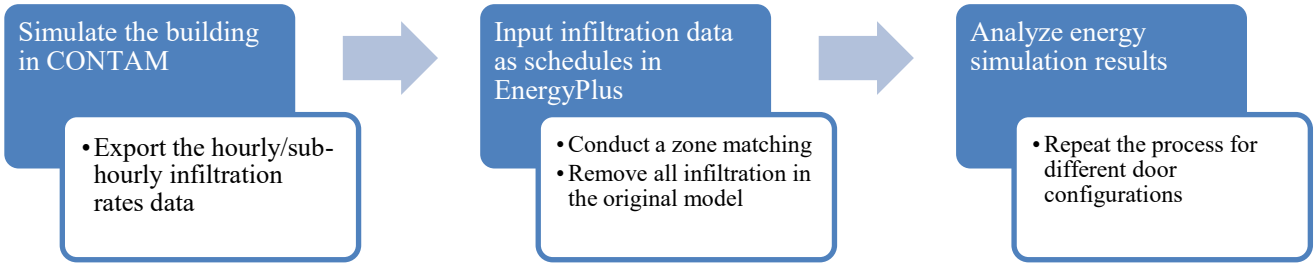

Figure 51. General process for the Energy Simulation using CONTAM-EnergyPlus Method

Table 19. Number of the calculations and simulations using CONTAM-EnergyPlus

	CONTAM Simulations		Energy Simulations	
	Main Cases	Sensitivity	Main Cases	Sensitivity
Strip Mall Building	45	46	45	46
Outpatient Healthcare Building	90	140	90	115
Total	321		296	

It is important to note that CONTAM simulations consider outdoor hourly weather and wind conditions as well as building specific internal and external airflow (internal zone interactions) during the simulations.

5.2.6.1 CONTAM Simulations

The CONTAM simulations were conducted using CONTAM 3.1 ("CONTAM User Manual," n.d.). The CONTAM weather file creator tool was used to convert the TMY3 files to suitable WTH files (for all the 16 locations). The time-step used for the airflow simulations is 1 Hour

(matching the weather data): a number of simulations were conducted and it showed that the results obtained for sub-hourly time-step matched the hourly data.

5.2.6.2 Calculating Infiltration Reduction

The annual infiltration reductions calculated and presented in the results is based on the total infiltration reduction calculated based on the EnergyPlus total infiltration outputs (kg). Since negative airflow rates are ignored by EnergyPlus, the total infiltration was considered to be the most indicative of the reductions. The reductions in percentage are calculated using the same method proposed for the energy saving (Equation 31 - while changing the energy to air infiltration in kg). For the strip mall building, where all the building zones have entrance doors, the infiltration is calculated based on the sum of all infiltration in all zones. For the outpatient healthcare building, however, the infiltration in the "Lobby" zone only (entrance zone - where the entrance zone is located) was considered (APPENDIX (E) shows a plan of the building). This of course may lead to higher reductions to be calculated in the outpatient healthcare building, where the reduction is local, as opposed to the strip mall where the reduction is more global.

5.2.6.3 Sensitivity Study

The sensitivity of the energy simulation results to the following parameters is analyzed for both buildings:

- door usage frequency: The door usage (P_h) is varied by ±30% (with 10% intervals) for the air curtain door cases and the variance in energy consumption calculated (For CZ-4A and CZ-7). The building's energy consumption with air curtain doors are also compared to the vestibule door vas for the +30% and -30% cases
- building orientation: the original building orientation (North) is varied for the two buildings in CZ-4A, CZ-7 and CZ-8 (orientation of the building was changed in both CONTAM and EnergyPlus). For the air curtain door cases the variance in energy consumption is calculated and the results are also compared to the vestibule door cases.
- wind pressure coefficient: the original wind pressure coefficient profile used in CONTAM (Swami & Chandra, 1987) - presented in APPENDIX (E) - is varied by ±20% (with 10% intervals) for the air curtain door cases and the variance in energy

consumption calculated in CZ-4A and CZ-7. The building's energy consumption with air curtain doors are also compared to the vestibule door for the +20% and -20% cases

Considering the effect of wind direction on the infiltration rates calculated, the average weighted prevailing wind directions in summer and winter in all 16 climate zones are presented in APPENDIX (E).

Some additional cases were conducted to study the sensitivity of the energy simulations results of the outpatient healthcare building to the entrance door interaction in CZ-4 and CZ-7 (removal of leakage from CONTAM model - varied from full interaction to full sealing) and to the entrance door location (in 5 different locations in the building) in CZ-8 and in all 16 zones for 1 location ("Vestibule" Zone). In addition, the sensitivity of the air curtain door savings to the air curtain unit's temperature operation control was assessed in CZ-3C. The detailed results of the sensitivity study are presented in APPENDIX (G).

5.2.7 Comparison between ASHRAE and CONTAM-EnergyPlus Methods

Table 20 presents a comparison between the ASHRAE Method and the CONTAM-EnergyPlus Method highlighting the differences and similarities between both. It is important to note that further details are presented in sections 5.2.5, 5.2.6 and 5.2.6.

Table 20. Comparison between the ASHRAE and CONTAM-EnergyPlus Methods

	ASHRAE Method	**CONTAM-EnergyPlus Method**
Calculation of Pressure Difference Across the Door	Based on R_p factor from ASHRAE (2009) at 16 °C (design value)	Using weather specific airflow simulations for each climate zone location (based on weather & building properties)
Single/Vestibule Door Coefficient	Based on the findings of Dr. Yuill (1996) and the door usage of each building model	Based on the findings of Dr. Yuill (1996) and the door usage of each building model
Air Curtain Door Coefficients and Infiltration	Based on the correlated curves for the air curtain with a person under the jet for air supply of 20 m/s and 20° outwards. Correction factors used to account for door usage	Based on the correlated curves for the air curtain with a person under the jet for air supply of 20 m/s and 20° outwards. Correction factors used to account for door usage

Table 19. Continued

	ASHRAE Method	CONTAM-EnergyPlus Method
Door Infiltration Modeling	Infiltration for the doors is modeled flow/zone input in EnergyPlus controlled with weekly and daily schedules based on the door	Infiltration is modeled through input of exported hourly infiltration data from CONTAM for each zone. The infiltration includes all infiltration sources (door and non-door sources)
Building Infiltration (non-door infiltration)	Considered by the original infiltration/exterior-wall inputs in the energy models	Considered within the airflow simulation results. The original energy model inputs are removed
When Air Curtain door not Operating	Single door infiltration used are used through a ERL program in EnergyPlus	Single door model is used in CONTAM through a control program
Comments	Uses design pressure differences which might exceed or strongly differ from real pressure conditions of the buildings	Estimates the pressure difference using weather file which can lead to more accurate estimations
Conclusion	A method can be used in preliminary basis to understand the savings trend of infiltration reduction. However, the magnitude of the savings can be distorted.	More refined method for estimating air infiltration reduction through envelopes. The method is building and weather specific and can provide more realistic estimates of energy savings

5.3 Results and Discussion

In this section, the main results of the energy simulations conducted using the ASHRAE Method and the CONTAM-EnergyPlus Method for the strip mall and outpatient healthcare building commercial reference building models (Deru et al., 2011) are presented and discussed. Moreover, the results of the sensitivity study conducted for both simulation methods are presented. More details of the calculations and results are presented in APPENDIX (F) and APPENDIX (G).

5.3.1 Energy Simulations using ASHRAE Method

5.3.1.1 Infiltration Rates through Entrance Doors

Following the methods proposed in section 5.2.5 (Wang, 2013; Cho et al., 2010; Yuill, 1996) regarding the ASHRAE Method, the infiltration rates through the 3 door scenarios investigated were calculated for the two buildings and are presented in Table 21. The air curtain door is seen

to reduce the air infiltration rate through the entrance doors in all the cases with an average reduction of 62% (for all the 6 cases presented in Table 21). As seen in Table 21, and based on the door time of use (T_h) calculated using Equation 14, the air curtain operated a maximum of 0.24 hours per hour (approx. 15 minutes per hour) during the peak door-opening frequency of the outpatient healthcare building. It is important to note that the infiltration rates presented in Table 21 are used for all climate zone locations since the ASHRAE Method is not location depended.

Figure 52 compares the peak air infiltration rates for the three door scenarios in the two buildings (the entrance door for a large store in the strip mall building and the entrance door of the outpatient healthcare building):

- For the strip mall building' large store entrance with a peak door usage of 34 P_h, the vestibule door's air infiltration is 0.508 m^3/s and air curtain door's air infiltration is 0.196 m^3/s. Thus the air curtain door reduced 61% of the infiltration from the vestibule door.
- For the outpatient healthcare building's entrance with peak door usage of 123 P_h, the vestibule door's air infiltration rate is 1.815 m^3/s and the air curtain door's air infiltration rate is 0.646 m^3/s. Thus the air curtain door reduced 64% of the infiltration from the vestibule door.

Table 21. Infiltration rates calculated for the buildings using the ASHRAE Method

Building		Door Usage (P_h)		Air Infiltration Rates Q (m^3/s) @ 16 °C			Air Curtain Operation (h/h)*	Air Curtain Door Infiltration Reduction**
				Single Door	Vestibule Door	Air Curtain Door		
Outpatient		Peak	123	2.938	1.815	0.646	0.240	64%
		Off Peak	12	0.300	0.177	0.066	0.026	63%
Strip Mall	Large Store	Peak	34	0.853	0.508	0.196	0.073	61%
		Off Peak	3	0.076	0.045	0.018	0.007	61%
	Small Store	Peak	16	0.404	0.239	0.093	0.035	61%
		Off Peak	2	0.051	0.030	0.012	0.004	61%

** *The air curtain operation time (presented as operating hour/hour at the different usage rates) was calculated based on the door usage time* (Wang & Zhong, 2014a; Yuill, 1996)

**Percent reductions in comparison to the vestibule door's air infiltration rates presented in the table*

It is important to note that, as proposed by the ASHRAE Method, the rates presented in Table 21 are used for all climate zones throughout all the year.

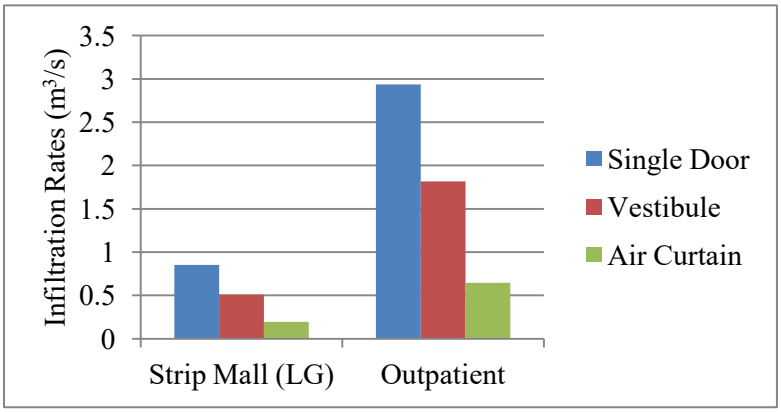

Figure 52. Peak air infiltration rates calculated for the 3 door scenarios investigated for the 2 buildings

5.3.1.2 Energy Simulations

Using the infiltration rates presented in Table 21, the energy simulations for the 2 reference building models were completed and the results are presented in Table 22, Figure 53 and Figure 54. The detailed results, obtained using the ASHRAE Method, are presented in APPENDIX (F).

As seen in Table 22, the air curtain doors' national weighted-average energy savings are 6.52% (46.47 MJ/m^2 or 12.91 kWh/m^2) for the strip mall building and 0.90% (11.97 MJ/m^2 or 3.33 kWh/m^2) and the outpatient healthcare building when compared to vestibule doors in CZ 3-8 and single doors in CZ 1-2. Generally, it is observed that the air curtain doors realize more savings, when compared to vestibules, in the colder climate zones. As seen in Table 22 and based on the buildings' operation schedules and location specific weather, the national weighted-average of the air curtain units' annual fan energy is 548.16 kWh (0.26 kWh/ m^2) for the strip mall building (for 10 air curtain units) and 314.37 kWh (0.08 kWh/m^2) for the outpatient healthcare building (for 1 air curtain unit).

Table 22. Air curtain door energy savings using ASHRAE Method

Climate Zone		Base Case	Strip Mall Building			Outpatient Healthcare Building		
			Air Curtain fan Energy* (kWh/m^2)	Energy Savings (kWh/m^2)	Energy Savings (%)	Air Curtain fan Energy* (kWh/m^2)	Energy Savings (kWh/m^2)	Energy Savings (%)
1A	Miami	Single Door	0.09	1.97	1.18%	0.03	1.37	0.34%
2A	Houston	Single Door	0.18	10.05	5.48%	0.05	2.07	0.54%
2B	Phoenix	Single Door	0.34	23.33	12.37%	0.10	2.77	0.75%
3A	Memphis	Vestibule Door	0.25	9.43	5.02%	0.07	2.61	0.68%
3B	El-Paso	Vestibule Door	0.22	-6.45	-3.95%	0.06	2.39	0.70%
3C	San Francisco	Vestibule Door	0.03	-11.04	-7.84%	0.01	3.10	0.97%
4A	Baltimore	Vestibule Door	0.28	14.29	7.02%	0.08	3.17	0.87%
4B	Albuquerque	Vestibule Door	0.27	7.58	4.53%	0.08	2.98	0.88%
4C	Salem	Vestibule Door	0.26	7.91	4.25%	0.07	3.67	1.11%
5A	Chicago	Vestibule Door	0.35	25.94	10.73%	0.09	3.80	1.02%
5B	Boise	Vestibule Door	0.35	19.82	9.89%	0.10	3.64	1.07%
5C	Vancouver	Vestibule Door	0.33	17.84	8.84%	0.09	3.82	1.16%
6A	Burlington	Vestibule Door	0.38	37.30	14.41%	0.10	4.26	1.14%
6B	Helena	Vestibule Door	0.40	32.19	13.89%	0.11	4.03	1.14%
7	Duluth	Vestibule Door	0.43	49.62	16.88%	0.12	5.13	1.32%
8	Fairbanks	Vestibule Door	0.47	72.48	18.67%	0.13	7.28	1.62%
National Weighted Average			0.26	12.91	**6.52%**	0.08	3.33	**0.90%**

**Air Curtain Energy is the end use energy consumption of the air curtain units (all units in the building) for 1 year of operation (depending on weather, operation schedule and door-opening frequency)*

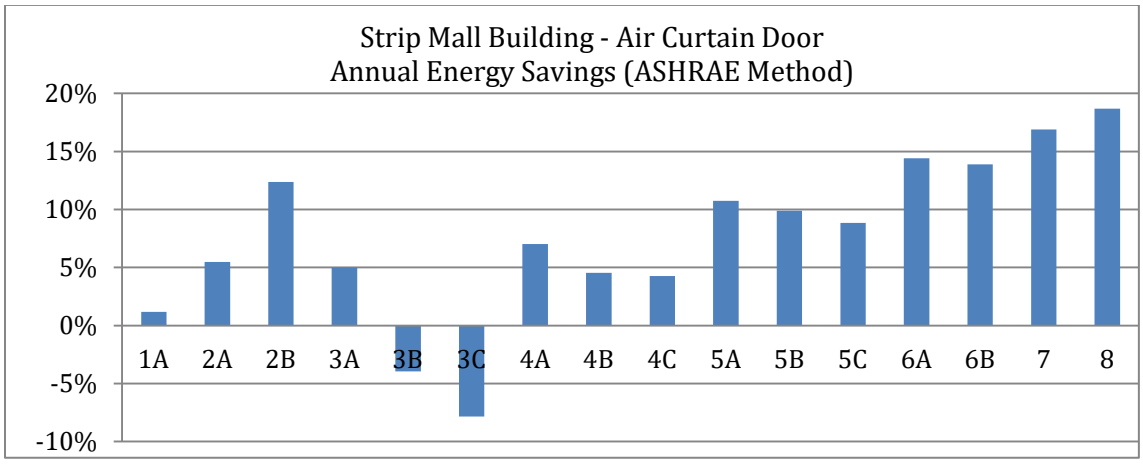

Figure 53. Air curtain door percent annual energy savings in the strip mall building using ASHRAE Method

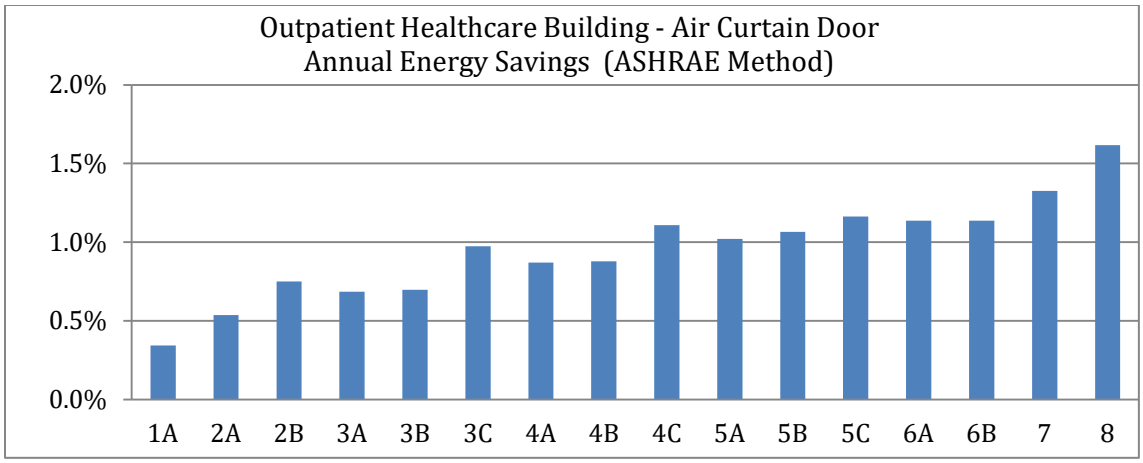

Figure 54. Air curtain door percent annual energy savings in the outpatient healthcare building using ASHRAE Method

As seen in Figure 53, air curtain door savings in the strip mall building range from 18.67% to -7.84% (where negative values indicate additional energy consumption). In the strip mall building, air curtain doors save energy in comparison to vestibule doors in 11 out of the 13 climate zone locations. However, air curtain doors show additional energy consumption in CZ 3B and 3C. Also, air curtain doors save energy in comparison to single door in CZ 1A, 2A and 2B. In the strip mall building, the excess energy used with air curtain doors in CZ 3B and 3C (seen in Table 22 and Figure 53) is mainly due to the idleness (lack of operation) of the air curtain units. This lack of operation is mainly resulting from the moderate weather conditions in these climate zone locations: the temperature falls within a range that does not activate the air curtain unit (based on the air curtain control parameters used for the simulations and presented in section 2.4.4.1.). As seen in Table 22, this idleness is indicated by the low air curtain energy consumption in CZ 3B and 3C in relation to other locations in CZ-3 to CZ-8 (climate zones with vestibule door baseline). It is important to note that, when the simulating the strip mall building with the air curtain door with no temperature control (air curtain door operates whenever the door is in use), 7.11% (positive) savings can be achieved when compared to the vestibule case as seen in Table 26 - APPENDIX (F) shows the details of the sensitivity conducted for the air curtain temperate control in CZ 3 for both buildings.

As seen in Figure 54, the air curtain door savings in the outpatient healthcare building range from 1.62% to 0.34%. Air curtain doors in the outpatient healthcare building save energy in

comparison to vestibule doors in all 16 climate zones simulated (compared to vestibules in CZ 3-8 and single doors in CZ 1-2).

Table 23. Energy consumption at sample climate zones and the calculated savings (%) for the vestibule door and the air curtain door in the strip mall building using the ASHRAE Method

Strip Mall Building (ASHRAE Method)			
Climate Zone	3A	4A	8
Single Door (MJ/m^2)	762.31	856.42	1734.68
Vestibule Door (MJ/m^2)	676.94	733.03	1397.59
Air Curtain Door (MJ/m^2)	642.98	681.59	1136.66
Vestibule Door Saving (Vestibule Door Vs. Single Door)	11.20%	14.41%	19.43%
Air Curtain Door Savings (Air Curtain Door Vs. Vestibule Door)	5.02%	7.02%	18.67%

Table 24. Energy consumption (at sample climate zones) and the calculated savings (%) for the vestibule door and the air curtain door in the outpatient healthcare building using the ASHRAE Method

Outpatient Healthcare Building (ASHRAE Method)			
Climate Zone	3A	4A	8
Single Door (MJ/m^2)	1372.15	1312.48	1623.53
Vestibule Door (MJ/m^2)	1371.25	1311.77	1621.55
Air Curtain Door (MJ/m^2)	1361.87	1300.35	1595.33
Vestibule Door Saving (Vestibule Door Vs. Single Door)	0.07%	0.05%	0.12%
Air Curtain Door Savings (Air Curtain Door Vs. Vestibule Door)	0.68%	0.87%	1.62%

Table 23 and Table 24 show the energy simulation results for the annual building energy consumption using the ASHRAE Method with the three doors scenarios (namely: single doors, vestibule doors and air curtain doors) for CZ-3A, CZ-4A and CZ-8 (as sample climate zones). The tables support PNNL's findings regarding the saving impact of vestibules (Cho et al., 2010). More importantly, the air curtain door savings in both building are also clear. The full end use energy data for both building models in all other climate zones are presented in APPENDIX (F).

When comparing the energy simulation results obtained using the ASHRAE Method to previously published study by PNNL (Cho et al., 2010) some differences are observed. It is important to note that (as presented in sections 2.4.3 and 5.2.5.1) the door size used in PNNL's study was 0.9 x 2.1 m (1.89 m^2) as opposed to the 2 x 2.4 m (4.80 m^2) door that is used in this

research. Based on the method presented in 5.2.5.1 regarding the infiltration rates calculation using the ASHRAE Method, the amount of air infiltration through the entrance doors in this research is about 2.5 times larger than that in PNNL's study (Cho et al., 2010); thus leading to the observed exaggerations in the energy saving of the vestibule and air curtain doors. For example, in the strip mall building - Table 64 in APPENDIX (G) -, the maximum calculated vestibule door savings in this research is 19.43% (in CZ-8) as opposed to the reported 7.67% in PNNL's study (Cho et al., 2010). However, considering that the infiltration rates calculated in this research are 2.5 times higher, the ratios are correct.

As explained in section 5.2.6.2, for the strip mall building, all the building (full volume of the building) is affected by air infiltration, thus the whole building energy savings are a good indication of the savings realized by air curtains. However, in the outpatient healthcare building, only the "Lobby" zone is affected by infiltration. Table 25 shows the total energy transfer in the "Lobby" zone only for CZ 4A - Baltimore (as a sample climate zone) for the vestibule and air curtain door.

Table 25. Total energy transfer (CZ 4A) and the reduction (%) for the vestibule door and the air curtain door in the outpatient healthcare building's Lobby zone using the ASHRAE Method

Outpatient Healthcare Building (ASHRAE Method) - "Lobby" Zone	
Climate Zone	4A
Vestibule Door (MJ)	5478.64
Air Curtain Door (MJ)	2853.47
Air Curtain Door Reduction in Energy Transfer to Zone (Air Curtain Door Vs. Vestibule Door)	47.9%

5.3.1.3 Sensitivity Study for the ASHRAE Method

Following the similar method to that proposed in the PNNL study on vestibule doors (Cho et al., 2010), the sensitivity of the calculated infiltration rates to the exterior temperature and the door usage frequency was assessed for the 3 entrance door scenarios in the outpatient healthcare building. The results of this sensitivity are summarized in Figure 55 and Figure 56. The detailed results of this sensitivity study are provided in APPENDIX (F).

As seen in Figure 55, the air curtain door's air infiltration rates are consistently lower than the vestibule door under all temperature conditions. The air curtain door reduced the air infiltration

rate through vestibule doors by 40% at -40 °C, 64% at 16 °C (baseline) and 75% at 38 °C. Also, as seen in Figure 56, the air curtain door's air infiltration rates are consistently lower than the vestibule infiltration rates at all variation in the door usage (P_h). The air curtain door reduced the air infiltration rates of the vestibule doors by 64% in all cases. The air curtain unit operated for 0.175 hour per hour (approx. 10 minutes per hour) at a door usage frequency of 86 P_h, 0.24 hour per hour (approx. 15 minutes per hour) at a door usage frequency of 123 P_h (baseline) and 0.3 hour per hour (approx. 20 minutes per hour) at a door usage frequency of 160 P_h.

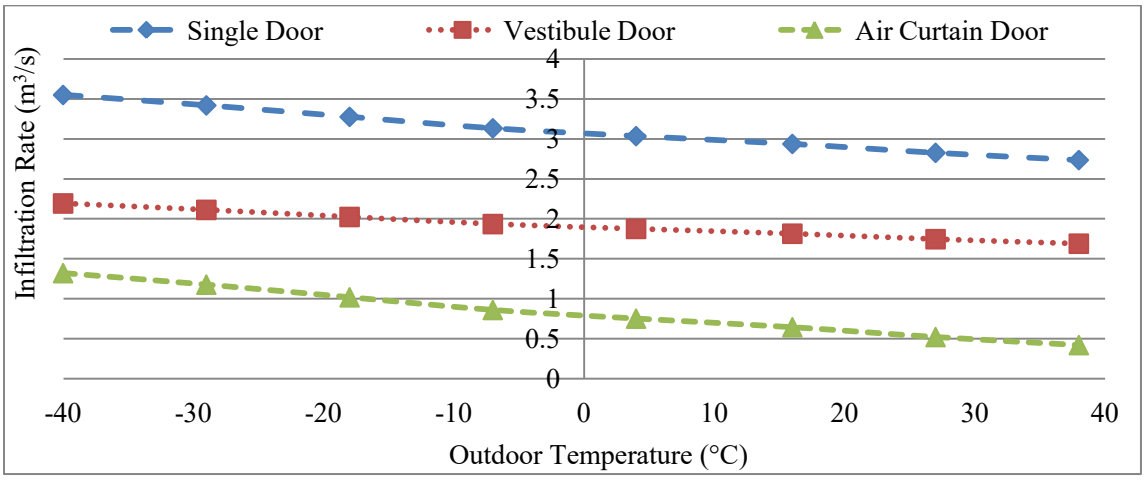

Figure 55. Effect of the outdoor temperature on the calculated infiltration rates for the 3 entrance door scenarios during peak door-opening frequency in the outpatient healthcare building

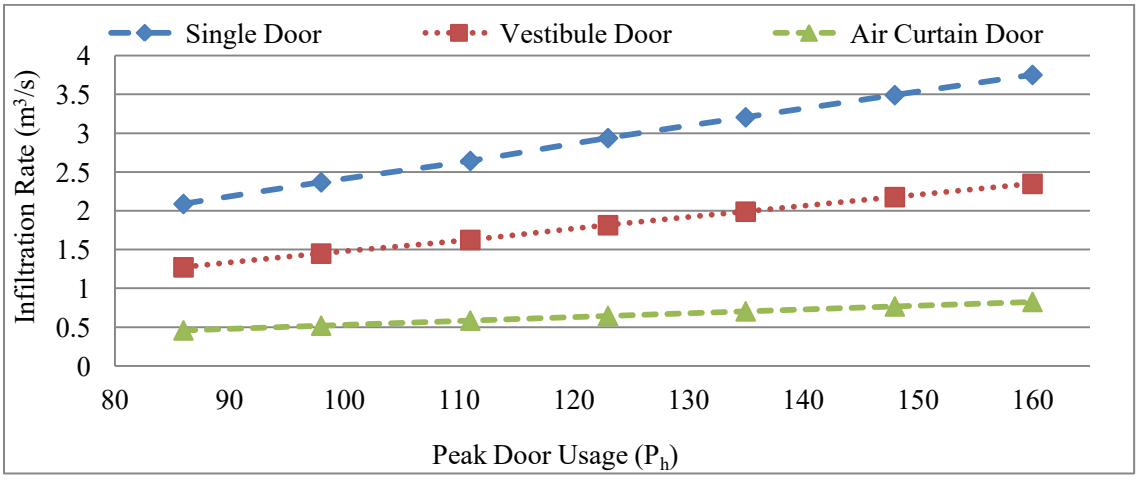

Figure 56. Effect of the door-opening frequency on the calculated infiltration rates for the 3 entrance door scenarios in the outpatient healthcare building

Table 26. Energy savings sensitivity to air curtain door temperature control in the CZ-3C

		Strip Mall		Outpatient Healthcare	
Air Curtain Temperature Control (Where T is the temperature range in ° C where the unit operates)		**30 < T < 10 (Baseline)**	Always ON (No temp. Control)	**30 < T < 10 (Baseline)**	Always ON (No temp. Control)
3C- San Francisco	Energy Saving	**-7.84%**	7.11%	**0.97%**	0.89%

Table 26 presents the sensitivity of the energy savings to the air curtain temperature control. Removing the temperature control in the strip mall building increases the savings achieved by the air curtain door while, in the outpatient healthcare building, the savings are reduced.

5.3.2 Energy Simulations using CONTAM-EnergyPlus Method

5.3.2.1 Energy Simulations

Following the methods proposed and presented in section 5.2.6 regarding the CONTAM-EnergyPlus, whole building annual airflow and energy simulations for the two buildings were completed. The results and discussions of the energy simulations are summarized in the Table 27, Figure 57 and Figure 58. The detailed results, obtained using the CONTAM-EnergyPlus Method, are presented in APPENDIX (G).

Table 27. Air curtain door energy savings using CONTAM for infiltration calculation

Climate Zone		Base Case	Strip Mall Building			Outpatient Healthcare Building		
			Air Curtain fan Energy* (kWh/m^2)	Energy Savings (kWh/m^2)	Energy Savings (%)	Air Curtain fan Energy* (kWh/m^2)	Energy Savings (kWh/m^2)	Energy Savings (%)
1A	Miami	Single Door	0.09	3.59	2.28%	0.03	-0.10	-0.02%
2A	Houston	Single Door	0.18	1.30	0.81%	0.05	-0.10	-0.03%
2B	Phoenix	Single Door	0.34	3.57	2.21%	0.10	-0.14	-0.04%
3A	Memphis	Vestibule Door	0.25	1.99	1.10%	0.07	-0.21	-0.05%
3B	El-Paso	Vestibule Door	0.22	-0.04	-0.03%	0.06	0.25	0.07%
3C	San Francisco	Vestibule Door	0.03	-0.60	-0.44%	0.01	-0.35	-0.11%
4A	Baltimore	Vestibule Door	0.28	4.13	2.09%	0.08	0.94	0.25%
4B	Albuquerque	Vestibule Door	0.27	1.30	0.81%	0.08	1.05	0.30%
4C	Salem	Vestibule Door	0.26	4.64	2.53%	0.07	0.19	0.05%
5A	Chicago	Vestibule Door	0.35	10.86	4.36%	0.09	4.14	1.02%
5B	Boise	Vestibule Door	0.35	4.73	2.50%	0.10	2.65	0.74%
5C	Vancouver	Vestibule Door	0.33	5.58	2.98%	0.09	6.53	1.86%
6A	Burlington	Vestibule Door	0.38	14.33	5.35%	0.10	0.89	0.22%
6B	Helena	Vestibule Door	0.40	7.77	3.53%	0.11	9.90	2.54%
7	Duluth	Vestibule Door	0.43	18.53	5.94%	0.12	0.09	0.02%
8	Fairbanks	Vestibule Door	0.47	31.77	7.71%	0.13	-1.38	-0.27%
National Weighted Average			0.26	4.20	**2.21%**	0.08	1.33	**0.34%**

**Air Curtain Energy is the end use energy consumption of the air curtain units' for 1 year of operation (depending on weather, operation schedule and door-opening frequency)*

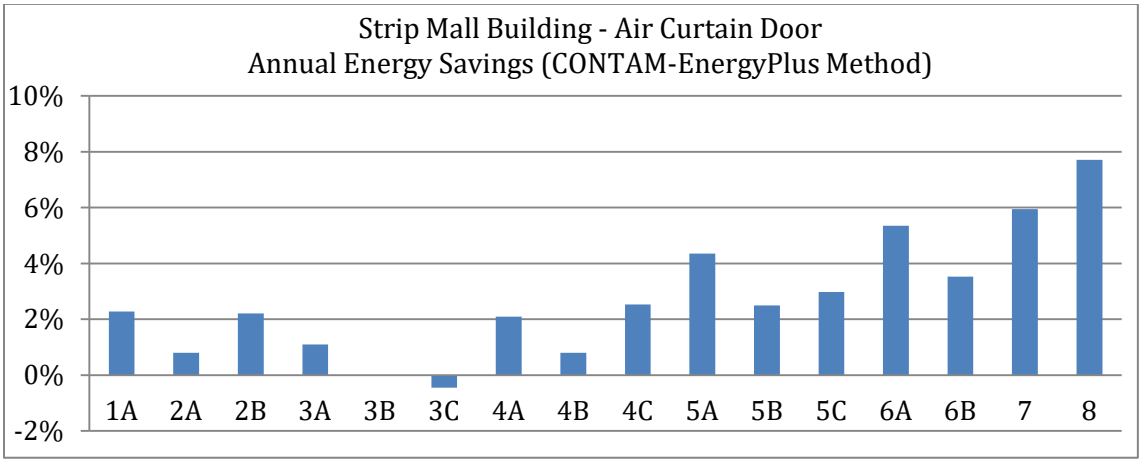

Figure 57. Air curtain door percent annual energy savings in the strip mall building using the CONTAM-EnergyPlus Method

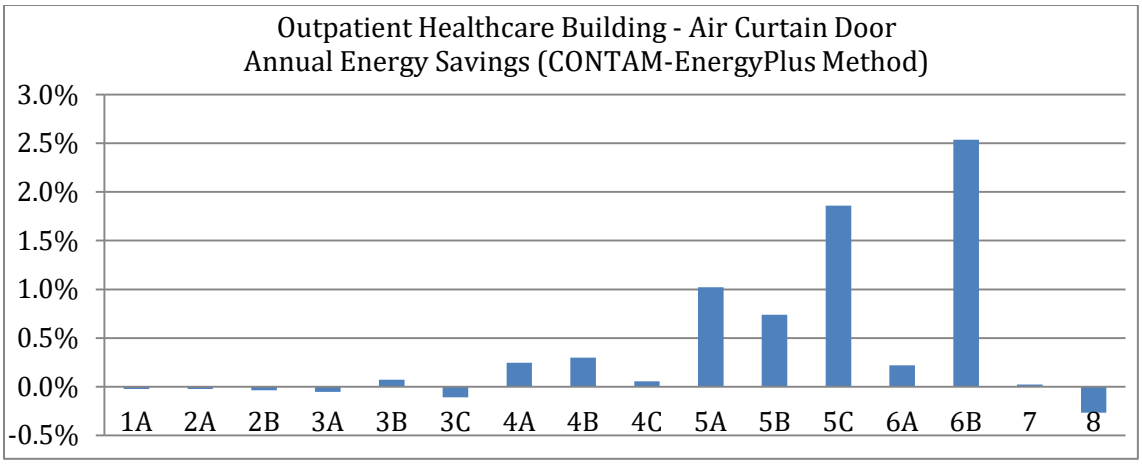

Figure 58. Air curtain door percent annual energy savings in the outpatient healthcare building using the CONTAM-EnergyPlus Method

As seen in Table 27, the air curtain doors' national weighted-average energy savings are 2.21% (15.15 MJ/m^2 or 4.20 kWh/m^2) for the strip mall building and 0.34% (4.80 MJ/m^2 or 1.33 kWh/m^2) in the outpatient healthcare building when compared to vestibule doors in CZ 3-8 and single doors in CZ 1-2. Again, as presented in section 5.3.1.2, the national weighted-average of the air curtain units' annual fan energy is 548.16 kWh (0.26 kWh/ m^2) for the strip mall building (for 10 air curtain units) and 314.37 kWh (0.08 kWh/ m^2) for the outpatient healthcare building (for 1 air curtain unit).

As seen in Figure 57, air curtain door savings in the strip mall building range from 7.71% to -0.44%. Again, the air curtain doors save energy in comparison to vestibule doors in 11 out of the 13 climate zone locations. However, air curtain doors consume additional energy in CZ 3B and 3C in comparison to vestibule doors. Also, air curtain doors save energy in comparison to single door in CZ 1A, 2A and 2B. It is observed that in the strip mall building the air curtain doors save more energy in comparison to vestibule doors in the cold climate zone locations.

As seen in Figure 58, the air curtain door savings in the outpatient healthcare building range from 2.54% to -0.27%. The air curtain doors save energy in comparison to vestibule doors in 10 out of the 13 climate zone locations. However, air curtain doors consume additional energy In CZ 3A, 3C and 8 in comparison to vestibules. In the outpatient healthcare building, air curtain doors also consume more energy in comparison to single door in CZ 1A, 2A and 2B. It is observed that when using the CONTAM-EnergyPlus Method, the air curtain door savings trend

across the climate zones changes: better savings are realized in the colder climate zones up to CZ 6B with decreasing savings in CZ 7 & 8.

Table 28 and Table 29 show the energy simulation results for the annual building energy consumption using the CONTAM-EnergyPlus Method with the three doors scenarios for CZ-3A, CZ-4A and CZ-8 (as sample climate zones). The tables generally support the findings of the previous published work with this infiltration modeling method regarding the saving impact of vestibules (Cho et al., 2010) and also show the air curtain doors' saving impact in both building models.

In Table 29, for the outpatient healthcare building in CZ-8, the vestibule door is seen to consume more energy than the single door (0.51 MJ/m^2 more energy). Based on additional simulations conducted for this building in this specific climate zone - presented in APPENDIX (F) - and the calculated infiltration reduction in the entrance zone (the results indicate reduction in the infiltration in the entrance zone - namely the "Lobby" zone), this increased energy usage was related to the increase of air infiltration in surrounding zones (zones other than the entrance zone). Due to the strong stack effect generated in the building by large temperature differences in this arctic region (along with other factors such as the wind direction), the decrease in infiltration in the entrance zone, led to an increase of infiltration in other zones in the building (since the airflow simulations consider the interactions of all internal zones). It is suggested that further investigation is needed on the special conditions that extreme cold climate zones pose on the airflow of large buildings (such as the outpatient healthcare building). In addition, the saving impact of the different envelope related design solutions have to be critically and further assessed in these extreme climate zones. The full end-use energy data for both building models in all other climate zones are presented in APPENDIX (F).

Table 28. Energy consumption at sample climate zones and the calculated savings (%) for the vestibule door and the air curtain door in the strip mall building using the CONTAM-EnergyPlus Method

Strip Mall Building (CONTAM Method)			
Climate Zone	3A	4A	8
Single Door (MJ/m^2)	663.39	724.56	1546.78
Vestibule Door (MJ/m^2)	653.47	711.11	1483.94
Air Curtain Door (MJ/m^2)	646.31	696.24	1369.56
Vestibule Door Saving (Vestibule Door Vs. Single Door)	1.50%	1.86%	4.06%
Air Curtain Door Savings (Air Curtain Door Vs. Vestibule Door)	1.10%	2.09%	7.71%

Table 29. Energy consumption (at sample climate zones) and the calculated savings (%) for the vestibule door and the air curtain door in the outpatient healthcare building using the CONTAM-EnergyPlus Method

Outpatient Healthcare Building (CONTAM Method)			
Climate Zone	3A	4A	8
Single Door (MJ/m^2)	1413.7	1378.22	1866.43
Vestibule Door (MJ/m^2)	1413.47	1377.57	1866.94
Air Curtain Door (MJ/m^2)	1414.23	1374.19	1871.91
Vestibule Door Saving (Vestibule Door Vs. Single Door)	0.02%	0.05%	-0.03%
Air Curtain Door Savings (Air Curtain Door Vs. Vestibule Door)	-0.05%	0.25%	-0.27%

Table 64 in APPENDIX (G) presents the full end-use energy savings of all doors using the two methods in the two buildings. The table indentifies the over-estimation of savings (national and local) that could result from using the ASHRAE method.

Once again as presented in section 5.2.6.2, Table 30 shows the total energy transfer in the "Lobby" zone only for CZ 4A - Baltimore (as a sample climate zone) for the vestibule and air curtain door.

Table 30. Total energy transfer (CZ 4A) and the reduction (%) for the vestibule door and the air curtain door in the outpatient healthcare building's Lobby zone using the CONTAM-EnergyPlus Method

Outpatient Healthcare Building (CONTAM-EnergyPlus Method) - "Lobby" Zone	
Climate Zone	4A
Vestibule Door (MJ)	4374.19
Air Curtain Door (MJ)	2765.77
Air Curtain Door Reduction in Energy Transfer to Zone (Air Curtain Door Vs. Vestibule Door)	36.77%

5.3.2.2 Annual Infiltration Reductions

Analyzing the infiltration data gathered for the two buildings, the results of the total infiltration reductions (in kg) realized by the air curtain doors in the entrance zone of the buildings are presented in Table 31. The detailed infiltration analysis is presented in APPENDIX (G). It is important to note that all the of strip mall building (100% of the floor area - 10 stores) is considered to be the entrance zone (these zones have multiple large exterior openings). In the outpatient healthcare building only the "Lobby" zone (1 zone of the 118 total zones) is considered to be the entrance zone (this zone the entrance door is considered the main exterior opening). As seen in Table 31, the air curtain door's national weighted average annual air infiltration reduction in the entrance zone(s) was 4.60% in the strip mall building (global for all building) and 40.70% in the outpatient healthcare building (local for the entrance zone). The infiltration reductions realized by the air curtain doors, presented in Table 31, are influenced by (and consider) the door-opening frequency and the air curtain operation time

Table 31. Total annual infiltration reduction by the use of air curtain door (CONTAM-EnergyPlus Method)

Climate Zone		Base Case	Strip Mall Building	Outpatient Healthcare Building
Infiltration Based on			10 Stores*	1 Entrance zone**
1A	Miami	Single Door	5.00%	7.10%
2A	Houston	Single Door	6.40%	18.40%
2B	Phoenix	Single Door	38.90%	21.50%
3A	Memphis	Vestibule Door	-2.60%	31.80%
3B	El-Paso	Vestibule Door	-4.50%	8.70%
3C	San Francisco	Vestibule Door	-5.90%	-7.90%
4A	Baltimore	Vestibule Door	0.20%	37.40%
4B	Albuquerque	Vestibule Door	-2.10%	26.60%
4C	Salem	Vestibule Door	-1.60%	25.80%
5A	Chicago	Vestibule Door	10.90%	50.20%
5B	Boise	Vestibule Door	3.70%	41.70%
5C	Vancouver	Vestibule Door	3.70%	34.20%
6A	Burlington	Vestibule Door	4.70%	55.60%
6B	Helena	Vestibule Door	5.70%	42.90%
7	Duluth	Vestibule Door	6.90%	53.40%
8	Fairbanks	Vestibule Door	11.20%	62.00%
National Weighted Average			**4.60%**	**40.70%**

**The total annual infiltration is calculated for 10 entrance zones (10 stores) which have openings other than the entrance doors.*

***The total annual infiltration is calculated in lobby (as the main entrance door zone).*

Figure 59 shows a sample of the infiltration rates obtained from the airflow simulations of the outpatient healthcare building with a vestibule. Clear variations in the infiltration rates can be seen which are based on the pressure difference calculated across the door at each time step. It is clear that in warmer months, mid-range of the x-axis, more exfiltration takes place, while in the colder months' infiltration rates are higher. It is also important that in all the year, the design rate of 1.815 m3/s calculated using the ASHRAE Method (presented in Table 21) is never reached.

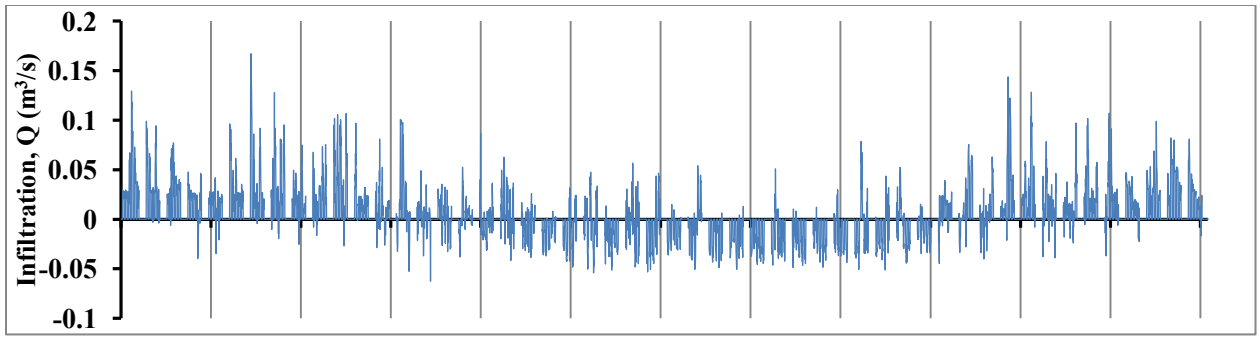

Figure 59. Sample of infiltration rates through the year obtained from airflow simulations for the outpatient healthcare building with a vestibule door (gridlines are months)

It is observed that for the strip mall building, where all of the building's surface area is considered as the entrance zone, small infiltration reductions can lead to large energy savings. It is also observed in the strip mall building, where the stores have multiple openings to the exterior, that the entrance door's air infiltration represents a small fraction of the air infiltration to the building. This is indicated by the small global infiltration reductions realized by the different doors as seen in Table 31.

In contrast, in the outpatient healthcare building, the air infiltration through the door represents the main portion of the air infiltrated to the entrance zone ("Lobby" Zone). The infiltration reductions seen in Table 31 are representative of this relation. In the outpatient healthcare building, where the entrance zone represent a small portion (less than 5%) of the total building surface area, it is seen that the total building energy savings are not directly related to the infiltration reduction realized in the entrance zone separately. Again, due to the connectivity of the interior zones of the buildings in airflow simulations conducted (all interior zones are connected by openings, leakages and to all surrounding and top zones), the buildings' response to infiltration changes in one zone may vary depending on outdoor or indoor parameters. Unlike the ASHRAE Method, where the door infiltration only effects the entrance door (with all other infiltration rates in the building unchanged), the CONTAM-EnergyPlus Method considers all the building as unified multi-zone system making the relation between infiltration reduction and energy savings non-direct. The connectivity of interior zones can lead to changes in pressure, flow and infiltrations in other zones (zones other than the entrance zone). This is further investigated in the sensitivity study (section 5.3.2.3).

Figure 60 and Figure 61 show the air curtain door infiltration reduction in comparison to vestibules and the percent total ON time for the air curtain units in ratio to the total operation hours of the building.

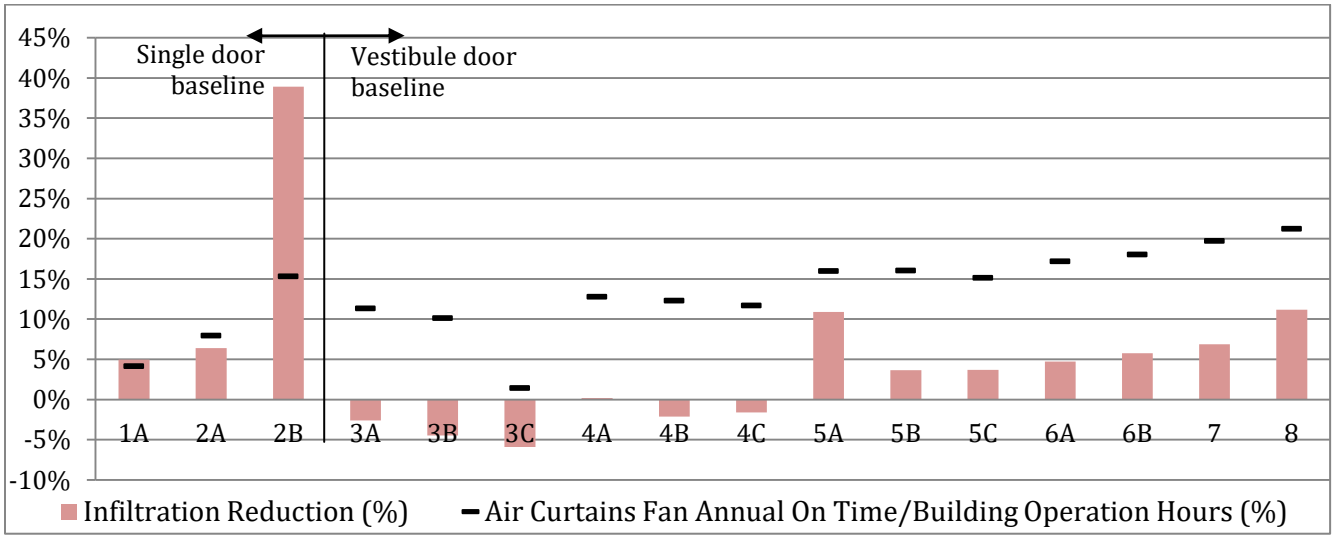

Figure 60. Air curtain door annual infiltration reduction and total air curtain units ON-time (for 10 stores) in the strip mall building

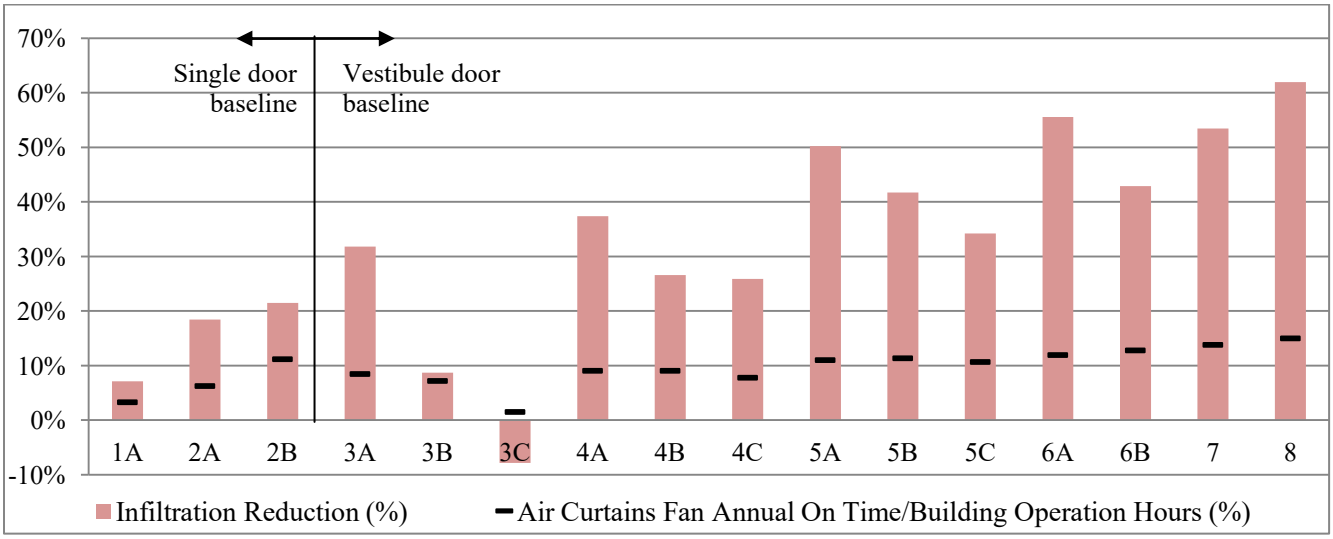

Figure 61. Air curtain door annual infiltration reduction and total air curtain units ON-time in the outpatient healthcare building

Overlaying the infiltration reduction realized by the air curtain doors in each of the two buildings and the air curtain units' operation hours shows a direct relation (when comparing climate zones with the same baseline case - i.e. vestibule or single door baseline cases). In each of the buildings

simulated, the more the air curtain units operated, the higher the annual infiltration reduction achieved by air curtain door.

5.3.2.3 Sensitivity of Energy Simulations using the CONTAM-EnergyPlus Method

Following the methods proposed in section 5.2.6.3, the sensitivity of the energy usage of the two buildings to the variance in door-opening frequency, the pressure coefficient and the orientation of the buildings was analyzed using the CONTAM-EnergyPlus Method (in a number of climate zones). The details of these results and additional sensitivity cases are presented in APPENDIX (G).

5.3.2.3.1 Sensitivity to door usage frequency

As seen in Table 32, Figure 62 and Figure 63, the air curtain doors in both buildings generally sustain their energy savings in comparison to vestibule doors with variance in the door-usage rates. Figure 62 shows that, in the strip mall building, the higher the door-opening frequency the higher the energy savings the air curtain door can achieve when compared to vestibule doors (energy savings increase by 0.58% in CZ-4A and 2.78% in CZ-7 with variation from -30% to 30% from the baseline case). However, Figure 63 shows that, in outpatient healthcare building, the changes in energy savings with the variance in the door-opening frequency are minimal with a slight decrease in savings for higher door usage frequencies (energy savings decreased by 0.02% in CZ-4A and 0.13% in CZ-7 with variation from -30% to 30% from the baseline case).

Table 32. Air curtain door annual energy savings' sensitivity to door usage frequency

Door Usage Percent Variation from Baseline			-30%	**0% (Baseline)**	30%	-30%	**0% (Baseline)**	30%
Climate Zone		Base Case	Strip Mall Building			Outpatient Healthcare Building		
4A	Baltimore	Vestibule Door	1.54%	**2.09%**	2.12%	0.25%	**0.25%**	0.23%
7	Duluth	Vestibule Door	4.36%	**5.94%**	7.14%	0.09%	**0.02%**	-0.04%

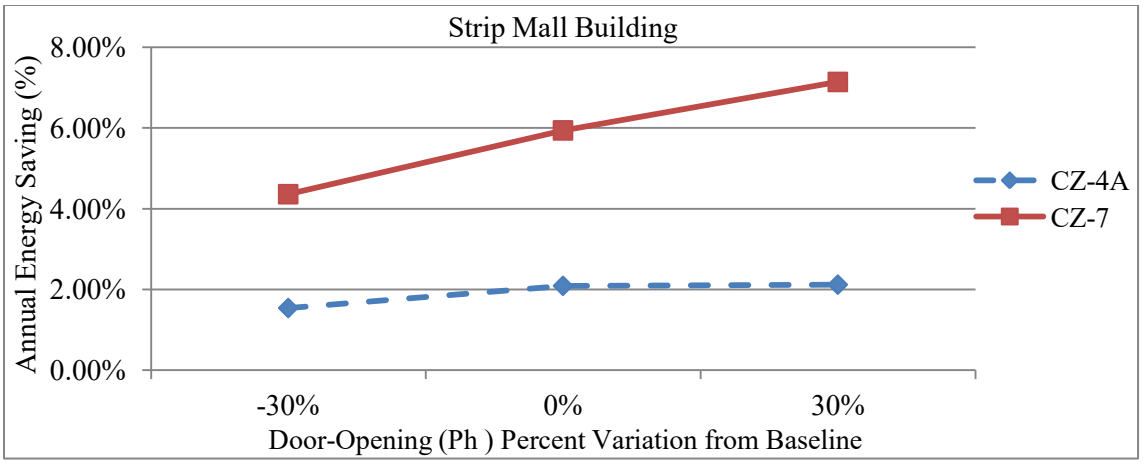

Figure 62. Air curtain door annual energy savings' sensitivity to door-opening frequency in the strip mall building

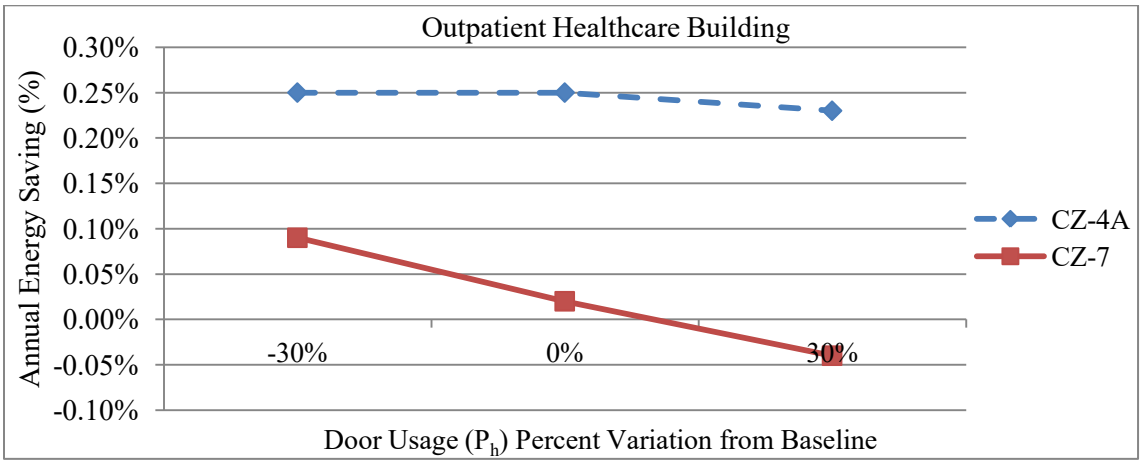

Figure 63. Air curtain door annual energy savings' sensitivity to door-opening frequency in the outpatient healthcare building

5.3.2.3.2 Sensitivity to wind pressure coefficients (outdoor pressure)

As seen in Table 33, Figure 64 and Figure 65, the air curtain door is able to sustain energy savings in comparison to vestibule doors with variance in the wind pressure coefficients in both buildings. Figure 64 shows that, in the strip mall building, the variation in the wind pressure coefficients has small or negligible effect on the air curtain door energy savings when compared to vestibule doors (energy savings decreased by 0.42% in CZ-4A and 0.29% in CZ-7 with variation from -20% to 20% from the baseline case). Figure 65 shows that, in the outpatient healthcare building, the air curtain door continues to save energy when compared to vestibules with variance in air pressure coefficients with slight increases in the savings for higher pressure

coefficients (energy savings increased by 0.15% in CZ-4A and 0.02% in CZ-7 with variation from -20% to 20% from the baseline case).

Table 33. Air curtain door annual energy savings' sensitivity to wind pressure coefficients

Pressure Coefficients Percent Variation from Base case			-20%	**0% (Baseline)**	20%	-20%	**0% (Baseline)**	20%
Climate Zone		Base Case	Strip Mall Building			Outpatient Healthcare Building		
4A	Baltimore	Vestibule Door	2.31%	**2.09%**	1.89%	0.17%	**0.25%**	0.32%
7	Duluth	Vestibule Door	6.09%	**5.94%**	5.80%	0.01%	**0.02%**	0.03%

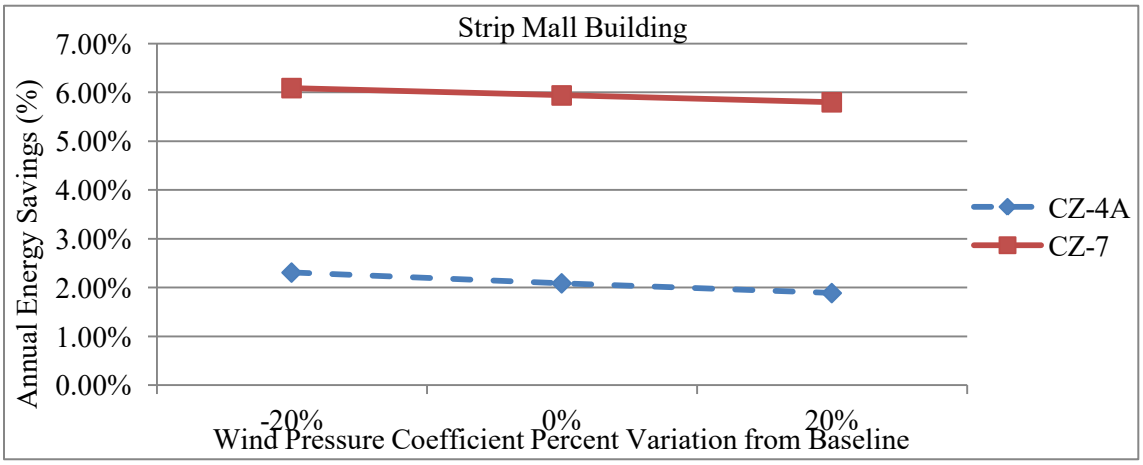

Figure 64. Air curtain door annual energy savings' sensitivity to wind pressure coefficients in the strip mall building

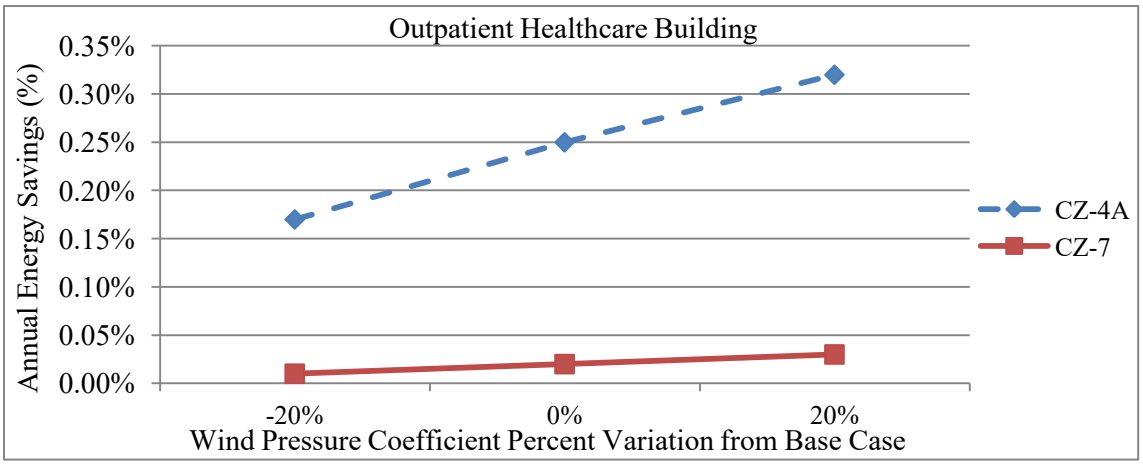

Figure 65. Air curtain door annual energy savings' sensitivity to wind pressure coefficients in the outpatient healthcare building

The detailed results are presented in APPENDIX (G) and the details of the pressure coefficients values used in the energy simulations are discussed in the methodology of this chapter in section 5.2.6.3.

5.3.2.3.3 Sensitivity to building orientation

As seen is Table 34, Figure 66 and Figure 67, the change in the buildings' orientation results in small variations in the energy savings of the two buildings. In the strip mall building, as seen in Figure 66, the air curtain doors continue to realize savings with variance in the building orientation for all the 3 climate zone locations simulated. Due to the smaller energy savings in the outpatient healthcare building, as seen in Figure 67, the variance in the building orientation make the air curtain door save or consume more energy when compared to the vestibule door.

Once again, comparing the infiltration reduction in the entrance zone(s) (seen in Table 35) and the air curtain door energy savings (seen in Table 34) indicates a direct relationship for the strip mall building and a more complex relation in the outpatient healthcare building model. Thus, when comparing air curtain doors to vestibule doors in the strip mall building, the higher the infiltration reduction, the higher the energy saving. However, in the outpatient healthcare building, this is not always the case: for example, in climate zone 4A (Baltimore), the infiltration reduction in the west orientation is 44.2% with 0.04% energy savings and 37.4% in the north orientation with 0.25% energy savings. For the outpatient healthcare building, the data shows independent reaction to the variation of orientations in each climate location.

Table 34. Air curtain door annual energy savings' sensitivity to building orientation

Building Orientation			**North (Baseline)**	East	South	West	**North (Baseline)**	East	South	West
Climate Zone		Base Case	Strip Mall Building				Outpatient Healthcare Building			
4A	Baltimore	Vestibule Door	**2.09%**	2.23%	3.64%	3.74%	**0.25%**	0.05%	0.06%	0.04%
7	Duluth	Vestibule Door	**5.94%**	5.37%	6.58%	7.26%	**0.02%**	-0.13%	0.06%	-0.08%
8	Fairbanks	Vestibule Door	**7.71%**	7.77%	7.97%	7.50%	**-0.27%**	-0.43%	-0.06%	0.05%

It is important to note that, the standard deviation in the total energy consumption of the two buildings with variance in the orientation indicate that air curtain door(s) is less affected by the building orientation when compared to vestibule door(s) - based on the standard deviation data presented in APPENDIX (G). A more stable performance is expected (energy consumption) for

the buildings with air curtains than when with vestibules. APPENDIX (E) presents the details of the prevailing wind directions in each climate zone location.

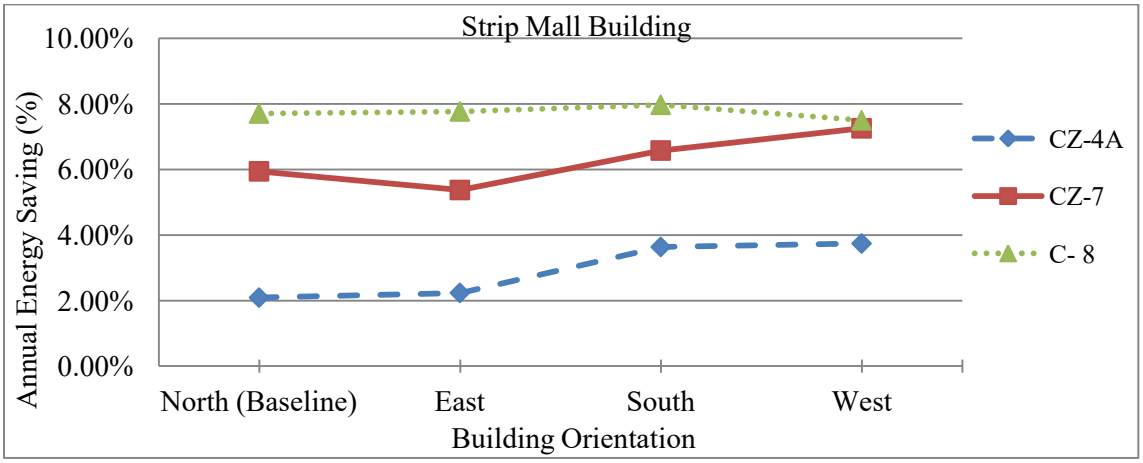

Figure 66. Air curtain door annual energy savings' sensitivity to building orientation in the strip mall building

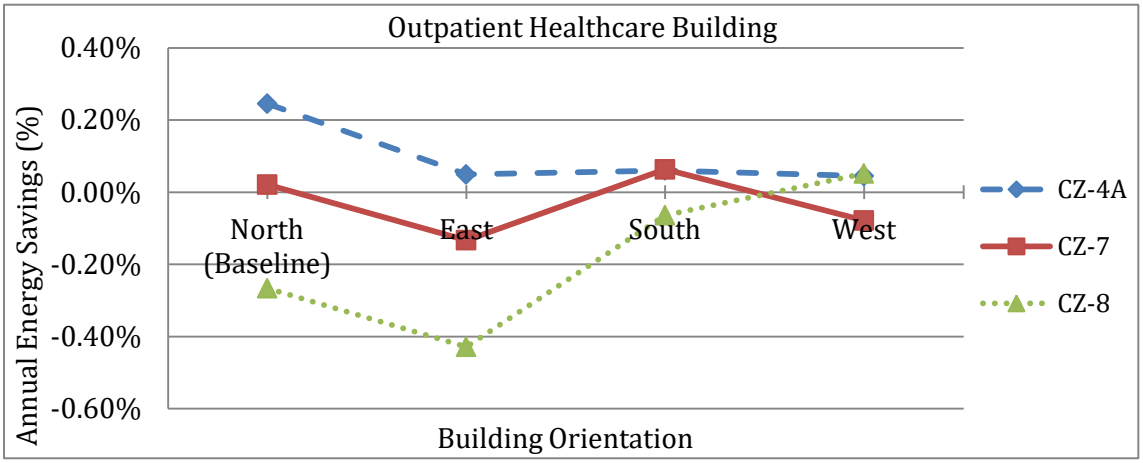

Figure 67. Air curtain door annual energy savings' sensitivity to building orientation in the outpatient healthcare building

Table 35. Air curtain door annual infiltration reduction sensitivity to building orientation

Building Orientation			**North (Baseline)**	East	South	West	**North (Baseline)**	East	South	West
Climate Zone		Base Case	Strip Mall Building				Outpatient Healthcare Building			
4A	Baltimore	Vestibule Door	**0.20%**	1.00%	3.80%	3.10%	**37.40%**	36.80%	40.70%	44.20%
7	Duluth	Vestibule Door	**6.90%**	6.90%	9.30%	8.60%	**53.40%**	54.50%	54.70%	60.90%
8	Fairbanks	Vestibule Door	**11.20%**	12.10%	12.30%	10.90%	**62.00%**	64.00%	64.60%	65.30%

5.3.2.3.4 Sensitivity to air curtain temperature control

As presented in section 5.2.5.2, the sensitivity of the air curtain door savings (air curtain door vs. vestibule door) to the air curtain temperature control parameters was quantified in CZ-3C (San Francisco). The air curtain door was simulated with no temperature control and compared to the vestibule door results presented in Table 27. Similarly to the sensitivity of this parameter when simulated with the ASHRAE method presented in section 5.2.5.2, the strip mall shows more savings (moving from negative to positive savings) with no temperature control. However, in contrast to the ASHRAE method, the outpatient healthcare building also shows more savings when the air curtain is Always On (no temperature control). This indicates that further investigation might be needed for the optimum temperature control parameters for each climate zone.

Table 36. Energy savings sensitivity to air curtain door temperature control in the CZ-3C

		Strip Mall		Outpatient Healthcare	
Air Curtain Temperature Control (Where T is the temperature range in ° C where the unit operates)		**30 < T < 10 (Baseline)**	Always ON (No temp. Control)	**30 < T < 10 (Baseline)**	Always ON (No temp. Control)
3C- San Francisco	Energy Saving	**-0.44%**	0.38%	**-0.11%**	0.61%

5.3.2.3.5 Sensitivity of the outpatient healthcare building to door location and internal zones' interaction

As suggested in the methodology of this chapter in section 5.2.6.3, a number of simulations were conducted in order to investigate the effect of the door location on the outpatient healthcare building. The details of this study are presented in APPENDIX (G).

It is found that when simulating the outpatient healthcare building with the entrance door in the "Lobby" zone, the vestibule doors showed a national weighted average energy savings of 0.08% when compared to single doors and the air curtain door saved 0.34% of energy when compared to vestibule doors. However, when simulating the building with the entrance door in the "Vestibule" zone, the vestibule doors showed a national weighted average energy savings of 0.00% when compared to single doors and the air curtain door saved -0.07% (consumed an additional 0.07%) of energy when compared to vestibule doors (refer to Figure 94 in APPENDIX (E) for the zones' location).

It was also seen that in certain extreme cold climate zones (such as CZ-8), when the CONTAM-EnergyPlus Method is used, the outpatient healthcare building with vestibule door is seen to consume more energy than the building with single door. This observation is related to the interactions of the entrance zone to the surrounding zones of the building (internal zones' interaction). The results of the sensitivity study indicate that, when the interaction between the internal zones is considered in CONTAM, the outpatient healthcare building uses more energy in CZ-8 with a vestibule door than when with a single door. Also the building with the air curtain door used even more energy than with a vestibule. This increase in energy usage is despite the fact that, in the entrance zone, the vestibule door reduced 8.7% of the yearly infiltration of the single door and that the air curtain door reduced 62% of yearly vestibule door infiltration. However, when removing (sealing) the interaction between the entrance zone (i.e. the lobby) and its surrounding, the vestibule door and the air curtain door showed energy savings (when compared to their respective baseline case) and showed higher yearly infiltration reductions (in percentage).

Based on the analysis of the results, these observations were linked to the strong stack effect generated in the building and the increase of infiltration rates in surrounding zones when more air tight (doors that provide better sealing/higher resistance to flow) are used in the entrance door. However, these observations can be the topic of future research since they are specific to extreme climate conditions.

5.4 Conclusion

Based on the obtained air curtain correlations from CFD presented in Chapter 4 and the methods proposed by Yuill (1996) and Wang (2013), the whole building EnergyPlus simulations were conducted using two methods of infiltration calculations: the ASHRAE Method, which uses design pressure values (R_p) and the CONTAM-EnergyPlus Method, which uses hourly infiltration data obtained through airflow simulations using CONTAM.

In the two reference building energy models simulated, namely the strip mall and outpatient healthcare buildings, energy simulations using both infiltration calculation methods showed that (a summary of the findings is provided in Table 37):

- air curtain doors save energy on a national weighted average level for the 15 climate zone locations (of the USA) when compared to vestibule doors in climate zones 3 - 8 and to single doors in climate zones 1 & 2.
- air curtain doors significantly reduce the total annual infiltration through the entrance door in comparison to vestibule doors and single doors.
- the infiltration reduction realized by air curtain doors is directly related to the operation hours of the air curtain: the longer the air curtain operates, the more infiltrations are reduced in comparison to single doors or vestibule doors.

Considering the space saving benefit of air curtains and their lower initial costs, it is concluded that air curtains are a valid energy saving alternative to the vestibule doors in climate zones 3 to 8 and a valuable energy saving addition in climate zones 1 & 2.

The sensitivity study using the CONTAM-EnergyPlus Method shows that the building orientations, entrance door locations, door usage rates, connectivity and interactions of internal zones, as well as the weather conditions all affect air infiltrations/exfiltration of the building, and consequently the resultant energy performance for the 3 entrance door scenarios - section 5.3.2.3, APPENDIX (F) and APPENDIX (G). Particularly, the weather conditions and the interaction of the building's internal zones cannot be overlooked as they are seen to significantly affect the buildings' energy performance. Also, as mentioned previously, the hours of operation of the air curtain have a major impact on the energy savings the air curtain door modeled (section 05.3.2.2).

Table 37. Summary of energy simulation results for the two building models of interest

		Strip Mall Building		Outpatient Healthcare Building	
		ASHRAE Method	CONTAM Method	ASHRAE Method	CONTAM Method
Total Annual Infiltration Reduction	National Weighted Average*	NA	4.6%**	NA	40.7%**
	Comments		Reduction in total annual infiltration in 10 stores with multiple exterior openings (10 entrances door & other large openings)		Reduction in total annual infiltration in 1 zone with 1 exterior openings (1 entrance door)
Total Annual Energy Savings	National Weighted Average*	6.52% 12.91 kWh/m^2	2.21% 4.20 kWh/m^2	0.90% 3.33 kWh/ m^2	0.34% 1.33 kWh/m^2
	Range	18.67% ~ -7.84%	7.71% ~ -0.44%	1.62% ~ 0.34%	2.54% ~ -0.27%
	Comments	Energy savings in 14 climate zones	Energy savings in 14 climate zones	Energy Savings in 16 climate zones	Energy savings in 10 climate zones
Air curtain Energy Consumption	National Weighted Average*	548.16 kWh		314.37 kWh	

** Savings are calculated by comparison to vestibule doors in climate zones 3-8 and single doors in climate zone 1-2.*
***Reductions obtained by the airflow simulation method were calculated based on the total infiltration in Kg of air obtained from simulations, they consider other factors other than the entrance door infiltration (other openings, weather and schedule*

Finally, and based on the data presented in this chapter, it is concluded that simulating the buildings using the design infiltration rates (ASHRAE, 2009) calculation method (ASHRAE Method) might lead to exaggerations in the savings calculated for both the vestibule doors and the air curtain doors - section 5.3.1 and APPENDIX (F). It is also concluded that the airflow simulations method for infiltration rates calculation (CONTAM-EnergyPlus Method) can provide more accurate estimates for the annual building's infiltration rates and energy consumption (section 5.3.2).

6 CONCLUSIONS

Considering the significant impact that air infiltration through large openings has on the total energy consumption of buildings, this research aimed to investigate the energy saving impact of air curtain doors in commercial buildings. The research had three main components (tasks), an experimental study, a numerical (CFD) simulation study and an energy simulation study.

In regards to the experimental validation, an experimental chamber (the CUBE) equipped with an air curtain was constructed and used to validate the CFD modeling methods of air curtains available in the literature (Wang, 2013) and the models available to estimate and correlate the air curtain infiltration characteristics (Wang & Zhong, 2014a). The results of the numerical simulations conformed to the experimental infiltration rates measured through the chamber's air curtain door, within the pressure difference range of -2 Pa to 20 Pa. Also, the airflow fields measured using PIV at the test chamber were similar to the velocity fields obtained by the numerical simulations. It was concluded that the CFD modeling method of air curtains proposed by Wang (2013) was valid and accurate in capturing the performance of air curtain doors and that the correlation methods proposed by Wang el al. (Wang & Zhong, 2014a) can accurately estimate the infiltration rates through the door. In addition, the experimental tests at the CUBE chamber found that:

- The infiltration rates measured through the air curtain door are significantly lower than the measured infiltrations through the single door
- The infiltration rates measured through the air curtain door are significantly lower than the measured and later theoretically calculated infiltrations through a vestibule door of the same size by Yuill (1996)
- The higher the air curtain supply speed, the better the air curtain performs, i.e. it is able to continue to operate in the optimum condition at higher pressure differences.
- The larger the outward angle of the air curtain supply, the better it is able to reduce air infiltrations.
- The performance of the air curtain door tested was barely affected by the outdoor wind of up to 10 m/s and continued to maintain its better performance in comparison to the single and vestibule door.

- The presence of a person in the doorway may slightly improve the air curtain performance by blocking air infiltrations.
- Particle image velocimetry (PIV) data captured for the airflows at the air curtain door confirms that the three airflow regions of air curtains found the previous study by Wang et al. (Wang & Zhong, 2014a): namely, inflow breakthrough and optimum conditions. By the visualization of the flow fields, the PIV data are also consistent with, and support, the findings from the blower door tests.
- For both the single door and the air curtain door, the CFD simulation results of the CUBE chamber agree well with the measured data in the chamber.

Following the validation of the CFD modeling methods, an extensive numerical study of more than 600 CFD cases was conducted using ANSYS Fluent 14 (ANSYS, 2011). The performance of air curtain doors with air supply of 10, 15 and 20 m/s and 10°, 15° and 20° outwards, and with and without people in the doorway was compared within the pressure difference range of -30 Pa to 60 Pa. The air curtain door with an air supply of 20 m/s and 20° outward and with a person in the doorway was found to have the best performance within the pressure range indicated out of all the simulated cases. Following the methods proposed by Wang et al (Wang & Zhong, 2014a; Wang, 2013), the correlations for the mentioned air curtain door were developed for a full door opening cycle and were used in whole building energy analysis of the strip mall and outpatient healthcare DOE model reference buildings in EnergyPlus.

Whole building EnergyPlus simulations were conducted using two methods of infiltration calculations: the ASHRAE Method (which uses a constant design pressure values as proposed by ASHRAE and used by PNNL in the development of the energy models), and the airflow simulation method (CONTAM-EnergyPlus Method), which uses hourly infiltration data calculated through airflow simulation using CONTAM. In the 2 buildings, both simulation methods showed that, on a national-average level, air curtain doors reduce air infiltration and save energy. It was also concluded that the CONTAM-EnergyPlus Method is more realistic in calculating infiltration rates and their related energy losses. In contrasts, the ASHRAE Method was observed to result in exaggerations in infiltration reductions and energy savings. In addition, for the 2 reference building models simulated, both simulation methods showed that:

- Air curtain doors significantly reduce total annual infiltrations in comparison to vestibule doors and single doors.
- The reduction of infiltration in the entrance zone of the buildings is directly related to the operation hours of the air curtain: the longer the air curtain operates, the more infiltrations are reduced in comparison to single doors or vestibule doors.
- For the climate zones investigated, air curtain doors continue to save energy in both buildings in comparison to vestibule doors with variations in the door usage frequency and wind pressure coefficients.
- The sensitivity study using the airflow simulation method shows that the building orientations, entrance door locations, door usage rates, connectivity and interactions with internal zones, as well as the weather conditions all affect air infiltration/exfiltration of the building, and consequently the resultant energy performance for the three entrance door scenarios. Particularly, the weather conditions and the interaction of the building's internal zones cannot be overlooked and they are shown to significantly affect the buildings' energy performance. Also, as mentioned previously, the hours of operation of the air curtain (which could be controlled by the operation temperature range) had a major impact on the energy savings the air curtain door modeled.

Considering the space saving benefit of air curtains and their lower initial costs, air curtains are concluded to be a valid and energy saving alternative to vestibule doors in climate zones 3 to 8 and a valuable energy saving addition in climate zones 1 & 2.

6.1 Recommendations for Future Research

The results of this research and the extensive review of literature conducted reveal the following future research opportunities:

- Developing a comprehensive model that can estimate the air curtain doors' performance (for air curtains with different supply characteristics - speeds and angles)
- Developing better control methods for air curtain doors during operation and dynamic control methods for the units based on more advanced environmental sensing
- Investigating the relation between the air curtains' supply uniformity (different models or construction of units) and performance

- Optimizing the temperature control of air curtain units in different climate zone locations
- Further investigating the effect of outdoor wind, temperature difference, supply angle on the air curtain doors performance as well as the effect of people presence in the doorway
- Investigating the relation between the buildings parameters (size, number of zones, height, door size and operation schedules) on the energy savings achieved from reductions in air infiltration through doors
- Investigating the effect of outdoor weather/climate conditions on entrance door air infiltration in buildings (especially in extreme cold weather)
- Investigating the effect airflow in buildings (airflow network) have on the end-savings in large buildings
- Reevaluating the saving impact of vestibules doors using the airflow simulation method considering the differences presented in this thesis

Figure 68 clarifies the relation between the different proposed future studies.

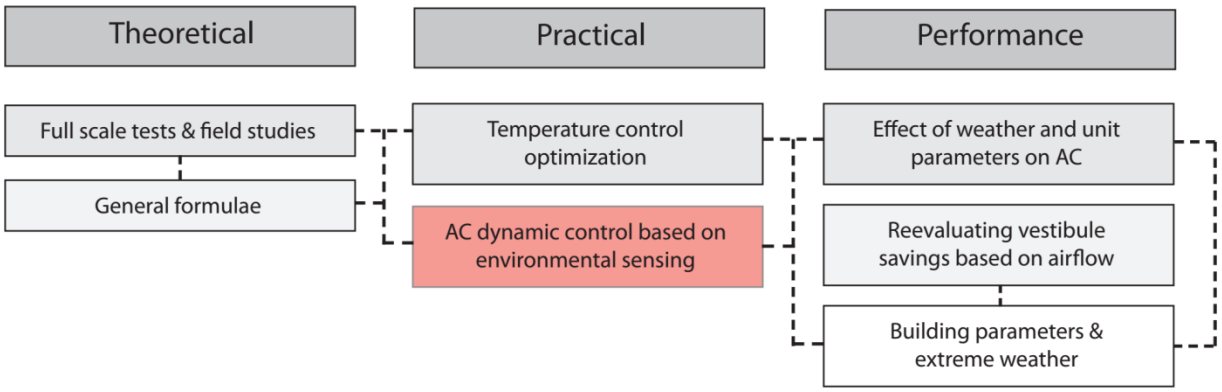

Figure 68. Relation between the different proposed future studies

REFERENCES

Adrian, R. J. (2005). Twenty years of particle image velocimetry. *Experiments in Fluids*, *39*(2), 159–169.

Air Movement and Control Association International. (2012a). Application Manual for Air Curtains. *Publication 222-08 (R2012)*, *08*.

Air Movement and Control Association International. (2012b). Laboratory Methods of Testing Air Curtain Units for Aerodynamic Performance Rating. *ANSI / AMCA Standard 220-05*, *05*.

Alamdari, F. (1997). *Air Curtains commercial applications - Application Guide 2/97*. *The Building Services Research and Information Association*. Berkshire: BSRIA.

ANSYS. (2011). *ANSYS FLUENT User's Guide – Release 14.0*. *ANSYS*. Canonsburg, PA.

ASHRAE. (2006). *ASHRAE Handbook: Refrigeration*. Atlanta: American Society of Heating, Refrigerating and Air Conditioning Engineers.

ASHRAE. (2007). *ASHRAE Handbook–HVAC Applications*. Atlanta: American Society of Heating, Refrigerating and Air Conditioning Engineers.

ASHRAE. (2009). *ASHRAE Handbook–Fundamentals*. Atlanta: American Society of Heating, Refrigerating and Air Conditioning Engineers, Inc.

ASHRAE. ASHRAE standard 90.1-2010: Energy Standard for Buildings Except Low-Rise Residential Buildings, ASHRAE/IESNA Standard (2010).

Belleghem, M. Van, Verhaeghe, G., T'Joen, C., Huisseune, H., De Jaeger, P., & De Paepe, M. (2012). Heat Transfer Through Vertically Downward-Blowing Single-Jet Air Curtains for Cold Rooms. *Heat Transfer Engineering*, *33*(June 2013), 1196–1206.

Bosbach, J., Kühn, M., Wagner, C., Raffel, M., Resagk, C., Puits, R., & Thess, A. (2006). Large Scale Particle Image Velocimetry of Natural and Mixed Convection 2 . Measurement of Convective Air Flow on Large Scales, 26–29.

Bryant, R. A., & Johnsson, E. L. (n.d.). *Large-Scale Particle Image Velocimetry Measurements of a Fire-Induced Doorway Flow*. Maryland.

Building Technologies Office: EnergyPlus Energy Simulation Software. (n.d.). Retrieved December 1, 2015, from http://apps1.eere.energy.gov/buildings/energyplus/

Cao, G., Sivukari, M., Kurnitski, J., & Ruponen, M. (2010). PIV measurement of the attached plane jet velocity field at a high turbulence intensity level in a room. *International Journal*

of Heat and Fluid Flow, *31*(5), 897–908.

Cao, G., Sivukari, M., Kurnitski, J., Ruponen, M., & Seppänen, O. (2010). Particle Image Velocimetry (PIV) application in the measurement of indoor air distribution by an active chilled beam. *Building and Environment*, *45*(9), 1932–1940.

Cao, X., Liu, J., Jiang, N., & Chen, Q. (2014). Particle image velocimetry measurement of indoor airflow field: A review of the technologies and applications. *Energy and Buildings*, *69*, 367–380.

Chen, Y. G. (2009). Parametric evaluation of refrigerated air curtains for thermal insulation. *International Journal of Thermal Sciences*, *48*(10), 1988–1996.

Cho, H., Liu, B., & Gowri, K. (2010). Energy Saving Impact of ASHRAE 90.1 Vestibule Requirements: Modeling of Air Infiltration through Door Openings. *Pacific Northwest National Laboratory*, (November). Retrieved from http://www.pnl.gov/main/publications/external/technical_reports/PNNL-20026.pdf

Commercial Prototype Building Models | Building Energy Codes Program. (n.d.). Retrieved December 1, 2015, from https://www.energycodes.gov/commercial-prototype-building-models

CONTAM User Manual. (n.d.). Retrieved December 1, 2015, from http://www.bfrl.nist.gov/IAQanalysis/CONTAM/userguide.htm

CONTAM Weather File Creator. (n.d.). Retrieved December 4, 2015, from http://www.bfrl.nist.gov/IAQanalysis/software/WEATHERprogram.htm

Costa, J. J., Oliveira, L. a., & Silva, M. C. G. (2006). Energy savings by Aerodynamic Sealing with a Downward-Blowing Plane Air Curtain - A Numerical Approach. *Energy and Buildings*, *38*(10), 1182–1193.

Crawley, D. (1998). Which weather data should you use for energy simulations of commercial buildings? *American Society of Heating Refrigerating and Air-Conditioning*, 1–18. Retrieved from http://apps1.eere.energy.gov/buildings/energyplus/pdfs/bibliography/whichweatherdatashouldyouuseforenergysimulations.pdf

Cremers, I. B. E. (2012). *Air Curtains : faster is not always better!*

Dantec Dynamics, & Nova Instruments. (2012). *DynamicStudio imaging platform*.

Deru, M., Field, K., Studer, D., & Benne, K. (2011). US Department of Energy commercial

reference building models of the national building stock. *National Laboratory of the U.S. Department of Energy*, (February 2011). Retrieved from http://www.nrel.gov/docs/fy11osti/46861.pdf

DG-700 Pressure and Flow Gauge - The Energy Conservatory. (n.d.). Retrieved December 4, 2015, from http://products.energyconservatory.com/dg-700-pressure-and-flow-gauge/

Emmerich, S. J., & Persily, A. K. (1998). Energy Impacts of Infiltration and Ventilation in U.S. Office Buildings Using Multizone Airflow Simulation. In *IAQ and Energy 98 Conference* (pp. 191–203). New Orleans.

Foster, A. M., Swain, M. J., Barrett, R., D'Agaro, P., & James, S. J. (2006). Effectiveness and optimum jet velocity for a plane jet air curtain used to restrict cold room infiltration. *International Journal of Refrigeration*, *29*(5), 692–699.

Goel, S., Rosenberg, M., Athalye, R., & Xie, Y. (2014). Enhancements to ASHRAE Standard 90.1 Prototype Building Models. *Pacific Northwest National Laboratory*, (April). Retrieved from http://www.energycodes.gov/sites/default/files/documents/PrototypeModelEnhancements_2014_0.pdf

Goubran, S., Qi, D., & Wang, L. (Leon). (2015). Annual Energy Saving Impact of Air Curtains in Commercial Reference Buildings. In *ISHVAC-COBEE* (p. 8). Tianjin.

Gowri, K., Winiarski, D., & Jarnagin, R. (2009). Infiltration Modeling Guidelines for Commercial Building Energy Analysis. *Contract*, (September), 21.

Hart, D. P. (2000). PIV error correction. *Experiments in Fluids*, *29*(1), 13–22.

Hayes, F. C. (1968). *Heat Transfer Characteristics of the Air Curtain: A Plane Jet Subjected to Transverse Pressure and Temperature Gradients*. University of Illinois.

Hayes, F. C., & Stoecker, W. F. (1969). Design Data For Air Curtains. *ASHRAE Transactions*, 168–180.

Hayes, F. C., & Stoecker, W. F. (1969). Heat transfer characteristics of the air curtain. *ASHRAE Transactions 75*, *75*, 153–167.

Howell, R. (2008). *Design & Application Guide: Air Curtains*. *Leading Edge*. Retrieved from http://www.cartographicperspectives.org/index.php/journal/article/view/1220

Indac, S. (2011). *Determination of the climate separation efficiency of Biddle air curtains Doorflow HP-200 and Indac S200 under laboratory conditions*. Netherlands.

Jaramillo, J., Oliva, A., Perez-Segarra, C. D., & Oliet, C. (2008). Application of Air Curtains in Refrigerated Chambers. In *Proceedings of the 12th International Refrigeration and Air Conditioning at Purdue* (pp. 1–8). Perdue University.

Jarnagin, R., & Bandyopadhyay, G. (2010). Weighting Factors for the Commercial Building Prototypes Used in the Development of ANSI/ASHRAE/IENSA Standard 90.1. *Pacific Northwest National Laboratory*, (January). Retrieved from http://www.pnl.gov/main/publications/external/technical_reports/PNNL-19116.pdf

Jiang, W., Gowri, K., Lane, M., Thornton, B., & Liu, B. (2009). Technical Support Document: 50% Energy Savings Design Technology Packages for Highway Lodging Buildings. *Pacific Northwest National Laboratory*, (September).

Johnson, D., Thomas, P., Kordecki, L., & Berner International Corporation. (2008). Air Curtains : a Proven Alternative to Vestibule Design. *Berner International Corp.*

Landau, L. D., & Lifshitz, E. M. (1987). *Fluid Mechanics*. (McGraw-Hill, Ed.)*Image Rochester NY* (Vol. 6). Pergamon Press.

Laser Optical CCD and sCMOS Cameras | Dantec Dynamics. (n.d.). Retrieved December 1, 2015, from http://www.dantecdynamics.com/ccd-and-scmos-cameras

Lawton, E. B., & Howell, H. (1995). Energy Saving Using Air Curtain Installed in High Traffic Doorway. *ASHRAE Transactions*, *101*(2), 136–143.

Li, A., Qin, E., Xin, B., Wang, G., & Wang, J. (2010). Experimental analysis on the air distribution of powerhouse of Hohhot hydropower station with 2D-PIV. *Energy Conversion and Management*, *51*(1), 33–41.

Liu, M. (1992). *Study of air infiltration energy consumption*. Texas A&M University. Retrieved from http://repository.tamu.edu/handle/1969.1/6463

Mahajan, G., Cho, H., Shanley, K., & Kang, D. (2015). Comprehensive modeling of airflow rate through automatic doors for low-rise buildings. *Building and Environment*, *87*, 72–81.

Minneapolis Duct Blaster® System - The Energy Conservatory. (n.d.). Retrieved December 4, 2015, from http://products.energyconservatory.com/minneapolis-duct-blaster-system/

National Institute of Standards and Technology. (2014). CONTAM Results Export Tool Description. Retrieved March 23, 2015, from http://www.bfrl.nist.gov/IAQanalysis/webapps/contam_results_exporter/desc.htm

New Wave Research. (2004). Solo PIV - Nd : YAG Laser Systems.

Ng, L. C., Emmerich, S. J., & Persily, A. K. (2014). An Improved Method of Modeling Infiltration in Commercial Building Energy Models. In *2014 ASHRAE/IBPSA Building Simulation Conference* (pp. 308–315). Atlanta.

Ng, L. C., Musser, A., Persily, A. K., & Emmerich, S. J. (2012). *Airflow and indoor air quality models of DOE reference commercial buildings*. *National Institute of Standards and Technology*. Retrieved from http://www.bfrl.nist.gov/IAQanalysis/docs/Tech Note 1734 - CONTAM reference bldgs.pdf

Nicklas Karlsson. (2013). *Air Infiltration through Building Entrances*. Chalmers University of Technology. Retrieved from http://publications.lib.chalmers.se/records/fulltext/184752/184752.pdf

Pappas, T. C., & Tassou, S. A. (2003). Numerical Investigations into the Performance of Doorway Vertical Air Curtains in Air-Conditioned Spaces. *ASHRAE Transactions*, *109*(1), 7.

Polidoro, B., Ng, L. C., Dols, W. S., & Emmerich, S. J. (2015). *NIST Technical Note 1873: CONTAM To EnergyPlus Infiltration Features of the CONTAM Results Export Tool*. Gaithersburg.

Qi, D., Goubran, S., Zmeureanu, R., & Wang, L. L. (2015). Effect of People on Infiltration of Building Entrance with Air Curtains. In *ISHVAC-COBEE* (p. 9). Tianjin.

Raffel, M., Willert, C. E., Wereley, S., & Kompenhans, J. (2013). *Particle Image Velocimetry: a Practical Guide*. Berlin: Springer-Verlag Berlin Heidelberg.

Sage action Inc. (2002). *SA/TM BUBBLE GENERATOR MODEL 5 CONSOLE*. ITHACA.

Scarano, F., Ghaemi, S., Caridi, G., Bosbach, J., Dierksheide, U., & Sciacchitano, A. (2014). On the use of helium filled soap bubbles for large-scale Tomographic PIV wind tunnel experiments. In *17th International Symposium on Applications of Laser Techniques to Fluid Mechanics* (pp. 7–10). Lisbon.

Scarano, F., Ghaemi, S., Caridi, G., Bosbach, J., Dierksheide, U., & Sciacchitano, A. (2015). On the use of helium - filled soap bubbles for large - scale Tomographic PIV wind tunnel experiments. *Experiments in Fluids*, *56*(42), 7–10.

Sirén, K. (2003a). Technical dimensioning of a vertically upwards blowing air curtain - Part II. *Energy and Buildings*, *35*(7), 681–695.

Sirén, K. (2003b). Technical dimensioning of a vertically upwards-blowing air curtain - Part I.

Energy and Buildings, *35*(7), 697–705.

Stein, J., & Kung, F. (2012). *Retail Building Guide for Entrance Energy Efficiency Measures*. Golden, CO (United States). Retrieved from http://www.osti.gov/servlets/purl/1037934/

Sun, Y., & Zhang, Y. (2007). An Overview of Room Air Motion Measurement: Technology and Application. *HVAC&R Research*, *13*(6), 929–950.

Swami, M. V., & Chandra, S. (1987). Procedures for calculating natural ventilation airflow rates in buildings. In *FSEC* (p. -163–86). Florida: Florida Solar Energy Center.

The Energy Conservatory. (2007). Operating Instructions for the Minneapolis Digital Pressure And Fan Flow Gauge (Model DG-3), (February), 2004–2007.

The Energy Conservatory. (2015). Minneapolis Duct Blaster ®. Minneapolis: The Energy Conservatory.

Thornton, B., Wang, W., Huang, Y., Lane, M., & Liu, B. (2010). Technical Support Document: 50% Energy Savings for Small Office Buildings. *Pacific Northwest National Laboratory*, (April). Retrieved from http://www.pnl.gov/main/publications/external/technical_reports/PNNL-19341.pdf

Thornton, B., Wang, W., Xie, Y., Cho, H., Liu, B., & Zhang, J. (2011). Achieving the 30% Goal : Energy and Cost Savings Analysis of ASHRAE Standard 90.1-2010. *Pacific Northwest National Laboratory*, 370.

TRNSYS. (n.d.). Retrieved December 1, 2015, from http://sel.me.wisc.edu/trnsys/features/

US DOE. (2010). EnergyPlus Engineering Reference. *The Reference to EnergyPlus Calculations*. Retrieved from http://apps1.eere.energy.gov/buildings/energyplus/pdfs/engineeringreference.pdf

Van der Mass, J. (1992). Annex 20 : Air Flow Patterns within Buildings Airflow through Large Openings. *International Energy Agency*. Lausanne. Retrieved from http://scholar.google.com/scholar?hl=en&btnG=Search&q=intitle:Air+Flow+Through+Large+Openings+in+Buildings#2

Verhaeghe, G., & Belleghem, M. Van. (2010). Study of air curtains used to restrict infiltration into refrigerated rooms. In *7th International conference on Heat Transfer, Fluid Mechanics and Thermodynamics (HEFAT 2010)* (p. 8). Antalya, Turkey.

Wang, L. (Leon). (2013). *Investigation of the Impact of Building Entrance Air Curtain on Whole Building Energy Use*. *Air Movement and Control Association*. Retrieved from

http://www.amca.org/UserFiles/file/Energy Initiative Web Pages/Air Curtain Study.pdf

Wang, L. (Leon), & Zhong, Z. (2014a). An approach to determine infiltration characteristics of building entrance equipped with air curtains. *Energy and Buildings*, *75*, 312–320.

Wang, L. (Leon), & Zhong, Z. (2014b). Whole Building Annual Energy Analysis of Air Curtain Performance in Commercial Building. In *eSim*. Ottawa.

Yuill, G. K. (1996). *Impact of High Use Automatic Doors on Infiltration*. *ASHRAE Research Project 763-TRP*. Pennsylvania.

Yuill, G. K., Upham, R., & Hui, C. (2000). Air leakage through automatic doors. *ASHRAE Transactions*, *106*(2), 145–160.

Zhang, J., Athalye, R., Hart, R., Rosenberg, M., & Xie, Y. (2013). Energy and Energy Cost Savings Analysis of the IECC for Commercial Buildings. *Pacific Northwest National Laboratory*, (August).

APPENDIX (A)

Experimental Design Methodology

Experimental Design

Chamber as Proposed by Project Team

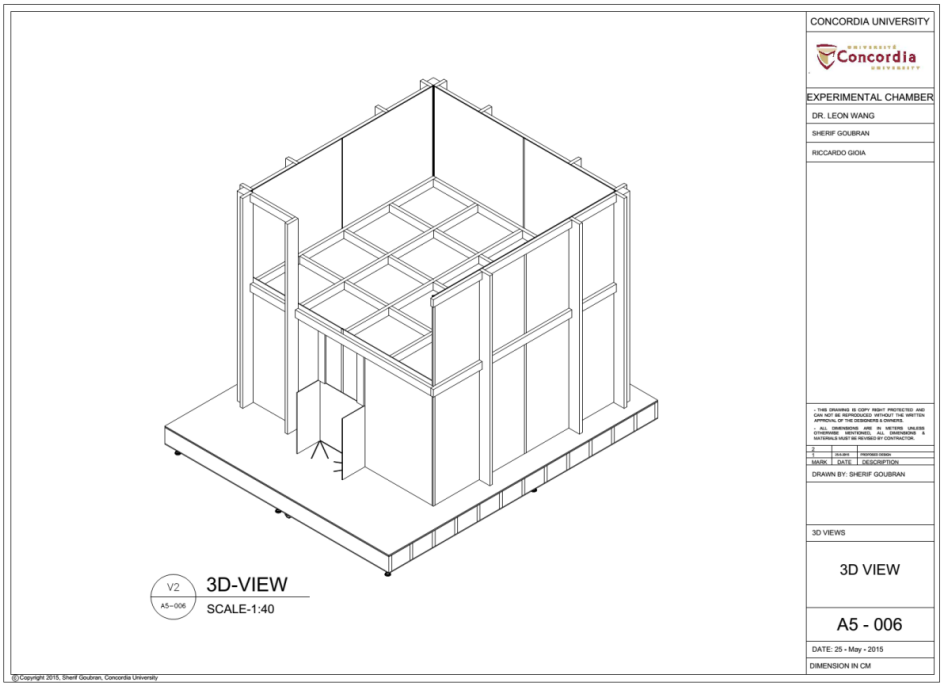

Figure 69. Sample technical drawing for chamber design prepared by the project team

Build Test Chamber (CUBE)

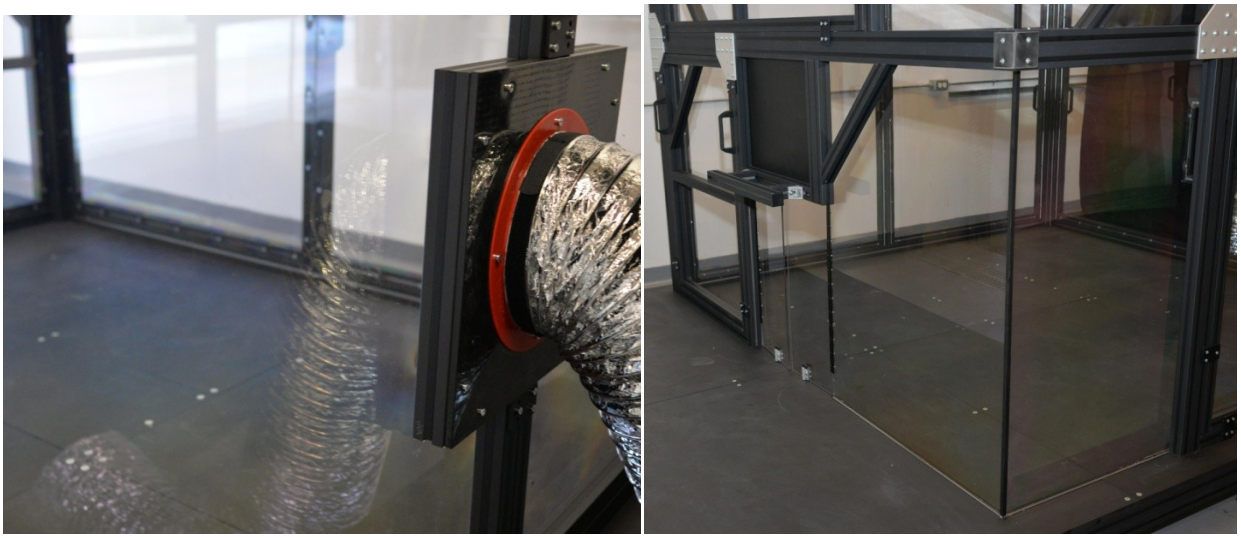

Figure 70. The fan duct (right) and the PIV clear corner of the CUBE (pictures provided by MËKANIC)

HFSB System

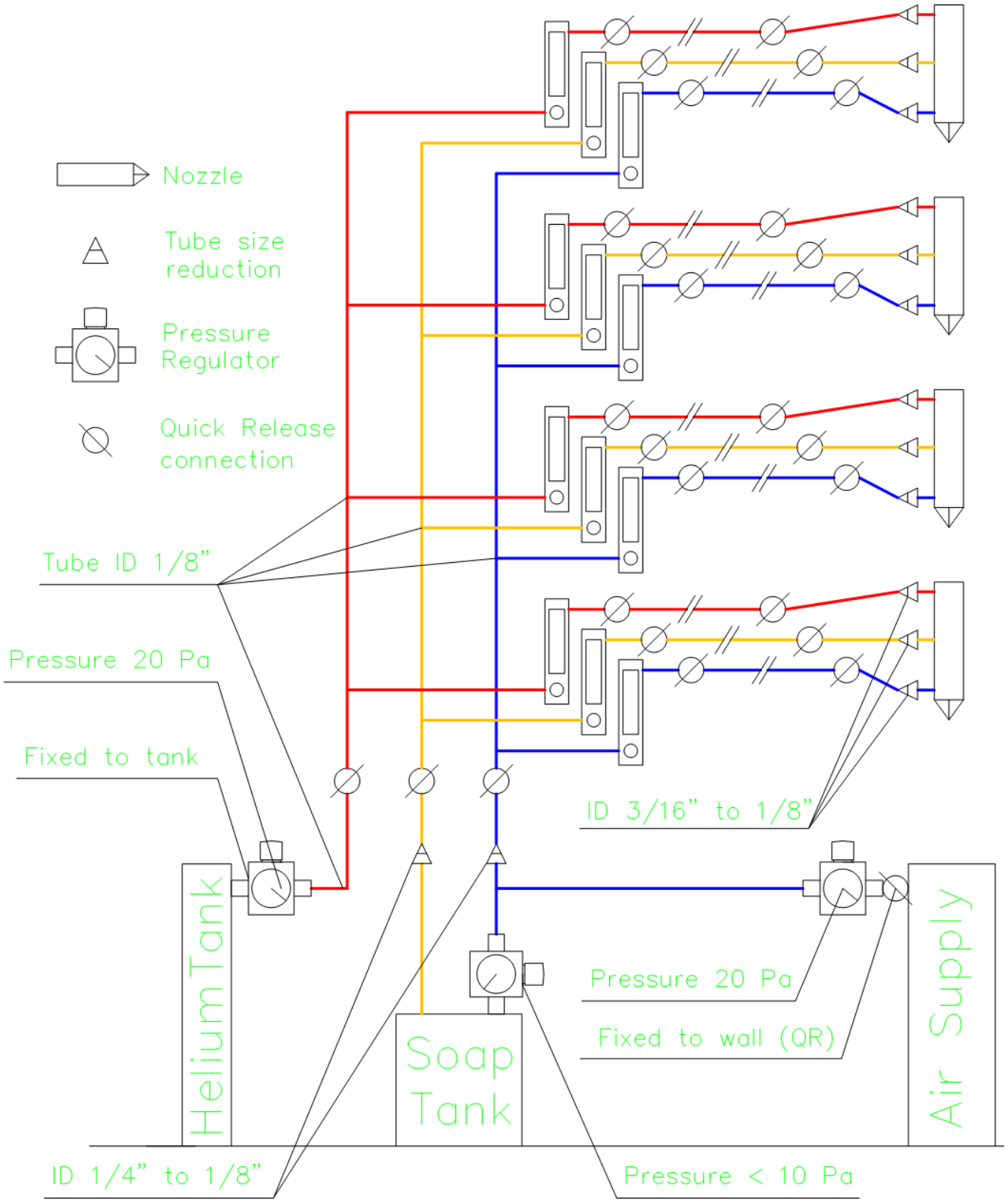

Figure 71. HFSB system diagram

Air Curtain Unit Supply Profile Data

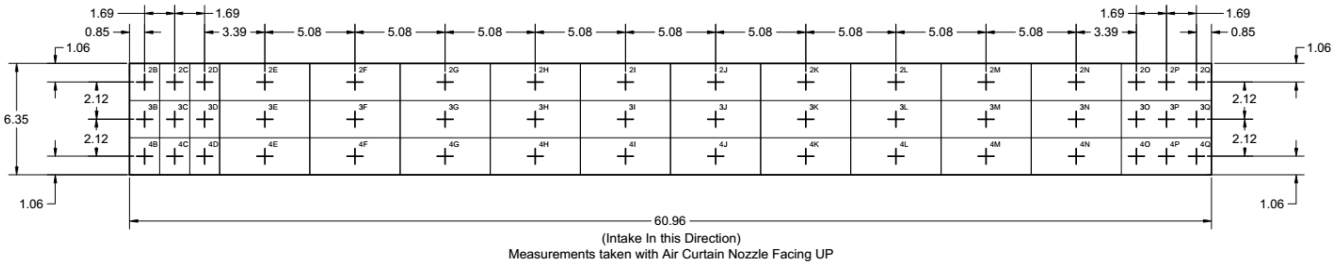

Figure 72. Air curtain supply speed measurement points

Table 38. Air curtain supply profile with 40 Hz VFD configuration (R1 near the door)

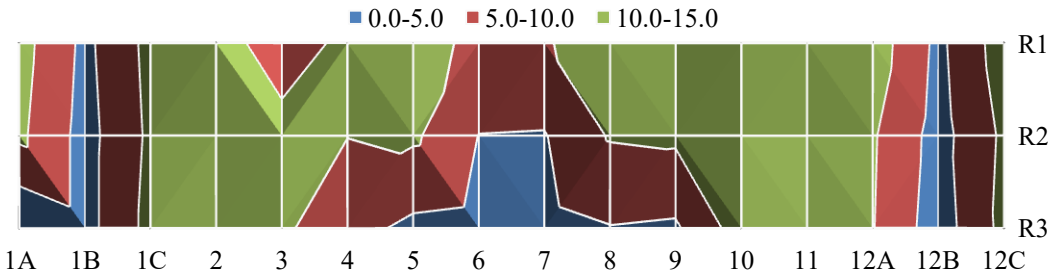

Average Speed	9.10 m/s
Standard Deviation	3.61 m/s
Average variance	39.67%

Table 39. Air curtain supply profile with 60 Hz VFD configuration (R1 near the door)

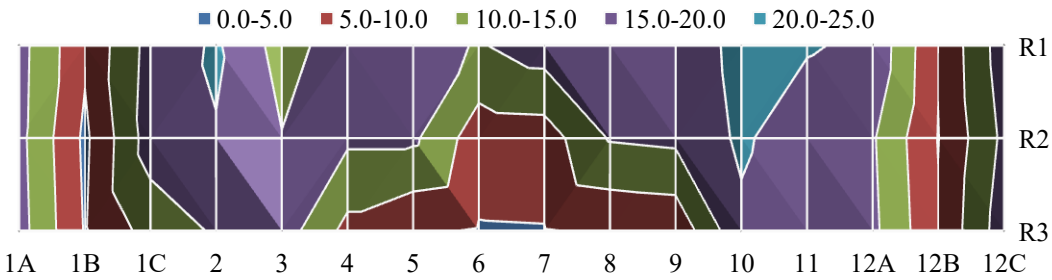

Average Speed	13.75 m/s
Standard Deviation	5.50 m/s
Average variance	40.10%

PIV Seeding

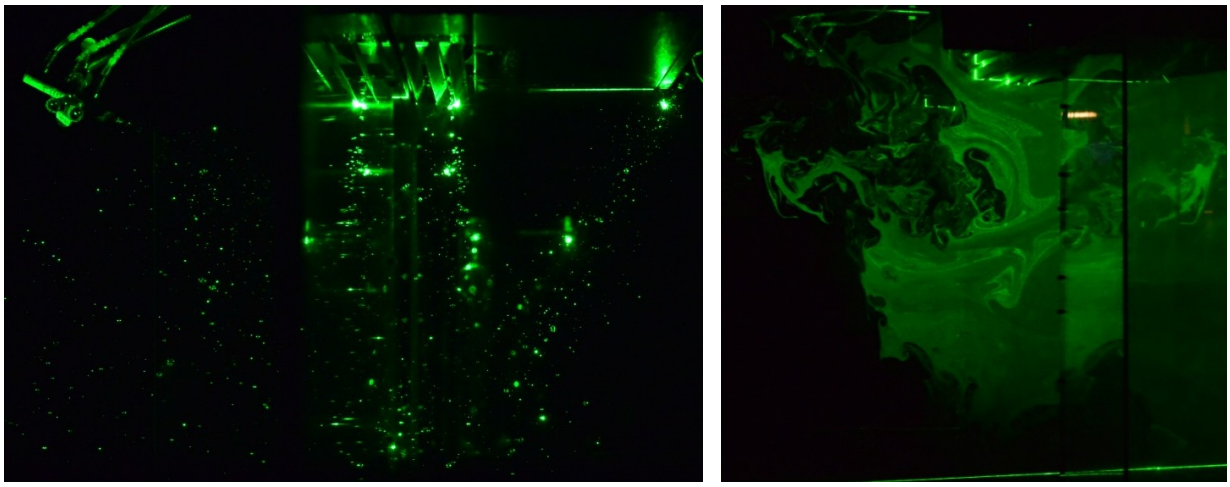

Figure 73. Seeding with HFSB (left) and some trials with fog (right) (pictures provided by MËKANIC)

Effect of People on Performance

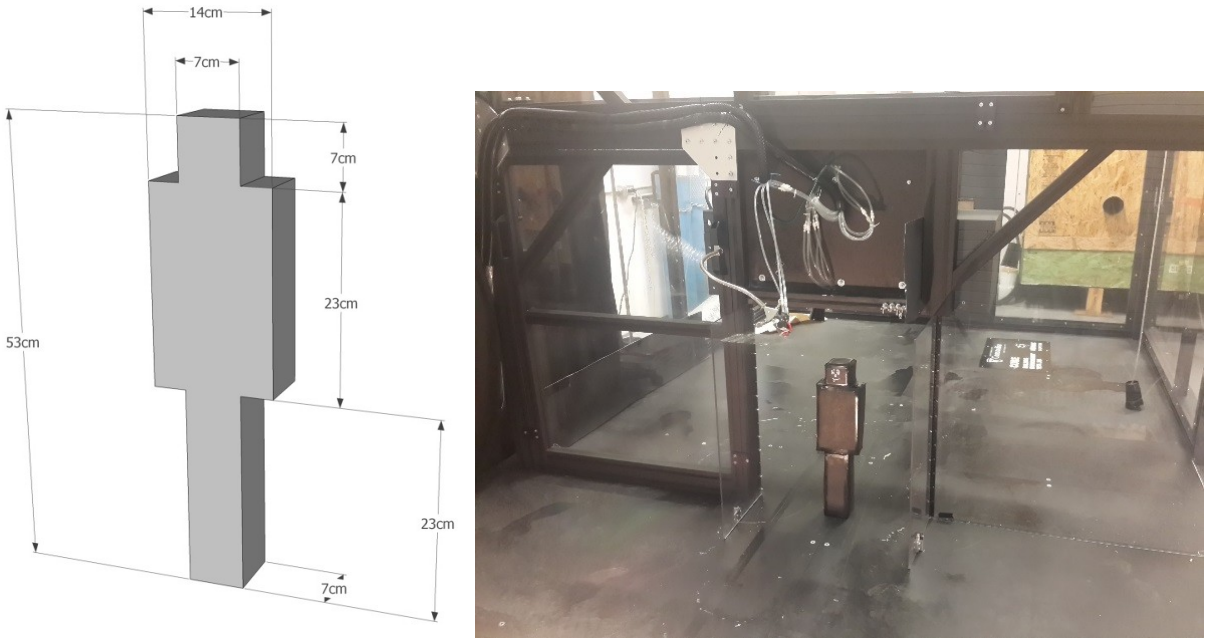

Figure 74. Details of the person model used (left) and the model placed in the doorway

Chamber Air Tightness Tests (Systematic Error in Flow Measurements)

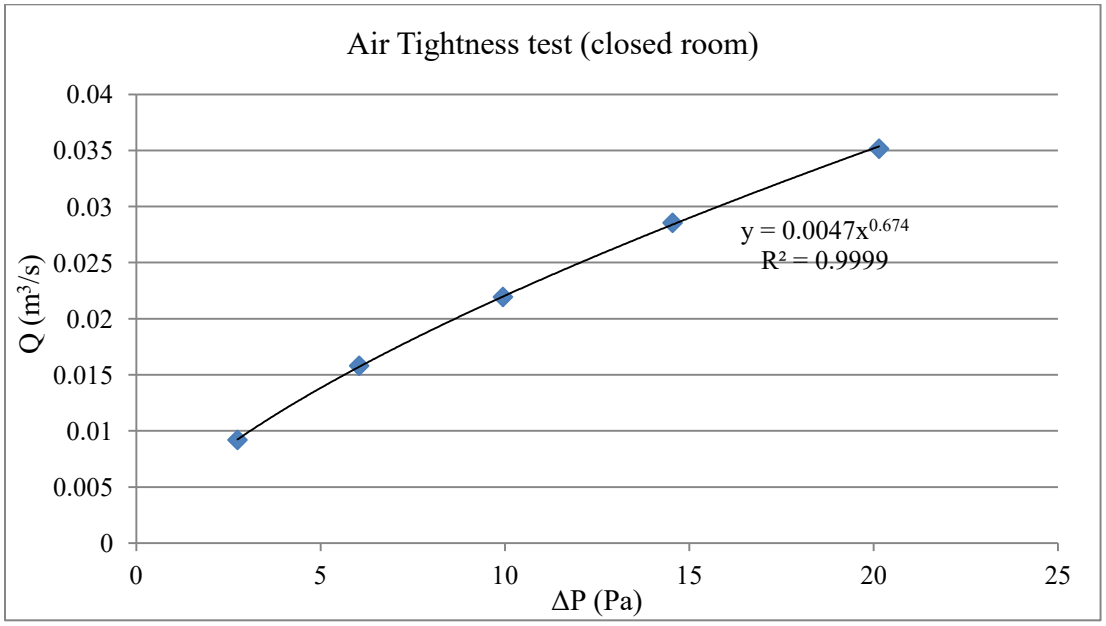

Figure 75. Chamber air tightness test: air infiltration with closed doors under varying pressure conditions used to calculate the error in the experimental flow measurements

APPENDIX (B)

Detailed Experimental Results

Blower-Door Tests

Single Door

Table 40. Raw experimental data for the air infiltration through the single door with 2 measurement points

Q (CFM)	Exp. 1 ΔP (in-out)	Exp. 2 ΔP (in-out)
800	-1.2	-1.3
700	-1	-0.9
600	-0.7	-0.7
500	-0.5	-0.4
400	-0.3	-0.3
300	-0.2	-0.2
0	0	0
-300	0.2	0.1
-400	0.3	0.2
-500	0.4	0.3

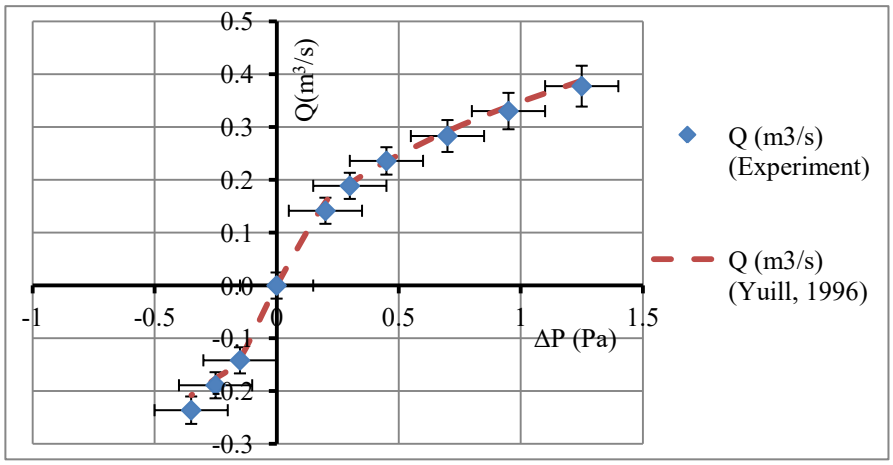

Figure 76. Averaged single door experimental infiltration with error range compared to empirical infiltration curve (Yuill, 1996) with an average error of 3.48%

Air Curtain Door (Average Supply of 9.1 m/s at 20°)

Table 41. Raw experimental data (2 measured points) for the air infiltration through the air curtain door (Average Supply of 9.1 m/s at 20°)

Q (CFM)	Exp. 1 ΔP (in-out)	Exp. 2 ΔP (in-out)
700	-10.4	-10.3
600	-9.9	-9.8
550	-9.6	-9.4
500	-9.2	-9.1
450	-8.8	-8.6
400	-8.5	-8.3
325	-7.5	-7.7
250	-7	-6.8
150	-6.4	-6.2
0	-5.4	-5.2
-120	-4.6	-4.8
-300	-2.8	-2.7
-400	-1.6	-1.7
-500	-0.6	-0.6
-600	0.1	0

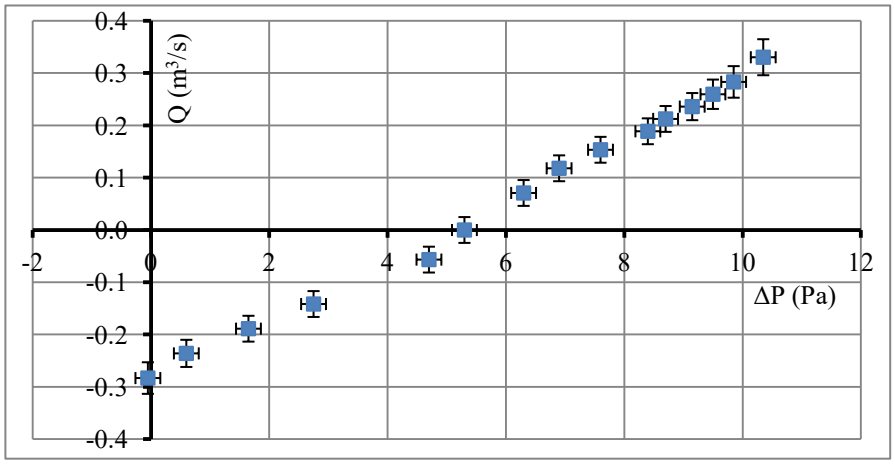

Figure 77. Averaged air curtain door (Average Supply of 9.1 m/s at 20°) experimental infiltration

Air Curtain Door (Average Supply of 13.75 m/s at 20°)

Table 42. Raw experimental data (2 measured points) for the air infiltration through the air curtain door (Average Supply of 13.75 m/s at 20°)

Q (CFM)	Exp. 1 ΔP (in-out)	Exp. 2 ΔP (in-out)
740	-19.1	-19.2
650	-18.2	-18.2
600	-17.6	-17.5
550	-17	-16.9
500	-16.6	-16.5
450	-16	-16.1
400	-15.4	-15.6
350	-14.9	-14.8
300	-14.5	-14.3
225	-13.7	-13.9
150	-12.7	-12.6
0	-11.5	-11.6
-190	-10.4	-10.2
-300	-8.9	-8.7
-400	-6.9	-6.7
-500	-5.2	-5.2
-600	-3.8	-3.9

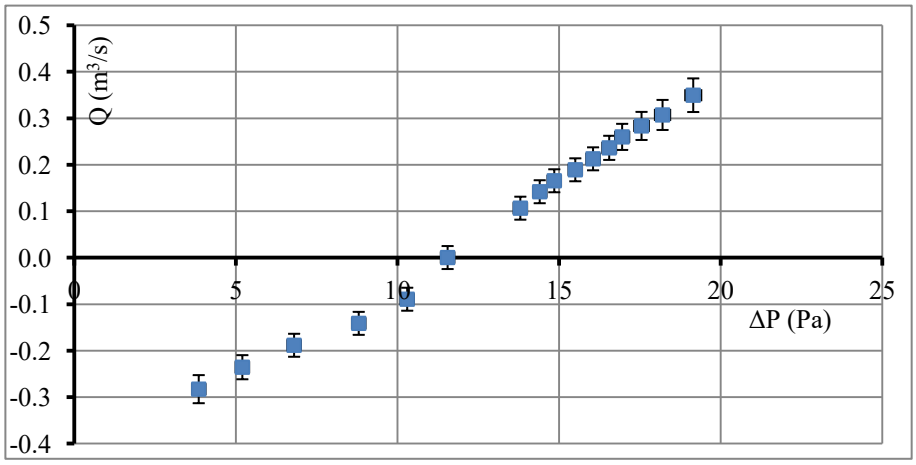

Figure 78. Averaged air curtain door (Average Supply of 13.75 m/s at 20°) experimental infiltration

Effect of Wind on Air Curtain Door (Average Supply of 13.75 m/s at 20°)

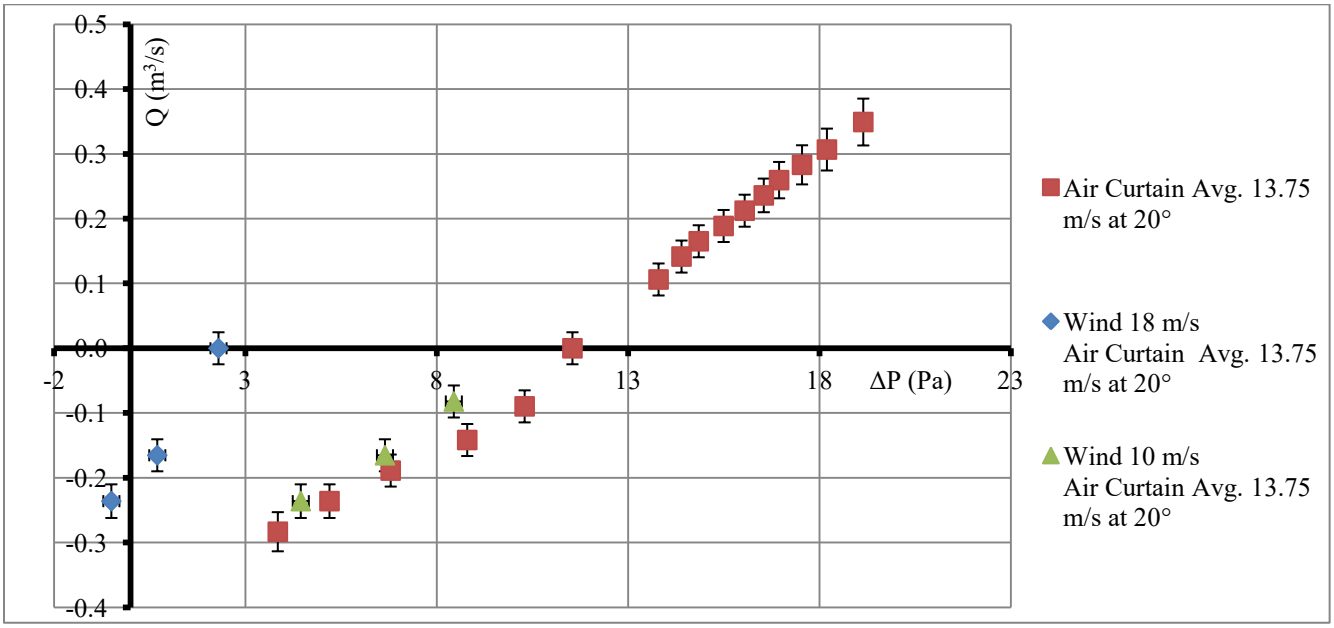

Figure 79. Effect of external wind on the air curtain door (Average Supply of 13.75 m/s at 20°) experimental infiltration

Effect of Presence of People on Air Curtain Door (Average Supply of 13.75 m/s at 20°)

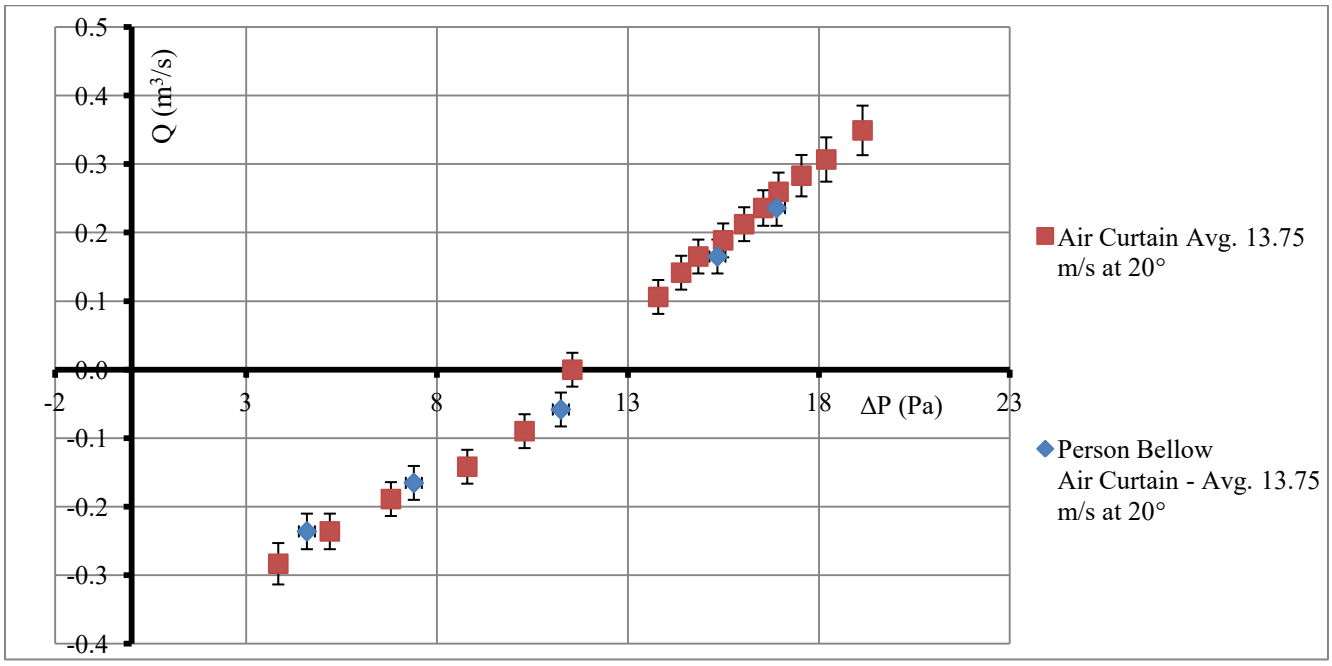

Figure 80. Effect of presence of people under the air curtain jet on the air curtain door (Average Supply of 13.75 m/s at 20°) experimental infiltration

Effect of Supply angle Air Curtain Door (Average Supply of 13.75 m/s)

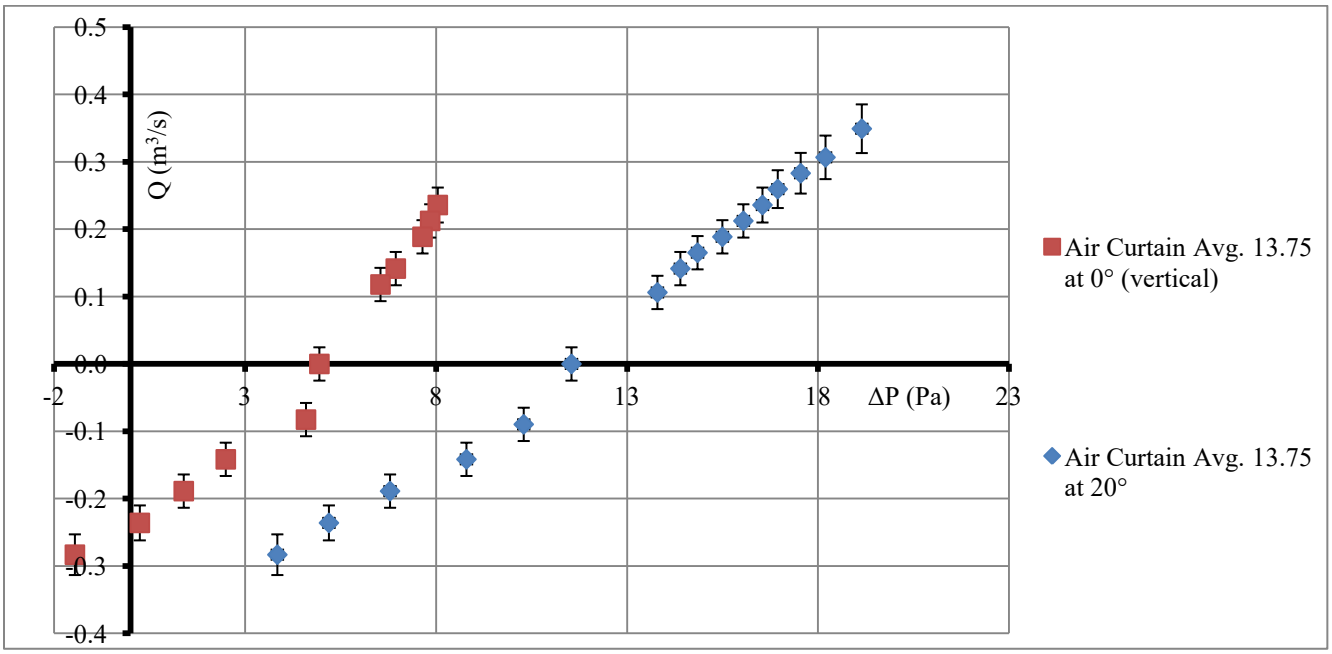

Figure 81. Effect of air supply angle on the air curtain door (Average Supply of 13.75 m/s) experimental infiltration

Differences in Airflow Rates between Experiments and Correlations

Table 43. Difference between the experimental and correlated flow rates for the air curtain with avg. supply of 13.75 m/s at 20°

ΔP (out - in) - (Pa)	Experiment - (m^3/s)	Correlation - (m^3/s)	Difference
19.15	0.3492	0.3236	7.35%
18.2	0.3068	0.2815	8.23%
17.55	0.2832	0.2521	10.98%
16.95	0.2596	0.2244	13.53%
16.55	0.2360	0.2057	12.81%
16.05	0.2124	0.1820	14.28%
15.5	0.1888	0.1555	17.61%
14.85	0.1652	0.1236	25.17%
14.4	0.1416	0.1011	28.60%
13.8	0.1062	0.0705	33.60%
11.55	0.0000	-0.0492	100.00%
10.3	-0.0897	-0.0776	13.43%
8.8	-0.1416	-0.1141	19.44%
6.8	-0.1888	-0.1679	11.07%
5.2	-0.2360	-0.2170	8.05%
3.85	-0.2832	-0.2647	6.51%
	Average		20.67%

Table 44. Difference between the experimental and correlated flow rates for the air curtain with avg. supply of 9.1 m/s at 20°

ΔP (out - in) - (Pa)	Experiment - (m^3/s)	Correlation - (m^3/s)	Difference
10.35	0.3304	0.4060	22.88%
9.85	0.2832	0.3682	30.04%
9.5	0.2596	0.3412	31.46%
9.15	0.2360	0.3138	32.96%
8.7	0.2124	0.2776	30.73%
8.4	0.1888	0.2530	34.04%
7.6	0.1534	0.1852	20.74%
6.9	0.1180	0.1228	4.11%
6.3	0.0708	0.0668	5.61%
5.3	0.0000	-0.0328	100.00%
4.7	-0.0566	-0.0731	-29.03%
2.75	-0.1416	-0.1187	-16.19%
1.65	-0.1888	-0.1521	-19.43%
0.6	-0.2360	-0.1977	-16.22%
0	-0.2832	-0.2670	-5.72%
	Average		15.07%

PIV Data and CFD Flow Fields

Door Side-Plane

Average supply speed 9.1 m/s at 20°

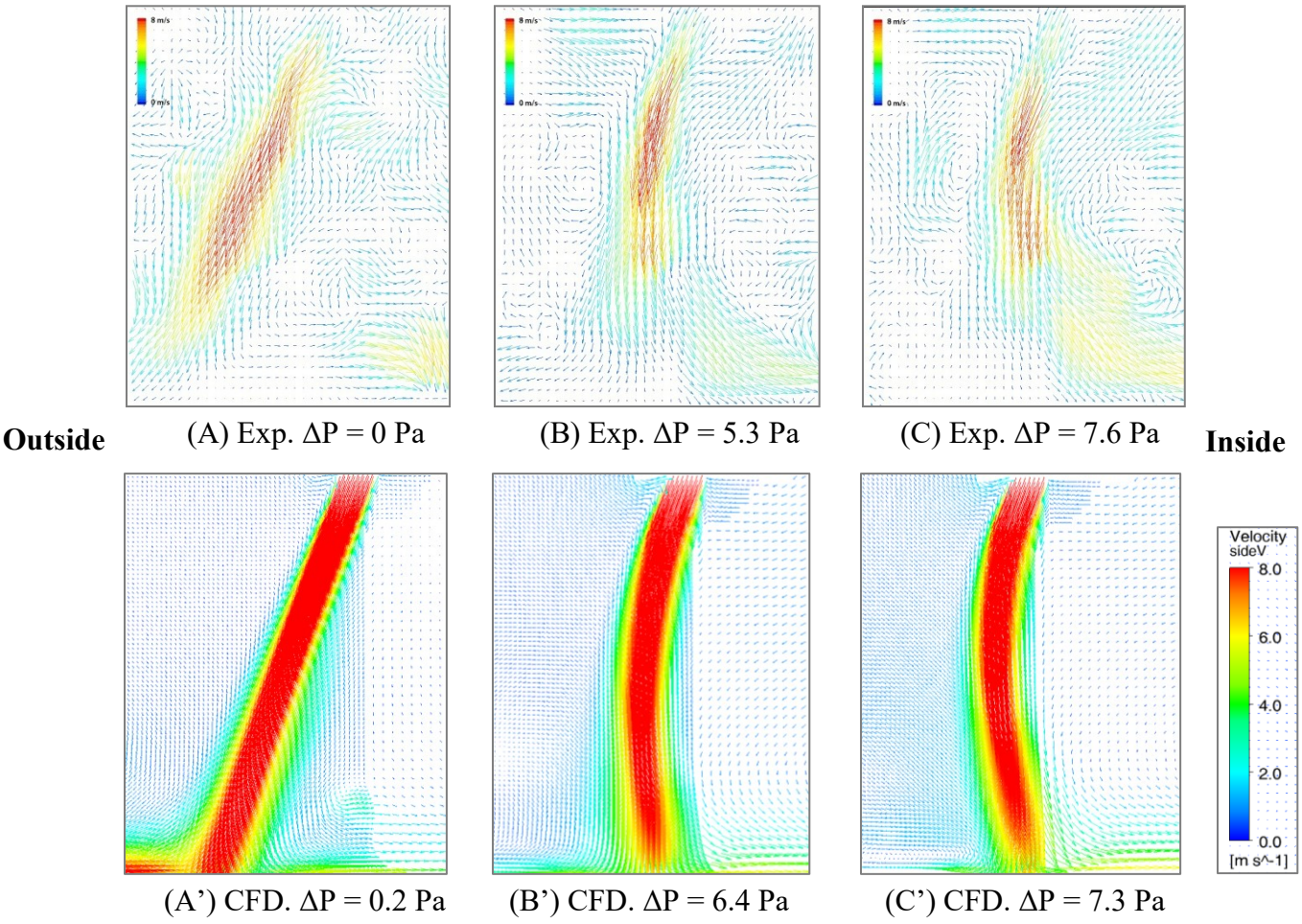

Figure 82. Additional comparison between experimental and CFD simulation flow visualization at door side-plane for the air curtain with an average supply speed of 9.1 m/s at 20° - (A) is outflow breakthrough and (B) & (C) are inflow breakthrough

Average supply speed 13.75 m/s at 20°

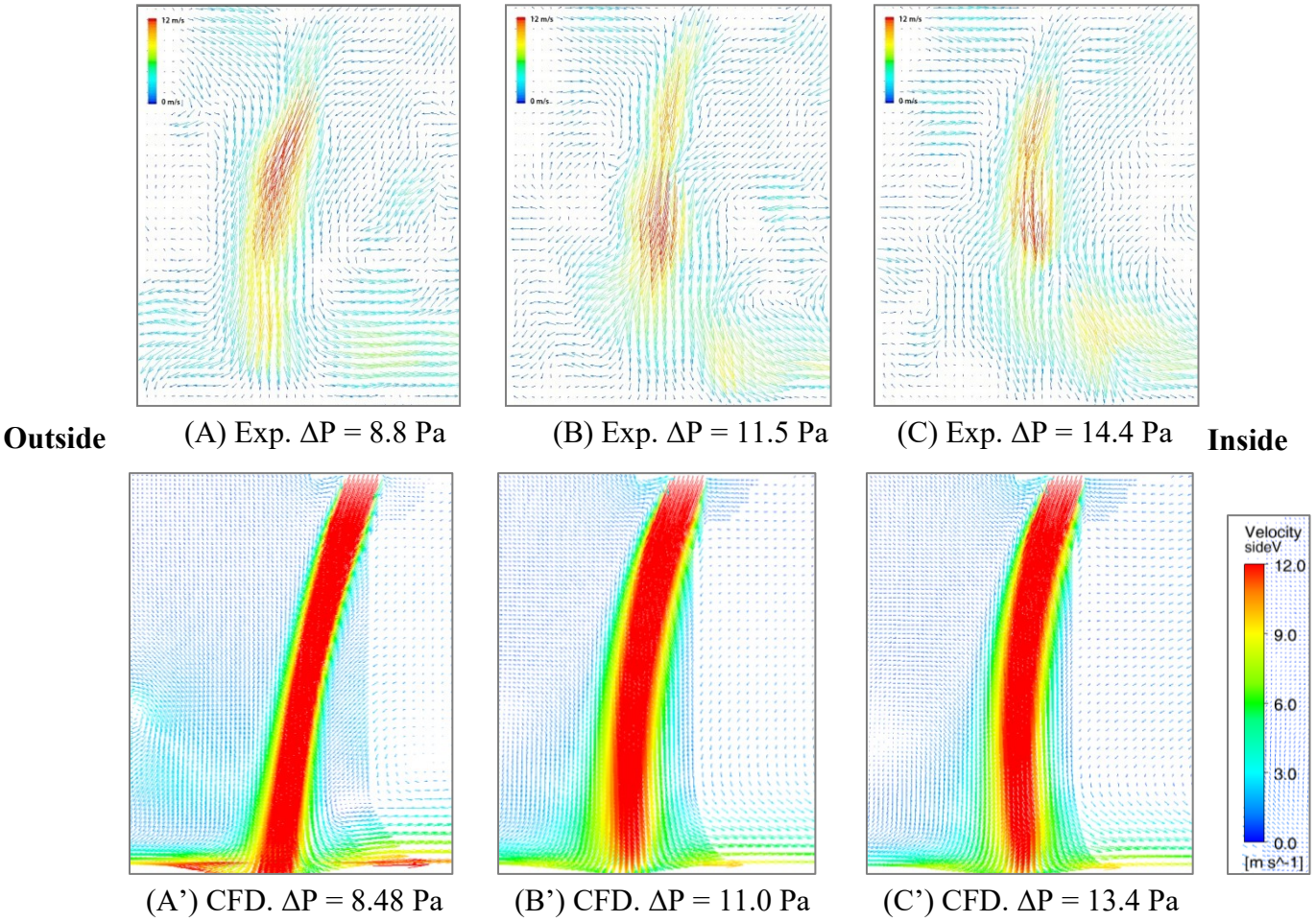

Figure 83. Additional comparison between experimental and CFD simulation flow visualization at door side-plane for the air curtain with an average supply speed of 13.75 m/s at 20° - (A) is optimum condition and (B) & (C) are inflow breakthrough

Door Mid-Plane

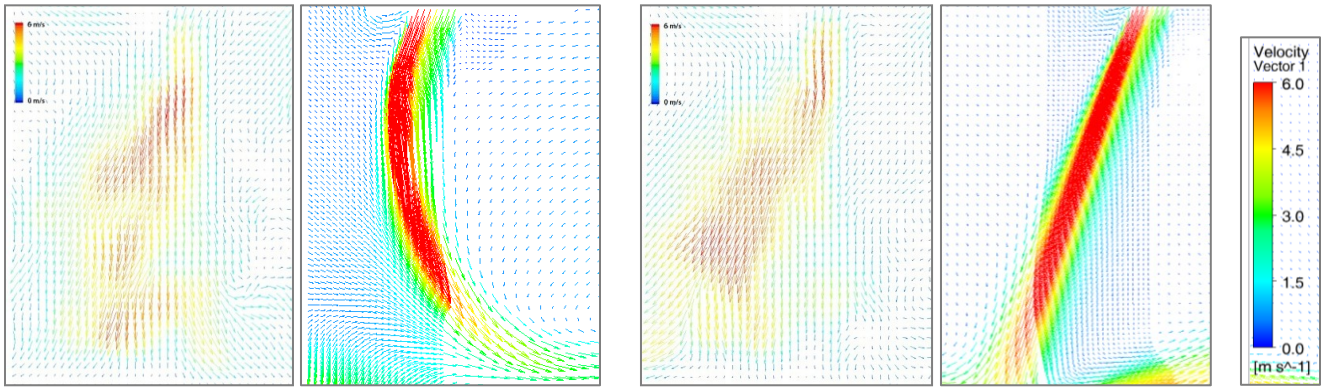

(A) Exp. ΔP = 4.7 Pa (A') CFD. ΔP = 3.6 Pa (B) Exp. ΔP = 0 Pa (B') CFD. ΔP = 0.2 Pa

Outside **Inside**

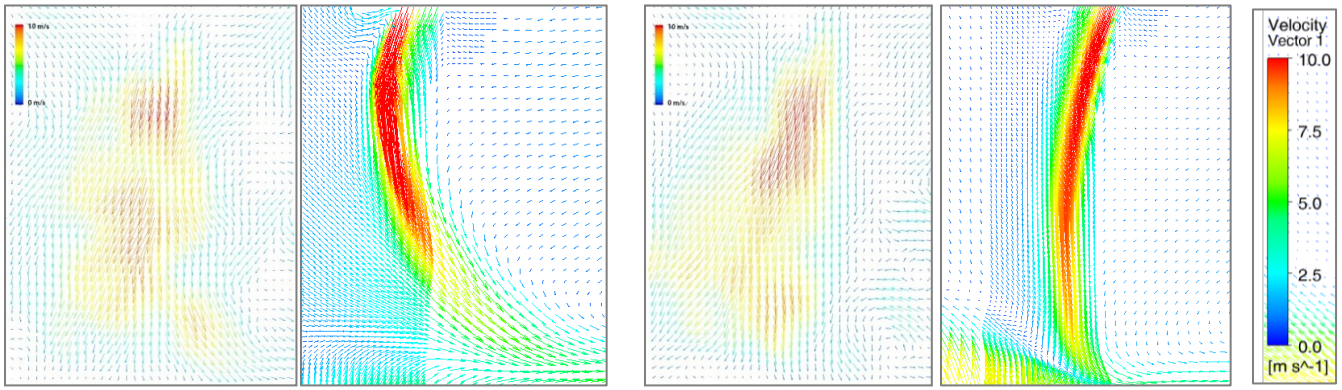

(C) Exp. ΔP = 16.0 Pa (C') CFD. ΔP = 17.1 Pa (D) Exp. ΔP = 4.0 Pa (D') CFD. ΔP = 4.7 Pa

Figure 84. Additional comparison between experimental and CFD simulation flow visualization at door mid-plane for the air curtain with an average supply speed of 9.1 m/s for (A) & (B) and 13.75 m/s for (C) & (D) at 20° - (A) & (C) are inflow breakthrough, (B) & (D) are outflow breakthrough

Effect of Wind on Air curtain Performance

Outside

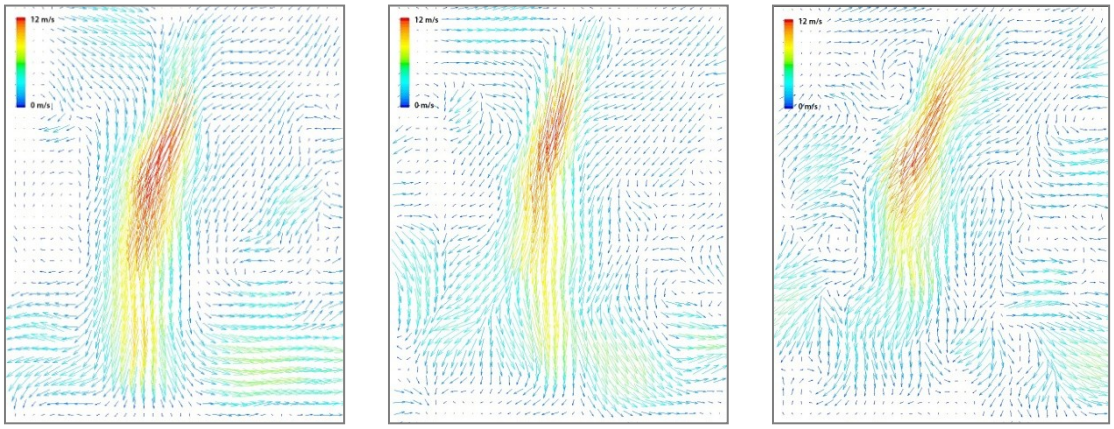

Inside

(A) No wind (B) 10 m/s wind (C) 18 m/s wind

Figure 85. Additional PIV visualization at the door side-plane with average air curtain supply speed of 13.75 m/s at 20° outwards for (A) no wind and no person, (B) 10 m/s wind and (C) 18 m/s wind

APPENDIX (C)

CFD Simulation Methodology

Total CFD Simulations Conducted

Table 45. CFD simulation cases for full-size building entrance.

	Winter Mode	**Summer Mode**
Outdoor Temperature (˚C)	-40, - 20, 10	25, 30, 40
Indoor Temperature (˚C)	21	24
Pressure Difference (Pa)	-20, -10, -5, -3.5, -2.5, -1.5, -1, -0.5, 0, 10, 20, 30, 40	
Door Opening Angle (˚)	10, 30, 45, 60, 90 (for 90 with and without people below the air curtain)	
Air Curtain Velocity (m/s)	10,15,20	
Air supply angle (^{0})	10,15,20	
Total CFD Runs	**(Total 810) 620 in this study**	

APPENDIX (D)

Detailed Simulation Results

Effect of Supply speed on Air Curtain Door Performance

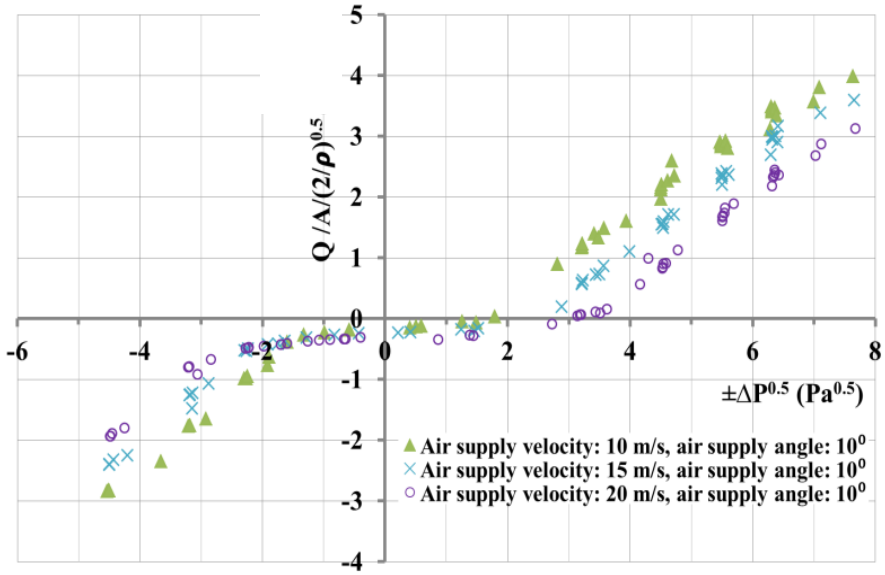

Figure 86. Performance the fully open air curtain door with air speed of 10, 15 & 20 m/s at 10°

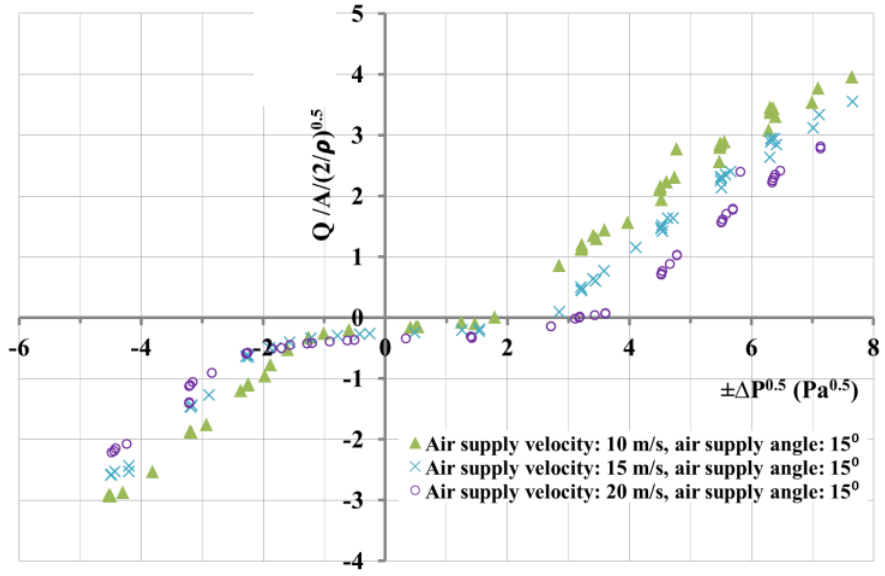

Figure 87. Performance the fully open air curtain door with air speed of 10, 15 & 20 m/s at 15°

Effect of Supply Angle on Air Curtain Door Performance

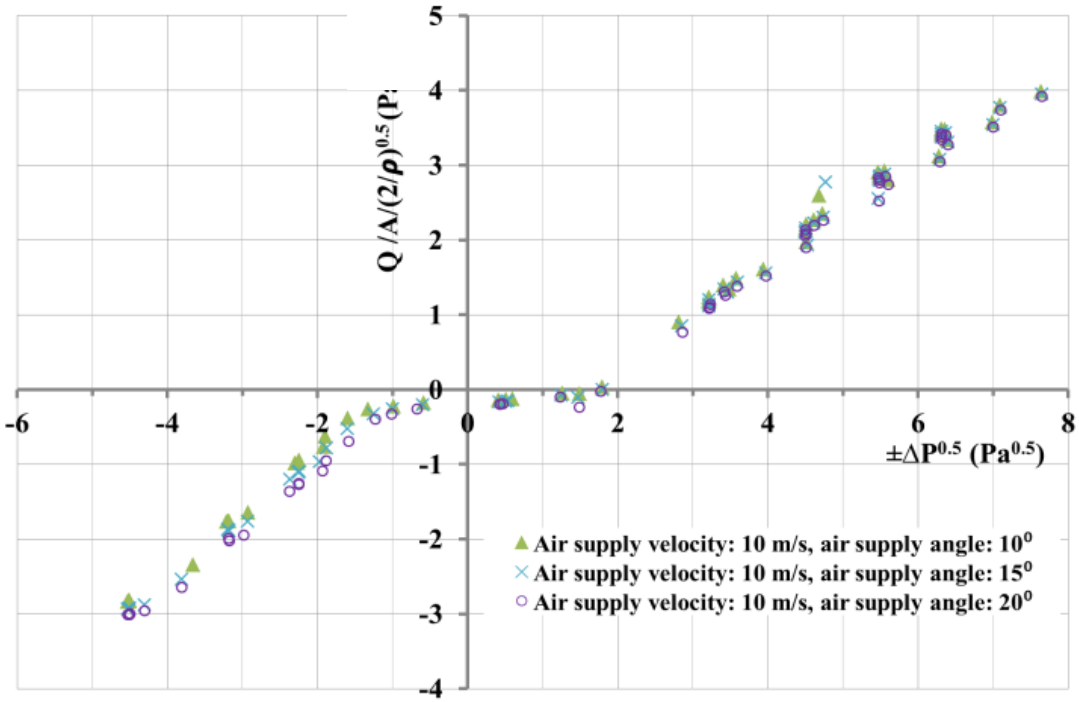

Figure 88. Performance the fully open air curtain door with air angle of 10°, 15° & 20° at 10 m/s

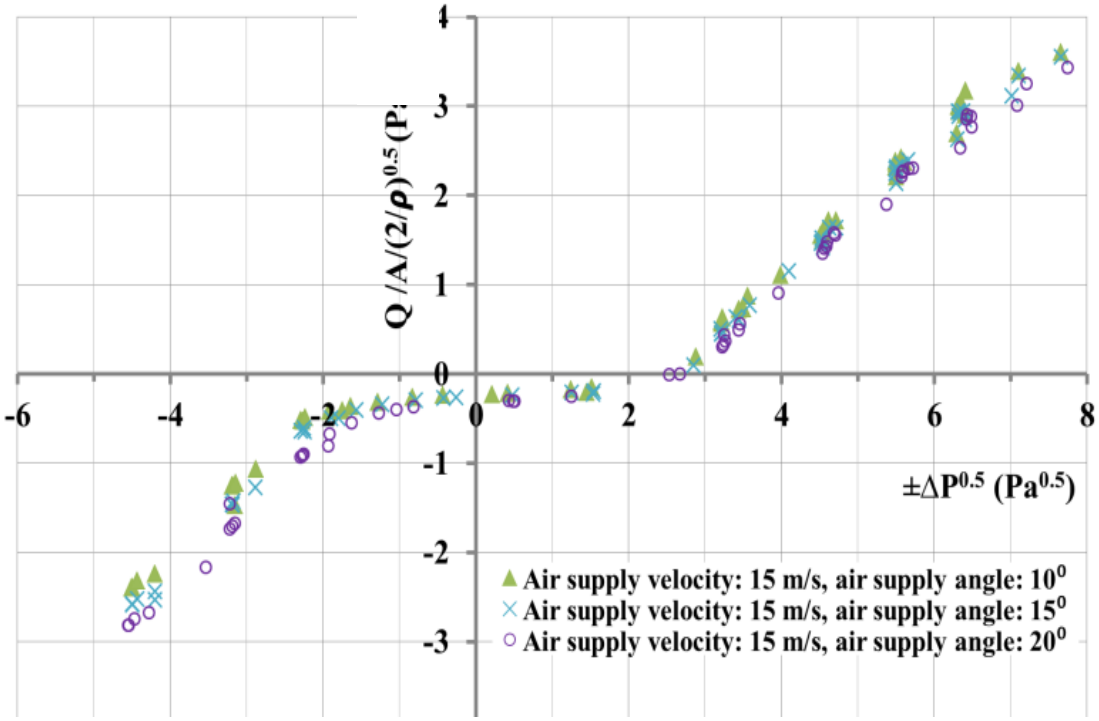

Figure 89. Performance the fully open air curtain door with air angle of 10°, 15° & 20° at 15 m/s

Performance of Air Curtain Door with Air Supply of 20 m/s & 15 m/s at 20°

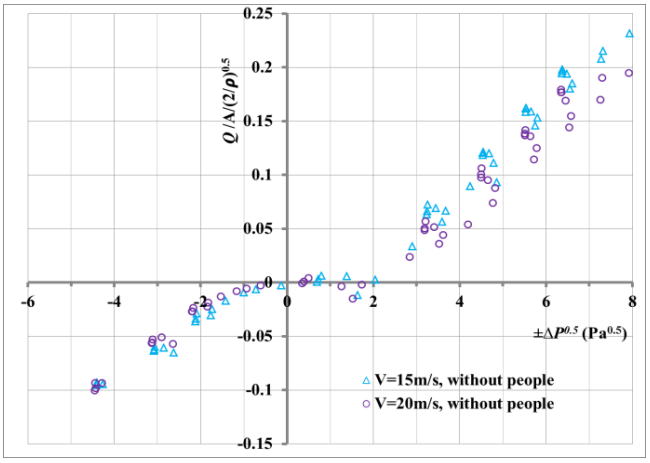

(A) Door Open 10°

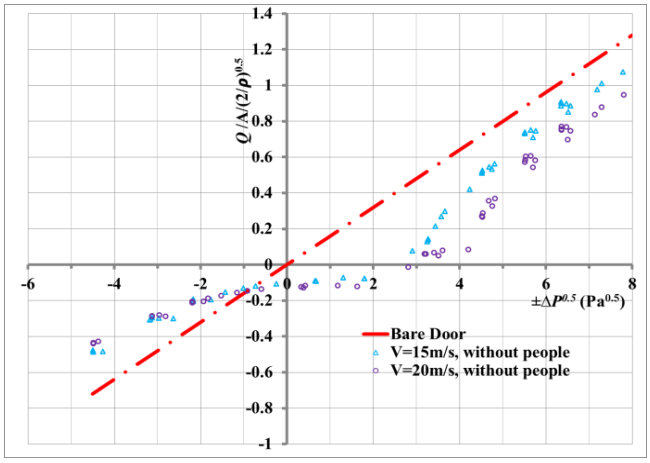

(B) Door Open 30°

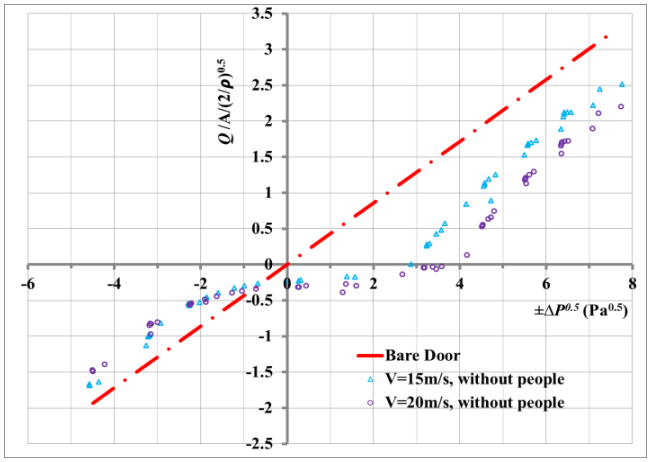

(C) Door Open 30°

Figure 90. Air curtain door infiltration with air curtain supply at 15 & 20 m/s at 20° outwards with the double door (both door leaves) open at (A) 10° (B) 30° and (C) 60°

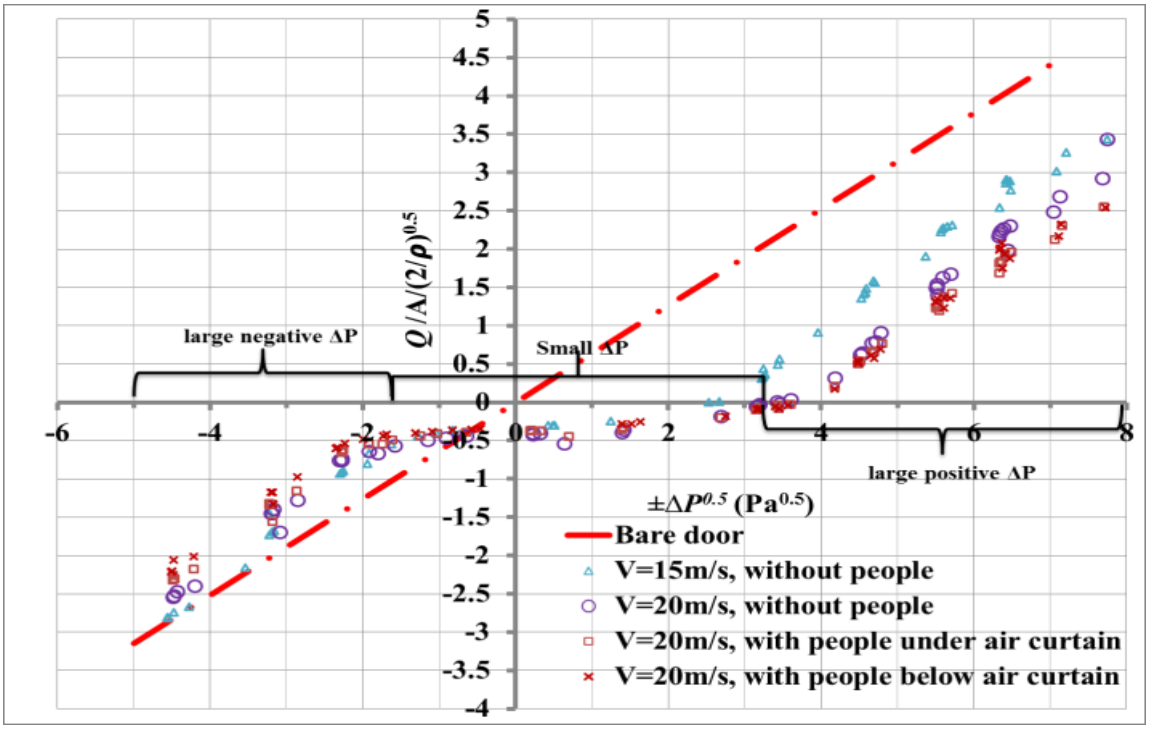

Figure 91. Air curtain door infiltration with air curtain supply at 15 & 20 m/s at 20° outwards with the double door (both door leaves) open at 90° considering people below and under the air curtain

Table 46. Discharge flow coefficients and flow modifiers for different door opening angles

Pressure scheme	Large positive pressure difference		Small pressure difference		Large Negative pressure difference	
Coefficient / Door opening angle	C_D	D_D	C_D	D_D	C_D	D_D
15 m/s without people						
10°	0.0397	-0.0703	0	0	0.0259	0.0181
30°	0.212	-0.4842	0.0232	-0.1073	0.1175	0.0465
60°	0.5346	-1.3975	0.0739	-0.2417	0.4756	0.4986
90°	0.7297	-1.9305	0.1221	-0.3344	0.8272	0.944
20 m/s without people						
10°	0.0357	-0.0707	0	0	0.0269	0.0259
30°	0.2175	-0.6748	0.0284	-0.1303	0.0969	0.0016
60°	0.5494	-1.8893	0.0586	-0.3473	0.42	0.4264
90°	0.77	-2.7647	0.1047	-0.4335	0.8114	1.0851
20 m/s with people below air curtain						
90°	0.6641	-2.439	0.0825	-0.3832	0.7502	1.0377

Table 47. Calculated door coefficients and flow modifiers for a full door operation cycle for the air curtain door (20 m/s at 20° supply) (ΔP_{uc}=10.66 Pa & ΔP_{lc}=-3.84 Pa)

	P_H	C	D
Infiltration (Inflow)	20	0.1472	-0.5204
	50	0.3695	-1.3090
	100	*0.7299*	*-2.5918*
	200	1.3775	-4.9033
	400	2.3537	-8.3948
Optimum	20	0.0190	-0.0844
	50	0.0481	-0.2112
	100	*0.0957*	*-0.4162*
	200	0.1822	-0.7833
	400	0.3133	-1.3353
Exfiltration (Outflow)	20	0.1440	0.1828
	50	0.3652	0.4671
	100	*0.7295*	*0.9406*
	200	1.3932	1.8116
	400	2.4038	3.1471

Table 48. Calculated door coefficients and flow modifiers for a full door operation cycle for the air curtain door with a person below the air curtain (20 m/s at 20° supply) (ΔP_{uc}=11.2 Pa & ΔP_{lc}=-3.86 Pa)

	P_h	C	D
Infiltration (Inflow)	20	0.1316	-0.4722
	50	0.3286	-1.1833
	100	*0.6459*	*-2.3333*
	200	1.2122	-4.3947
	400	2.0615	-7.4963
Optimum	20	0.0158	-0.0769
	50	0.0395	-0.1918
	100	*0.0781*	*-0.3763*
	200	0.1475	-0.7048
	400	0.2520	-1.1965
Exfiltration (Outflow)	20	0.1350	0.1757
	50	0.3416	0.4488
	100	*0.6809*	*0.9030*
	200	1.2976	1.7376
	400	2.2349	3.0163

APPENDIX (E)

Energy Simulations Methodology

CONTAM Airflow Models

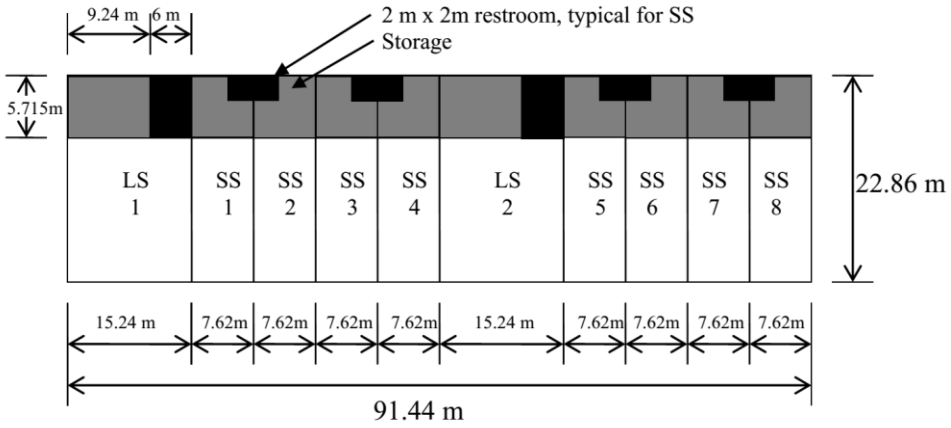

Figure 92. Strip mall building model plan drawing (Ng et al., 2012)

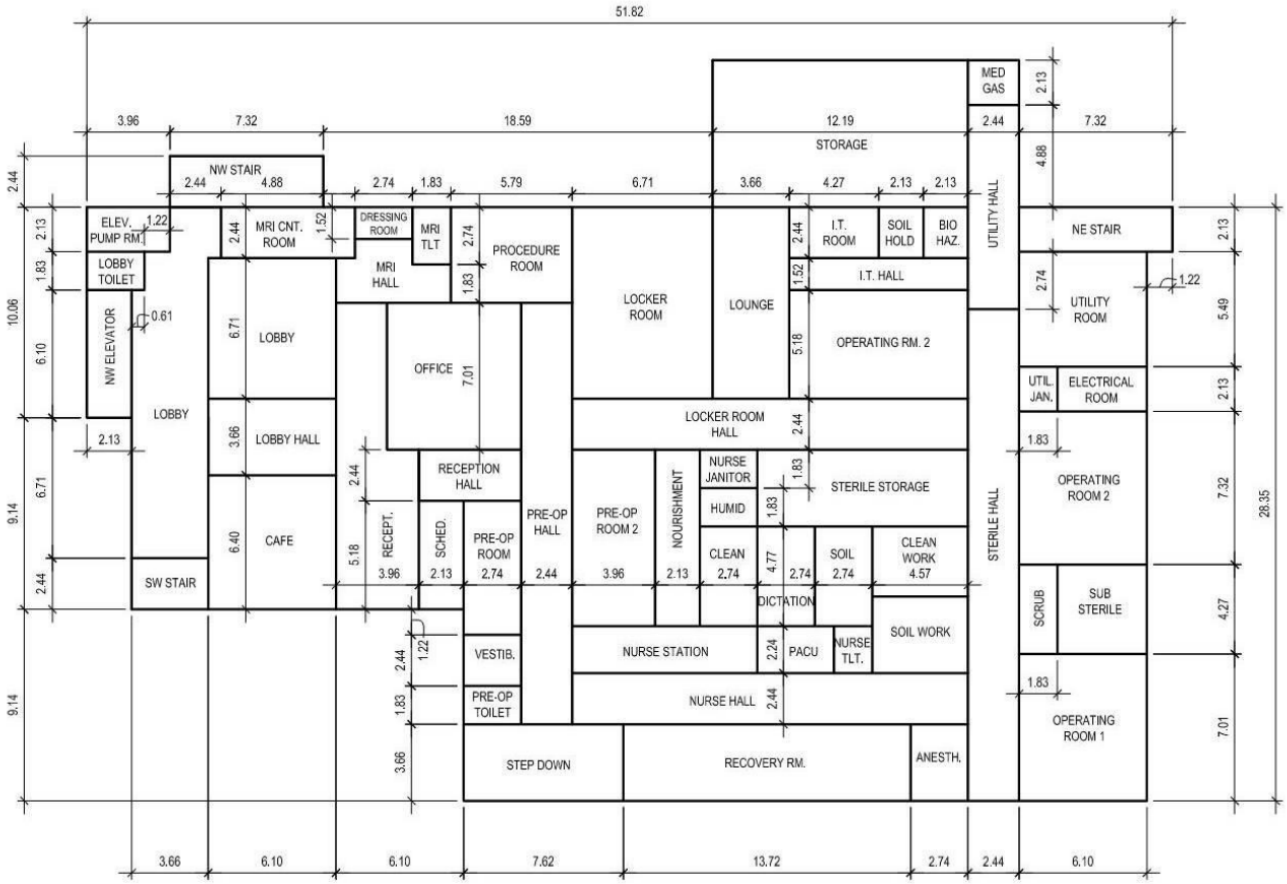

Figure 93. Outpatient healthcare building model plan drawing (Ng et al., 2012)

Zone Matching for Building Models

Table 49. Zone matching for the strip mall building CONTAM and EnergyPlus models

CONTAM	EnergyPlus
1_LG1restroom	Large Store 1
1_LG1storage	
1_LGstore1	
1_LG2restroom	Large Store 2
1_LG2storage	
1_LGstore2	
1_SM1restroom	Small Store 1
1_SM1storage	
1_SmStore1	
1_SM2restroom	Small Store 2
1_SM2storage	
1_SmStore2	
1_SM3restroom	Small Store 3
1_SM3storage	
1_SmStore3	
1_SM4restroom	Small Store 4
1_SM4storage	
1_SmStore4	
1_SM5restroom	Small Store 5
1_SM5storage	
1_SmStore5	
1_SM6restroom	Small Store 6
1_SM6storage	
1_SmStore6	
1_SM7restroom	Small Store 7
1_SM7storage	
1_SmStore7	
1_SM8restroom	Small Store 8
1_SM8storage	
1_SmStore8	

Table 50. Zone matching for the outpatient healthcare building CONTAM and EnergyPlus models

CONTAM	EnergyPlus
1_Anesthesia infiltration	Floor 1 Anesthesia
1_Cafe infiltration	Floor 1 Cafe
1_DressingRoom infiltration	Floor 1 Dressing Room

1_ElecrtricalRoom infiltration	Floor 1 Electrical Room
1_ElevatorPumpRm infiltration	Floor 1 Elevator Pump Room
1_Lobby infiltration	Floor 1 Lobby
1_LobbyToilet infiltration	Floor 1 Lobby Toilet
1_Lockerroom infiltration	Floor 1 Locker Room
1_MedGas infiltration	Floor 1 Med Gas
1_MRIControlRm infiltration	Floor 1 MRI Control Room
1_MRIToilet infiltration	Floor 1 MRI Toilet
1_NEStair infiltration	NE Stair
1_NWElevator infiltration	NW Elevator
1_NWStair infiltration	NW Stair
1_OperatingRoom1 infiltration	Floor 1 Operating Room 1
1_OperatingRoom2 infiltration	Floor 1 Operating Room 2
1_PreOpRoom1 infiltration	Floor 1 Pre-Op Room 1
1_PreOpToilet infiltration	Floor 1 Pre-Op Toilet
1_ProcedureRoom infiltration	Floor 1 Procedure Room
1_Reception infiltration	Floor 1 Reception
1_RecoveryRoom infiltration	Floor 1 Recovery Room
1_Scheduling infiltration	Floor 1 Scheduling
1_StepDown infiltration	Floor 1 Step Down
1_SterileHall infiltration	Floor 1 Sterile Hall
1_Storage infiltration	Floor 1 Storage
1_SubSterile infiltration	Floor 1 Sub-Sterile
1_SWStair infiltration	SW Stair
1_UtilityHall infiltration	Floor 1 Utility Hall
1_UtilityRoom infiltration	Floor 1 Utility Room
1_Vestibule infiltration	Floor 1 Vestibule
2_Conference infiltration	Floor 2 Conference
2_Exam1 infiltration	Floor 2 Exam 1
2_Exam2 infiltration	Floor 2 Exam 2
2_Exam3 infiltration	Floor 2 Exam 3
2_Exam4 infiltration	Floor 2 Exam 4

2_Exam5 infiltration	Floor 2 Exam 5
2_Exam6 infiltration	Floor 2 Exam 6
2_Exam7 infiltration	Floor 2 Exam 7
2_Exam8 infiltration	Floor 2 Exam 8
2_Exam9 infiltration	Floor 2 Exam 9
2_ExamHall1 infiltration	Floor 2 Exam Hall 1
2_ExamHall2 infiltration	Floor 2 Exam Hall 2
2_ExamHall3 infiltration	Floor 2 Exam Hall 3
2_ExamHall4 infiltration	Floor 2 Exam Hall 4
2_ExamHall5 infiltration	Floor 2 Exam Hall 5
2_ExamHall6 infiltration	Floor 2 Exam Hall 6
2_Janitor infiltration	Floor 2 Janitor
2_NEStair infiltration	NE Stair
2_NWElevator infiltration	NW Elevator
2_NWStair infiltration	NW Stair
2_Office infiltration	Floor 2 Office
2_Reception infiltration	Floor 2 Reception
2_ReceptionHall infiltration	Floor 2 Reception Hall
2_SWStair infiltration	SW Stair
2_Utility infiltration	Floor 2 Utility
2_Work infiltration	Floor 2 Work
2_WorkHall infiltration	Floor 2 Work Hall
2_WorkToilet infiltration	Floor 2 Work Toilet
3_DressingRoom infiltration	Floor 3 Dressing Room
3_ElevatorHall infiltration	Floor 3 Elevator Hall
3_Humid infiltration	Floor 3 Humid
3_Janitor infiltration	Floor 3 Janitor
3_Locker infiltration	Floor 3 Locker
3_Lounge infiltration	Floor 3 Lounge
3_LoungeToilet infiltration	Floor 3 Lounge Toilet
3_Mechanical infiltration	Floor 3 Mechanical
3_MechanicalHall infiltration	Floor 3 Mechanical Hall
3_NEStair infiltration	NE Stair
3_NWElevator infiltration	NW Elevator
3_NWStair infiltration	NW Stair
3_Office infiltration	Floor 3 Office
3_OfficeHall infiltration	Floor 3 Office Hall
3_OfficeToilet infiltration	Floor 3 Office Toilet

3_PhysicalTher1 infiltration	Floor 3 Physical Therapy 1
3_PhysicalTher2 infiltration	Floor 3 Physical Therapy 2
3_PysTherTlt infiltration	Floor 3 Physical Therapy Toilet
3_Storage1 infiltration	Floor 3 Storage 1
3_Storage2 infiltration	Floor 3 Storage 2
3_SWStair infiltration	SW Stair
3_Treatment infiltration	Floor 3 Treatment
3_Undeveloped1 infiltration	Floor 3 Undeveloped 1
3_Undeveloped2 infiltration	Floor 3 Undeveloped 2
3_Utility infiltration	Floor 3 Utility
3_Work infiltration	Floor 3 Work

Entrance Door in the Outpatient Healthcare building

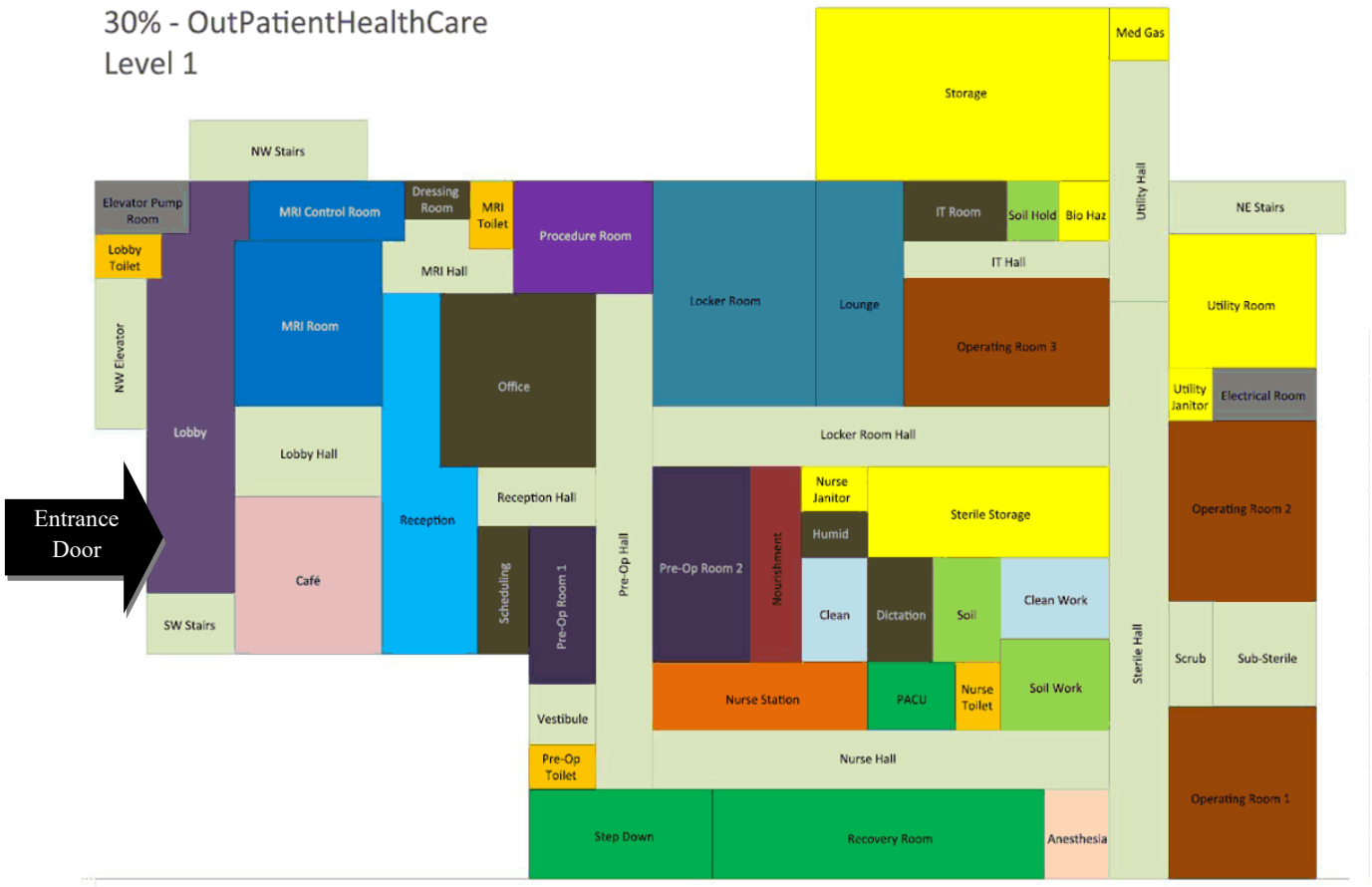

Figure 94. Entrance door location in the outpatient healthcare building (Deru et al., 2011)

ERL Air Curtain Control EMS Program in EnergyPlus

```
EnergyManagementSystem:Program,
    AC_SM_PRO,                !- Name
    IF (TEMP > 30) || (TEMP < 10),  !- Program Line 1
        IF (Hour >= 8) && (Hour < 10),
        Set AC_CONTROL_SM = 0.004456042,
        ELSEIF (Hour >= 10) && (Hour < 18),
        Set AC_CONTROL_SM = 0.035097289,
        ELSEIF (Hour >= 18) && (Hour < 20),
        Set AC_CONTROL_SM = 0.004456042,
        ENDIF,
    ElSE,
        Set AC_CONTROL_SM = 0 ,
    ENDIF;
```

Figure 95. Control program to control the air curtain operation in energy plus

Air Curtain Doors Model in CONTAM

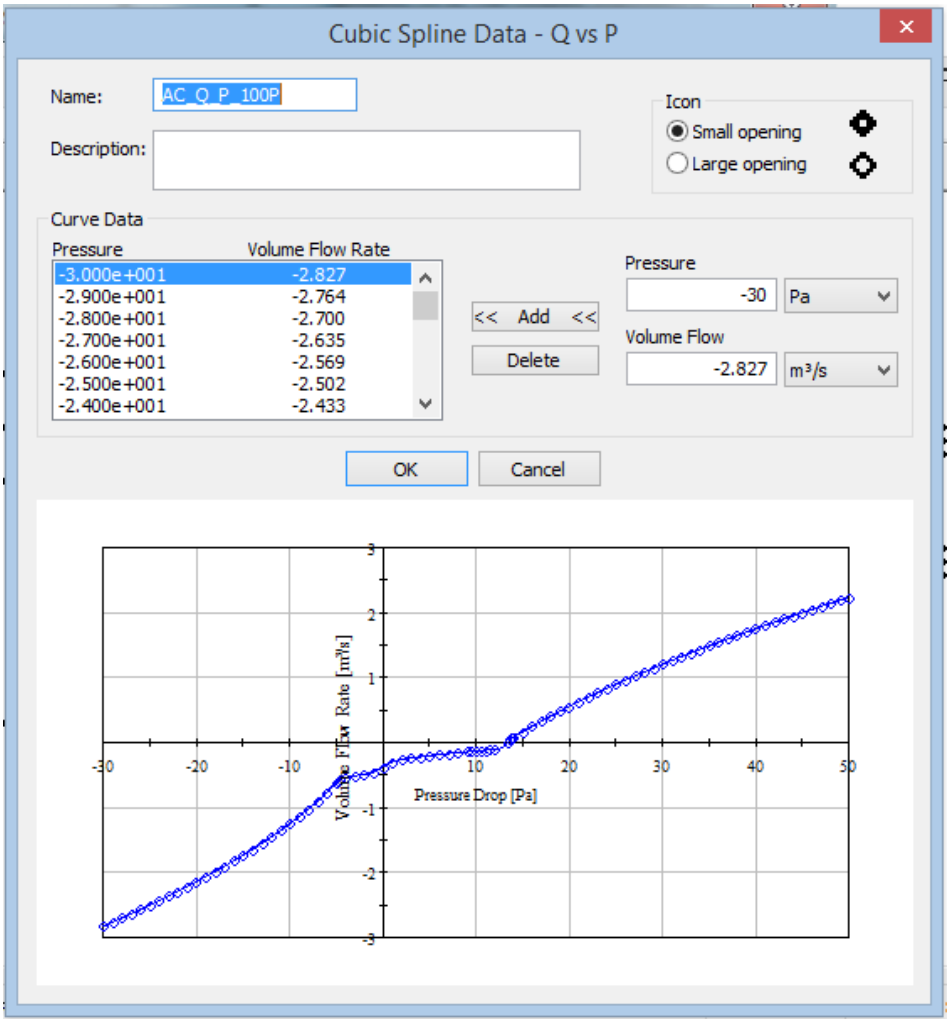

Figure 96. Cubic-Spline data for the air curtain door as input in CONTAM

Door Coefficients

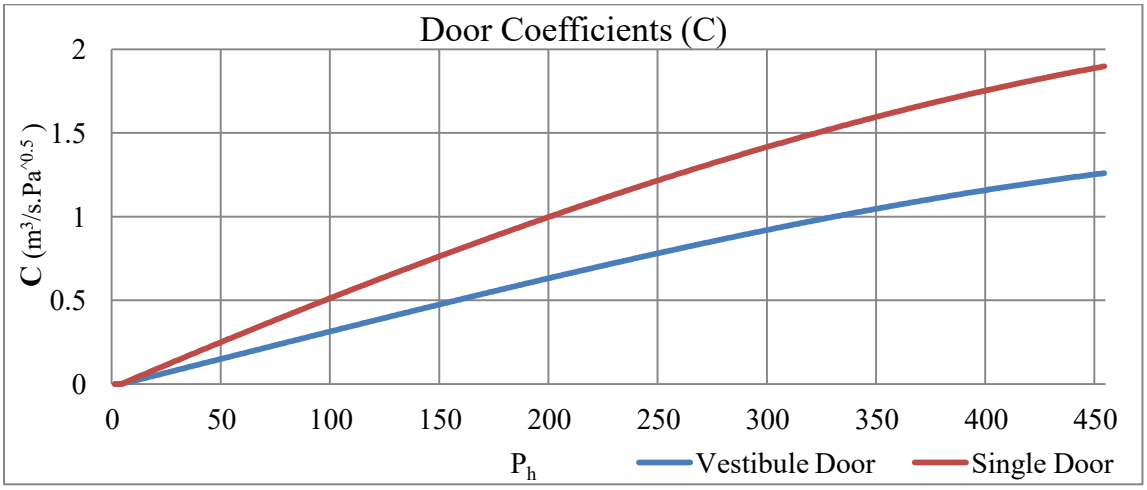

Figure 97. Flow Coefficients for a door size 2 × 2.4 m calculated based on Yuill's model (Yuill, 1996)

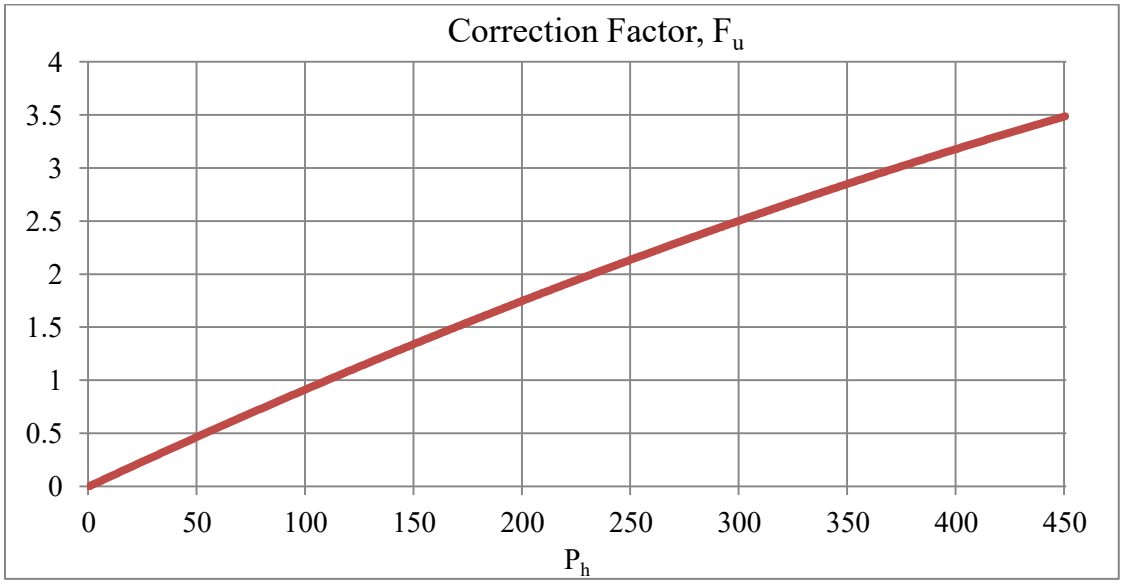

Figure 98. Air curtain door correction factors in reference to 100 P_h (for an air curtain with a supply speed of 20 m/s at 20° with a person below in a door size of 2 × 2.4 m); Calculated based on model proposed by Wang (2013)

Energy Simulations

ASHRAE Method

Table 51. Simulation for the selection of reference models version (2004-2010-2013)

Climate zones 1 & 2	3 ×1 = 3 (No Vestibule)
Climate zones 3 to 8	13 × 2 = 26
Total for each building model version	29
For 2 building models	58
For 3 model version	**174**

Table 52. Simulations for the buildings using the ASHRAE Method for the 3 doors scenarios

Climate zones 1 & 2	3 ×2 = 6 (No Vestibule)
Climate zones 3 to 8	13 × 3 = 26
Total for each model	45
For 2 building models	**90**

CONTAM-EnergyPlus Method

Please note each EnergyPlus simulation has a analogous CONTAM simulation.

Table 53. Simulations for the buildings using the CONTAM-EnergyPlus Method for the 3 doors scenarios

Climate zones 1 & 2	3 ×2 = 6 (No Vestibule)
Climate zones 3 to 8	13 × 3 = 26
Total	45
For 2 building models	**90**

Table 54. Simulations for the buildings using the CONTAM-EnergyPlus Method for the 3 doors scenarios

Rate of door use: -30%, -20%, -10%, 10%,20%,30%	32 (2 climate zones - 2 door types)
Orientation: S, W, E	36 (3 climate zones - 2 door types)
Varying wind pressure coefficient: -20%, -10%, 10%,20%	24 (2 climate zones - 2 door types)
Internal zone connectivity	15 (1 building -1 climate zone - 3 door types)
Entrance door location	54 (1 building -16 climate zone - 3 door types)
Total	**161**

Sensitivity Study for the CONTAM-EnergyPlus Method

Wind Pressure Coefficients

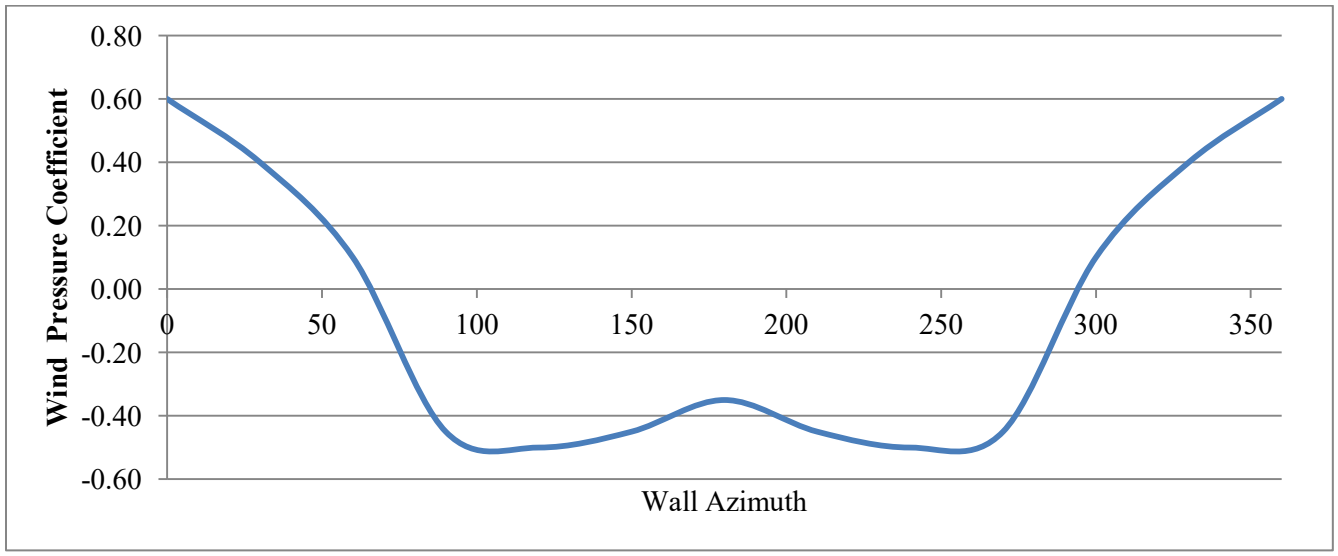

Figure 99. Original wind pressure coefficients used in CONTAM models (Swami & Chandra, 1987)

Wind Direction

Table 55. Weighted average wind directions in summer and winter for the 16 climate zone locations based on TMY3 weather files

	Summer Weighted Average Wind Direction (°From North)	Winter Weighted Average Wind Direction (°From North)
1A	138 (S42°E)	174 (S6°E)
2A	155 (S25°E)	183 (S3°W)
2B	185 (S5°W)	161 (S19°E)
3A	179 (S1°E)	188 (S8°W)
3B	196 (S16°W)	197 (S17°W)
3C	267 (S87°W)	229 (S49°W)
4A	200 (S20°W)	236 (S56°W)
4B	194 (S14°W)	210 (S30°W)
4C	217 (S27°W)	183 (S3°W)
5A	182 (S2°W)	219 (S39°W)
5B	246 (S66°W)	193 (S13°W)
5C	196 (S16°W)	161 (S19°E)
6A	214 (S34°W)	224 (S44°W)
6B	242 (S62°W)	257 (S77°W)
7	197 (S17°W)	240 (S60°W)
8	198 (S18°W)	173 (S7°E)

APPENDIX (F)

ASHRAE Method

Strip Mall Reference Building Model

Table 56. Air curtain door annual energy savings in the strip mall building using ASHRAE infiltration rates calculation method

	1A*	2A*	2B*	3A	3B	3C	4A	4B	4C	5A	5B	5C	6A	6B	7	8
	Miami	Houston	Phoenix	Memphis	El-Paso	San Francisco	Baltimore	Albuquerque	Salem	Chicago	Boise	Vancouver	Burlington	Helena	Duluth	Fairbanks
Vestibule Door (MJ/m^2)	601.80	660.04	678.97	676.94	587.11	506.77	733.03	601.92	669.74	870.29	721.59	726.50	932.10	834.10	1057.92	1397.59
Air Curtain Door (MJ/m^2)	594.70	623.86	594.98	642.98	610.32	546.50	681.59	574.64	641.27	776.89	650.25	662.26	797.81	718.21	879.30	1136.66
Savings (MJ/m2)	7.10	36.18	83.99	33.96	-23.21	-39.73	51.44	27.28	28.47	93.40	71.34	64.24	134.29	115.89	178.62	260.93
Energy Savings (%)	1.18%	5.48%	12.37%	5.02%	-3.95%	-7.84%	7.02%	4.53%	4.25%	10.73%	9.89%	8.84%	14.41%	13.89%	16.88%	18.67%

National weighted-average air curtain door annual energy savings		National weighted-average air curtain units energy use
46.47 (MJ/m^2)	6.52%	548.16 kWh

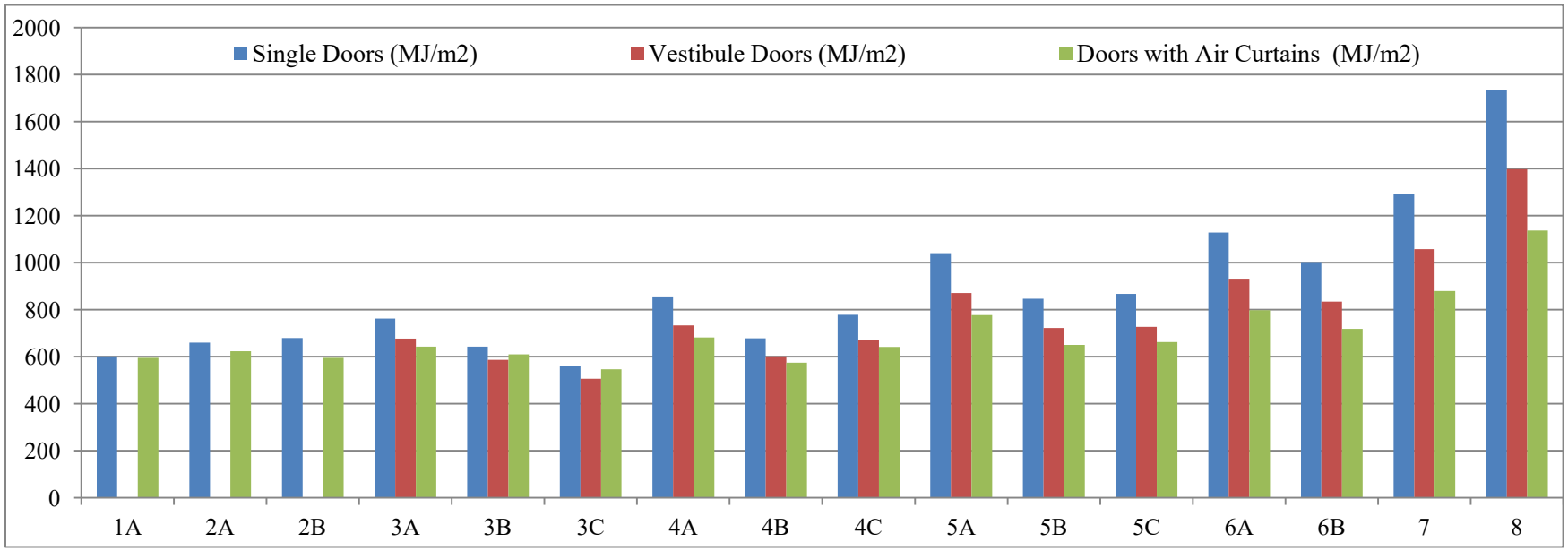

Figure 100. Strip mall building's annual energy consumption based on ASHRAE infiltration rates calculation method for the 3 entrance door scenarios

**Baseline of comparison for CZ 1A, 2A & 2B is the single door case since vestibule doors are not required by ASHRAE 90.1 for this building in these locations*

Outpatient Healthcare Reference Building Model

Table 57. Air curtain door annual energy savings in the outpatient healthcare building using ASHRAE infiltration rates calculation method

	1A*	2A*	2B*	3A	3B	3C	4A	4B	4C	5A	5B	5C	6A	6B	7	8
	Miami	Houston	Phoenix	Memphis	El-Paso	San Francisco	Baltimore	Albuquerque	Salem	Chicago	Boise	Vancouver	Burlington	Helena	Duluth	Fairbanks
Vestibule Door (MJ/m2)	1435.96	1386.42	1329.66	1371.25	1235.93	1146.07	1311.77	1221.24	1191.06	1339.91	1230.01	1180.94	1346.63	1275.75	1393.22	1621.55
Air Curtain Door (MJ/m2)	1431.03	1378.98	1319.68	1361.87	1227.32	1134.91	1300.35	1210.52	1177.86	1326.24	1216.91	1167.20	1331.31	1261.24	1374.76	1595.33
Savings (MJ/m2)	4.93	7.44	9.98	9.38	8.61	11.16	11.42	10.72	13.20	13.67	13.10	13.74	15.32	14.51	18.46	26.22
Energy Savings (%)	0.34%	0.54%	0.75%	0.68%	0.70%	0.97%	0.87%	0.88%	1.11%	1.02%	1.07%	1.16%	1.14%	1.14%	1.32%	1.62%

National weighted-average air curtain door annual energy savings		National weighted-average air curtain units energy use
11.97 (MJ/m2)	0.90%	314.37 kWh

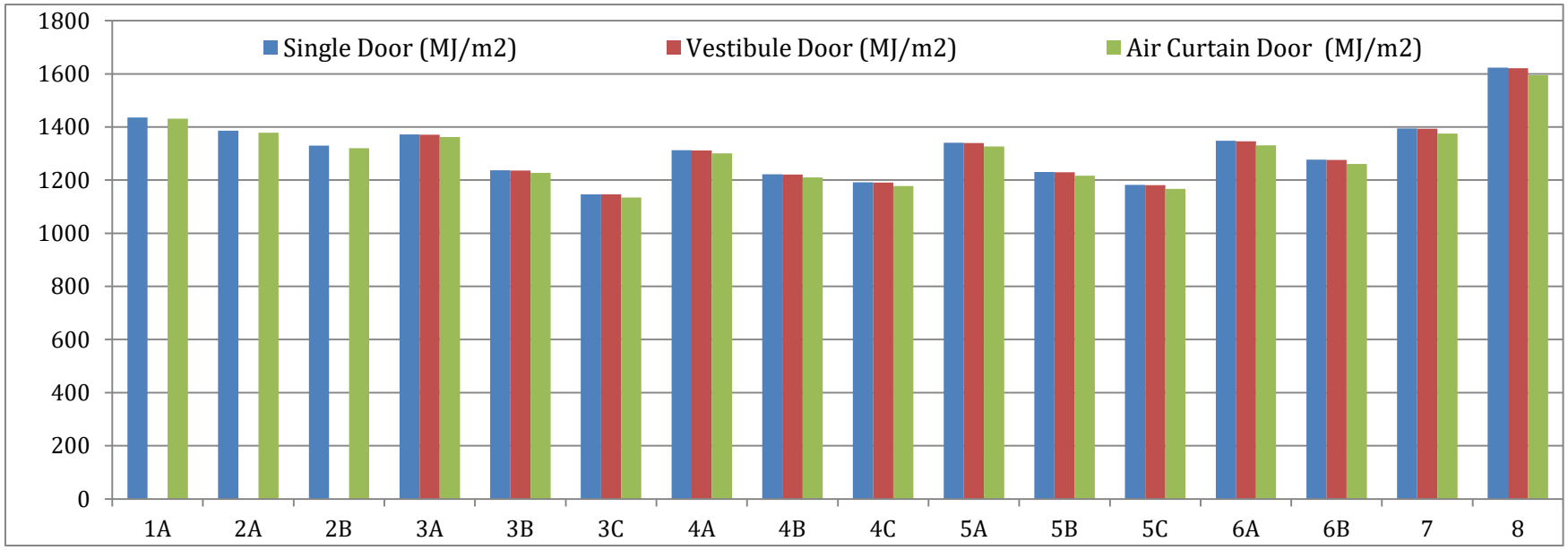

Figure 101. Outpatient healthcare building's annual energy consumption based on ASHRAE infiltration rates calculation method for the 3 entrance door scenarios

**Baseline of comparison for CZ 1A, 2A & 2B is the single door case since vestibule doors are not required by ASHRAE 90.1 for this building in these locations*

Sensitivity Study for the Infiltration Rates Calculated using the ASHRAE Method

Table 58. Effect of the outdoor temperature on the calculated infiltration rates for the 3 entrance door scenarios during peak door-opening frequency in the outpatient healthcare building

Outdoor Temperature (°C)	Single Door		Vestibule Door		Air Curtain Door		
	Peak Infiltration (m3/s)	Percentage Variation from baseline	Peak Infiltration (m3/s)	Percentage Variation from baseline	Peak Infiltration (m3/s)	Percentage Variation from baseline	Percent Reduction from Vestibule Door Infiltration
-40	3.550	20.84%	2.194	20.84%	1.322	104.74%	39.72%
-29	3.420	16.41%	2.113	16.41%	1.178	82.45%	44.23%
-18	3.276	11.53%	2.024	11.53%	1.020	57.94%	49.61%
-7	3.133	6.65%	1.936	6.65%	0.862	33.43%	55.49%
4	3.035	3.33%	1.876	3.33%	0.754	16.71%	59.81%
16 (Baseline)	**2.938**	**-**	**1.815**	**-**	**0.646**	**-**	**64.42%**
27	2.827	-3.77%	1.747	-3.77%	0.524	-18.94%	70.03%
38	2.736	-6.87%	1.690	-6.87%	0.423	-34.54%	74.99%

Table 59. Effect of the door-opening frequency on the calculated infiltration rates for the 3 entrance door scenarios in the outpatient healthcare building

Percentage Variation in Door-usage Frequency (%)	Door Usage (P_h)	Single Door		Vestibule Door		Air Curtain Door				
		Peak Infiltration (m3/s)	Percentage Variation from baseline	Peak Infiltration (m3/s)	Percentage Variation from baseline	Peak Infiltration (m3/s)	Percentage Variation from baseline	Percent Reduction From Vestibule Door Infiltration	Air Curtain Units Operation (h/h)	Percentage Variation from baseline
-30	86	2.089	-28.90%	1.272	-29.91%	0.459	-28.94%	63.93%	0.175	-27.25%
-20	98	2.368	-19.40%	1.449	-20.17%	0.520	-19.45%	64.10%	0.197	-18.16%
-10	111	2.643	-10.02%	1.625	-10.46%	0.586	-9.28%	63.95%	0.220	-8.59%
0 (Baseline)	**123**	**2.938**	**-**	**1.815**	**-**	**0.646**	**-**	**64.42%**	**0.240**	-
10	135	3.206	9.12%	1.989	9.60%	0.705	9.17%	64.56%	0.260	8.36%
20	148	3.492	18.87%	2.177	19.93%	0.769	19.00%	64.70%	0.281	17.18%
30	160	3.752	27.72%	2.349	29.39%	0.826	27.96%	64.81%	0.300	25.09%

Sensitivity of Energy Savings to Air Curtain Temperature

Table 60. Effect of air curtain temperature control on energy consumption and savings in CZ-3 for the strip mall building

Air Curtain Temperature Control (Where T is the temperature range in ° C where the unit operates)		**30 < T < 10 (Baseline)**	40 < T < 10	30 < T < 20	Always ON (No temp. Control)
3C San Francisco	Air Curtain Door (MJ/m²)	**546.51**	546.51	477.1	470.72
	Vestibule Door (MJ/m²)	**506.77**			
	Energy Savings	**-7.84%**	-7.84%	5.85%	7.11%
	Units Energy (GJ)	**0.24**	0.23	5.04	5.79
	Units On-Time (Hrs/Year)	**63**	61	1333	1532

Table 61. Effect of air curtain temperature control on energy consumption and savings in CZ-3 for the outpatient healthcare building

Air Curtain Temperature Control (Where T is the temperature range in ° C where the unit operates)		**30 < T < 10 (Baseline)**	40 < T < 10	30 < T < 20	Always ON (No temp. Control)
3C San Francisco	Air Curtain Door (MJ/m²)	**1134.91**	1134.91	1135.75	1135.92
	Vestibule Door (MJ/m²)	**1146.07**			
	Energy Savings	**0.97%**	0.97%	0.90%	0.89%
	Units Energy (GJ)	**0.18**	0.18	2.49	2.9
	Units On-Time (Hrs/Year)	**48**	48	659	767

APPENDIX (G)

CONTAM-EnergyPlus Method

Strip Mall Reference Building Model

Table 62. Air curtain door annual energy savings in the strip mall building using CONTAM for infiltration calculation

	1A*	2A*	2B*	3A	3B	3C	4A	4B	4C	5A	5B	5C	6A	6B	7	8
	Miami	Houston	Phoenix	Memphis	El-Paso	San Francisco	Baltimore	Albuquerque	Salem	Chicago	Boise	Vancouver	Burlington	Helena	Duluth	Fairbanks
Doors Azimuth (° From North)	180															
Vestibule door (MJ/m2)	568.32	579.51	582.67	653.47	558.94	489.83	711.11	581.68	660.13	897.43	681.34	674.06	963.86	792.42	1122.48	1483.94
Air Curtain door (MJ/m2)	555.38	574.84	569.81	646.31	559.08	492.00	696.24	576.99	643.41	858.33	664.32	653.97	912.26	764.44	1055.77	1369.56
Savings (MJ/m^2)	12.94	4.67	12.86	7.16	-0.14	-2.17	14.87	4.69	16.72	39.10	17.02	20.09	51.60	27.98	66.71	114.38
Energy Savings (%)	2.28%	0.81%	2.21%	1.10%	-0.03%	-0.44%	2.09%	0.81%	2.53%	4.36%	2.50%	2.98%	5.35%	3.53%	5.94%	7.71%

National weighted-average air curtain door annual energy savings	
15.15 (MJ/m2)	2.21%

National weighted-average air curtain units energy use
548.16 kWh

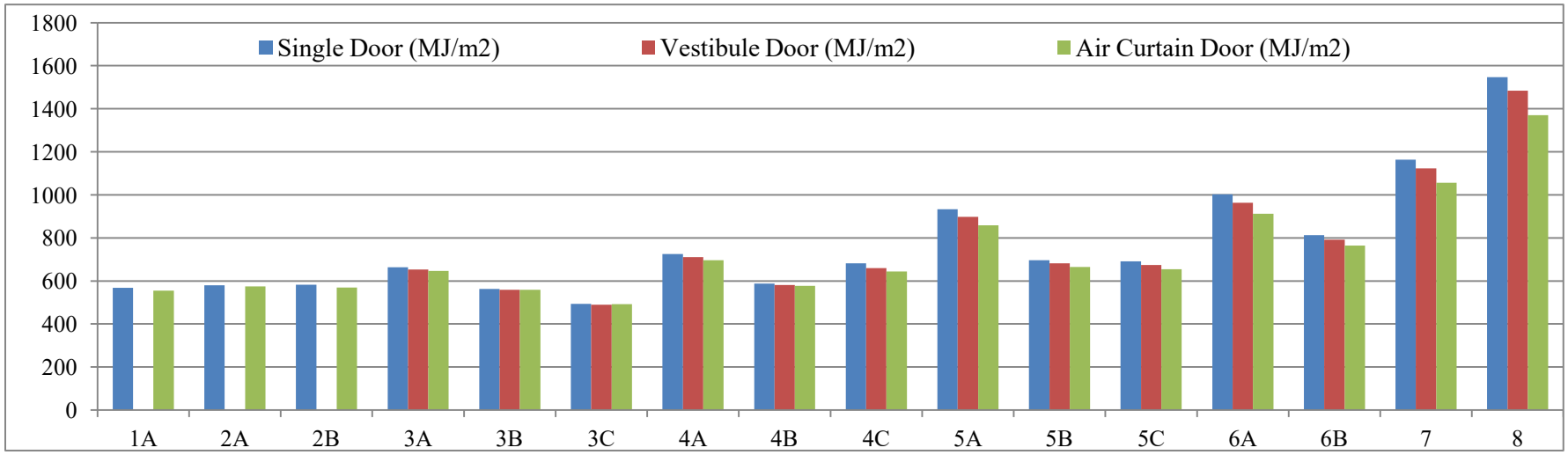

Figure 102. Strip mall building's annual energy consumption based on CONTAM infiltration rates calculation method for the 3 entrance door scenarios

**Baseline of comparison for CZ 1A, 2A & 2B is the single door case since vestibule doors are not required by ASHRAE 90.1 for this building in these locations*

Outpatient Healthcare Reference Building Model

Table 63. Air curtain door annual energy savings in the outpatient healthcare building using CONTAM for infiltration calculation

	1A*	2A*	2B*	3A	3B	3C	4A	4B	4C	5A	5B	5C	6A	6B	7	8
	Miami	Houston	Phoenix	Memphis	El-Paso	San Francisco	Baltimore	Albuquerque	Salem	Chicago	Boise	Vancouver	Burlington	Helena	Duluth	Fairbanks
Doors Azimuth (° From North)	270															
Vestibule door (MJ/m2)	1447.49	1412.19	1338.67	1413.47	1254.07	1169.73	1377.57	1256.95	1243.23	1456.49	1291.32	1263.49	1477.64	1404.81	1568.02	1866.94
Air Curtain door (MJ/m2)	1447.84	1412.55	1339.17	1414.23	1253.18	1171.00	1374.19	1253.18	1242.55	1441.59	1281.79	1239.99	1474.42	1369.18	1567.69	1871.91
Savings (MJ/m2)	-0.35	-0.36	-0.50	-0.76	0.89	-1.27	3.38	3.77	0.68	14.90	9.53	23.50	3.22	35.63	0.33	-4.97
Energy Savings (%)	-0.02%	-0.03%	-0.04%	-0.05%	0.07%	-0.11%	0.25%	0.30%	0.05%	1.02%	0.74%	1.86%	0.22%	2.54%	0.02%	-0.27%

National weighted-average air curtain door annual energy savings		National weighted-average air curtain units energy use
4.80 (MJ/m2)	0.34%	314.47 kWh

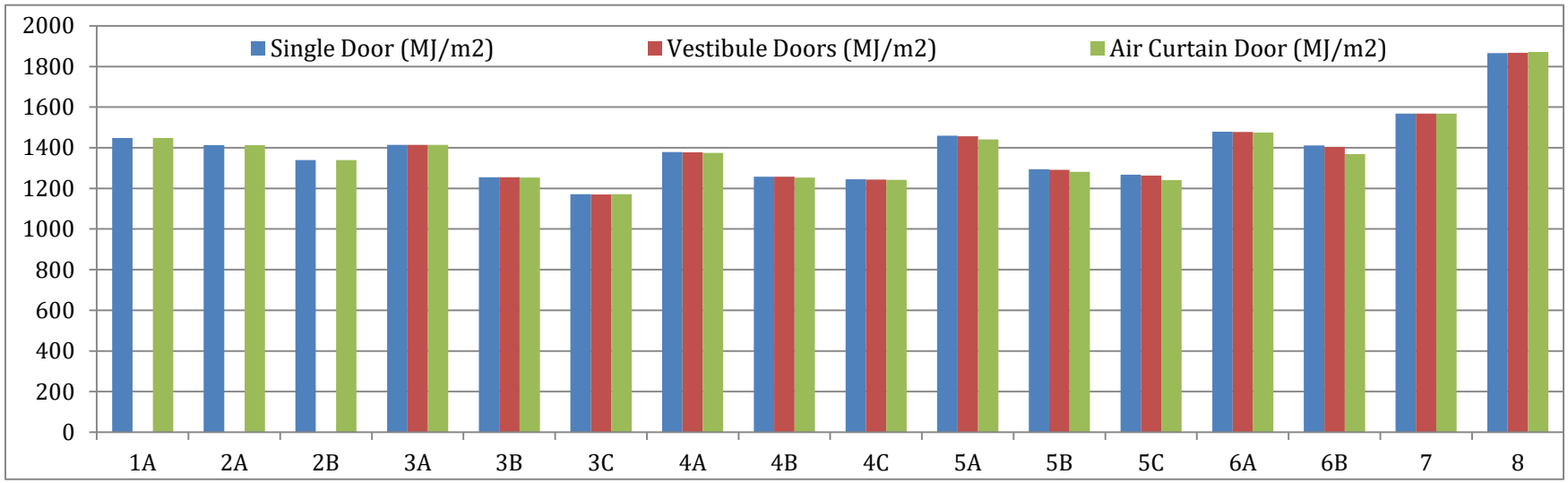

Figure 103. Outpatient healthcare building's annual energy consumption based on CONTAM infiltration rates calculation method for the 3 entrance door scenarios

**Baseline of comparison for CZ 1A, 2A & 2B is the single door case since vestibule doors are not required by ASHRAE 90.1 for this building in these locations*

Table 64. Compiled calculated savings for vestibule doors and air curtain doors using both simulation methods

			Strip Mall Building				Outpatient Healthcare Building			
Infiltration Modeling Method			ASHRAE		CONTAM-EnergyPlus		ASHRAE		CONTAM-EnergyPlus	
Climate Zone		Base Case for Air Curtain Savings Calculation	Vestibule Door Vs. Single Door	Air Curtain Vs. Base Case	Single Door Vs. Vestibule Door	Air Curtain Vs. Base Case	Vestibule Door Vs. Single Door	Air Curtain Vs. Base Case	Single Door Vs. Vestibule Door	Air Curtain Vs. Base Case
1A	Miami	Single Door	-	1.18%	-	2.28%	-	0.34%	-	-0.02%
2A	Houston	Single Door	-	5.48%	-	0.81%	-	0.54%	-	-0.03%
2B	Phoenix	Single Door	-	12.37%	-	2.21%	-	0.75%	-	-0.04%
3A	Memphis	Vestibule	11.20%	5.02%	1.50%	1.10%	0.07%	0.68%	0.02%	-0.05%
3B	El-Paso	Vestibule	8.67%	-3.95%	0.60%	-0.03%	0.06%	0.70%	0.05%	0.07%
3C	San Francisco	Vestibule	9.97%	-7.84%	0.73%	-0.44%	0.08%	0.97%	0.15%	-0.11%
4A	Baltimore	Vestibule	14.41%	7.02%	1.86%	2.09%	0.05%	0.87%	0.05%	0.25%
4B	Albuquerque	Vestibule	11.20%	4.53%	1.11%	0.81%	0.06%	0.88%	0.09%	0.30%
4C	Salem	Vestibule	13.90%	4.25%	3.17%	2.53%	0.08%	1.11%	0.08%	0.05%
5A	Chicago	Vestibule	16.38%	10.73%	3.88%	4.36%	0.07%	1.02%	0.22%	1.02%
5B	Boise	Vestibule	14.72%	9.89%	2.21%	2.50%	0.07%	1.07%	0.17%	0.74%
5C	Vancouver	Vestibule	16.23%	8.84%	2.42%	2.98%	0.08%	1.16%	0.35%	1.86%
6A	Burlington	Vestibule	17.36%	14.41%	3.82%	5.35%	0.08%	1.14%	0.05%	0.22%
6B	Helena	Vestibule	16.83%	13.89%	2.44%	3.53%	0.08%	1.14%	0.48%	2.54%
7	Duluth	Vestibule	18.24%	16.88%	3.57%	5.94%	0.11%	1.32%	-0.01%	0.02%
8	Fairbanks	Vestibule	19.43%	18.67%	4.06%	7.71%	0.12%	1.62%	-0.03%	-0.27%
National Weighted Average			**11.00%**	**6.52%**	**1.90%**	**2.21%**	**0.06%**	**0.90%**	**0.08%**	**0.34%**

Total Air Infiltration using CONTAM for infiltration calculation & Air Curtain Units Operation Details

Strip Mall Reference Building Model

Table 65. Total air infiltration in the entrance door zone for the 3 entrance door scenarios in the strip mall building

	1A	2A	2B	3A	3B	3C	4A	4B	4C	5A	5B	5C	6A	6B	7	8
Single Door (kg x10)	2464674	2833976	2720399	3203397	2480474	3462986	3446171	2796289	3910517	4525493	2985527	3460119	4810371	3060473	4780097	4801899
Vestibule Door (kg x10)	-	-	-	2895671	2235304	3248873	3157135	2544377	3458924	4113348	2749530	3157513	4375384	2833005	4397914	4387817
Air Curtain Door (kg x10)	2342595	2652577	1662073	2971063	2335226	3441339	3151945	2598520	3514895	3665739	2648954	3041174	4168317	2670551	4095686	3897404

Table 66. Air curtain units (10 air curtains) operation details for the strip mall building

	1A	2A	2B	3A	3B	3C	4A	4B	4C	5A	5B	5C	6A	6B	7	8
Air Curtain Fan Energy (kWh)	191.67	366.67	705.56	522.22	466.67	66.67	588.89	566.67	538.89	736.11	738.89	697.22	791.67	830.56	908.33	977.78
Air Curtain Fan Energy fraction from Annual Building Energy Consumption	0.06%	0.11%	0.21%	0.14%	0.14%	0.02%	0.15%	0.17%	0.14%	0.15%	0.19%	0.18%	0.15%	0.19%	0.15%	0.12%
Air Curtain Fan Annual On Time (Hrs)	182.54	349.21	671.96	497.35	444.44	63.49	560.85	539.68	513.23	701.06	703.70	664.02	753.97	791.01	865.08	931.22
Air Curtains Fan Annual On Time/Building Operation Hours (%)	4.2%	8.0%	15.3%	11.4%	10.1%	1.4%	12.8%	12.3%	11.7%	16.0%	16.1%	15.2%	17.2%	18.1%	19.8%	21.3%

Outpatient Healthcare Reference Building Model

Table 67. Total air infiltration in the entrance door zone for the 3 entrance door scenarios in the outpatient healthcare building

	1A	2A	2B	3A	3B	3C	4A	4B	4C	5A	5B	5C	6A	6B	7	8
Single Door (kg)	596327	908970	1111400	1845470	2543810	6296940	3539240	2291190	2133210	3848550	2775940	3872380	3547650	4557570	5045960	4871610
Vestibule Door (kg)	-	-	-	1688210	2277670	5662990	3222940	2071750	1961630	3501490	2533710	3530830	3241800	4106040	4583980	4450030
Air Curtain Door (kg)	553817	741524	872878	1151790	2079290	6108320	2017870	1521100	1454570	1743760	1476870	2322980	1440770	2345590	2133910	1693210

Table 68. Air curtain unit (1 air curtain) operation details for the outpatient healthcare building

	1A	2A	2B	3A	3B	3C	4A	4B	4C	5A	5B	5C	6A	6B	7	8
Air Curtain Fan Energy (kWh)	108.33	205.56	366.67	277.78	236.11	50.00	297.22	297.22	255.56	361.11	372.22	350.00	391.67	419.44	452.78	491.67
Air Curtain Fan Energy fraction from Annual Building Energy Consumption	0.01%	0.01%	0.03%	0.02%	0.02%	0.00%	0.02%	0.02%	0.02%	0.02%	0.03%	0.03%	0.03%	0.03%	0.03%	0.02%
Air Curtain Fan Annual On Time (Hrs)	103.17	195.77	349.21	264.55	224.87	47.62	283.07	283.07	243.39	343.92	354.50	333.33	373.02	399.47	431.22	468.25
Air Curtains Fan Annual On Time/Building Operation Hours (%)	3.3%	6.3%	11.2%	8.5%	7.2%	1.5%	9.1%	9.1%	7.8%	11.0%	11.4%	10.7%	12.0%	12.8%	13.8%	15.0%

Sensitivity Study

Sensitivity to Door Usage Frequency

Strip Mall Building

Table 69. Air curtain door annual energy savings' sensitivity to door-opening frequency in the strip mall building

		4A Baltimore							7A Duluth						
Door Usage Small Store (People/Hour)	Peak	11	13	14	16	18	19	21	11	13	14	16	18	19	21
	Off-Peak	1	1	1	2	2	2	2	1	1	1	2	2	2	2
Door Usage Large Store (People/Hour)	Peak	24	27	31	34	37	41	44	24	27	31	34	37	41	44
	Off-Peak	2	3	3	3	4	4	4	2	3	3	3	4	4	4
Door Usage Variance from Baseline case		-30%	-20%	-10%	0% (Baseline)	10%	20%	30%	-30%	-20%	-10%	0% (Baseline)	10%	20%	30%
Door Azimuth (From North)		180							180						
Vestibule (MJ/m2)		703.79			711.11			714.14	1099.22			1122.48			1140.99
Difference from Base (MJ/m2)		-7.32			0.00			3.03	-23.26			0.00			18.51
Difference from Base Case (%)		-1.03%			0.00%			0.43%	-2.07%			0.00%			1.65%
Air Curtain (MJ/m2)		692.98	694.13	694.92	696.24	697.17	698.04	698.99	1051.31	1052.83	1053.99	1055.77	1057.09	1058.07	1059.49
Difference from Base (MJ/m2)		-3.26	-2.11	-1.32	0.00	0.93	1.80	2.75	-4.46	-2.94	-1.78	0.00	1.32	2.30	3.72
Difference from Base Case (%)		-0.47%	-0.30%	-0.19%	0.00%	0.13%	0.26%	0.39%	-0.42%	-0.28%	-0.17%	0.00%	0.13%	0.22%	0.35%
Air Curtain Vs. Vestibule Savings (MJ/m2)		10.81			14.87			15.15	47.91			66.71			81.50
Air Curtain Vs. Vestibule Savings (%)		1.54%			2.09%			2.12%	4.36%			5.94%			7.14%
Total Air Curtain Units Energy (kWh)		394.44	455.56	494.44	613.89	650.00	686.11	738.89	605.56	702.78	761.11	908.33	1002.78	1061.11	1138.89
Total Air Curtain Units Energy (MJ/m2)		0.37	0.43	0.47	0.58	0.62	0.65	0.70	0.57	0.67	0.72	0.86	0.95	1.00	1.08
Total Air Curtain Fans Energy Fraction from Annual Consumption (%)		0.0539%	0.0621%	0.0673%	0.0834%	0.0882%	0.0930%	0.1000%	0.0545%	0.0632%	0.0683%	0.0814%	0.0898%	0.0949%	0.1017%
Standard Deviation Vestibule (MJ/m2)		5.32							20.93						
Standard Deviation Air Curtain (MJ/m2)		2.17							2.95						

Outpatient Healthcare Building

Table 70. Air curtain door annual energy savings' sensitivity to door-opening frequency in the outpatient healthcare building

		4A							7A						
		Baltimore							Duluth						
Door Usage (People/Hour)	Peak	86	98	111	123	135	148	160	86	98	111	123	135	148	160
	Off-Peak	9	10	11	12	14	15	16	9	10	11	12	14	15	16
Door Usage Variance from Baseline case		-30%	-20%	-10%	0% (Baseline)	10%	20%	30%	-30%	-20%	-10%	0% (Baseline)	10%	20%	30%
Door Azimuth (From North)		270							270						
Vestibule (MJ/m2)		1377.12			1377.57			1377.96	1568.12			1568.02			1567.84
Difference from Base (MJ/m2)		-0.45			0.00			0.39	0.10			0.00			-0.18
Difference from Base Case (%)		-0.03%			0.00%			0.03%	0.01%			0.00%			-0.01%
Air Curtain (MJ/m2)		1373.72	1373.81	1374.00	1374.19	1374.31	1374.58	1374.74	1566.71	1567.03	1567.37	1567.69	1567.91	1568.28	1568.44
Difference from Base (MJ/m2)		-0.47	-0.38	-0.19	0.00	0.12	0.39	0.55	-0.98	-0.66	-0.32	0.00	0.22	0.59	0.75
Difference from Base Case (%)		-0.03%	-0.03%	-0.01%	0.00%	0.01%	0.03%	0.04%	-0.06%	-0.04%	-0.02%	0.00%	0.01%	0.04%	0.05%
Air Curtain Vs. Vestibule Savings (MJ/m2)		3.40			3.38			3.22	1.41			0.33			-0.60
Air Curtain Vs. Vestibule Savings (%)		0.25%			0.25%			0.23%	0.09%			0.02%			-0.04%
Air Curtain Fan Energy (kWh)		216.67	244.44	269.44	297.22	325.00	347.22	372.22	330.56	372.22	413.89	452.78	497.22	530.56	569.44
Air Curtain Fan Energy (MJ/m2)		0.21	0.23	0.25	0.28	0.31	0.33	0.35	0.31	0.35	0.39	0.43	0.47	0.50	0.54
Air Curtain Fan Energy Fraction from Annual Consumption (%)		0.0149%	0.0168%	0.0186%	0.0205%	0.0224%	0.0239%	0.0256%	0.0200%	0.0225%	0.0250%	0.0273%	0.0300%	0.0320%	0.0344%
Standard Deviation Vestibule (MJ/m2)		0.42							0.14						
Standard Deviation Air Curtain (MJ/m2)		0.38							0.64						

Sensitivity to Wind Pressure Coefficients (Outdoor Pressure)

Strip Mall Building

Table 71. Air curtain door annual energy savings' sensitivity to wind pressure coefficients in the strip mall building

	4A					7				
	Baltimore					Duluth				
Wind Pressure Coefficient Variance from Base case	-20%	-10%	0% (Base Case)	10%	20%	-20%	-10%	0% (Base Case)	10%	20%
Door Azimuth (From North)	180					180				
Vestibule (MJ/m2)	716.03		711.11		708.18	1134.56		1122.48		1113.41
Difference from Base (MJ/m2)	4.92		0.00		-2.93	12.08		0.00		-9.07
Difference from Base Case (%)	0.69%		0.00%		-0.41%	1.08%		0.00%		-0.81%
Air Curtain (MJ/m2)	699.47	697.35	696.24	695.15	694.79	1065.46	1059.03	1055.77	1051.35	1048.84
Difference from Base (MJ/m2)	3.23	1.11	0.00	-1.09	-1.45	9.69	3.26	0.00	-4.42	-6.93
Difference from Base Case (%)	0.46%	0.16%	0.00%	-0.16%	-0.21%	0.92%	0.31%	0.00%	-0.42%	-0.66%
Air Curtain Vs. Vestibule Savings (MJ/m2)	16.56		14.87		13.39	69.10		66.71		64.57
Air Curtain Vs. Vestibule Savings (%)	2.31%		2.09%		1.89%	6.09%		5.94%		5.80%
Total Air Curtain Fans Energy (kWh)	588.89					908.33				
Total Air Curtain Fans Energy (MJ/m2)	0.28					0.43				
Total Air Curtain Fans Energy Fraction from Annual Consumption (%)	0.0402%	0.0403%	0.0404%	0.0405%	0.0405%	0.0402%	0.0405%	0.0406%	0.0408%	0.0409%
Standard Deviation Vestibule (MJ/m2)	3.97					10.61				
Standard Deviation Air Curtain (MJ/m2)	1.89					6.55				

Outpatient Healthcare Building

Table 72. Air curtain door annual energy savings' sensitivity to wind pressure coefficients in the outpatient healthcare building

	4A					7				
	Baltimore					Duluth				
Wind Pressure Coefficient Variance from Baseline	-20%	-10%	0% (Baseline)	10%	20%	-20%	-10%	0% (Baseline)	10%	20%
Door Azimuth (From North)	270					270				
Vestibule (MJ/m2)	1374.92		1377.57		1380.54	1567.24		1568.02		1568.10
Difference from Base (MJ/m2)	-2.65		0.00		2.97	-0.78		0.00		0.08
Difference from Base Case (%)	-0.19%		0.00%		0.22%	-0.06%		0.00%		0.01%
Air Curtain (MJ/m2)	1372.65	1373.28	1374.19	1375.04	1376.18	1567.03	1567.00	1567.69	1567.74	1567.67
Difference from Base (MJ/m2)	-1.54	-0.91	0.00	0.85	1.99	-0.66	-0.69	0.00	0.05	-0.02
Difference from Base Case (%)	-0.11%	-0.07%	0.00%	0.06%	0.14%	-0.04%	-0.04%	0.00%	0.00%	0.00%
Air Curtain Vs. Vestibule Savings (MJ/m2)	2.27		3.38		4.36	0.21		0.33		0.43
Air Curtain Vs. Vestibule Savings (%)	0.17%		0.25%		0.32%	0.01%		0.02%		0.03%
Air Curtain Fan Energy (kWh)	297.22					452.78				
Air Curtain Fan Energy (MJ/m2)	0.28					0.43				
Air Curtain Fan Energy Fraction from Annual Consumption (%)	0.0205%	0.0205%	0.0205%	0.0205%	0.0204%	0.0273%	0.0273%	0.0273%	0.0273%	0.0273%
Standard Deviation Vestibule (MJ/m2)	2.81					0.48				
Standard Deviation Air Curtain (MJ/m2)	1.40					0.38				

Sensitivity to Building Orientation

Strip Mall Building

Table 73. Air curtain door annual energy savings' sensitivity to building orientation in the strip mall building

	4A				7				8			
	Baltimore				Duluth				Fairbanks			
Building Orientation	North (Baseline)	East	South	West	North (Baseline)	East	South	West	North (Baseline)	East	South	West
Doors Azimuth (From North)	180	270	0	90	180	270	0	90	180	270	0	90
Vestibule (MJ/m2)	711.11	735.31	742.35	755.28	1122.48	1158.76	1163.68	1184.75	1483.94	1489.95	1520.23	1481.72
Air Curtain (MJ/m2)	696.24	718.88	715.36	727.02	1055.77	1096.49	1087.13	1098.79	1369.56	1374.18	1399.00	1370.61
Savings (MJ/m2)	14.87	16.43	26.99	28.26	66.71	62.27	76.55	85.96	114.38	115.77	121.23	111.11
Savings (%)	2.09%	2.23%	3.64%	3.74%	5.94%	5.37%	6.58%	7.26%	7.71%	7.77%	7.97%	7.50%
Total Air Curtain Fans Energy (kWh)	588.89				908.33				977.78			
Total Air Curtain Fans Energy (MJ/m2)	1.01				1.56				1.68			
Total Air Curtain Fans Energy Fraction from Annual Consumption (%)	0.1457%	0.1411%	0.1418%	0.1395%	0.1482%	0.1427%	0.1439%	0.1424%	0.1230%	0.1225%	0.1204%	0.1229%
Average Vestibule Door (MJ/m2)	736.01				1157.42				1493.96			
Average Air Curtain Door (MJ/m2)	714.38				1084.55				1378.34			
Average Savings (MJ/m2)	21.64				72.87				115.62			
Average Savings for 4 Orientations (%)	2.94%				6.30%				7.74%			
Standard Deviation Vestibule Door (MJ/m2)	18.55				25.88				17.86			
Standard Deviation Air Curtain (MJ/m2)	13.04				19.84				13.92			

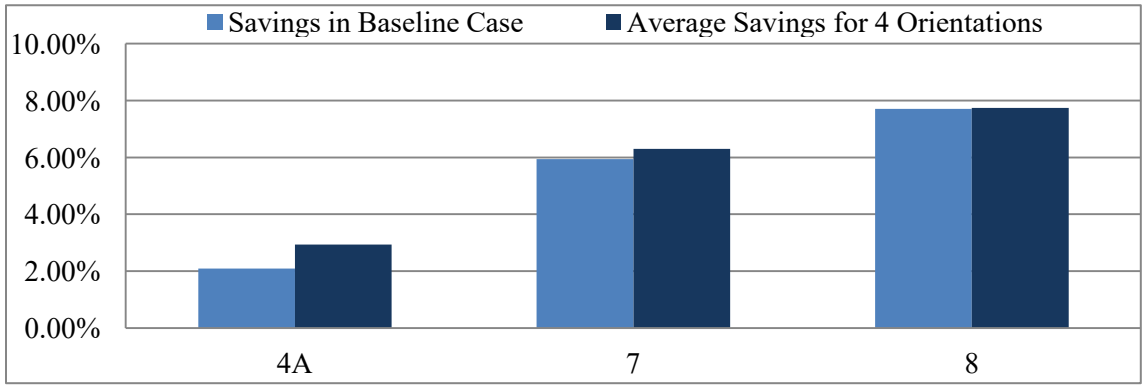

Figure 104. Air curtain door annual energy savings for the baseline case and the average for the 4 orientations in the strip mall building

Table 74. Air curtain door annual infiltration reduction's sensitivity to building orientation in the strip mall building

	4A				7				8			
	Baltimore				Duluth				Fairbanks			
Building Orientation	North (Baseline)	East	South	West	North (Baseline)	East	South	West	North (Baseline)	East	South	West
Door Azimuth (° From North)	180	270	0	90	180	270	0	90	180	270	0	90
Annual Air Infiltration with Vestibule in 10 Stores (Kg)	31571352	32625355	32624202	35842301	43979142	46627726	43926184	48703650	43878175	42232820	43843265	43019373
Annual Air Infiltration with Air Curtains in 10 Stores (Kg)	31519458	32310818	31368642	34729228	40956863	43423519	39825819	44497831	38974042	37110503	38447110	38326819
Infiltration Reduction (Kg)	51894	314536	1255561	1113073	3022279	3204207	4100365	4205819	4904133	5122317	5396155	4692554
Infiltration Reduction (%)	0.2%	1.0%	3.8%	3.1%	6.9%	6.9%	9.3%	8.6%	11.2%	12.1%	12.3%	10.9%

Table 75. Air curtain Door air heating and cooling energy savings (sample calculation for CZ-4A)

	4A							
	Baltimore							
	HVAC Air Cooling Loads				HVAC Air Heating Loads			
Building Orientation	North (Baseline)	East	South	West	North (Baseline)	East	South	West
Door Azimuth (From North)	180	270	0	90	180	270	0	90
Vestibule (J)	4.79E+11	4.95E+11	4.46E+11	5.01E+11	5.31E+11	5.70E+11	5.88E+11	6.05E+11
Air Curtain (J)	4.81E+11	4.99E+11	4.48E+11	5.01E+11	5.04E+11	5.40E+11	5.41E+11	5.56E+11
Savings (J)	-2.42E+09	-3.37E+09	-2.24E+09	2.15E+08	2.69E+10	2.97E+10	4.72E+10	4.89E+10
Savings (%)	-0.51%	-0.68%	-0.50%	0.04%	5.06%	5.22%	8.03%	8.08%
Average Vestibule (J)	4.80E+11				5.74E+11			
Average Air Curtain (J)	4.82E+11				5.35E+11			
Average Savings (J)	-1.95E+09				3.82E+10			
Average Savings for 4 Orientations (%)	-0.41%				6.66%			

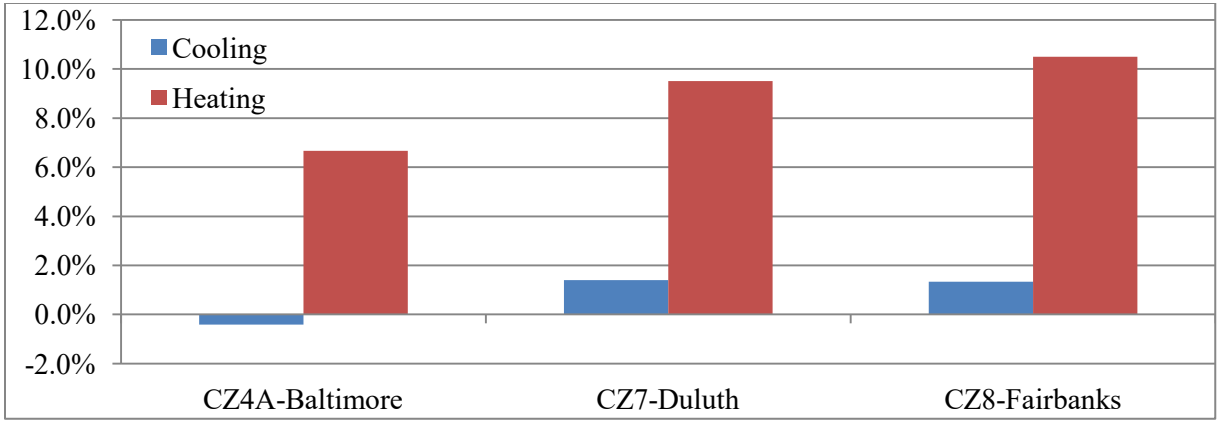

Figure 105. Air curtain door average air heating and cooling energy savings for 4 orientations in the strip mall building

Outpatient Healthcare Building

Table 76. Air curtain door annual energy savings' sensitivity to building orientation in the outpatient healthcare building

Building Orientation	4A Baltimore				7 Duluth				8 Fairbanks			
	North (Baseline)	East	South	West	North (Baseline)	East	South	West	North (Baseline)	East	South	West
Door Azimuth (From North)	270	0	90	180	270	0	90	180	270	0	90	180
Vestibule (MJ/m2)	1377.57	1385.14	1373.91	1382.17	1568.02	1586.61	1567.82	1580.64	1866.94	1867.40	1863.21	1874.46
Air Curtain (MJ/m2)	1374.19	1384.46	1373.08	1381.55	1567.69	1588.72	1566.83	1581.88	1871.91	1875.40	1864.40	1873.49
Savings (MJ/m2)	3.38	0.68	0.83	0.62	0.33	-2.11	0.99	-1.24	-4.97	-8.00	-1.19	0.97
Savings (%)	0.25%	0.05%	0.06%	0.04%	0.02%	-0.13%	0.06%	-0.08%	-0.27%	-0.43%	-0.06%	0.05%
Air Curtain Fan Energy (kWh)	297.22				452.78				491.67			
Air Curtain Fan Energy (MJ/m2)	0.28				0.43				0.47			
Air Curtain Fan Energy Fraction from Annual Consumption (%)	0.0205%	0.0203%	0.0205%	0.0204%	0.0273%	0.0270%	0.0273%	0.0271%	0.0249%	0.0248%	0.0250%	0.0248%
Average Vestibule (MJ/m2)	1379.70				1575.77				1868.00			
Average Air Curtain (MJ/m2)	1378.32				1576.28				1871.30			
Average Savings (MJ/m2)	1.38				-0.51				-3.30			
Average Savings for 4 Orientations (%)	0.10%				-0.03%				-0.18%			
Standard Deviation Vestibule (MJ/m2)	4.96				9.39				4.70			
Standard Deviation Air Curtain (MJ/m2)	5.56				10.79				4.82			

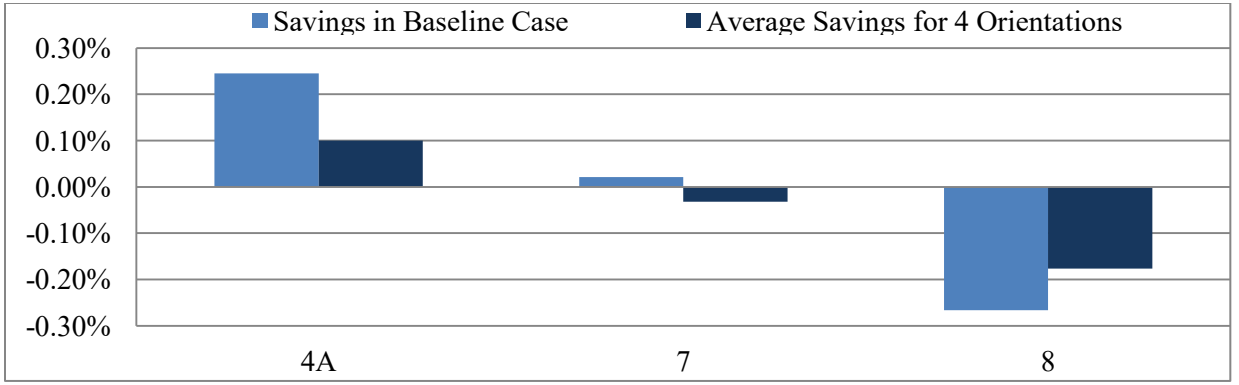

Figure 106. Air curtain door annual energy savings for the baseline case and the average for the 4 orientations in the outpatient healthcare building

Table 77. Air curtain door annual infiltration reduction's sensitivity to building orientation in the outpatient healthcare building

	4A				7				8			
	Baltimore				Duluth				Fairbanks			
Building Orientation	North (Baseline)	East	South	West	North (Baseline)	East	South	West	North (Baseline)	East	South	West
Door Azimuth (° From North)	270	0	90	180	270	0	90	180	270	0	90	180
Annual Air Infiltration in Lobby with Vestibule (Kg)	3222940	1983230	1928530	2452870	4583980	3366830	3641460	3467500	4450030	4474450	4283100	4513920
Annual Air Infiltration with in Lobby with Air Curtain (Kg)	2017870	1253920	1143580	1368120	2133910	1533080	1650730	1354480	1693210	1609010	1516350	1565590
Infiltration Reduction (Kg)	1205070	729310	784950	1084750	2450070	1833750	1990730	2113020	2756820	2865440	2766750	2948330
Infiltration Reduction (%)	37.4%	36.8%	40.7%	44.2%	53.4%	54.5%	54.7%	60.9%	62.0%	64.0%	64.6%	65.3%

Table 78. Air curtain Door air heating and cooling energy savings (sample calculation for CZ-4A)

	4A							
	Baltimore							
	HVAC Air Cooling Loads				HVAC Air Heating Loads			
Building Orientation	North (Baseline)	East	South	West	North (Baseline)	East	South	West
Door Azimuth (From North)	270	0	90	180	270	0	90	180
Vestibule (J)	3.08E+12	3.12E+12	3.06E+12	3.09E+12	1.58E+12	1.60E+12	1.57E+12	1.60E+12
Air Curtain (J)	3.07E+12	3.11E+12	3.06E+12	3.09E+12	1.57E+12	1.60E+12	1.57E+12	1.59E+12
Savings (J)	8.08E+09	4.98E+09	3.69E+09	3.93E+09	8.85E+09	9.26E+08	2.52E+09	2.52E+09
Savings (%)	0.26%	0.16%	0.12%	0.13%	0.56%	0.06%	0.16%	0.16%
Average Vestibule (J)	3.09E+12				1.59E+12			
Average Air Curtain (J)	3.08E+12				1.58E+12			
Average Savings (J)	5.17E+09				3.70E+09			
Average Savings for 4 Orientations (%)	0.17%				0.23%			

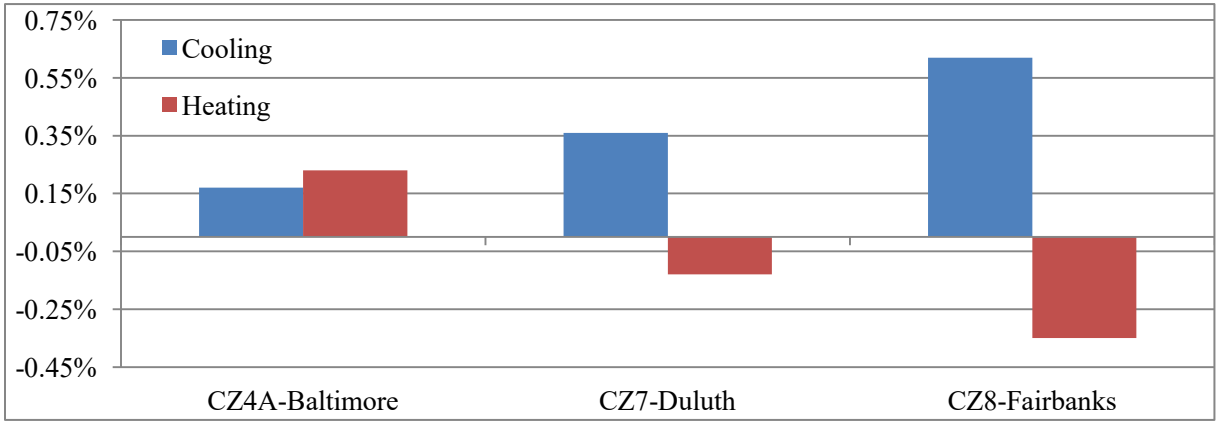

Figure 107. Air curtain door average air heating and cooling energy savings for 4 orientations in the outpatient healthcare building

Sensitivity to Air Curtain Door Temperature Control

Table 79. Effect of air curtain temperature control on energy consumption and savings in CZ-3 for the strip mall building

Air Curtain Temperature Control (Where T is the temperature range in ° C where the unit operates)			**30 < T < 10 (Baseline)**	Always ON (No temp. Control)
3C	San Francisco	Air Curtain Door (MJ/m²)	**492.00**	487.98
		Vestibule Door (MJ/m²)	**489.83**	
		Energy Savings (%)	**-0.44%**	0.38%
		Units Energy (GJ)	**0.24**	5.79
		Units On-Time (Hrs/Year)	**63**	1532

Table 80. Effect of air curtain temperature control on energy consumption and savings in CZ-3 for the outpatient healthcare building

Air Curtain Temperature Control (Where T is the temperature range in ° C where the unit operates)			**30 < T < 10 (Baseline)**	Always ON (No temp. Control)
3C	San Francisco	Air Curtain Door (MJ/m²)	**1171.00**	1162.62
		Vestibule Door (MJ/m²)	**1169.73**	
		Energy Savings (%)	**-0.11%**	0.61%
		Units Energy (GJ)	**0.18**	2.9
		Units On-Time (Hrs/Year)	**48**	767

Outpatient Healthcare Building Sensitivity to Door Location & Zone Interaction

Table 81. Outpatient healthcare building in CZ-8: vestibule & air curtain doors percent annual energy savings for 5 entrance door locations

Door Location	Outpatient Healthcare Building	
	Vestibule Door Vs. Single Door	Air Curtain door Vs. Vestibule Door
Lobby (Baseline for this study)	**-0.03%**	**-0.27%**
Reception	-0.04%	-0.39%
Procedure Room	-0.02%	-0.07%
Utility Room	0.02%	-0.24%
Vestibule (Default model Entrance Location)	0.05%	-0.18%

Table 82. Outpatient healthcare building: vestibule & air curtain door percent annual energy savings

Entrance Door Location		"Vestibule" Zone (Default Model Entrance Zone for Model)		"Lobby" Zone (Baseline Entrance Zone for this Study)		Baseline for Air Curtain Savings Calculation
Climate Zone		Vestibule Door Vs. Single Door	Air Curtain Door Vs. Baseline	Vestibule Door Vs. Single Door	Air Curtain Door Vs. Baseline	
1A	Miami	-	-0.03%	-	-0.02%	Single Door
2A	Houston	-	-0.06%	-	-0.03%	Single Door
2B	Phoenix	-	-0.10%	-	-0.04%	Single Door
3A	Memphis	0.00%	-0.12%	0.02%	-0.05%	Vestibule
3B	El-Paso	0.00%	-0.09%	0.05%	0.07%	Vestibule
3C	San Francisco	0.00%	-0.01%	0.15%	-0.11%	Vestibule
4A	Baltimore	0.00%	-0.07%	0.05%	0.25%	Vestibule
4B	Albuquerque	0.00%	-0.06%	0.09%	0.30%	Vestibule
4C	Salem	0.00%	-0.05%	0.08%	0.05%	Vestibule
5A	Chicago	0.01%	-0.04%	0.22%	1.02%	Vestibule
5B	Boise	0.00%	-0.04%	0.17%	0.74%	Vestibule
5C	Vancouver	0.00%	0.13%	0.35%	1.86%	Vestibule
6A	Burlington	0.01%	-0.10%	0.05%	0.22%	Vestibule
6B	Helena	0.00%	0.13%	0.48%	2.54%	Vestibule
7	Duluth	0.01%	-0.07%	-0.01%	0.02%	Vestibule
8	Fairbanks	0.05%	-0.18%	-0.03%	-0.27%	Vestibule
National Weighted Average		**0.00%**	**-0.07%**	**0.08%**	**0.34%**	

Table 83. Outpatient healthcare building in CZ-8: vestibule & air curtain doors percent annual air infiltration reduction for 5 entrance door locations

Door Location	Outpatient Healthcare Building	
	Vestibule Door Vs. Single Door	Air Curtain door Vs. Vestibule Door
Lobby (Baseline for this study)	**8.70%**	**62.00%**
Reception	9.50%	70.80%
Procedure Room	1.50%	25.00%
Utility Room	0.00%	-0.30%
Vestibule (Default model Entrance Location)	0.90%	26.80%

Table 84. Outpatient healthcare building (door in "Lobby" zone) in CZ-8: vestibule & air curtain doors percent annual energy savings for different internal zones interactions

Leakage Condition	Outpatient Healthcare Building	
	Vestibule Door Vs. Single Door	Air Curtain Door Vs. Vestibule Door
Base Case	**-0.03%**	**-0.27%**
Only Large Opening	0.00%	-0.12%
Only Wall Leakages	0.08%	-0.18%
1 Ceiling Leakage	0.02%	-0.10%
No Leakages (Sealed Zone)	0.02%	0.01%

Table 85. Outpatient healthcare building (door in "Lobby" zone) in CZ-8: vestibule & air curtain doors percent annual air infiltration reduction for different internal zones interactions

Leakage Condition	Outpatient Healthcare Building	
	Vestibule Door Vs. Single Door	Air Curtain Door Vs. Vestibule Door
Base Case	**8.70%**	**62.00%**
Only Large Opening	7.60%	81.50%
Only Wall Leakages	3.30%	48.00%
1 Ceiling Leakage	0.60%	94.40%
No Leakages (Sealed Zone)	24.70%	75.80%

Table 86. Details of leakage and openings conditions for the different internal zones interaction cases

Leakage Condition	Comments
Base Case	All Openings (doors & vents) and all leakages
Only Large Opening	Only doors and vents
Only Wall Leakages	Only wall/ceiling leakages
1 Ceiling Leakage	Only 1 leakage connecting zone to upper floor
No Leakages (Sealed Zone)	Zone only connected to outdoor - separate from surroundings